



Jaworska, Katarzyna (2017) Understanding age-related differences in the speed of information processing of complex object categories measured with electroencephalography (EEG). PhD thesis.

<http://theses.gla.ac.uk/8112/>

Copyright and moral rights for this work are retained by the author

A copy can be downloaded for personal non-commercial research or study, without prior permission or charge

This work cannot be reproduced or quoted extensively from without first obtaining permission in writing from the author

The content must not be changed in any way or sold commercially in any format or medium without the formal permission of the author

When referring to this work, full bibliographic details including the author, title, awarding institution and date of the thesis must be given

Enlighten:Theses
<http://theses.gla.ac.uk/>
theses@gla.ac.uk



University
of Glasgow | Institute of Neuroscience
& Psychology

UNDERSTANDING AGE-RELATED
DIFFERENCES IN THE SPEED OF
INFORMATION PROCESSING OF COMPLEX
OBJECT CATEGORIES MEASURED WITH
ELECTROENCEPHALOGRAPHY (EEG)

Katarzyna Jaworska

MA, MSc

Submitted in fulfilment of the requirements for the
Degree of Doctor of Philosophy

School of Psychology
Institute of Neuroscience and Psychology
College of Medical, Veterinary and Life Sciences
University of Glasgow

April 2017

ABSTRACT

Ageing is associated with differences in visual function which can be observed, for example, as a decline in performance on face and object processing tasks. One of the most prominent accounts of age-related decrement in perceptual and cognitive tasks alike is that of a reduction in information processing speed (Salthouse, *Psychological Review* 1996, 103:403). Differences in myelin integrity in some parts of the cortex, as well as in neuronal responsivity are physiologically plausible as the origins of the age-related slowing-down of information processing. However, little research to date has directly investigated age-related slowing-down of visual information processing in humans. Previously, Rousselet et al. (*Frontiers in Psychology* 2010, 1:19) reported a 1ms/year delay in face visual processing speed in a sample of 62 subjects aged ~20-80, using event-related potentials (ERPs). This result was replicated in another 59 subjects, and was independent of stimulus luminance and senile miosis (Bieniek et al. *Frontiers in Psychology* 2013, 4:268). To go beyond differences in average brain activity and interpret previous findings, in the first study (Chapter 2) we investigated what information is coded by early face ERPs in younger and older observers. In a detection task, young and older observers each categorized 2,200 pictures of faces and noise textures revealed through Gaussian apertures ("Bubbles"). Using reverse correlation and Mutual Information (MI), we found that the presence of the left eye elicited fastest detection in both age groups. Older observers relied more on the eyes to be accurate, suggesting a strategy difference between groups. In both age groups, the presence of the eye contralateral to the recording electrode modulated single-trial ERPs at lateral-occipital electrodes, but this association was weaker in older observers and delayed by about 40 ms. We also observed a differentiated coding of the eyes across groups: in younger observers, both the N170 latency and amplitude coded the contralateral eye, whereas it was only the N170 amplitude in older adults. The latency modulation in younger adults was also higher in the right than in the left hemisphere, but very similar across hemispheres in older adults. Our results suggest that face detection in ageing is associated with delayed and weaker processing of the same face features, and point to potential coding differences. On the notion that incomplete or occluded stimuli (such as Bubbled images) might differentially affect older adults' ability to perform a perceptual task, in the second study (Chapter 3) we sought to understand whether the age-related differences in eye sensitivity were preserved in a face context. Two groups of observers, young and older, performed a face detection task in which the visibility of the eye region was modulated in a parametric manner by adding phase noise. This way, we could investigate the modulation of ERPs by increasing information available in the eye region,

when the face context was preserved (or absent – in control conditions). In line with behavioural results reported in Chapter 2, modulating the visibility of the left eye had a greater effect on reaction times across older participants, and this modulation increased with decreasing face context information in older adults. Contralateral eye sensitivity was weaker than that reported in Chapter 2 and did not differ between young and older observers, suggesting that coding of the eye by the N170 acts differently when the eye is revealed through Bubble masks and when it is presented in the face context. In Chapter 4, we investigated potential origins of the large N170 responses to textures observed in a sample of older participants before (Rousselet et al. BMC Neuroscience 2009, 10:114), and quantified age-related delays in visual processing speed of stimuli other than faces: houses and letters. Two groups of participants performed three simple detection tasks: face detection, house detection, and letter detection. Perceiving textures in the context of a face detection task, but not house detection or letter detection, influenced ERP responses to textures in older participants only to a small extent and after 200 ms post-stimulus, suggesting that the large N170 responses to textures are unlikely due to a top-down influence of the task at hand. Furthermore, visual processing speed of faces, houses and letters was delayed to a smaller extent than that predicted by the original study and depended on the nature of categorical comparisons made. Overall, our results fill the big gap in the literature concerned with age-related slowing of *information* processing: using Bubbles, we have presented direct evidence that processing of the same facial information is slower (and weaker) in ageing. However, quantifying visual processing speed using categorical designs yielded mixed evidence for the theory of slower information processing in ageing, pointing to the need for carefully designed visual stimuli in ageing research, and for careful selection of control stimuli for comparisons.

ABSTRACT	2
TABLE OF FIGURES	7
CHAPTER 2	7
CHAPTER 3	7
CHAPTER 4	7
TABLE OF TABLES	8
CHAPTER 2	8
CHAPTER 3	8
CHAPTER 4	8
ACKNOWLEDGMENTS	9
LIST OF PUBLICATIONS	10
CHAPTER 1: INTRODUCTION	11
GENERAL SLOWING DOWN WITH AGEING	12
OVERVIEW OF AGE-RELATED STRUCTURAL DIFFERENCES AND CHANGES IN THE BRAIN	13
AGE-RELATED CHANGES TO WHITE MATTER MICROSTRUCTURE	14
STRUCTURAL CORRELATES OF AGE-RELATED COGNITIVE DECLINE	16
NEURONAL RESPONSIVITY	17
AGE-RELATED SLOWING OF VISUAL PROCESSING	20
AIMS OF THE THESIS	24
CHAPTER 2: PROCESSING OF THE SAME FACE FEATURES IS DELAYED BY 40 MS AND WEAKER IN HEALTHY AGEING	27
INTRODUCTION	27
MATERIALS AND METHODS	29
PARTICIPANTS	29
STIMULI	30
PROCEDURE	31
EEG RECORDING AND PRE-PROCESSING	31
ELECTRODE SELECTION	33
STATISTICAL ANALYSES	33
MEASURES OF EFFECT SIZE	34
MUTUAL INFORMATION	34
MUTUAL INFORMATION: CONTINUOUS APPROACH	35
MUTUAL INFORMATION: CLASSIFICATION IMAGES	36
ERP ONSET ANALYSES	37
TOPOGRAPHIC ANALYSES	38

RESULTS	39
BEHAVIOURAL RESULTS	39
EVENT-RELATED POTENTIALS	43
BRAIN INFORMATION CONTENT	46
TIME COURSE OF INFORMATION PROCESSING	49
ERP FEATURE-OF-INTEREST ANALYSIS	53
DISCUSSION	57
CHAPTER 3: AGE-RELATED DIFFERENCES IN EYE SENSITIVITY WITH AND WITHOUT THE FACE CONTEXT	63
INTRODUCTION	63
MATERIALS AND METHODS	65
PARTICIPANTS	65
STIMULI	66
PROCEDURE	69
EEG RECORDING AND PRE-PROCESSING	69
STATISTICAL ANALYSES.....	71
MEASURES OF EFFECT SIZE	71
MUTUAL INFORMATION.....	71
50% INTEGRATION TIME	72
ELECTRODE SELECTION	73
RESULTS	75
BEHAVIOURAL RESULTS	75
MUTUAL INFORMATION.....	79
AGE-RELATED DIFFERENCES IN EYE SENSITIVITY WHEN FACE CONTEXT IS PRESENT	83
AGE-RELATED DIFFERENCES IN EYE SENSITIVITY WHEN FACE CONTEXT IS ABSENT	85
MUTUAL INFORMATION ABOUT CATEGORICAL DIFFERENCES BETWEEN FACE AND TEXTURE...87	
REVERSE ANALYSIS	94
EVENT-RELATED POTENTIALS.....	100
DISCUSSION	104
CHAPTER 4: TOP-DOWN EFFECTS ON THE PERCEPTION OF TEXTURES IN THE CONTEXT OF OBJECT DETECTION TASKS	112
INTRODUCTION	112
METHODS	115
PARTICIPANTS	115
STIMULI	116

PROCEDURE.....	117
EEG RECORDING AND PRE-PROCESSING.....	119
STATISTICAL ANALYSES.....	120
MEASURES OF EFFECT SIZE.....	120
MUTUAL INFORMATION.....	120
50% INTEGRATION TIME.....	121
ELECTRODE SELECTION.....	122
TOPOGRAPHIC ANALYSES.....	123
RESULTS.....	124
BEHAVIOURAL RESULTS.....	124
EVENT-RELATED POTENTIALS.....	127
BRAIN SENSITIVITY: MUTUAL INFORMATION.....	129
CATEGORICAL DIFFERENCES: OBJECTS.....	129
CATEGORICAL DIFFERENCES: TEXTURES.....	132
AGE-RELATED DIFFERENCES IN BRAIN SENSITIVITY TO BASELINE VS. TASK-RELATED TEXTURES.....	134
AGE-RELATED DIFFERENCES IN IMAGE STRUCTURE SENSITIVITY.....	136
DISCUSSION.....	139
CHAPTER 5: GENERAL DISCUSSION.....	145
LIMITATIONS AND FUTURE DIRECTIONS.....	150
APPENDICES.....	154
APPENDIX A.....	154
SUPPLEMENTARY RESULTS.....	154
EFFECT SIZES FOR BRAIN SENSITIVITY TO IMAGE STRUCTURE.....	154
COMPARISON OF MI VALUES OBTAINED WITH DIFFERENT METHODS.....	155
SUPPLEMENTARY FIGURES.....	157
APPENDIX B.....	163
SUPPLEMENTARY RESULTS.....	163
MUTUAL INFORMATION ABOUT CATEGORICAL DIFFERENCES BETWEEN FACE AND TEXTURE (OTL).....	164
REVERSE ANALYSIS (OTL).....	171
APPENDIX C.....	175
REFERENCES.....	178

TABLE OF FIGURES

CHAPTER 2

Figure 1 Age-related differences in behavioural classification images.	40
Figure 2 Behavioural modulation by eye visibility.	42
Figure 3 Group-average ERPs.....	46
Figure 4 Age-related differences in ERP information content.	48
Figure 5 Time-courses of the maximum MI across pixels.....	51
Figure 6 Onsets of afferent activity to the visual cortex.	52
Figure 7 ERP modulation as a function of eye visibility in face trials.	54

CHAPTER 3

Figure 8 Examples of stimuli.	68
Figure 9 Electrode locations.....	74
Figure 10 Behavioural results.	76
Figure 11 Age-related differences in eye sensitivity with face context present.	84
Figure 12 Age-related differences in eye sensitivity with face context absent.	86
Figure 13 MI(face/noise, ERP) at OTR.	89
Figure 14 Scatterplots of individual maximum MI, latency and 50% integration times.	90
Figure 15 Modulation of ERPs by eye visibility at OTR.....	97
Figure 16 Group-average modulation of the N170 by eye visibility at OTR.	97
Figure 17 Event-related potentials.	101

CHAPTER 4

Figure 18 Stimuli.	117
Figure 19 Electrode location.	123
Figure 20 Event-related potentials.	128
Figure 21 Categorical differences between full images.	131
Figure 22 Age-related categorical differences between textures.	133
Figure 23 Age-related differences in brain sensitivity to baseline vs. task-related textures.	135
Figure 24 Age-related differences in sensitivity to image structure.....	137

TABLE OF TABLES

CHAPTER 2

Table 1 Visual test scores.	30
Table 2 Effect size estimates for group differences in high vs. low eye visibility.	42
Table 3 Effect size estimates for group differences in N170 latency and amplitude.	44
Table 4 Effect size estimates for eye coding by the N170.	56
Table 5 Amplitude modulation by eye visibility.	56

CHAPTER 3

Table 6 Visual and cognitive test scores.	66
Table 7 Behavioural results: accuracy scores.	77
Table 8 Behavioural results: reaction times.	78
Table 9 MI(eye, RT).	80
Table 10 Condition differences in MI(eye, RT): left eye advantage.	81
Table 11 Condition differences in MI(eye, RT): effects of decreasing stimulus information available from the face.	82
Table 12 Categorical differences: maximum MI.	91
Table 13 Categorical differences: MI latency.	92
Table 14 Categorical differences: 50% integration times.	93
Table 15 Group-average N170 latency and amplitude modulation by eye visibility at OTR.	98
Table 16 Group differences in the N170 latency and amplitude modulation at OTR.	99
Table 17 N170 latency and amplitude averaged across young and older participants.	102
Table 18 Group differences in the N170.	103

CHAPTER 4

Table 19 Visual and cognitive test scores.	116
Table 20 Behavioural results: reaction times.	125
Table 21 Behavioural results: percent correct.	126

ACKNOWLEDGMENTS

First and foremost, I would like to express my thanks to my supervisor, Dr Guillaume Rousselet for the continuous support of my PhD study and related research, for his patience, kindness, always timely advice, and for sharing his immense knowledge with great enthusiasm. Thank you for helping me grow as a scientist. It has been a truly inspiring experience to work in your lab.

Besides my supervisor, I would like to thank the rest of the extended lab group I had the honour of being part of: Prof. Philippe Schyns for insightful comments and discussions, Dr Robin Ince for sharing his immense technical knowledge, Fei Yi, Hannah Gilman and Vicky Nicholls for sharing the joys of EEG, as well as students Morika Georgieva and Marsella for tremendous help with data collection. In particular, I would like to thank Dr Nicola van Rijsbergen. Nicola – thank you for being there professionally and personally, for the discussions, sharing ideas and for your words of comfort.

The work undertaken for this thesis would have been impossible without the volunteers who dedicated their time for science. I am profoundly grateful to both young and older volunteers alike, for taking the time out of their busy schedules and sometimes travelling long distances to participate in this research. The older adults' remarkable source of energy and wonderful chat kept me going through the many recording sessions. I can only hope that in my retirement I am still as energetic, motivated, curious and kind as those older adults.

I also thank my parents for their continued support, motivation and encouragement.

Dziękuję Rodzicom – za nieustające wsparcie i życzliwość oraz za to, że zawsze we mnie wierzyliście.

Last but not least, to Maciej – thank you for being with me and pushing me to keep going.

This work was supported by the BBSRC DTP (WestBio) studentship.

LIST OF PUBLICATIONS

Jaworska, K., Yi, F., Ince, R.A.A., Schyns, P.G., & Rousselet, G.A. (in prep). Processing of the same face features is delayed by 40 ms and weaker in healthy ageing. *Manuscript in preparation*.

Ince, RAA, **Jaworska, K**, Gross, J, Panzeri, S, van Rijsbergen, NJ, Rousselet, GA, Schyns, PG (2016). The deceptively simple N170 reflects network information processing mechanisms involving visual feature coding and transfer across hemispheres. *Cerebral Cortex*, 26(11), 4123-4135.

van Rijsbergen, NJ, **Jaworska, K**, Rousselet, GA, & Schyns, PG (2014). With age comes representational wisdom in social signals. *Current Biology*, 24(23), 2792-2796.

CHAPTER 1: INTRODUCTION

It is well understood that ageing is associated with differences in visual function that may have a profound impact on older adults' performance of everyday visual tasks (Owsley, 2011). For example, older adults have impaired contrast sensitivity (Owsley, Sekuler, & Siemsen, 1983; Sekuler & Hutman, 1980) and visual acuity (Gittings & Fozard, 1986), they also perform worse on a variety of perceptual tasks, including orientation discrimination (Betts, Sekuler, & Bennett, 2007), motion perception (Bennett, Sekuler, & Sekuler, 2007), contour integration (Roudaia, Bennett, & Sekuler, 2008), as well as face and object processing (Boutet & Faubert, 2006). In particular, face recognition is one of the most commonly reported difficulties in the ageing population (Boutet, Taler, & Collin, 2015). Studies show that face and facial expression recognition can be affected in addition to general functioning impairments in ageing (e.g. in memory), suggesting that face-specific factors may be subject to age-related decline (Boutet et al., 2015; Hildebrandt, Wilhelm, Schmiedek, Herzmann, & Sommer, 2011).

Evidence that faces may be processed in a qualitatively different way than other objects comes from behavioural studies, neuroimaging studies showing specialized regions for face processing (Grill-Spector, Knouf, & Kanwisher, 2004; Haxby, Hoffman, & Gobbini, 2000; Nancy Kanwisher, McDermott, & Chun, 1997), as well as neurophysiological studies showing a double dissociation between specific impairments in the recognition of faces following a lesion to the temporal lobe (i.e. prosopagnosia) and non-face objects (i.e. object agnosia). In addition, most objects are supposedly processed on the basis of their individual parts or components (features), which offers advantages such as allowing recognition of partly visible objects, or regardless of the configuration of parts (e.g. when rotated). To the contrary, it has been suggested that faces are processed in a different, more "holistic" way (Piepers & Robbins, 2012). Even though the term itself is controversial and subject to an ongoing debate regarding its exact nature, many studies have presented evidence that the recognition of faces nevertheless relies on the processing of configural information (Daphne Maurer, Grand, & Mondloch, 2002; McKone & Robbins, 2011). Configural information can refer to first-order relational properties, i.e. the basic configuration of face features – eyes above the nose, itself above the mouth; or second-order properties, i.e. variations in the spacing between and positioning of the features in individual faces (Daphne Maurer et al., 2002).

A deficit in encoding configural information has been proposed as one of the accounts of impoverished face recognition in ageing, although evidence to support this hypothesis is

mixed (for a review, see Boutet et al., 2015). On a similar note, perceptual deterioration of sensory abilities such as visual acuity or contrast sensitivity cannot fully account for an age-related impoverishment on face recognition tasks (Boutet et al., 2015). Additionally, Boutet et al. (2015) point out that a variety of stimulus manipulations and testing conditions make it difficult to compare results in the literature and obtain an understanding of processes underlying age-related deficits. As such, a comprehensive understanding of age-related deterioration on face processing, and its underlying mechanisms is still missing from the literature.

GENERAL SLOWING WITH AGEING

One of the most prevalent accounts of behavioural differences between young and older adults is that of an age-related slowing down of neural processing speed (Salthouse, 1996), broadly defined as how fast one can execute the mental operations needed to complete the task at hand (Salthouse, 2000). According to this view, a lot of age-related variance across cognitive (e.g. memory, reasoning, spatial abilities) and perceptual tasks, as well as sensory variables, such as visual acuity or auditory sensitivity is shared (Baltes & Lindenberger, 1997; Verhaeghen & Salthouse, 1997), and can be accounted for by inter-individual differences in processing speed (Salthouse & Ferrer-Caja, 2003).

The reduction in processing speed leading to cognitive impairment has been proposed to operate via two mechanisms: the limited time mechanism and the simultaneity mechanism (Salthouse, 1996). The limited time mechanism posits that relevant cognitive processes are performed too slowly to be successfully completed in the available time. In other words, if complex operations depend on the quality of information processed in simpler operations, then less information processed in simpler operations (due to slowing) will lead to impairment in higher-order cognitive processes. This mechanism would be particularly relevant in tasks requiring an external time limit or other restrictions on the time available for processing, such as the presence of concurrent task demands. It would also predict a more pronounced effect on the speed and accuracy of complex operations. According to the simultaneity mechanism, slow processing reduces the amount of simultaneously available information needed for higher level processing. Simultaneously available information, which could be indexed, for example, by some measures of working memory, might decrease in availability (quality or quantity) over time. As such, a longer time required to process the information might result in its impoverishment or degradation by the time it is needed for a higher-level operation, suggesting a cumulative effect of ageing-related slowing on higher-order tasks, or perception of higher order stimuli, or both.

Salthouse (1996, 2000) speculated about a number of neurophysiological mechanisms that could account for the age-related slowing, including loss of nerve cells or demyelination, impairment on functioning of neurotransmitters, or reduced synchronization of activation patterns across multiple neural networks. However, his theory has not been tested thoroughly because the concept of processing speed on a neural level is not unitary and may reflect activity across multiple neural networks responsible for information processing. Specifically, it is still unclear what the neural bases for the observed behavioural differences in face perception are, and at which stages of the visual processing system the ageing-related deficits first occur.

OVERVIEW OF AGE-RELATED STRUCTURAL DIFFERENCES AND CHANGES IN THE BRAIN

Postmortem studies revealed a wide range of changes that occur in the aged brain: reduced overall weight and volume, enlarged ventricles and sulcal expansion, loss of and changes to the myelin structure, loss and shrinkage of neuronal bodies in the neocortex, the hippocampus and the cerebellum, loss of dendritic spines, and others (for a review, see Raz & Rodrigue, 2006). Overall, a reduction of about 10% for the total number of neurons in neocortex was observed between the ages of 20 and 90, or about 0.18% per annum (Pakkenberg & Gundersen, 1997). However, the structural changes are not uniformly distributed across the brain but are rather a function of the brain region and cortical lamina. Ageing affects the volume changes especially in the frontal cortex and the hippocampus while, for example, the visual cortex is relatively spared (Uylings & de Brabander, 2002).

A similar pattern of results was obtained in vivo using manual volumetry of the healthy ageing brain using magnetic resonance imaging (for a review, see Raz, 2005). Across cerebral cortex, the frontal areas were associated with the greatest decline of volume in ageing, followed by the temporal cortex. Parietal and occipital cortices revealed relatively smaller differences.

Not only are brain regions affected differentially by ageing, but also the loss of gray and white matter seem to follow different trajectories across life span. Several cross-sectional studies reported that on a global level, gray matter volume decreases linearly from reaching its maximum in childhood, whereas white matter increases linearly into young adulthood, followed by a long-lasting plateau and a steady decline only in the old age (Raz, 2005). A similar trajectory of change was observed on a regional level in the brain

areas most susceptible to ageing (prefrontal and temporal cortices) – gray matter volume decreased in a linear fashion, whereas white matter followed a quadratic relationship with age, peaking in mid-40s and then declining (Bartzokis, 2001). A similar, non-linear decline in prefrontal white matter was observed in a longitudinal study over a 5-year period (Raz et al., 2005), with the deterioration beginning in the fifth decade of life.

AGE-RELATED CHANGES TO WHITE MATTER MICROSTRUCTURE

Apart from changes in the volume of gray and white matter, white matter microstructure is susceptible to the effect of ageing, and has been proposed to account for altered connectivity between brain regions (Raz, 2005). Myelin deformation and loss associated with healthy ageing has been thoroughly demonstrated both in animal models (Peters, 2002, 2009) and in humans (Marnier, Nyengaard, Tang, & Pakkenberg, 2003). Pathological changes that can compromise white matter integrity consist of accumulation of dark cytoplasm pockets that are produced by splitting of the major nerve, formation of spherical cytoplasmic cavities (“balloons”); continued production of redundant myelin so that a sheath is too large for the enclosed axon; and formation of double sheaths in which one layer of compact myelin is surrounded by another one (Peters, 2002).

In monkeys, significant losses of myelinated nerve fibers were reported in optic nerve (Sandell & Peters, 2002), the anterior commissure (Sandell & Peters, 2003), the fornix and the splenium of corpus callosum (Peters, 2009a).

Such losses of myelinated nerve fibers could result in disconnection between parts of the central nervous system and, in turn, lead to cognitive decline. For example, association between cognitive decline and myelinated nerve loss was found in monkey anterior commissure, which provides interhemispheric connections between the temporal lobes, as well as the orbitofrontal cortex and the amygdala (Peters, 2009b; Sandell & Peters, 2003).

The frequency of occurrence of myelin sheaths deformation in prefrontal cortex, splenium of the corpus callosum (Peters & Sethares, 2002) and anterior commissure (Sandell and Peters, 2003), but not in primary visual cortex (Peters, Moss, & Sethares, 2001; Peters, Moss, & Sethares, 2000) also correlate significantly with the decline in cognitive behavior that occurs with increasing age in monkeys (Peters, 2002). The reason for such an association might be that damage to myelin sheaths results in a decrease in conduction velocity along nerve fibers (Peters, 2002; Xi, Liu, Engelhardt, Morales, & Chase, 1999). This, in turn, would disrupt the timing of sequential events in

neuronal circuits and could lead to slowing of responses as occurs in older individuals (Peters, 2002; Salthouse, 1996).

A decrease in axonal conduction velocity could account for the observed age-related increase in latency of visual information processing in cortical areas V1 and V2 in old monkeys (Wang, Zhou, Ma, & Leventhal, 2005). Specifically, visual response latencies of cells in layer 4 of area V1, which receives afferent inputs from the lateral geniculate nucleus (LGN) of the thalamus and projects to the remaining layers of V1 and from there to V2, were similar in young and old monkeys and occurred at around 53 ms. Latencies recorded outside of layer 4 in area V1 were longer in senescence, and occurred at 70 ms in young, and 84 ms in old monkeys. In area V2, response latencies occurred at 82 ms in young, and at 114 ms in old monkeys. As such, visual information processing was delayed in ageing by 13 ms in V1 and by 32 ms in V2. Information also took longer to travel from area V1 to V2 (about 10 ms in young and about 20 ms in old monkeys), and the range of latencies observed in both areas was greater in old (30 ms in V1, 60 ms in V2) than in young (15 ms in V1, 30 ms in V2) monkeys indicating that intracortical information processing and the intercortical information transfer slow down during old age.

In humans, similarly to monkeys, a 27-45% decrease in the lengths of myelinated nerve fibers (Marner et al., 2003; Tang, Nyengaard, Pakkenberg, & Gundersen, 1997), or a 10% decrease per decade (Marner et al., 2003) has been observed. White matter integrity can be studied in humans by the means of diffusion tensor imaging (DTI), an MRI modality that measures the magnitude and direction of water diffusion. Diffusion anisotropy can be quantified with a number of measures, such as fractional anisotropy (FA) or apparent diffusion coefficient (ADC). In ageing, degradation of white matter typically decreases FA values and, as such, those measures can be used to quantify white matter integrity in aged adults.

In a review of DTI studies investigating white matter changes in ageing, it was reported that major reductions of FA measures occur in frontal regions of interest (ROIs) relative to more posterior ROIs (Gunning-Dixon, Brickman, Cheng, & Alexopoulos, 2009). This pattern of changes seems to be in line with the “retrogenesis” (or “last-in-first-out”) hypothesis (Bender, Völkle, & Raz, 2016; Brickman et al., 2012), which states that fibers that myelinate early in development (such as sensory cortices) are thought to be more robust than later-myelinated fibers (such as in frontal cortices) and thus might be less susceptible to age-related damage.

Recently, a study combining magnetoencephalographic (MEG) measures of neural processing speed with magnetic resonance imaging (MRI) measures of white- and gray-matter reported evidence for a direct relationship between neural slowing and brain atrophy (Price et al., 2016). Specifically, visual delay was mediated by differences in white-matter microstructure in the optic radiation, as opposed to auditory delay which was mediated by gray-matter differences in auditory cortex, suggesting dissociable effects on neural processing speed (Price et al., 2016).

STRUCTURAL CORRELATES OF AGE-RELATED COGNITIVE DECLINE

Under the hypothesis that white matter degradation with age leads to changes in conduction time, and thus in processing speed, recent studies have increasingly focused on the role of white matter as the biological basis underlying the cognitive slowing down (Eckert, 2011). For example, differences in white matter integrity in late-myelinating regions were correlated with cognitive processing speed (Charlton et al., 2006; Vernooij et al., 2008), or measures of executive functioning involving attentional set-shifting and working memory (Charlton et al., 2006; Charlton, Schiavone, Barrick, Morris, & Markus, 2010; Kennedy & Raz, 2005; Schiavone, Charlton, Barrick, Morris, & Markus, 2006). Measures of white matter degradation in the anterior limb of the internal capsule were also associated with slower reaction times in older individuals (Madden et al., 2004).

The association between white matter degradation and behavioural measures seems to be specifically restricted to the late-myelinating brain regions. For example, Lu and colleagues (2011) reported correlations between cognitive processing speed and white matter integrity in the frontal lobes and the genu of the corpus callosum, which connects the prefrontal cortices of the left and right hemispheres. On the other hand, the correlation was not significant in the splenium of the corpus callosum, which contains primarily sensory (visual) axons that tend to be fully and heavily myelinated in early childhood.

In an attempt to link white matter connectivity to age-related difficulties in visual processing, Thomas et al. (2008) studied white matter integrity along two major tracts that pass through the fusiform face area (FFA) in the fusiform gyrus, which forms part of the “core” of the distributed neural network subserving the perception of faces, along with other regions such as the occipital face area (OFA) and the superior temporal sulcus (STS) (Haxby, Petit, Ungerleider, & Courtney, 2000; Ishai et al., 2005). However, there is growing evidence of reliance on a more widespread or “extended” cortical network including the amygdala and insula, as well as the inferior frontal gyrus, which might

contribute to some aspects of face perception (Haxby et al., 2000; Ishai et al., 2005). In light of the findings that face processing may be mediated by a distributed network of feedforward, feedback, and horizontal connections between regions of the ventral visual stream and frontal cortices (Haxby et al., 2000; Ishai et al., 2005), a reduction in connectivity could have clear adverse consequences in face processing. Keeping this proposition in mind, Thomas et al. (2008) reported that age was associated with a smaller number of fibers in the inferior fronto-occipital fasciculus (IFOF), specifically in the right hemisphere. They also observed an age-related decrement in perceptual processing of visual stimuli that was larger for faces than for cars. The ability to discriminate faces was correlated with white matter integrity of the IFOF in the right hemisphere, although no statistics were reported so the association between brain and behaviour should be treated with caution. In sum, age-related deficit in the perception of faces could be due to the alteration of long-range connections between the ventral pathway and the prefrontal cortex (Thomas et al., 2008), suggesting a potential breakdown or “disconnection” in the circuitry of the neural networks mediating face perception. It is yet unclear what role the frontal cortex might play in the processing of facial information, but suggestions have been made that it might be important for perceptual decision-making (D. Maurer et al., 2007), maintaining face representations in a working memory task (Druzgal & D’Esposito, 2003), or modulating activity in the fusiform gyrus with feedback connections when perceptual difficulty increases (Platek et al., 2006; Summerfield et al., 2006). Whatever the underlying function of the frontal cortices is, current research seems to converge on an idea that increased functional activation in certain brain regions is at the same time associated with disrupted connectivity between regions (for a review, see Sala-Llonch, Bartres-Faz, & Junque, 2015), pointing out that task performance (e.g. slowing down) in young and older adults may be due to involvement of very different cortical networks.

NEURONAL RESPONSIVITY

Apart from gray and white matter losses, as well as deterioration to white matter integrity, other age-related changes can be seen on the level of neuronal responsivity to visual stimuli even in sensory cortices such as V1. For example, Schmolesky and colleagues (2000) reported significant degradation of orientation and direction selectivity in single neurons found in monkey primary visual cortex (area V1), accompanied by increased spontaneous and visually evoked activities that affected the signal to noise ratio of the responses. Less sensitivity to contrast and direction selectivity, enhanced visual response amplitudes, and higher levels of spontaneous activity were also found in V2

(Wang et al., 2005; Yu, Wang, Li, Zhou, & Leventhal, 2006) and in middle temporal visual area (MT) (Liang et al., 2010; Yang et al., 2008). In addition to a decrease in the stimulus selectivity, increased neuronal response latency was also reported in inferotemporal cortex (IT) of awake monkeys viewing images of real world objects and shapes (Csete, Bognár, Csibri, Kaposvári, & Sály, 2015). Altogether, these findings can also be related to Salthouse's (1996) theory because a lower signal to noise ratio might mean that accumulation of information in neuronal populations occurs over longer periods of time (Wang et al., 2005).

Ageing also seems to affect different visual areas in a progressive manner, in line with Salthouse's (1996) proposition that slowing at lower stages of information processing has a cumulative effect on higher stages. For example, very little age-related differences were found in the dorsal lateral geniculate nucleus (dLGN) (Schmolesky et al., 2000; Spear, 1993) compared with V1, whereas area V1 in turn was less severely affected by age than V2 (Wang et al., 2005; Yu et al., 2006) or MT (Liang et al., 2010; Yang et al., 2008). Ageing also had a greater effect on complex than simple cells within area V1 (Liang et al., 2012), suggesting that ageing effects increase along the hierarchical level of visual processing pathway. In line with this finding, longer processing times were found in old monkeys' V2 than V1 (Wang et al., 2005).

Altogether, consistent reports of decreased neuronal selectivity and increased response amplitudes to optimal, as well as non-optimal stimuli are in line with a hypothesis of an age-related degradation of inhibitory intracortical connections (Lustig, Hasher, & Zacks, 2007; Schmolesky et al., 2000) It has been proposed that inhibitory connections are mediated by the neurotransmitter gamma-aminobutyric acid (GABA), and that age may be associated with decreased GABAergic inhibition in visual cortices (Hua, Kao, Sun, Li, & Zhou, 2008; Leventhal, Wang, Pu, Zhou, & Ma, 2003; Schmolesky et al., 2000). For example, administration of GABA agonist to neurons in area V1 improved their orientation and direction selectivity, as well as decreased their peak visual response and spontaneous background activity, thereby increasing signal-to-noise ratio (Leventhal et al., 2003). On the other hand, strong effects of GABA agonist administration was only seen in some cells of monkey V1, leaving it possible that factors other than degradation of GABA-mediated inhibition may also be involved in age-related visual changes.

A recent neurocomputational model has proposed similar changes occurring in the human brain (S.-C. Li, 2005). Specifically, age-related changes to the efficacy of various neurotransmitter systems (e.g. dopaminergic, GABAergic) could reduce cortical neuron responsivity and increase neural noise, thereby resulting in less distinctive neural

representations elicited by different stimuli (Li, 2005). Some evidence for this account comes from studies using functional magnetic resonance imaging (fMRI) to study responses of specific brain regions to visual stimuli (Burianová, Lee, Grady, & Moscovitch, 2013; Park et al., 2004; Park et al., 2012; Payer et al., 2006; Voss et al., 2008a). For example, Park and colleagues (2004) reported that regions of the ventral visual cortex that in young adults responded most strongly to particular stimulus categories, such as faces or houses, became less specialized in older adults. This de-differentiation of neural responses could manifest either as an increased activation to non-preferred visual categories with little change in the response to the preferred category, or as a decrease in activation to the preferred category. Such dissociation in neural changes has been observed for faces (Park et al. 2012), where increased responses to non-preferred stimuli were observed in the fusiform face area (FFA) and decreased responses to faces were observed in the “extended” face network (Ishai, 2008; Ishai, Schmidt, & Boesiger, 2005).

Furthermore, a few studies reported that, unlike younger adults, older adults showed similar neural responses to both repetitions of the same face and different faces, thus showing no adaptation to face repetitions (Burianová et al., 2013; Lee, Grady, Habak, Wilson, & Moscovitch, 2011). Lack of adaptation suggests that different neuronal populations, which are supposed to be tuned to different identities, are responding less distinctively and have overlapping representations (*broad tuning*). In addition to broader tuning of neural responses in ventral face processing regions, ageing was also associated with increased functional connectivity between the fusiform gyrus in the right hemisphere and medial frontal cortex (Burianova et al., 2013), as well as with an additional recruitment of frontal and parietal regions (Lee et al., 2011). Such over-recruitment of brain regions in older compared with young adults could be thought to compensate for impaired activity in visual processing regions (Grady et al., 1994; Payer et al., 2006) – a phenomenon termed the ‘posterior-anterior shift with ageing’ (PASA) (Davis, Dennis, Daselaar, Fleck, & Cabeza, 2008). The suggestion that over-recruitment of brain regions is compensatory comes from several studies that show a relationship between additional recruitment of frontal brain regions and better behavioural performance in older adults (for reviews, see Grady, 2012; Grady, 2008). However, this relationship is not always present, suggesting that over-recruitment might reflect less efficient use of neural resources rather than compensation (Grady, 2008, 2012).

A distributed network of regions in parietal and prefrontal cortex has also been shown to be important for top-down control of visual perception (Bar, 2003; Gilbert & Li, 2013; Gilbert & Sigman, 2007). Top-down modulation can be thought of as any mechanism by

which cognitive influences and higher-order representations, such as attention or expectation, impinge upon earlier steps in information processing (Gilbert & Li, 2013). Such influences can have both a facilitatory effect by which neural responses to relevant stimuli are enhanced, as well as an opposite effect where suppression of irrelevant information takes place (Gazzaley, Cooney, Rissman, & D'Esposito, 2005). In an influential framework unifying perceptual and top-down factors, Gazzaley and colleagues proposed that ageing is associated with a selective deficit in the ability to inhibit irrelevant information (Gazzaley et al., 2008, 2005; Gazzaley & D'Esposito, 2007; Hasher & Zacks, 1988). In a working memory paradigm, young and older participants were asked to comply with three different instructions: Remember faces and Ignore scenes, Remember scenes and Ignore faces, and Passively view faces and scenes without attempting to remember or evaluate them. The enhancement metric was calculated as a difference between BOLD signal in visual cortex on Remember trials versus Passive view trials, whereas the suppression metric was the difference between Passive view and Ignore trials. In young adults, there was enhancement of activity associated with stimuli relevant to the task (both faces and scenes) and suppression of activity associated with those irrelevant – but only for scenes (Gazzaley et al., 2005). Older adults revealed a pronounced deficit in the suppression of irrelevant information relative to younger adults. In a follow-up study using electroencephalography (EEG), a significant age-related suppression deficit on the P1 amplitude and the N170 latency in the right hemisphere was found, in the setting of preserved enhancement (Gazzaley et al., 2008; Zanto, Toy, & Gazzaley, 2010).

AGE-RELATED SLOWING OF VISUAL PROCESSING

Altogether, changes in the myelination throughout the cortex, as well as in neuronal responsiveness in monkey cortex (possibly reflected as de-differentiation of neural responses in the human brain) are physiologically plausible as the origins of the age-related slowing-down of information processing. However, our understanding of the slowing down of visual processing speed in humans is still elusive. Recent studies employing EEG, because of its high temporal resolution that makes it possible to record neurophysiological responses to stimuli with a millisecond precision, have attempted to shed some light on this issue.

Overall, research on components thought to reflect primarily the sensory processing of visual or auditory stimuli (such as the P1, N1 and P2) presents mixed evidence for age-related deficiencies (for a review, see D. Friedman, 2011). Early sensory components seem to be consistently associated with increased amplitudes in ageing, suggesting

deficiencies in inhibitory processing (De Sanctis et al., 2008), but not necessarily with latency delays.

More specifically, comparing early responses to complex visual stimuli (e.g. faces, letters, houses) between young and older adults revealed mixed results. The first 200 ms after stimulus onset is sufficient for the visual system to elicit responses reflecting sensitivity to the higher-order content of the image, such as object category along the occipital-temporal pathway in young adults (Rousselet, Husk, Bennett, & Sekuler, 2008; VanRullen & Thorpe, 2001). Whether age affects this early processing of visual stimuli remains inconclusive. Some ageing studies reported that event-related potentials (ERPs) in the first 200 ms, in particular the N170 – an ERP component related to visual object recognition/categorization, were delayed by about 10 – 20 ms in older compared with young participants viewing images of faces (Daniel & Bentin, 2012; Gazzaley et al., 2008; Nakamura et al., 2001; Wiese, Schweinberger, & Hansen, 2008), letters (Falkenstein, Yordanova, & Kolev, 2006), and letter-number pairs (De Sanctis et al., 2008). Other studies did not find any age-related delays in the first 200 ms of processing faces (Chaby, George, Renault, & Fiori, 2003; Chaby, Jemel, George, Renault, & Fiori, 2001; Gao et al., 2009; Pfütze, Sommer, & Schweinberger, 2002) but reported ageing effects on later stages visual processing, after 400 ms (Chaby et al., 2001).

In line with this finding (Chaby et al., 2001), consistent age-related delays are observed for longer-latency components associated with higher-order processing stages (such as the N2b or P3) (D. Friedman, 2011; Polich, 1996, 1997). Accordingly, studying indices of stimulus processing, sensorimotor integration and motor-related processing revealed that age did not affect latencies of early processes associated with stimulus processing or response selection, but did affect motor response generation (Kolev, Falkenstein, & Yordanova, 2006; Yordanova, Kolev, Hohnsbein, & Falkenstein, 2004). As such, age-related behavioural slowing might not be associated with ubiquitous delays across different stages of processing but rather be both task-dependent and process-specific (Bashore, Van Der Molen, Ridderinkhof, & Wylie, 1997), therefore speaking against the theory of general slowing (Salthouse, 1996). Given the inconsistency of findings from early time-domain components, studying event-related *oscillations* (i.e. EEG responses in different frequency bands, such as theta, alpha and gamma) might prove useful for revealing specific differences in sensory processing in young and older adults (Yordanova, Kolev, & Başar, 1998). For example, Yordanova et al. (1998) found age-dependent differences in alpha (8-13 Hz) and theta (4-8 Hz) band activity in the absence of significant differences for the time-domain N1 and P2 components. Other differences due to age include a decrease in magnitude of delta (2-4 Hz) power in occipital cortex,

as well as of low- (8-10.5 Hz) and high-band (10.5-13 Hz) alpha power in parietal, occipital, temporal and limbic areas (Babiloni et al., 2006). However, not all studies show consistent age-related differences in modulations of event-related oscillations. For example, both lower and upper alpha activity, related to the sensory and motor response processing had similar modulations in young and older adults, suggesting that alterations in alpha oscillatory networks with age may depend on the stimuli applied (Schmiedt-Fehr, Mathes, & Basar-Eroglu, 2009).

Similarly, the discrepancies in the results obtained with studies focusing on early ERPs could also be due to a number of factors such as low-level stimulus characteristics, but also task demands and statistical measures used to assess group differences. More importantly, focusing analyses on ERP peaks assumes that peaks reflect interesting information about the underlying neural processes. However, peaks are ill-defined in terms of selectivity to categories and processes (Schyns, Jentzsch, Johnson, Schweinberger, & Gosselin, 2003; Smith, Gosselin, & Schyns, 2007) and there is no reason to believe that an ERP peak is equivalent to a single functional brain component (Luck, 2005). Furthermore, comparing latencies from the same peak across different age groups presumes that one peak indexes the same neuronal processes over the life span, or that it responds to the same information (Rousselet et al., 2010). However, fMRI studies cited above seem to suggest this might not hold true in ageing, in a way that other brain areas might become involved in the same task in older adults, following a de-differentiated response of the areas responsible for visual processing (Grady, 2008).

Some of these limitations have recently been overcome by adopting an innovative, component-free approach to quantify age-related differences in the time course of visual processing of faces to which phase noise was added in a parametric manner (Rousselet et al., 2009). By contrasting evoked activity in response to images of faces and textures, it was shown that visual processing speed is reduced by about 1 ms per year (Rousselet et al., 2009, 2010), despite relatively small group differences on the N170 latency (about 8 – 13 ms) (Rousselet et al., 2009). Specifically, sensitivity to image structure was spread over a longer period of time, and over two peaks on older adults – one weaker in the 100 – 200 ms time window, and one stronger after 230 ms. In contrast, young participants' image sensitivity peaked in the time window of 100 – 200 ms (Rousselet et al., 2009, 2010). These results suggested a qualitative age-related shift in visual processing of complex objects that takes place around 47 years of age (Rousselet et al., 2009), pointing to a possibility that in older adults a later time window might become functionally equivalent to the early one in young adults, and speaking against analyses restricted to ERP peaks. This delayed sensitivity was driven by the same image

parameters in both young and older participants (Rousselet et al., 2009, 2010), although older participants needed more stimulus information (i.e. stimuli with a lower noise level) to achieve the same level of behavioural performance as younger participants. The age-related delay in the speed of visual processing was replicated in an independent sample of participants (Bieniek, Frei, & Rousselet, 2013) and was independent of stimulus luminance or pupil size, suggesting that the ageing effect is due to cortical, rather than optical origin (Bieniek et al., 2013). Another interesting finding was that the largest age-related ERP differences were found for stimuli with the lowest phase coherence, i.e. textures that did not contain any meaningful information (Rousselet et al., 2009). These large evoked responses to textures occurred in the same time window as the responses to faces, i.e. around 150 – 170 ms after stimulus onset. It remained unclear whether such responses arose because of de-differentiation of neural responses in the occipital-temporal brain regions in ageing, or due to processing of textures as meaningful stimuli by older adults, or some other influence.

Despite recent advances in our knowledge of age-related slowing of visual processing of faces, we still have a limited understanding of the age-related differences in visual cortical *information* processing. This is because we need to know *what* information the brain processes and *when*, in order to understand some of the steps of the information-processing network concerned with a particular image category (Schyns, Gosselin, & Smith, 2009). This can be achieved, for example by sampling the stimulus space in a randomized but principled manner, which can be then reverse-correlated with behavioural or brain responses to reveal information diagnostic (i.e. sufficient and necessary) to the task at hand (e.g. using Bubbles) (Gosselin & Schyns, 2001). We currently begin to have some understanding of the visual information processing of faces in young adults and its underlying neural correlates (Schyns, Gosselin, et al., 2009). For example, in a face detection task, presence of the left eye is important for behavioural and electrophysiological responses alike (Rousselet, Ince, van Rijsbergen, & Schyns, 2014). Specifically, presence of the contralateral eye in the image was associated with the modulation of single-trial EEG activity in the time window of the N170, in a way that more visibility of the eye was associated with earlier and larger N170 (Rousselet et al., 2014). Information about the eye can also be associated with ERPs independent of the task (Schyns et al., 2003; Smith, Gosselin, & Schyns, 2004), and the same time window can show sensitivity to other face regions, which are important for the task, such as the mouth in emotion categorization (Schyns, Petro, & Smith, 2007). Specifically, information encoding starts well before the peak of the N170 with the eyes (Schyns et al., 2007; Rousselet et al., 2014) and ends when enough stimulus information has been

accumulated to enable successful performance on the task (Schyns et al., 2007), suggesting that a peak of the ERP component (the N170 in this case) marks the end of a cascade of processes, rather than reflecting some perceptual process itself.

The use of “bubbled” stimuli has been of great importance for identifying the features used by human and animal (Issa & DiCarlo, 2012) observers in detection and discrimination tasks. However, because images are presented through a restricted number of small apertures, which introduce substantial manipulations of these stimuli, it has been suggested that use of this technique could qualitatively alter natural face processing or affect strategies used by observers (Macke & Wichmann, 2010; Murray & Gold, 2004). For example, Bubbles could force the observer to switch to feature-based processing as opposed to perceiving the face as a whole (Neath & Itier, 2014) or attend to local cues (albeit not in a face perception task, Murray & Gold, 2004). In addition, the features returned by this method may not be those, which are predictive of human behavior under natural viewing conditions or in different tasks (Macke & Wichmann, 2010; Murray & Gold, 2004). Finally, most information about the task is achieved with the presence of enough identification errors, i.e. when behaviour is maintained at some kind of a threshold, such as 75% accuracy. Nevertheless, a recent study has shown that even when visual degradation is introduced in the stimulus, a large amount of variance in face-specific abilities can be still captured suggesting that face processing mechanisms appear to be insensitive to the visual impoverishment of the face stimulus (Royer, Blais, Gosselin, Duncan, & Fiset, 2015). Furthermore, observers’ strategies were not found to be different on expression and gender discrimination tasks compared with another reverse correlation technique using Gaussian white noise (Gosselin & Schyns, 2004). Finally, in real world sensory information reaching the eyes often *is* incomplete, as objects occlude parts of the neighbouring objects and parts of themselves, and yet our everyday object recognition does not suffer (Gosselin & Schyns, 2004; Sekuler, Gold, Murray, & Bennett, 2000). The visual systems seems to effectively treat partly occluded objects as functionally complete, although completion takes some measurable time so that recognition of partly occluded objects is achieved slower than their fully visible counterparts (Sekuler et al., 2000). Altogether, the use of Bubbles is still warranted as a method for extracting stimulus features on which the visual system can base its computations in a given task.

AIMS OF THE THESIS

Whether visual *information* processing is affected by age-related slowing down remains elusive. In this thesis, we aimed to shed light on this issue by investigating some of the

information processing steps in the ageing brain using one of the simplest perceptual tasks: face detection. We aimed to understand *what* information the brain processes when it detects a face, and *when* this information is processed with respect to the young brain. We tackled these two questions in Chapter 2 using EEG, which offers high temporal resolution, ideally suited to study fast visual processes. In order to find out what facial information is used by young and older adults alike, we employed the Bubbles paradigm which samples stimulus space in a randomized yet principled manner, and reverse-correlated the stimulus information revealed in single trials with behavioural and brain responses.

Only two studies to date used reverse correlation techniques to study age-related behavioural differences in perception of faces. One of those studies investigated mental representations of age (van Rijsbergen, Jaworska, Rousselet, & Schyns, 2014) and the other one – of trustworthiness, anger and happiness judgments (Éthier-Majcher, Joubert, & Gosselin, 2013). In both studies, noise was added to grey-scale images of faces in order to introduce systematic variability of the image parameters, and classification images were computed to understand what features drove behavioural performance. Older adults had richer representations of age across all age categories (young, middle-aged and old) suggesting a more accurate depiction of socially relevant information than younger adults (van Rijsbergen et al., 2014). Internal representations of trust, anger and happiness were very similar across young and older adults, although judgments of trust were more related to judgments of happiness in young than in older adults (Éthier-Majcher et al., 2013). No study to date, on the other hand, used reverse correlation methods in a simple face detection task, either on the behavioural or brain imaging level.

We capitalized on the findings obtained in the sample of young participants (Rousselet et al., 2014), where behavioural and brain responses in a face detection task were driven by the presence of the (contralateral) eye in the image, and aimed to apply the same tools to study visual processing of faces in a detection task in older adults. In line with the theory of slower information processing in ageing (Salthouse, 1996), we hypothesized that processing of the same information (the contralateral eye) would be delayed in ageing. Experimental findings were in line with this hypothesis by showing a 40 ms delay in processing the contralateral eye in our sample of older adults.

In a follow-up study (Chapter 3), we sought to understand whether the age-related differences in eye sensitivity were preserved in a face context, on a notion that incomplete or occluded stimuli (such as Bubbled images) might differentially affect older adults' ability to perform a perceptual task. To our knowledge, only one study to date

(Daniel & Bentin, 2012) compared ERPs from young and older participants in response to whole images of faces and inner features only (i.e. the eyes, the nose and the mouth). Results of that study indicated an age-related sensitivity to global structure of the face visible as a reduction of the N170 amplitude when the face contour was eliminated (Daniel & Bentin, 2012). Unlike that study, however, we were not interested in comparing categorical responses to whole faces and/or inner components presented in isolation, but in measuring ERP responses to the visibility of the eye revealed in a parametric manner by adding phase noise in the eye region. This way, we could investigate the modulation of ERPs by increasing information available in the eye region, when the face context was preserved (or absent – in control conditions). We found that contralateral eye sensitivity was still observed in young and older adults alike, but to a lesser degree than in our first study, suggesting that coding of the eye by the N170 acts differently when the eye is revealed through Bubble masks and when it is presented in the face context.

Finally, in Chapter 4 we were interested in investigating potential origins of the large N170 responses to textures reported already in previous studies (Rousselet et al., 2009), as well as in Chapter 2. Our hypothesis was that differences between *texture* trials could be due to a perceptual expectation effect, whereby perceiving textures in the context of different detection tasks would influence ERP responses to textures in a top-down manner. However, we found little evidence to support this notion.

In the same study, we also sought to investigate whether the age-related delay in sensitivity to image structure obtained by comparing faces and textures (Rousselet et al., 2009, 2010) would generalize to other stimulus categories, such as houses or letters. To date, only a couple of studies reported age-related latency delays in the N170 responses to visually presented letters (Falkenstein et al., 2006) or letter-number pairs (de Sanctis et al., 2008). To avoid peak measurements, we adopted a similar approach to that described by Rousselet and colleagues (2009), where we contrasted ERPs elicited by faces, houses and letters with those elicited by textures, and quantified the age-related processing delays on this difference. We found that visual processing speed was delayed to a smaller extent than that predicted by the original study (Rousselet et al., 2009) and depended on the nature of categorical comparisons made.

CHAPTER 2: PROCESSING OF THE SAME FACE FEATURES IS DELAYED BY 40 MS AND WEAKER IN HEALTHY AGEING

INTRODUCTION

The human visual system undergoes many age-related changes that lead to slower processing (Rousselet et al., 2009, 2010) and reduced neuronal selectivity (Burianová, Lee, Grady, & Moscovitch, 2013; Park et al., 2004; Park et al., 2012). In particular, several studies have shown that face processing slows down by about 1 ms per year from 20 years of age onwards (Bieniek et al., 2013; Rousselet et al., 2009, 2010). The onset of the age-related delay in processing starts around 120 ms following stimulus onset, which suggests that this effect has a cortical origin (Bieniek, Bennett, Sekuler, & Rousselet, 2015; Bieniek et al., 2013). Consistent with this observation, the N170, an event-related potential (ERP) component associated with face processing (Bentin, Allison, Puce, Perez, & McCarthy, 1996; Itier, Alain, Sedore, & McIntosh, 2007; Rousselet, Ince, van Rijsbergen, & Schyns, 2014), is delayed in older participants (Gazzaley et al., 2008; Nakamura et al., 2001; Rousselet et al., 2009; Wiese, Schweinberger, & Hansen, 2008).

Indication of reduced neuronal selectivity comes from fMRI studies showing an age-related increase in brain responses to non-preferred stimuli in visual areas that respond preferentially to one stimulus category (e.g. faces) in young adults (Park et al., 2012). Our previous studies also indicate that a similar de-differentiation of EEG responses could occur in occipital-temporal brain regions (Rousselet et al., 2009). Specifically, Rousselet and colleagues (2009) reported a prominent peak in the time window of the N170 in response to phase noise in older participants (Bieniek et al., 2015; Rousselet et al., 2009, 2010). At the same time, the peak of discriminatory activity between face and texture trials was lower in older than in young participants in the time window of the N170, suggesting that the N170 might become less face-sensitive with age (Rousselet et al., 2009). As such, evoked responses in the time window of the N170 in older adults might reflect processing of non-diagnostic information (i.e. processing of textures as meaningful stimuli and/or processing of non-diagnostic face features) unlike in young adults (Rousselet et al., 2014; Schyns et al., 2007).

Other studies also suggest an age-related decrement in the behavioural ability to use facial information in perceptual tasks. For example, older adults had a reduced ability to detect configural changes when the eye region was modified (Slessor, Riby, & Finnerty, 2013), needed more stimulus information to reach the same behavioural performance as

younger adults in face categorisation tasks (Rousselet et al., 2009, 2010), were worse at facial identity matching when faces were shown in different views (Habak, Wilkinson, & Wilson, 2008), and seemed to be less efficient in extracting task-relevant information from horizontally-filtered faces (Chaby, Narme, & George, 2011; Obermeyer, Kolling, Schaich, & Knopf, 2012). Filtered images can test the influence of particular spatial frequencies on early visual processes (Dakin & Watt, 2009; Goffaux & Dakin, 2010), but they are only an approximation of what stimulus features drive face categorization performance.

Although ageing research has identified age-related differences in behaviour and brain activity using a variety of tasks and stimuli, how the information content of brain activity changes with age remains unknown. This is because previous studies investigating age-related differences on the N170 were based on categorical responses to whole faces. To go beyond average responses to image categories and understand what facial information is associated with electrophysiological responses in the time window of the N170, it is important to introduce stimulus variability in a principled manner and link single-trial brain activity to this stimulus variability. This can be done with reverse correlation methods, for example using Bubbles (Gosselin & Schyns, 2001) to sample stimulus space on a single-trial basis.

Previously, using Bubbles we have shown that the N170 to face images in young adults is driven by the presence of the contralateral eye (Rousselet et al., 2014; Schyns, Petro, & Smith, 2007; Smith, Gosselin, & Schyns, 2004; Van Rijsbergen & Schyns, 2009). However, it is unknown what facial information is associated with ERP responses to face images in older adults and whether the observed delay in neural responses (Rousselet et al., 2009) is due to slowed information processing in older adults (Salthouse, 1996), or de-differentiation of neural responses (Park et al., 2004) that might in turn lead to processing of non-diagnostic face features and longer times necessary to accumulate visual information (Wang et al., 2005).

To fill this gap in the field, in the current study we aimed to directly test what facial information is associated with both behavioural and brain responses in older adults in a face detection task. We address this question by using a Bubbles technique coupled with reverse correlation. We aim to determine how the first step in face processing, face detection, is affected by ageing. We hypothesize that in older adults, the N170 would be mostly sensitive to the presence of the left eye in the image (similarly to young adults), but processing of this feature would be delayed.

MATERIALS AND METHODS

PARTICIPANTS

Eighteen young (9 females, median age = 23, min 20, max 36) and nineteen older adults (7 females, median age = 66, min 60, max 86) participated in the study. Results from fifteen of the young participants have been reported previously (Rousselet et al. 2014). All older adults were community dwellers, recruited through advertising at the University of Glasgow, active age gym classes, and a newspaper article. Volunteers were excluded from participation if they reported any current eye condition (i.e., lazy eye, glaucoma, macular degeneration, cataract), had a history of mental illness, were currently taking psychotropic medications or used to take them, suffered from any neurological condition, had diabetes, or had suffered a stroke or a serious head injury. Volunteers were also excluded from participation if they had their eyes tested more than a year (for older volunteers) or two years (for younger volunteers) prior to the study taking place, in order to minimise the chances that volunteers did not have knowledge of an underlying eye condition. Two older participants reported having cataracts removed, and one older participant reported having undergone a laser surgery. These participants were included because their corrected vision did not differ from that of the others. Participants' visual acuity and contrast sensitivity were assessed in the lab on the day of the first session using a Colenbrander mixed contrast card set and a Pelli-Robson chart. All participants had normal or near-normal visual acuity as measured with the 63 cm viewing distance (computer distance) chart (Table 1). Three older participants had contrast sensitivity of 1.65, and all others had contrast sensitivity of 1.95 log units. Both values fell within the normal range of contrast sensitivity for that age group (Elliott, Sanderson, & Conkey, 1990). All young participants had contrast sensitivity of 1.95 log units and above. During the experimental session, participants wore their habitual correction if needed.

Table 1 Visual test scores.

Visual acuity scores are reported for high contrast (HC) and low contrast (LC) charts presented at the 63 cm viewing distance, and expressed as raw visual acuity scores (VAS). The corresponding logMAR scores are presented below in italics, where higher values indicate poorer vision and negative values represent normal vision (logMAR score of 0 corresponds to 20/20 vision). Square brackets indicate the minimum and maximum scores across participants in each age group. Contrast sensitivity (CS) scores for young and older participants correspond to median log units across all participants in each age group.

	HC 63	LC 63	CS
young	108 [95, 110] <i>-0.16 [0.10, -0.20]</i>	99 [94, 104] <i>0.02 [0.12, -0.08]</i>	1.95 [1.95, 2.25]
older	98 [93, 105] <i>0.04 [0.14, -0.10]</i>	89 [82, 95] <i>0.22 [0.36, 0.10]</i>	1.95 [1.65, 1.95]

The study was approved by the local ethics committee at the College of Science and Engineering, University of Glasgow (approval no. FIMS00740), and conducted in line with the British Psychological Society ethics guidelines. Informed written consent was obtained from each participant before the study. Participants were compensated £6/h.

STIMULI

We used a set of 10 grey-scaled front view photographs of faces, oval cropped to remove external features, and pasted on a uniform grey background (Gold et al., 1999). The pictures were about 9.3° x 9.3° of visual angle; the face oval was about 4.9° x 7.0° of visual angle. A unique image was presented on each trial by introducing phase noise (70% phase coherence) into the face images (Rousselet, Pernet, Bennett, & Sekuler, 2008). Textures were created by randomising the phase of the face images (0% phase coherence). All stimuli had the same amplitude spectrum, set to the mean amplitude of the face images. Face and texture images were revealed through ‘bubble masks’, i.e. masks containing 10 two-dimensional Gaussian apertures (sigma = 0.36°), with the constraint that the center of the aperture remained in the face oval (Rousselet et al., 2014). Information sampling was dense enough to allow very good behavioural performance without revealing too much of the stimuli (Rousselet et al., 2014). We wrote

our experiments in MATLAB using the Psychophysics Toolbox extensions (Brainard, 1997; Kleiner, Brainard, & Pelli, 2007; Pelli, 1997).

PROCEDURE

Testing was conducted in a sound-attenuated booth. The viewing distance of 80 cm was maintained with a chinrest. Participants were tested in two experimental sessions on separate days. During each session, participants were asked to minimise movement and blinking, or blink only when hitting a response button.

In each experimental session, participants completed 12 blocks of 100 trials each. The first block was a practice block of images without bubble masks. A set of 10 face identities and 10 unique noise textures, each repeated 5 times were randomized within each block. Each session lasted about 60 to 75 minutes, including breaks, but excluding EEG electrode application.

Within a block of trials, participants were asked to categorise images of faces and textures as fast and accurately as possible by pressing '1' for face, and '2' for texture on the numerical pad of a keyboard, using the index and middle finger of their dominant hand. After each block, participants could take a break, and they received feedback on their performance in the previous block and on their overall performance in the experiment (median reaction time and percentage of correct responses). The next block started after participants pressed a key indicating they were ready to move on.

Each trial began with a small black fixation cross (12 x 12 pixels, $0.4^\circ \times 0.4^\circ$ of visual angle) displayed at the centre of the monitor screen for a random time interval of 500 to 1000 ms, followed by an image of a face or a texture presented for 7 frames (~82 ms). After the stimulus, a blank grey screen was displayed until the participant responded. The fixation cross, the stimulus and the blank response screen were all displayed on a uniform grey background with mean luminance of $\sim 43 \text{ cd/m}^2$.

EEG RECORDING AND PRE-PROCESSING

EEG data were recorded at 512 Hz using a 128-channel Biosemi Active Two EEG system (Biosemi, Amsterdam, the Netherlands). Four additional UltraFlat Active Biosemi electrodes were placed below and at the outer canthi of both eyes. Electrode offsets were kept between $\pm 20 \mu\text{V}$.

EEG data were pre-processed using MATLAB 2013b and the open-source EEGLAB toolbox (Delorme et al., 2011; Delorme & Makeig, 2004). Data were first average-referenced and detrended. Two types of filtering were then performed. First, data were band-pass filtered between 1 Hz and 30 Hz using a non-causal fourth order Butterworth filter. Independently, another dataset was created in which data were pre-processed with fourth order Butterworth filters: high-pass causal filter at 2 Hz and low-pass non-causal filter at 30 Hz, to preserve accurate timing of onsets (Acunzo, MacKenzie, & van Rossum, 2012; Luck, 2005; Rousselet, 2012; Widmann & Schröger, 2012).

Data from both datasets were then downsampled to 500 Hz, and epoched between -300 and 1000 ms around stimulus onset. Mean baseline was removed from the causal-filtered data, and channel mean was removed from each channel in the non-causal-filtered data in order to increase reliability of Independent Component Analysis (ICA; Groppe, Makeig, & Kutas, 2009). Noisy electrodes and trials were then detected by visual inspection of the non-causal dataset, and rejected on a subject-by-subject basis. On average, more noisy channels were removed from older than from young participants' datasets (older participants: median 10, min 0, max 24; young participants: median 5, min 0, max 28; median difference = 4 [2, 7]). More noisy Bubble trials were also removed from older than from young participants' datasets (trials included in analyses, older participants: median 2130, min 1987, max 2180; young participants: median 2178, min 2023, max 2198; median difference = 42 [23, 64]).

Subsequently, ICA was performed on the non-causal filtered dataset using the Infomax algorithm as implemented in the *runica* function in EEGLAB (Delorme & Makeig, 2004; Delorme, Sejnowski, & Makeig, 2007). The ICA weights were then applied to the causal filtered dataset to ensure removal of the same components, and artifactual components were rejected from both datasets (median = 4, min = 1, max = 27 for one older participant who displayed excessive blink activity; the second max was 17). Then, baseline correction was performed again, and data epochs were removed based on an absolute threshold value larger than 100 μV and the presence of a linear trend with an absolute slope larger than 75 μV per epoch and R^2 larger than 0.3. The median number of bubble trials accepted for analysis was, out of 1100, for older participants: face trials = 1069 [min=999, max=1092]; noise trials = 1067 [min=986, max=1088]; for young participants: face trials = 1090 [min=1006, max=1100]; noise trials = 1089 [min=1014, max=1098]. Finally, we computed single-trial spherical spline current source density waveforms using the CSD toolbox (Kayser, 2009; Tenke & Kayser, 2012). CSD waveforms were computed using parameters 50 iterations, $m=4$, $\lambda=10^{-5}$. The head radius was arbitrarily set to 10 cm, so that the ERP units are $\mu\text{V}/\text{cm}^2$. The CSD

transformation is a spatial high-pass filtering of the data, which sharpens ERP topographies and reduces the influence of volume-conducted activity. CSD waveforms also are reference-free.

ELECTRODE SELECTION

Detailed analyses were performed on a subset of electrodes. The set of electrodes consisted of four posterior midline electrodes that have been previously shown to be sensitive to face features or conjunction of features: from top to bottom CPz, Pz, POz, Oz (Rousselet, Ince, van Rijsbergen, & Schyns, 2014; Schyns, Thut, & Gross, 2011). However, we report the results only from the Oz electrode because the other three showed weak mutual information values across the two groups. We also selected two posterior-lateral electrodes, one in the right hemisphere (right electrode, RE), and one in the left hemisphere (left electrode, LE). These electrodes were selected by measuring the difference between all bubble face trials and all bubble noise trials at all posterior-lateral electrodes, squaring it, and selecting the left and the right electrodes that showed the maximum difference in the period 130-250 ms. The selected lateral electrodes were P7/8, or PO7/8, or their immediate neighbours, which are electrodes typically associated with large face ERPs in the literature.

STATISTICAL ANALYSES

Statistical analyses were conducted using Matlab 2013b and the LIMO EEG toolbox (Pernet et al., 2011). Throughout the paper, square brackets indicate 95% confidence intervals computed using the percentile bootstrap technique, with 1000 bootstrap samples. Unless otherwise stated, median values are Harrell-Davis estimates of the 2nd quartile (Harrell & Davis, 1982).

MEASURES OF EFFECT SIZE

We estimated the size of the between-group differences using two robust techniques: Cliff's delta and the median of all pairwise differences. Cliff's *delta* (Cliff, 1996; Wilcox, 2006) is related to the Wilcoxon-Mann-Whitney U statistic and estimates the probability that a randomly selected observation from one group is larger than a randomly selected observation from another group, minus the reverse probability. Cliff's *delta* ranges from 1 when all values from one group are higher than the values from the other group, to -1 when the reverse is true. Completely overlapping distributions have a Cliff's *delta* of 0. In line with Cliff's delta approach, we also calculated all pairwise differences between young and older participants on the measures of interest (reaction times, percent corrects, N170 latencies and amplitudes), and took the median of the distribution of these differences. This way of measuring effect sizes enabled us to provide information about the typical difference between any two observations from two groups (Wilcox, 2012).

MUTUAL INFORMATION

We used mutual information (MI) to quantify the dependence between stimulus features and behavioural and brain responses. MI is a non-parametric measure that quantifies (in bits) the reduction in uncertainty about one variable after observation of another and has been used to study the selectivity of neural and behavioural responses to external stimuli (Ince, Petersen, Swan, & Panzeri, 2009; Magri, Whittingstall, Singh, Logothetis, & Panzeri, 2009a; Panzeri, Brunel, Logothetis, & Kayser, 2010; Schyns et al., 2011). The advantage of using the MI lies in its ability to detect associations of any order, whether linear or non-linear (for a more extensive evaluation, see Rousselet et al., 2014). We calculated MI from the standard definition (Ince et al., 2009), using the following formula:

$$I(B_i; R) = \sum_{b,r} P(b,r) \log_2 \frac{P(b,r)}{P(b)P(r)}$$

Where B_i represents the bubble mask value (pixel visibility) at pixel i and R represents the response of interest (either behavioural or EEG recording). $P(b)$ is the probability of pixel i having bubble mask falling inside bin b (of the 3 equiprobable bins, as using 3 bins yielded best results, Rousselet et al., 2014); $P(r)$ is the probability of the considered response falling inside bin r , and $P(b,r)$ is the joint probability of the coincidence of both events. $I(B_i; R)$ quantifies the reduction of uncertainty about the behavioural/neural response that can be gained from knowledge of the visibility of pixel i .

Here, we calculated several MI quantities in single participants: MI(PIX, RT) to establish the relationship between image pixels and reaction times; MI(PIX, CORRECT) to establish the relationship between image pixels and correct responses; MI(PIX, RESP) between pixels and response category; and MI(PIX, ERP) to establish the relationship between image pixels and ERPs. These quantities were computed separately for face and noise trials. To control for the variable number of trials in each participant arising as a result of EEG preprocessing, we scaled every MI quantity for every participant by a factor of $2N/n2$ (Ince, Mazzone, Bartels, Logothetis, & Panzeri, 2012), using the formula:

$$MI_{scaled} = MI \times 2 \times Nt \times \log_2,$$

where MI refers to mutual information values, and Nt is the number of trials. MI_{scaled} , therefore, reflects a measure of MI adjusted for a systematic upward bias in the information estimate that might arise due to limited data sampling, especially if the numbers of trials in the two age groups are systematically different. All group-difference analyses were performed using the scaled MI values.

MUTUAL INFORMATION: CONTINUOUS APPROACH

The binning approach described above can be sensitive to the problem of limited sampling bias. As such, we computed a new estimator of MI that can be used with continuous variables (Ince, Giordano, et al., 2016) and utilizes the concept of copulas (Nelsen, 2007), statistical structures that express the relationship between two random variables, independently of their marginal distributions.

In single participants, we calculated MI between visibility of the left eye (a scalar value obtained as a sum of pixel visibility within the circular left eye mask on each trial) and EEG voltage over the time period of -300 ms before to 1000 ms after stimulus onset. We also computed the temporal gradient of the EEG voltage (dEEG) on each trial in order to account for the temporal relationship between neighbouring time points, and then combined the EEG voltage and its temporal gradient into a bivariate response (*gradient MI*, see Table S1 in Appendix A). We then calculated the time course of MI about the eye visibility in the bivariate response: MI(eye, [EEG dEEG]). Considering the gradient response together with the voltage smoothes out the artifactual dips in MI time courses, occurring at time points of zero-crossings when EEG voltages change the sign. It also introduces information about the shape of the ERP, otherwise missing from just considering instantaneous amplitudes. As such, the bivariate time course provides a clearer picture of the time window(s) over which the EEG signal is modulated by the

changing stimulus (Ince, Giordano, et al., 2016). However, this analysis yielded group differences comparable to those obtained with the binning method (Table S1 in Appendix A). As such, the binning method was sensitive enough to provide a good description of age-related differences in eye coding.

MUTUAL INFORMATION: CLASSIFICATION IMAGES

We refer to MI between pixels and behaviour or ERPs as classification images: they reveal the image pixels associated with modulations of the responses. Classification images for the MI(PIX, ERP) analysis were computed at every time point within the first 400 ms following stimulus onset, using the non-causal and causal-filtered datasets, and at each of the 6 electrodes specified above. To provide a summary of the image pixels associated with the ERP distributions for every participant at every electrode, we saved the maximum MI across time points in the non-causal filtered dataset.

Single-subject analyses. In order to establish which parts of the classification image showed significant association with the behavioural performance or ERPs in face and noise trials, we performed a permutation test coupled with the Threshold-Free Cluster Enhancement (TFCE) technique (Smith & Nichols, 2009) on individual participants' data. First, the MI values were computed between the bubble masks and the response labels. The resulting classification images were then transformed with the TFCE technique. This technique boosts the height of spatially extended regions in the image without changing the location of their maxima. As such, clustered pixels will get much higher TFCE scores than individual ones, which combined with standard permutation testing alleviates the problem of multiple comparisons across many pixels (Pernet, Latinus, Nichols, & Rousselet, 2015; Rousselet et al., 2014; Smith & Nichols, 2009). TFCE parameters were $E=1$ and $H=2$. To estimate TFCE scores expected by chance, the trial labels were shuffled while keeping the bubble masks constant. The MI values were then computed and TFCE-scored again. This procedure was performed 1000 times. On every iteration of the permutation test, we saved the maximum TFCE value across pixels in order to create a distribution of TFCE values under the null hypothesis that the variables (pixel MI values and behavioural or ERP responses) are statistically independent. To obtain the image pixels associated with the response at the significance level of 0.05, the original TFCE scores were then compared against the 95th percentile of the permutation distribution. Following this analysis, data from two participants: one older and one young were excluded due to flat mutual information maps, resulting in a sample size of 17 young and 18 older participants.

Group analyses. In order to assess classification image differences between the two age groups, we first computed Cliff's *delta* on the MI values at every pixel separately. Similarly to the single-subject analyses, we then applied a permutation test in order to assess the statistical significance of these differences. However, instead of shuffling trial labels, we shuffled younger and older participants' labels while keeping the classification images constant. Then, we computed Cliff's *delta* on permuted classification images and saved the maximum *delta* score. This procedure was performed 1000 times in order to obtain a distribution of maximum *delta* scores under the null hypothesis that there are no differences in the classification images of the two age groups. We then compared the original *delta* scores against the 95th percentile of the permutation distribution.

Feature-of-interest analyses. We quantified how the presence of the eyes modulated behavioural and brain responses by averaging MI values inside an eye mask. To create the mask, we centred a circle (radius = 15 pixels) on the pixel that showed the maximum MI value in the group-averaged MI(PIX, ERP) classification image, separately for the left and for the right eye (as seen by the observer in the picture plane).

ERP ONSET ANALYSES

We quantified ERP onsets using the causal-filtered datasets. To control for multiple comparisons, we used a bootstrap temporal clustering technique as implemented in LIMO EEG (Pernet et al., 2015; Pernet et al., 2011).

ERP_{STD} onset. In order to determine whether age-related differences in timing of MI accumulation reflect differences in the onset of afferent activity to the visual cortex or information accumulation at later stages of visual processing, we looked at the time course of the standard deviation across electrodes of the mean ERP (ERP_{STD}). ERP_{STD} provides a compact description of the global ERP response, summarizing each participant's evoked brain activity across electrodes in one vector. This analysis was based on the notion that early visual activity can be characterized by a sudden increase in standard deviation of the mean ERP across electrodes. We computed the ERP_{STD} time course, and subtracted mean baseline from it in each individual participant. Then, we localised the first peak whose minimum height was five times the height of any peak in the baseline. Then, using ARESLab toolbox (Jekabsons, 2015), we built a piecewise-linear regression model with three basis functions using the Multivariate Adaptive Regression Splines (MARS; Friedman, 1991) method.

MI onset. We quantified MI onsets using the same technique as with ERP_{STD} onsets.

TOPOGRAPHIC ANALYSES

Topographic maps for each participant were computed from the whole-scalp MI(PIX, ERP) results at the individual MI peak latency. Individual topographic maps were normalised between 0 and 1, interpolated and rendered in a 67 x 67 pixel image using the EEGLAB function *topoplot*, and then averaged across participants in each age group. Using the interpolated head maps, we then computed a hemispheric lateralisation index for each participant. First, we saved the maximum pixel intensity in the left and the right hemisphere (lower left and right quadrants of the interpolated image), excluding the midline. Then, we computed the lateralisation index in each group as the ratio $(MI_{\text{left}} - MI_{\text{right}}) / (MI_{\text{left}} + MI_{\text{right}})$.

RESULTS

BEHAVIOURAL RESULTS

On average, older participants were less accurate and slower than younger participants. Mean percent correct was 82% [80, 85] in older participants, 93% [92, 94] in younger participants, group difference = -11 percentage points (PP) [-14, -8]. The group median of individual median reaction times (RT) was 576 ms [527, 604] in older participants, and 378 ms [349, 401] in young participants; group difference = 198 ms [148, 237].

On face trials, young participants were on average 91% correct and older participants were on average 75% correct (group difference = 15 PP [8, 19]). On noise trials, young participants were 96% correct and older participants were 92% correct (group difference = 4 PP [1, 13]). A larger group difference in percent corrects for face trials might suggest that older participants were more conservative on face trials, i.e. responded 'face' less often when there was a face, and there was a small interaction between trial type and age group (group difference of face-noise difference = 7 PP [0, 15]).

Both groups were also less accurate on Bubble trials compared with practice trials (difference_{bubble-practice}, young: -4 PP [-6, -3]; older: -15 PP [-18, -11]), with average accuracy in each group reaching 98% [97, 98] on practice trials. The difference was significantly larger in older than in young participants (group difference: -11 PP [-14, -7]).

Previously, Rousselet et al. (2014) showed that the presence of the left eye as seen by observers in the picture plane (hereafter, the left eye) was strongly associated with faster reaction times in a group of young participants. Here, we extend these results by showing that the RTs of almost all (N = 16/18) older participants, and all (N=17/17) young participants were modulated by the presence of the left eye (Figure 1A-B, top panel). The left eye region was also involved in modulating RTs in noise trials in a few older participants (N = 3), but the relationship was weak. The presence of right eye pixels influenced RTs in a few young and a few older participants (Figure 1B, top panel).

Pixels in the eye region were also strongly associated with correct responses in almost all older participants (N = 16, Figure 1A-B, third panel). In contrast, the association between the eye region and correct responses was significant in only a few young participants (N = 4). This suggests that whereas young participants correctly detected faces on the basis of any feature, older observers needed to see the eye region to be accurate. We confirmed this dissociation by directly comparing the average classification images between the two groups. Relative to young participants, older participants relied significantly more on the eyes (third panel, Figure 1C) in making accurate judgments. However, despite a slightly stronger mean MI across older participants, there was no

significant difference between the two groups in the effect of the presence of the left eye on reaction times (first panel, Figure 1C). None of these effects were observed for noise trials.

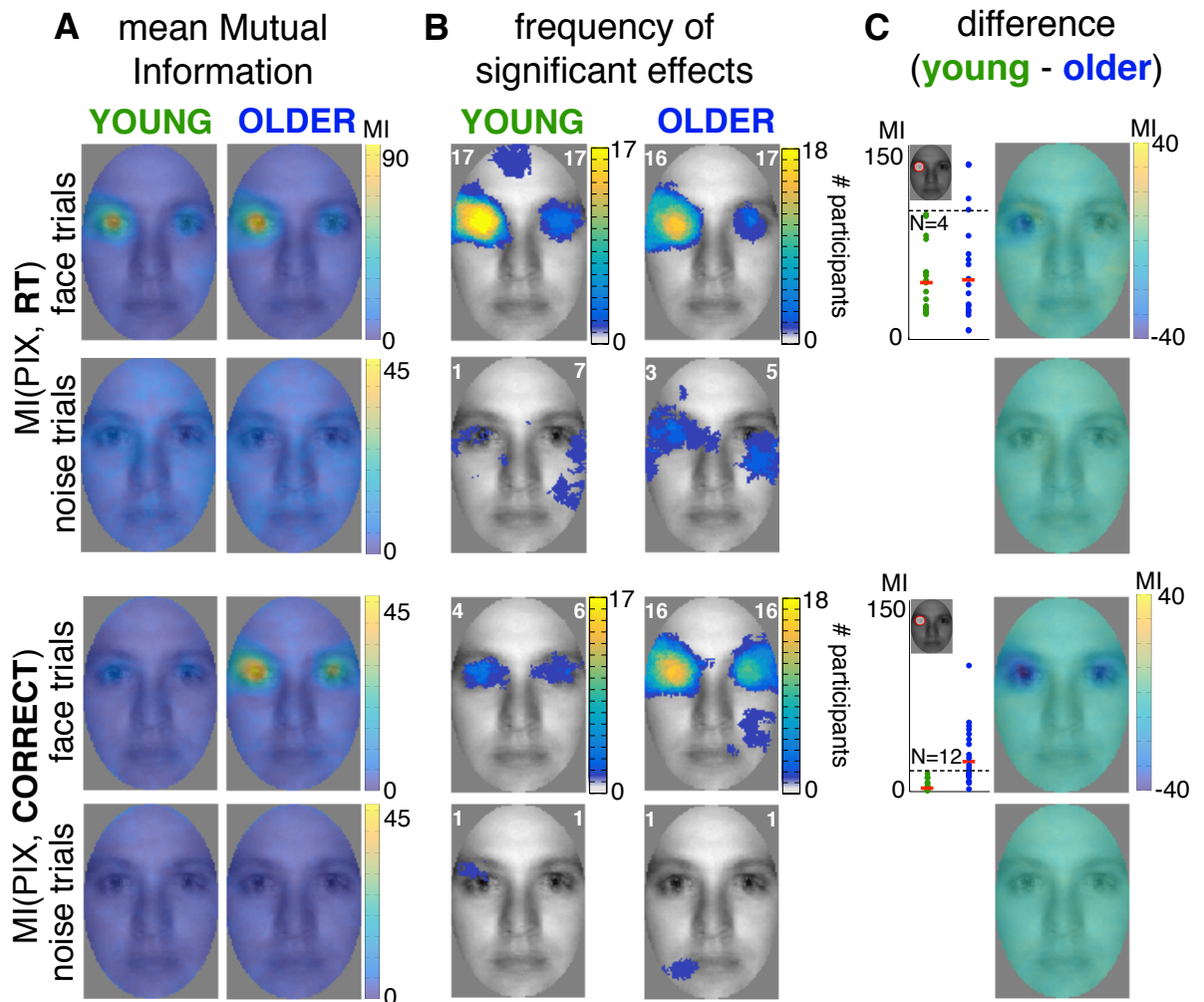


Figure 1 Age-related differences in behavioural classification images.

(A) Group-average MI maps for young and older participants. Each row corresponds to one analysis condition. The maximum average MI on face trials was stronger in the RT condition than in the CORRECT condition for both age groups, and is therefore presented on a different scale. **(B)** Number of participants showing significant effects. The white number in the left upper corner of every image corresponds to the maximum number of participants showing a significant effect at the same pixel, whereas the number in the right upper corner corresponds to the total number of participants showing significant effects at any pixel. **(C)** Differences in MI between young and older participants. Scatterplots show individual MI values averaged within the left eye mask (represented as a red circle in the face inset; for explanation, see *Methods*). Red bars correspond to medians across participants. Distributions of individual MI values were different between the groups for correct responses, with 12 older participants (and 4 older participants in the RT condition) showing stronger MI than the maximum MI across all young participants. Images on the right display the differences between young and older average MI maps for every condition.

We established that the presence of the eye(s) was associated with different behavioural responses across the two age groups. Using a reverse analysis (Rousselet et al., 2014), we then quantified by how much changing the information about the eyes would influence participants' behaviour. To this end, we first defined circular masks (radius = 15 pixels) for the left eye and the right eye. We then correlated single-trial Bubble masks with each eye mask, to provide an estimate of eye pixel visibility. We then split these correlations into ten equally populated bins ranging from the lowest to the highest correlation values. Next, we quantified the effect of eye visibility on behavioural judgments by calculating the RT and percent correct difference between the 10th and the 1st bin (Figure 2).

In our group of young observers, high left eye visibility led to, on average, 53 ms [45, 61] faster and 15 percentage points (PP) [10, 20] more accurate responses; when the right eye was present participants were 17 ms [10, 24] faster and 7 PP [4, 11] more accurate.

These effects were even stronger in older participants: they were 91 ms [68, 114] faster and 37 PP [25, 48] more accurate when the left eye was visible, and 16 ms [2, 30] faster and 28 PP [19, 36] more accurate when the right eye was visible (for effect sizes of group differences, see Table 2 and Figure 2).

All participants were generally faster and more accurate on trials where higher correlation between one or both eyes and Bubble mask visibility was observed (for detailed results, see Figures S1 – S5 in Appendix A). However, even when there was no eye visibility on any given trial, young participants were still able to discriminate face images from noise images above chance (median: 72%, min: 56%, max: 92%). On the other hand, older participants performed well below chance on trials without eye visibility, with only two older participants performing similarly to an average young participant (median: 31%, min: 9%, max: 94%).

In sum, here we show that in a face detection task, older participants use the same facial feature (the left eye) as young participants to make fast responses. However, whereas young participants can use any face feature to make a correct response, older observers rely predominantly on the eyes to do the same task. Both in reaction times and accuracy scores, the eye information revealed through the Bubble apertures modulates responses to a higher extent in older than in young participants. This suggests a different strategy in older observers, who use the presence of the eyes more to detect a face.

Table 2 Effect size estimates for group differences in high vs. low eye visibility.

Values correspond to differences in RT (expressed in milliseconds) and percent correct (percentage points). Values correspond to the median of all pairwise differences between each young and every older participant. A corresponding Cliff's *delta* is shown in italics. Square brackets indicate 95% confidence intervals.

	Accuracy scores		Reaction times	
	Face trials	Noise trials	Face trials	Noise trials
Left eye	-21.3 [-30.5, -10.3] <i>-0.71 [-0.93, -0.44]</i>	1.9 [-0.3, 3.8] <i>0.37 [-0.02, 0.70]</i>	40.6 [19, 60.3] <i>0.71 [0.41, 0.94]</i>	4.9 [-7.4, 13.2] <i>0.16 [-0.23, 0.54]</i>
Right eye	-19.2 [-26, -10.1] <i>-0.73 [-0.94, -0.44]</i>	4.0 [0.9, 6.7] <i>0.50 [0.12, 0.82]</i>	-2.5 [-16.2, 9.8] <i>-0.08 [-0.49, 0.31]</i>	11.2 [-7.9, 27.2] <i>0.25 [-0.17, 0.62]</i>

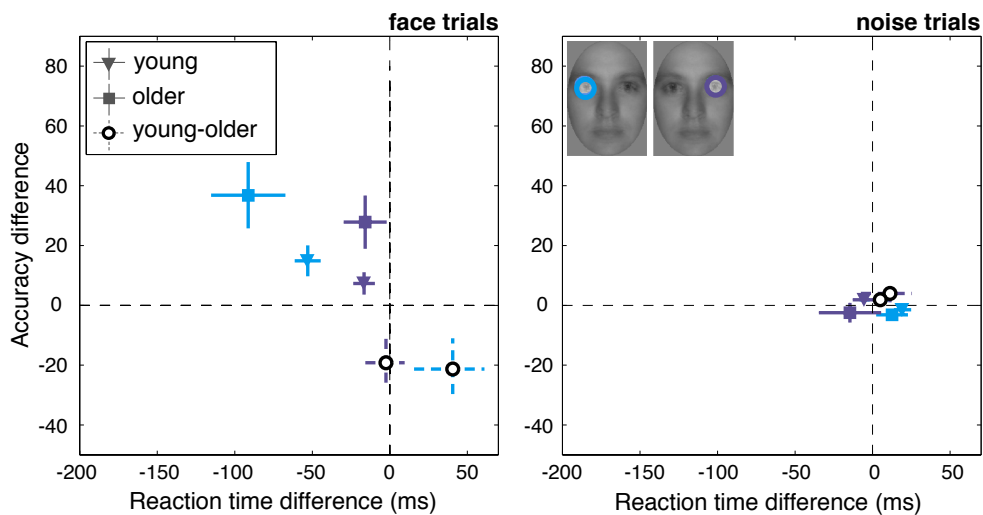


Figure 2 Behavioural modulation by eye visibility.

Each point corresponds to the difference between high and low visibility of the left (blue) and the right (purple) eye, separately for young (triangles) and older (squares) participants, and for face (left panel) and noise (right panel) trials. Median accuracy score and around median reaction time differences are marked with vertical and horizontal lines, respectively. Group differences (empty circles and dashed CI lines) show stronger modulation of accuracy scores by the presence of each eye in older participants, as well as stronger RT modulation by the presence of the left eye.

EVENT-RELATED POTENTIALS

We started by comparing the amplitude and latency of the N170 between the two age groups (Figure 3). We computed mean ERPs across trials for each participant, separately for face and noise trials, and for practice (without Bubbles) and regular (with Bubbles) trials. For ERPs recorded at the lateral-occipital electrode in the right hemisphere (RE), we then computed the N170 latency for individual participants as the latency of the minimum ERP in the time window of 110-230 ms following stimulus onset, and its corresponding amplitude.

We found a strong age difference in the amplitude difference between face and noise practice trials: the ratio of older to young participants' amplitude difference between face and noise trials was, on average, 33% (difference: $0.34 \mu\text{V}/\text{cm}^2$ [0.15, 0.48]; Table 3). There was no significant age difference on the N170 amplitude in practice face trials (difference: $0.09 \mu\text{V}/\text{cm}^2$ [-0.12, 0.24]). Rather, the effect was driven by the difference in practice noise trials: older participants' ERPs were much larger than those of young participants (difference: $0.45 \mu\text{V}/\text{cm}^2$ [0.26, 0.66]).

The N170 latencies in older participants were also significantly delayed compared with young participants: by 18 ms [9, 24] in practice face trials, and by 23 ms [9, 38] in practice noise trials. The age-related delay was similar across faces and noise textures (interaction between age and stimulus category = 6 ms [-3, 16]).

In trials with Bubbles, latencies in older participants were delayed similarly to practice trials: by 22 ms [10, 32] in face trials, and by 18 ms [7, 31] in noise trials.

However, due to sampling of face information on each trial our Bubble trials reflect a mixture of conditions that are not comparable to full faces. Therefore, comparing mean ERPs in practice and Bubble trials is not meaningful. As such, we ran a Mutual Information (MI) analysis in order to investigate how ERPs *varied* according to what stimulus information was revealed through Bubble apertures on a single trial level.

Table 3 Effect size estimates for group differences in N170 latency and amplitude.

Effect size estimates for group differences (young – older) in N170 latency (LAT; expressed in milliseconds) and amplitude (AMP; expressed in $\mu\text{V}/\text{cm}^2$). Values correspond to the median of all pairwise differences between each young and every older participant. A corresponding Cliff's *delta* is shown in italics. Square brackets indicate 95% confidence intervals.

Face	Noise	Face-Noise
Trials without Bubbles		
N170 LAT		
-18 [-24, -9]	-23 [-39, -9]	6 [-3, 16]
<i>-.64 [-.91, -.32]</i>	<i>-.51 [-.82, -.16]</i>	<i>.27 [-.13, .62]</i>
N170 AMP		
.09 [-.12, .24]	.45 [.24, .64]	-.34 [-.48, -.15]
<i>.16 [-.24, .51]</i>	<i>.74 [.46, .95]</i>	<i>-.78 [-.96, -.54]</i>
Trials with Bubbles		
N170 LAT		
-22 [-32, -9]	-18 [-33, -6]	-2 [-8, 3]
<i>-.59 [-.86, -.26]</i>	<i>-.52 [-.82, -.20]</i>	<i>-.13 [-.50, .26]</i>
N170 AMP		
-.18 [-.37, .03]	-.04 [-.18, .13]	-.15 [-.24, -.05]
<i>-.32 [-.65, .07]</i>	<i>-.11 [-.50, .26]</i>	<i>-.62 [-.85, -.34]</i>

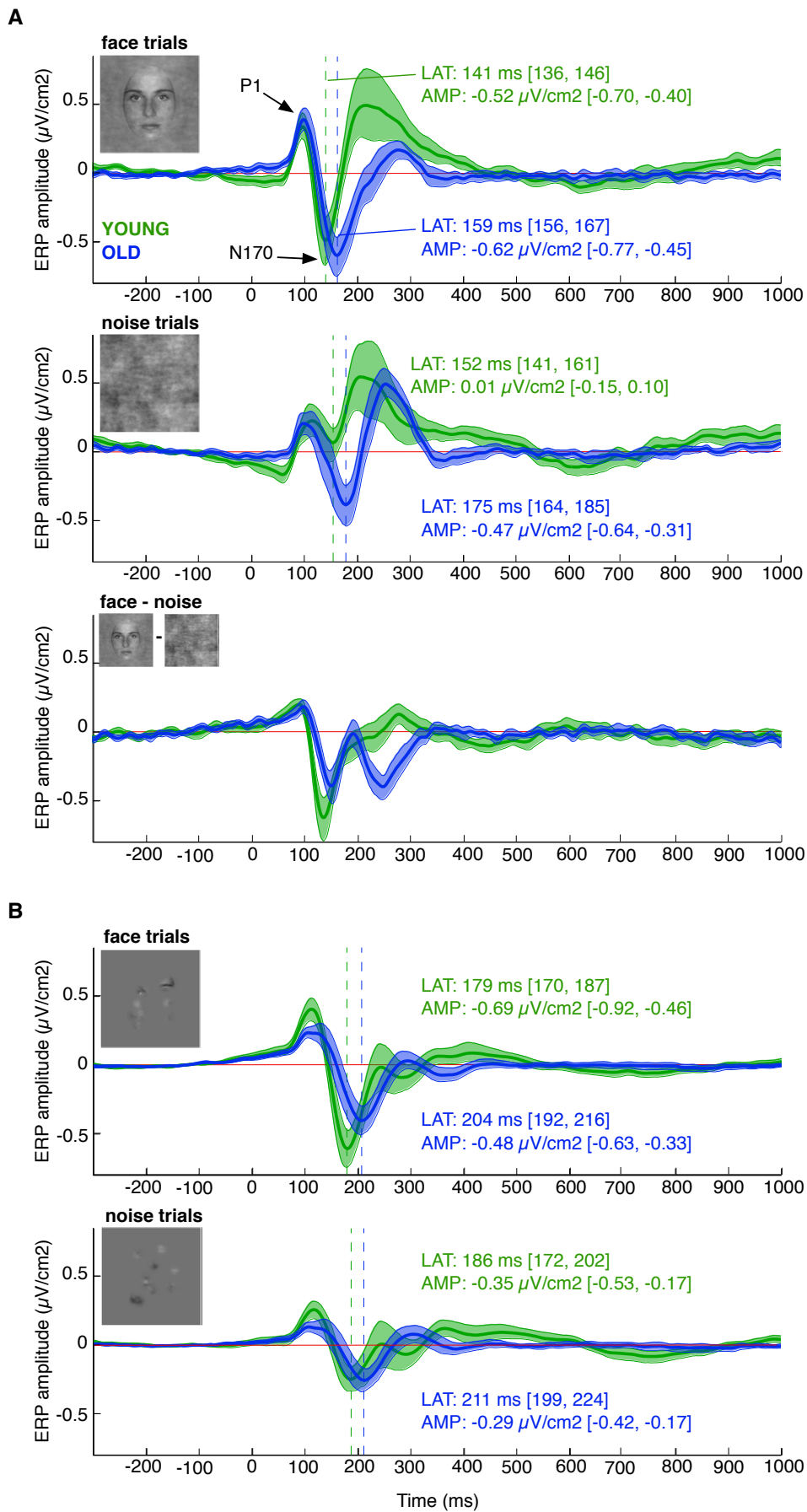


Figure 3 Group-average ERPs.

Group-average ERPs in young (green) and older (blue) participants, for face and noise trials. **(A)** Average ERPs calculated for practice trials (without Bubble masks). **(B)** Average ERPs for trials with Bubble masks. Values reported in the subplots correspond to median latencies and amplitudes of the N170 component.

BRAIN INFORMATION CONTENT

To reveal the stimulus features that modulated electrophysiological responses in each age group, we quantified MI between pixels and ERP responses at three electrodes of interest: lateral-occipital electrodes over the left (LE) and the right (RE) hemisphere, and a midline occipital electrode (Oz, Figure 4). We found that in both groups, single-trial ERPs at lateral posterior electrodes were mostly modulated by pixels in the contralateral eye area: the left eye region was associated with ERPs recorded at the right electrode, and the right eye region was associated with responses at the left electrode. However, this association was weaker and delayed in older participants.

At the left electrode (LE, Figure 4A, top panels), the group-average MI tended to cluster around the right (contralateral) eye. This effect was weaker in older participants and significant in a smaller number of older than young participants (Figure 4B, top panels). There was also some weak sensitivity to the left (ipsilateral) eye region in a few young participants. Sensitivity to each eye region was significantly stronger in young than in older participants (Figure 4C, top panels). To quantify the group effect, we averaged MI within the circular eye mask in each participant separately (see Figure 4 caption) and computed Cliff's *delta* on the median difference between young and older participants. There was a large effect size for the group difference in MI: Cliff's *delta* = 0.58 [0.21, 0.81].

There was no sensitivity to any image features in noise trials for either young or older participants, suggesting that MI found in face trials was not due to spatial attention. No sensitivity in noise trials also suggests that elevated amplitudes of the N170 to textures in older participants do not reflect any functional processing.

At the right electrode (RE, Figure 4A, middle panels), group-average MI was maximal in the region surrounding the contralateral (left) eye area in both young and older participants. It was, on average, significantly stronger across young compared with older participants (Figure 4C, middle panels). There was also a large effect size for the group difference in MI: Cliff's *delta* = 0.57 [0.19, 0.80]. The association between the presence

of the contralateral eye and ERPs was also somewhat stronger at RE than at LE, in line with the right-hemispheric preference for face processing.

The midline electrode (Oz, Figure 4A, bottom panels) showed generally weaker MI values than the lateral-posterior electrodes, and sensitivity to various face features (eyes, chin, mouth, nose, and forehead) in some participants in both age groups. Comparison of the MI values revealed stronger sensitivity to the right eye in young participants (Figure 4C, bottom panels). On the other hand, older participants had greater sensitivity to the forehead area. Additionally, on noise trials, one young and three older participants showed some sensitivity to face areas suggesting a low-level response to stimulation at this electrode (Rousselet et al., 2014).

We made sure not to miss any effects by computing the classification image for the MI(PIX, ERP) across all electrodes, which showed sensitivity to the left eye region in both young and older participants (Figure S6 in Appendix A).

Altogether, both in young and older participants, brain activity was mostly associated with the presence of the eyes at lateral electrodes, and with the presence of the eyes as well as other facial features at the midline electrode. Similarly to behavioural results, the same features were associated with ERP responses across groups. This association, however, was considerably stronger in young participants.

of the image shows individual MI values averaged within the right eye mask (for the left electrode), or the left eye mask (for the right electrode). The number in each scatterplot corresponds to the number of young participants whose MI values were greater than the maximum MI value across older participants (marked as a black dashed line). The image on the right displays the difference between average young and older MI maps for every condition.

TIME COURSE OF INFORMATION PROCESSING

Knowing what face areas were mostly associated with brain activity, we then investigated how this relationship unfolds over time. We found that processing of the same facial information was delayed by 40 ms in older participants compared to young participants.

To obtain the time courses of information processing, we saved the maximum MI across all pixels in the classification image computed at every time point, and then compared these time courses between age groups (Figure 5B). We observed a significant delay of 40 ms in MI peak latencies in older compared to young participants at both lateral electrodes (CI of the median difference in ms = [28, 65] at LE, [23, 57] at RE). At LE, MI peaked at 166 ms [159, 175] in young and at 205 ms [195, 241] in older participants (Figure 5B, top panel). At RE, peak latencies occurred at 164 ms [158, 168] in young, and 204 ms [184, 221] ms in older participants (Figure 5B, middle panel).

Using a measure similar to Rousselet et al. (2009, 2010), we found that it took older participants 23 ms [14, 33] more to integrate 50% of their MI time course at RE (median, young = 180 ms [174, 187]; older = 204 ms [197, 211]), and 25 ms [9, 38] at LE (median, young = 183 ms [172, 200]; older = 205 ms [201, 214]).

As expected from the classification image analysis, the MI peak was significantly smaller across older participants at both lateral electrodes. At LE, the peak MI amplitude in older participants was about 58% [36, 89] that of young participants, and 57% [42, 82] at RE.

MI peaked shortly before the peak of the N170 at both lateral electrodes in young participants (LE: 10 ms [4, 24]; RE: 8 ms [0, 16]), similarly to what was reported in Rousselet et al. (2014). This relationship, on the other hand, was not present across older participants (LE: 0 ms [-31, 8]; RE: 5 ms [-4, 18]).

We made sure not to miss any local maxima of information by plotting maximum MI across pixels and all electrodes in both young and older participants. The time courses

were very similar to those obtained for the displayed electrodes (Figure S6 in Appendix A).

Further evidence that we did not miss group effects which might have been localised in different brain regions in the two groups came from running a multivariate MI on all electrodes in each group. Comparing the maximum MI and its latency between young and older participants revealed similar results to those obtained with the electrodes of interest (see Table S1 in Appendix A).

Using the whole-scalp MI results, we found that MI was maximum at posterior-lateral electrodes in both groups (Figure 5C). MI tended to be more right-lateralised across older participants (lateralisation index for face trials = -0.18 [-0.31, -0.05] in young, -0.23 [-0.37, -0.09] in older participants). The group difference was not significant (young-older = 0.07 [-0.07, 0.21]).

In order to understand when the ageing differences in MI first occurred, we quantified MI onsets using causal-filtered data (Figure 5A). The median onsets were 129 ms in young participants at LE [109, 149], and 137 ms [128, 146] at RE. In older participants, MI onsets occurred slightly later: at 154 ms [137, 172] at LE, and at 151 ms [138, 164] at RE. Onsets of MI were significantly delayed by 25 ms [-46, -5] in older than in young participants only at LE. Although MI onsets were also delayed by 13 ms [-24, 1] in older participants at RE, the group difference was not significant.

There was also no significant difference in MI peak latencies (group difference: 3 ms [-13, 19]) between groups at the midline electrode: the latencies were observed at 162 ms [154, 180] in young and 154 ms [148, 172] in older participants (Figure 5B, bottom panel). Peak amplitude in older observers was 100% that of young participants (amplitude difference = -0.1 [-14, 14] units).

There were also no differences in group effects after computing MI using different methods (see Supplementary Results in Appendix A).

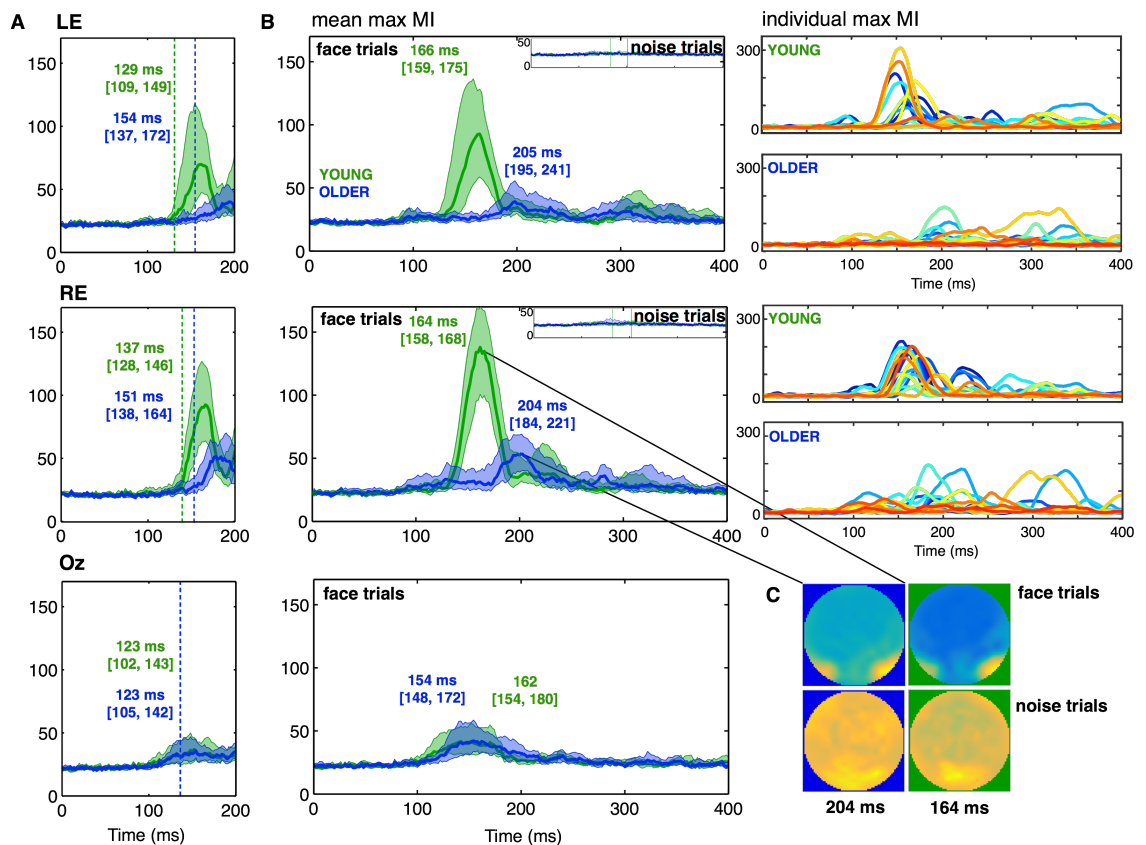


Figure 5 Time-courses of the maximum MI across pixels.

(A) Causal-filtered data. Time-courses of average MI values are presented for young (green) and older (blue) participants, for face trials only. The vertical lines mark the onset of the group effect. **(B)** Non-causal-filtered data. Time-courses of average MI values are presented for both face and noise (insets) trials. The vertical lines mark median latencies of maximum MI in both groups, obtained for face trials. The two panels on the right display individual participants' time-courses. In all graphs, shaded areas correspond to 95% confidence intervals around the 20% trimmed mean. **(C)** Group-averaged topographic maps.

Finally, we looked at the onsets of afferent activity to the visual cortex (Figure 6), using the ERP_{STD} data. Using Global Field Power (GFP), a measure similar to ERP_{STD}, Foxe and Simpson (2002) found that the mean onset latency of the first visual component C1 (said to represent initial occipital cortex activation) occurred at ~56 ms after stimulus presentation. Here, the onsets occurred at 68 ms [64, 72] in young participants, and at 69 ms [62, 75] in older participants and were possibly delayed with respect to this in Foxe and Simpson (2002) due to our stimuli not being optimal to elicit a C1. Importantly, we found no difference in the onsets of afferent activity across the two groups (difference = -0.5 ms [-7, 5]), suggesting there was no general delay in the onset of visual cortical activity in older participants.

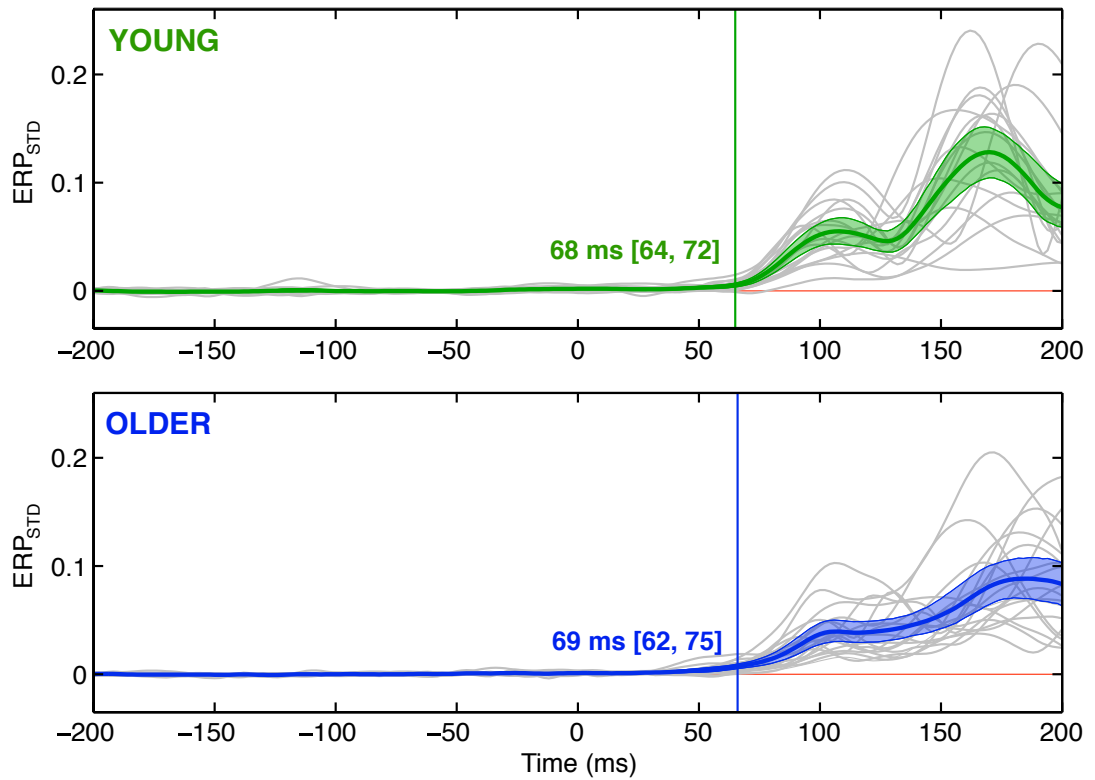


Figure 6 Onsets of afferent activity to the visual cortex.

Thin grey lines show individual participants' ERP_{STD} ($\mu\text{V}/\text{cm}^2$), the thick line shows the group average, and the shaded areas show 95% confidence intervals around the group mean. The vertical lines mark the onset of cortical activity in each group.

ERP FEATURE-OF-INTEREST ANALYSIS

So far, we have shown that the variability in single-trial ERP distributions was associated with the presence of the eyes in both young and older participants. However, this association was significantly weaker and delayed in older compared with younger participants at posterior lateral electrodes, and very similar across groups at the midline electrode.

Previously, we have also shown that in young participants, amplitude and latency distributions of single-trial ERPs were modulated by pixels in the eye area, but the N170 latency carried significantly more information about the contralateral eye than its amplitude, particularly at the right electrode (Rousselet et al., 2014). Here, we sought to investigate whether coding of the contralateral eye by the N170 latency was preserved in ageing. To this end, we used the same approach as in the behavioural analysis where we defined features of interest: the eye contralateral to the recording electrode, and the eye ipsilateral to the recording electrode. We then correlated single-trial Bubble masks with each feature, and computed MI between features and single-trial ERP distributions. Then, similarly to behavioural analysis, we split the correlation values for each feature of interest into 10 bins, and averaged the ERPs corresponding to each of the bins, separately for the left and right lateral electrodes. Presence of the eyes was associated with larger and earlier N170 at both electrodes in young participants. In contrast, in older participants, only the amplitude was modulated by the presence of the eyes (Figure 7A).

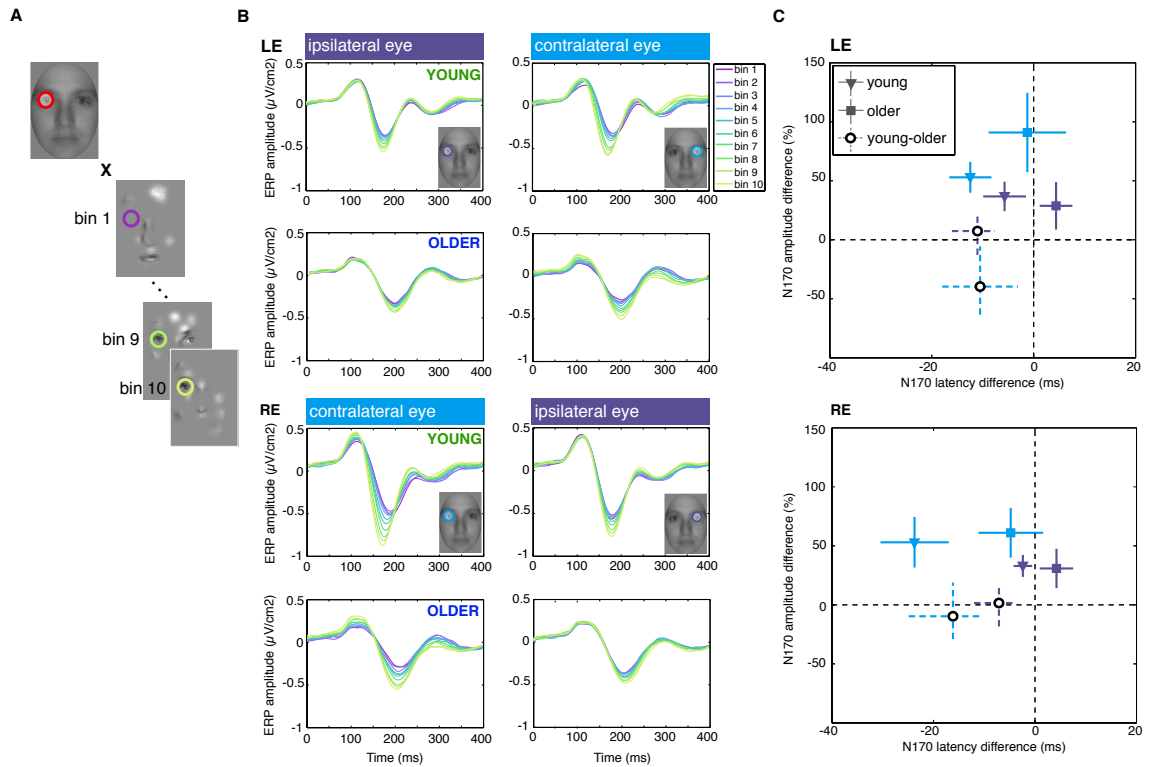


Figure 7 ERP modulation as a function of eye visibility in face trials.

(A) Feature-of-interest analysis. A left-eye mask (red) was correlated with Bubble masks on each trial. These correlation values were then binned, where bin 1 (purple) corresponds to no visibility of the left eye through Bubble masks; and bin 10 (yellow) corresponds to high visibility of the eye.

(B) Rows correspond to face trials in young and older participants at the left electrode (top two), and at the right electrode (bottom two). Columns correspond to ERP modulations as a function of the visibility of the contralateral eye (blue) or the ipsilateral eye (purple). In young, but not in older participants, presence of the contralateral eye was associated with earlier and larger N170, particularly at the right electrode.

(C) Effects of eye visibility on the latency and amplitude differences between the 10th (high information) and the 1st (low information) bin ERPs, at the left (top) and right (bottom) lateral electrodes. Amplitude and latency modulations by the presence of the contralateral eye (blue) and ipsilateral eye (purple) are presented in both plots. Amplitude differences are expressed as proportion of the 1st bin ERP amplitudes, i.e. amplitude difference of 50% means that amplitude of bin 10 ERPs was 150% the size of the amplitude of bin 1 ERPs. Filled circles correspond to median ERP modulations across young participants; squares show medians across older participants, and empty circles show group differences in median of the pairwise differences. Vertical and horizontal bars correspond to 95% confidence intervals.

To quantify this effect, we computed the N170 amplitude and latency in every participant and every feature, for the lowest (bin 1) and the highest (bin 10) correlation values, separately for the left and right electrode. We defined the N170 as the first local minimum in the time window 150 to 250 ms following stimulus onset in ERPs low-pass filtered at 20 Hz using a fourth order Butterworth non-causal filter. We then computed the differences between high and low amplitude and latency values for each group separately. Results are presented in Figure 7B.

At the left electrode, the N170 in young participants was 12 ms [8, 17] earlier when the contralateral eye visibility was high compared to low, and 6 ms [2, 10] earlier when the ipsilateral eye visibility was higher. On the contrary, the N170 latency to the contralateral eye was not significantly modulated in older participants (difference = -1 ms [-9, 6]), and was *delayed* by 4 ms [1, 8] when the ipsilateral eye visibility was higher. At the right electrode, these effects were even stronger. The N170 was 24 ms [17, 31] earlier in young and only 5 ms [2, 11] earlier in older participants when more of the left eye was visible. The ipsilateral eye had opposite effects in the two groups: in young participants, the N170 latency to the presence of the right eye was shorter by 2 ms [1, 4], but longer by 4 ms [1, 8] in older participants.

We then directly tested the interaction between age and latency modulation, i.e. whether the difference in latency modulation by the presence of the contralateral eye versus the ipsilateral eye differs between the two age groups. Finally, we computed the effect size estimates for the group difference in the latency modulations at each electrode. We found a significant group effect at the right (difference: -9 ms [-16, -3]), but not the left electrode (difference: 2 ms [-5, 9]). This means that presence of the contralateral eye had a stronger effect on the N170 latency modulation in young participants, but not older participants, in the right hemisphere. This effect was not found in the left hemisphere. Altogether, the results suggest a differential ageing effect on eye coding mechanisms across hemispheres.

In terms of age effects on amplitude modulation (Figure 7B), the only significant group effect was found at the left electrode for Bubble visibility of the right eye: this was associated with 153% [140, 166] larger N170 amplitude in young, and 191% [157, 225] larger amplitude in older participants (Cliff's *delta*, -0.41 [-0.76, -0.02]; for group differences in latency and amplitude refer to Table 4). Other amplitude modulations were similar across the two groups (Tables 4 and 5).

In summary, our feature-of-interest analysis suggests modulation of the N170 latency and amplitude as a mechanism involved in face detection in young participants. This mechanism changes with ageing. Specifically, while face detection is associated with modulation of the N170 amplitude, there is no modulation of latency in older adults. Our results also point to the right hemisphere as the site where the mechanism is localised.

Table 4 Effect size estimates for eye coding by the N170.

Effect size estimates for group differences (young-older) in N170 latency (LAT) and amplitude (AMP) for different facial features visibility, at left (LE) and right electrode (RE). Values correspond to median latencies expressed in milliseconds, and median difference (percentage points) in amplitude. Square brackets indicate 95% confidence intervals. A corresponding Cliff's delta estimate is shown in italics.

	N170 LAT		N170 AMP	
	LE	RE	LE	RE
Left eye	-11 [-16, -7] <i>-0.79</i> [-0.97, -0.56]	-16 [-24, -11] <i>-0.77</i> [-0.92, -0.52]	7 [-14, 22] <i>0.16</i> [-0.24, 0.58]	-10 [-31, 17] <i>-0.16</i> [-0.54, 0.20]
Right eye	-11 [-18, -3] <i>-0.48</i> [-0.80, -0.11]	-7 [-12, -4] <i>-0.71</i> [-0.92, -0.44]	-40 [-64, -3] <i>-0.41</i> [-0.76, -0.02]	2 [-17, 14] <i>0.03</i> [-0.39, 0.41]

Table 5 Amplitude modulation by eye visibility.

Amplitude modulation for left and right eye visibility, at left (LE) and right (RE) electrode. Amplitude differences are expressed as proportion of the 1st bin ERP amplitudes, i.e. amplitude modulation of 137% means that amplitude of the 10th bin ERPs was 137% the size of the amplitude of the 1st bin ERPs. Square brackets indicate 95% confidence intervals.

	Young		Older	
	LE	RE	LE	RE
Left eye	137% [125, 150]	153% [132, 175]	129% [111, 150]	161% [141, 181]
Right eye	153% [140, 166]	133% [124, 142]	191% [157, 225]	131% [113, 149]

DISCUSSION

To understand visual information processing in ageing, we must start by asking what facial information the aged brain processes and when. Here, for the first time in a sample of older participants, we address these two questions by using reverse correlation to link facial stimulus space to behavioural and brain responses.

In the current study, we found that older adults used pixels around the eyes to detect faces, similarly to young adults. In particular, pixels around the left eye were associated with faster reaction times in both young and older participants. However, older adults were heavily dependent on the presence of the eyes to accurately detect faces, whereas young adults used any feature. These results suggest older participants used a different strategy to detect faces – they might be focusing on higher contrast information contained within the face, in line with previous studies showing that older adults require more contrast to detect and discriminate between faces (Lott, Haegerstrom-Portnoy, Schneck, & Brabyn, 2005; Owsley, Sekuler, & Boldt, 1981). The results pertaining to group differences in modulation of accuracies, however, should be treated with caution because young participants performance on Bubble trials was above 90% and, as such, could be regarded as being at ceiling. Given this high accuracy the task might not have been sensitive enough to elicit modulations of accuracy by face feature in young adults. As such, if performance of young participants was brought down, there might just as well be an observable association between presence of the eye, or other feature(s) and correct responses.

Having established what information participants use to perform a face detection task, we quantified when that information was coded in the brain. In young and older participants alike, we found that single-trial ERPs are mostly associated with the presence of eye pixels contralateral to the recording lateral-occipital electrodes. This association (measured with Mutual Information) was also stronger at right hemisphere electrodes in both groups, in line with the right hemisphere dominance for face processing (Sergent, Ohta, & MacDonald, 1992). However, Mutual Information (MI) was significant in a smaller number of older than young participants and weaker in older participants. MI time courses also peaked about 40 ms earlier in young than in older participants suggesting that processing of the same face feature is weaker and delayed in ageing. Altogether, our results of delayed diagnostic information processing seem to be in line with the theory of slowed information processing in ageing (Salthouse, 1996). These results, together with behaviour, suggest a double-dissociation in age-related changes to face processing: a stronger reliance on the eyes in making behavioural

judgments is coupled with weaker and delayed brain sensitivity to these features in older adults, relative to young adults.

The MI results were not due to our selection of electrodes. We made sure not to miss any effects by running the MI analysis on all electrodes and visualising maximum MI across electrodes in a classification image and a time course. Whole-scalp results, however, were very similar to those obtained on the electrode of interest (RE) suggesting that occipital-lateral electrodes showed maximum sensitivity to the eye region in both young and older observers.

The age-related delay in processing of the eye could not be attributed to the presence of Bubbles either. Bubbles can be thought of as a form of masking procedure that degrades the visual input and has been suggested to entail object completion (Tang et al., 2014). Processing occluded stimuli by the visual system may require additional resources to perform the task, leading to longer processing times (Sekuler, Gold, Murray, & Bennett, 2000). As such, any delay observed in a sample of older adults could be due to a combination of factors: a genuine slowing down of processing speed, as well as an increase in the time needed to process the occluded stimulus with respect to young adults. However, our ERP results show that the processing time of Bubbled images compared with full images was not different in young and in older participants. Specifically, even though processing of the Bubbled stimuli was delayed with respect to full images by about 20 ms in both young and older participants, there was no interaction between age and masking condition. In both practice (unmasked) and Bubble (masked) trials, the N170 latency to face images in older participants was delayed by about 20 ms (18 ms in practice trials and 22 ms in Bubble trials) with respect to that in young participants. This is in line with a recent study (Bieniek et al., 2013) showing that even though stimulus luminance affects the entire ERP time course in both young and older participants, it does not affect age-related differences in processing speed.

On the other hand, there is some indication that ageing may indeed affect perception of partially occluded objects on a behavioural level. For example, older participants were less accurate and needed more stimulus information in tasks requiring perceptual closure (Cremer & Zeef, 1987; Salthouse & Prill, 1988; Whitfield & Elias, 1992), perceptual organization (Kurylo, 2006), contour integration (Roudaia et al., 2008) or perception of incomplete/fragmented figures (Danziger & Salthouse, 1978; Lindfield & Wingfield, 1999; Lindfield, Wingfield, & Bowles, 1994). Lower accuracy was not due to diminished retinal illuminance associated with ageing (e.g. because of senile miosis or increased lenticular density), but rather due to some general inefficiency in utilizing

segment information as effectively as young adults (Danziger & Salthouse, 1978; Salthouse & Prill, 1988). The reason for such age-related deterioration in performance on tasks involving perception of fragmented pictures or perceptual closure remains elusive, but it has been suggested that perceptual difficulties arise as a result of slowing within a neural network (Salthouse & Mein, 1995; Salthouse, 1996). According to this hypothesis, slowing of the network responsible for a given task arises as a result of heightened noise or variability associated with the internal stimulus representation in the neural system (Salthouse & Lichty, 1985). This increased internal noise hypothesis has recently been tested behaviourally in studies investigating face perception across different views in older adults (Habak et al., 2008; Wilson, Mei, Habak, & Wilkinson, 2011). Results showing an increase in bandwidths for head orientation and a drop in performance were in line with the hypothesis that decreased neural inhibition between neural representations of different face views contributed to an increase in internal noise (see also Bennett, Sekuler, & Sekuler, 2007), albeit these studies did not measure neural inhibition directly. Evidence for increased internal noise, leading to a lower signal-to-noise ratio comes from monkey single-unit recordings (Schmolesky et al., 2000; Wang et al., 2005; Yang et al., 2008) and, indirectly, from fMRI studies in humans showing broader tuning of neural responses in ventral visual brain regions (Park et al., 2004, 2012).

The decrease in neural inhibition could explain the elevated responses to noise trials in the current study. We already reported that older adults show large N170-like responses to textures (Rousselet et al., 2009) and observed similar responses here. By investigating the information content of these noise trials in the current study, we shed some light on the potential origins of these responses. Specifically, we show that there was no significant information content on noise trials in either young or older participants. Lack of any information content on noise trials in the current study suggests that older adults are not processing textures as faces. Therefore, the large amplitude to textures might rather reflect some general activation to a visual stimulus without functional significance. Furthermore, lack of information on noise trials suggests that MI results on *face* trials were unlikely to be due to spatial attention to the eye region. If this were the case, we would have expected to observe some sensitivity to the eye area in noise trials as well. However, the effects of potential age-related differences in controlling spatial attention should not be ruled out completely. For example, a recent EEG study identified an age-related reduction of right-hemispheric control of spatial attention in a line bisection task (Learmonth, Benwell, Thut, & Harvey, 2017), in agreement with the “hemispheric asymmetry reduction in older adults” (HAROLD) model (Cabeza, 2002)

which proposes that cognitive function that are highly lateralised to one cerebral hemisphere in young adults become generally less lateralised in older adults. Although our results show that MI was right-lateralised in both young and older adults alike, this measure might not be sensitive enough to measure attentional biases in the two groups. Interestingly, our behavioural results suggested that both the left and the right eye regions were important for correct responses in older participants. However, with the present design it is not possible to say whether it was any eye available on a given trial that was associated with correct responses, or whether it was an integration of information from both eyes, and whether such integration (if found) was associated with a compensatory recruitment of the left hemisphere in older adults. Future studies should address this issue, for example by employing independent Bubbles sampling in the two visual hemifields and other paradigms aimed at testing feature integration.

The relationship between diagnostic information and the peak of the N170 has only been investigated in a sample of young participants so far (Ince, Jaworska, et al., 2016; Rousselet et al., 2014; Schyns et al., 2007). Specifically, coding of the eye starts well before the peak of the N170 (Rousselet et al., 2014; Schyns et al., 2007), and the N170 peaks when information diagnostic to the task at hand (e.g. the mouth in expressiveness task) has been integrated (Schyns et al., 2007). In a face detection task, since the contralateral eye provides the diagnostic information, the N170 peaks earlier and is larger in amplitude when visibility of the eye is higher (Rousselet et al., 2014). In the current study, we extended those results to a sample of older participants. Specifically, using reverse analysis we found that higher eye visibility was associated with larger amplitude of the N170 in older participants. However, there was no modulation of latency, contrary to young participants. Latency and amplitude modulation of the N170 by the contralateral eye was also larger in the right hemisphere in young, but not older participants, suggesting an age-related difference in coding of the eye by the N170.

Recently, Ince et al. (2016) also found that the *rebound* from the N170 peak codes the transferred ipsilateral eye from the other hemisphere, suggesting that the N170 reflects coding and transfer functions of an information-processing network involving both hemispheres. These results further support the notion that the peak of the N170 cannot be interpreted as an isolated event and that traditional ERP peak analyses should be abandoned in favour of investigating the entire time course of feature sensitivity (Rousselet & Pernet, 2011; Rousselet, Pernet, Caldara, & Schyns, 2011; Schyns et al., 2007).

To go beyond peak measurements, Rousselet et al. (2009, 2010; Bieniek et al., 2013, 2015) used an alternative measure that takes into account both the latencies and amplitudes of the entire ERP waveform, providing a cumulative index of the speed of visual processing. They reported that the earliest stage of image structure processing is spared in ageing, with onsets of face sensitivity taking place around 90 ms post-stimulus regardless of age. Ageing effects began at around 120 ms following stimulus onset and were the strongest at around 190 – 200 ms, with older adults being about 50 ms slower than young adults. Here, using a similar cumulative sum approach, we found that it took older participants only about 20 ms more to integrate 50% of their MI time course about contralateral eye sensitivity. In previous studies, older participants' maximum sensitivity to image structure was also spread over two time windows, one weaker around the same time as in young participants (100 – 200 ms post-stimulus) and one stronger, after 200 ms. As opposed to our results, the maximum sensitivity to image structure was also equally strong in both groups.

Results from previous studies left it unclear whether the second period of sensitivity reflected involvement of a different mechanism in older adults, e.g. top-down control (Gazzaley et al., 2008; Grady, 2008), or slowing down of visual processing with age. If the latter were true, this could mean that, in older participants, the later time window might become functionally equivalent to the N170 time window in young participants.

Here, we shed some light on this question by showing that the same information (contralateral eye sensitivity) is processed in the same time window of the N170 in young and older participants, but this processing is weaker and delayed in ageing. Our results also lack the second period of sensitivity found in previous studies, which might be the effect of applying Bubble masks to the images. As such, it would be interesting to compare how contralateral eye sensitivity is affected by ageing with the use of a different experimental manipulation. For example, visibility of the eye could be parametrically manipulated by adding different levels of phase noise to the eye region, thereby providing a direct comparison to results obtained previously (Rousselet et al., 2009, 2010; Bieniek et al., 2013, 2015).

In conclusion, here we show for the first time that the information content of early visual ERPs in older adults does not differ from that of young adults. Specifically, the contralateral eye region modulates ERPs in young and older adults alike, although the processing of the eye is weaker and delayed in ageing. This finding is coupled with an increased reliance on the presence of the eyes in the image on a behavioural level, suggesting a dissociation of behavioural and brain responses in older adults.

Furthermore, eye visibility modulates only the N170 amplitude in older adults, but both the latency and amplitude in young adults.

CHAPTER 3: AGE-RELATED DIFFERENCES IN EYE SENSITIVITY WITH AND WITHOUT THE FACE CONTEXT

INTRODUCTION

In order to understand whether young and older adults use the same facial information to perform a face detection task, and when this information is processed in the brain, we have recently used a Bubbles paradigm (Gosselin & Schyns, 2001) coupled with reverse correlation (Jaworska et al., in prep). Participants were presented with images of faces and textures revealed through ten Gaussian apertures placed randomly on each trial. By correlating reaction times with stimulus information in single trials, we have shown that young and older participants alike responded faster when the left eye was visible through the Bubble masks (Jaworska et al., in prep). However, older participants relied on the presence of the eyes much more to make correct responses, whereas any face feature was sufficient for young participants (Jaworska et al., in prep). Presence of the contralateral eye in the image also modulated single-trial brain activity measured with electroencephalography (EEG) in both young (Rousselet et al., 2014; Schyns et al., 2007; Van Rijsbergen & Schyns, 2009) and older adults (Jaworska et al., in prep). However, this association was weaker and delayed in older participants. As such, we have shown that in a face detection task, processing of the same diagnostic information (the contralateral eye) was slower in ageing.

Since only partial image information is presented through the Bubble masks, it has been suggested that the use of this technique may force the observer to attend to features rather than process the face as an overall gestalt, and that diagnostic information might not generalize to other experimental paradigms (Neath & Itier, 2014). Furthermore, older adults have been shown to perform worse on face recognition when the stimulus is degraded (Grady, Randy McIntosh, Horwitz, & Rapoport, 2000), as well as on object recognition from fragmented pictures (Danziger & Salthouse, 1978; Lindfield & Wingfield, 1999; Lindfield, Wingfield, & Bowles, 1994) or in tasks requiring perceptual closure (Cremer & Zeef, 1987; Salthouse & Prill, 1988; Whitfield & Elias, 1992). In line with these findings, older participants in our previous study were also generally less accurate in detecting a face from Bubbled images (Jaworska et al., in prep).

As such, two questions remain unanswered. First, would behavioural and EEG sensitivity to the visibility of the eye generalize beyond the Bubbles paradigm? Secondly, would age-related delay in processing of the eye still be present in a less degraded stimulus?

To answer these questions, we employed a new experimental paradigm in which we manipulated eye visibility parametrically by introducing phase noise into the eye region. Previously, Rousselet et al. (2008, 2009) manipulated the visibility of full face images by randomizing their phase spectra in a parametric manner, and reported phase effects that reached maximum in the time window of the N170 in young participants (Rousselet, Pernet, et al., 2008). In older participants, sensitivity to phase information peaked in two time windows: one early (<200 ms) and one late (>200ms, Rousselet et al., 2009). In the current study, alongside manipulating the eye visibility, the rest of the face remained intact, thereby providing a “face context” and a more ecologically valid stimulus than Bubbled images. We then compared the results with a complementary condition in which the eye visibility was still manipulated but the rest of the face was phase-randomized (“face context absent”). This condition was related to the Bubbles stimulus such that only a portion of the image was revealed through an eye aperture, but it differed in that only the eye region was revealed on each trial, and a smaller proportion of the face area was revealed than through Bubble masks.

Our hypotheses were that eye sensitivity in both face contexts would be associated with ERP modulation in the time window of the N170 in young adults, and that this sensitivity would be delayed in older adults.

MATERIALS AND METHODS

PARTICIPANTS

Twenty-four young (15 females, 3 left-handed; median age = 22, min = 20, max = 39) and twenty-three older adults (12 females, 3 left-handed; median age = 68, min = 59, max = 85) participated in the study. All young participants were recruited from the student body at the University of Glasgow. Older participants were local residents who had already taken part in the Bubbles study before (Jaworska et al., in prep) or were recruited from a local Active Age fitness class, the Retired Staff Association at the University of Glasgow, or through advertisement at a local optometrist. Young participants were recruited from the student body at the University of Glasgow. Volunteers were excluded from participation if they reported any current eye condition (i.e., lazy eye, glaucoma, macular degeneration, cataract, diabetic retinopathy), had a history of mental illness, were currently taking psychotropic medications or used to take them, suffered from any neurological condition, or had suffered a stroke or a serious head injury. Volunteers were also excluded from participation if they had their eyes tested more than a year (for older volunteers) or two years (for younger volunteers) prior to the study taking place, in order to minimise the chances that volunteers did not have knowledge of an underlying eye condition. Participants' visual acuity was assessed during their first experimental session using a Colenbrander mixed contrast card set (Colenbrander & Fletcher, 2004) for the 40 cm and 63 cm viewing distances, and the 6 m Bailey-Lovie Chart (Bailey & Lovie, 1980). Participants' contrast sensitivity was assessed with the Mars Letter Contrast Sensitivity set (Arditi, 2005). All participants had normal or corrected to normal visual acuity (Table 6) and contrast sensitivity of 1.72 log units and above, which fell within the normal range of contrast sensitivity for each age group (Haymes et al., 2006). In addition, older participants completed the Montreal Cognitive Assessment (MOCA) to screen for age-related cognitive impairment. MOCA scores of three older participants were one point below the normal threshold (more than or equal to 26 out of 30, Table 6) and the median score was 28 (min = 25, max = 30). Older participants also completed the Trail Making Test – part of the Delis-Kaplan Executive Function System (D-KEFS) (Delis, Kaplan, & Kramer, 2001) battery of tests to assess higher-order cognitive and executive functioning. Results of the Trail Making Test are reported in Table 6. During the experimental session, participants wore their habitual correction if needed.

The study was approved by the local ethics committee at the College of Science and Engineering, University of Glasgow (approval no. 300150007), and conducted in line with the British Psychological Society ethics guidelines. Informed written consent was obtained from each participant before they took part in the study. Participants were compensated £6 per hour.

Table 6 Visual and cognitive test scores.

Presented are visual acuity and contrast sensitivity (CS) scores for young and older participants, as well as MOCA and Trail Making Test Scores for older participants. Visual acuity scores are reported for high contrast (HC) and low contrast (LC) charts presented at the 40 cm, 63 cm and 6 m viewing distances, and expressed as raw visual acuity scores (VAS). Their corresponding logMAR scores are presented below in italics, where higher values indicate poorer vision and negative values represent normal vision (logMAR score of 0 corresponds to 20/20 vision). For Trail Making Test, scores are age-scaled composite scores for Number-Letter Switching (NLS) task versus: Visual Scanning (VS), Number Sequencing (NS), Letter Sequencing (LS), Composite Scaled Score (CSS), and Motor Speed (MS). Scores correspond to median across all participants in each age group. Square brackets indicate the minimum and maximum scores across participants in each age group.

	HC 40	LC 40	HC 63	LC 63	HC 600	LC 600	CS
young	103	95	105	94	103	95	1.84
	[93, 105]	[83, 103]	[97, 111]	[86, 105]	[89, 110]	[65, 103]	[1.72, 1.92]
	<i>-0.06 [0.14,</i>	<i>0.10 [0.34,</i>	<i>-0.10 [0.06,</i>	<i>0.12 [0.28,</i>	<i>-0.06 [0.22,</i>	<i>0.10 [0.70,</i>	
	<i>-0.10]</i>	<i>-0.06]</i>	<i>-0.22]</i>	<i>-0.10]</i>	<i>-0.20]</i>	<i>-0.06]</i>	
older	92	83	100	89	100	91	1.80
	[75, 105]	[65, 98]	[85, 110]	[75, 100]	[88, 105]	[75, 99]	[1.68, 1.88]
	<i>0.16 [0.50,</i>	<i>0.34 [0.70,</i>	<i>0.00 [0.30,</i>	<i>0.22 [0.50,</i>	<i>0.00 [0.24,</i>	<i>0.18 [0.50,</i>	
	<i>-0.10]</i>	<i>0.04]</i>	<i>-0.20]</i>	<i>0.00]</i>	<i>-0.10]</i>	<i>0.02]</i>	
	MOCA	D-KEFS Trail Making test: NLS vs. XXX					
		VS	NS	LS	CSS	MS	
older	28	12	11	12	11	10	
	[25, 30]	[10, 15]	[9, 15]	[9, 15]	[9, 15]	[9, 13]	

STIMULI

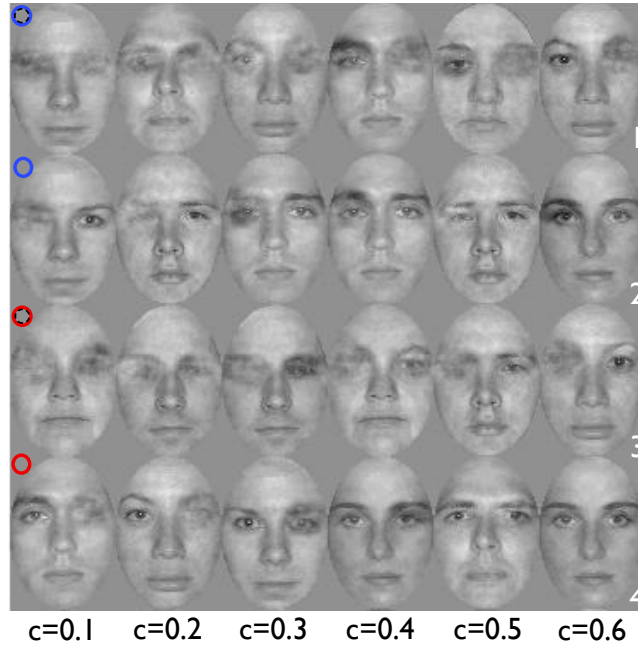
Participants were presented with a set of 10 grey-scaled front view photographs of faces (5 males and 5 females), oval cropped (9.3° x 6.4°) to remove external features, and pasted on a uniform grey background (Gold et al., 1999). All stimuli had the same amplitude spectrum and contrast variance (variance = 0.035). For each face identity, a

unique eye mask, including the eyebrow, was created by centring an ellipse on the pupil of each eye independently. As such, the eye mask for each identity varied slightly in shape and size. Each eye's aperture was smoothed with a Gaussian filter (standard deviation = 5 pixels).

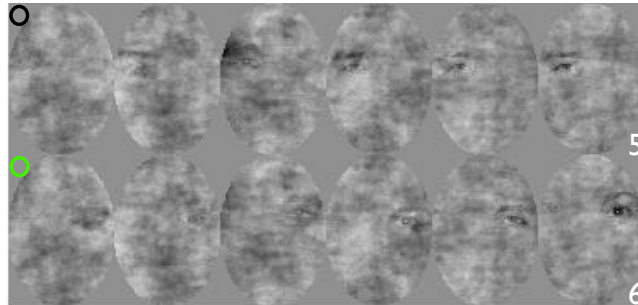
There were six experimental conditions: four in which the face context was present, and two in which the face context was absent (Figure 8). In the face context conditions, either the left or the right eye (as seen by observers in the picture plane) visibility was parametrically manipulated by adding phase noise. At the same time, the opposite eye to the one sampled was either present or absent. In the conditions without the face context, visibility of only one eye (the left or the right) was changed.

Noise in the sampled eye region was created by altering phase coherence of the face image, such that coherence varied across 60 levels from 1% to 60%. In conditions with the face context present (conditions 1 – 4, Figure 8A), the presence of the opposite eye was then manipulated by either completely randomizing phase coherence within the other eye aperture (0% coherence, 'eye absent', conditions 1 and 3) or leaving phase coherence intact (100% phase coherence, 'eye present', conditions 2 and 4). Both the sampled eye and the opposite eye were then combined with the face context. In conditions without the face context present (conditions 5 – 6, Figure 8A), either the left (condition 5) or the right eye (condition 6) visibility was manipulated in a similar manner to other conditions: by randomizing phase spectrum of a face image drawn at random. Independently, a texture was created by fully randomizing the phase spectrum of the same image. Then, the eye with added noise and the texture were combined. A set of textures, presented through the face oval, was also generated for the task of discriminating a face image from a texture image.

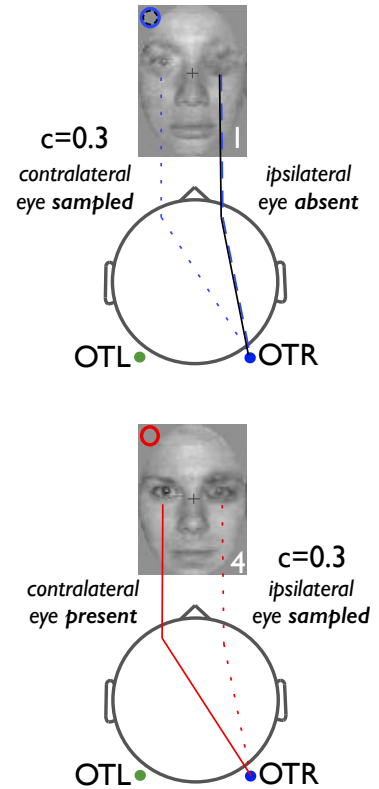
A face context conditions



no-face context conditions



B



- | |
|---------------------------------------|
| 1: sample Left eye, Right eye absent |
| 2: sample Left eye, Right eye present |
| 3: sample Right eye, Left eye absent |
| 4: sample Right eye, Left eye present |
| 5: sample Left eye |
| 6: sample Right eye |

Figure 8 Examples of stimuli.

(A) Experimental conditions. Columns correspond to examples of six phase coherence levels ($c = 0.1$ to 0.6 , or 10% to 60%) introduced to the sampled eye. Rows correspond to the six experimental conditions (numbers in the bottom right corner; see legend in the bottom right corner of the figure). Coloured circles in the top left corners correspond to condition coding used in ERP figures, reflecting an interaction between the visibility of the eyes in the stimulus and their coding in each hemisphere (either present in the hemifield contralateral or ipsilateral to the sensor of interest). **(B)** Example of stimulus coding with respect to analyses performed at the occipital-temporal sensor on the right hemisphere (OTR). Example stimuli are shown at coherence level of 30%. Top, a diagram depicting sampling of the eye contralateral to OTR while the ipsilateral eye is absent (condition 1). Bottom, sampling of the eye ipsilateral to OTR while the contralateral eye is present (condition 4).

PROCEDURE

All participants were tested in one experimental session consisting of a behavioural task and simultaneous EEG recordings. Participants sat in a dimly lit and sound-attenuated booth, and were given experimental instructions including a request to minimize movement and blinking, or to blink when hitting a response button.

The experimental session consisted of 18 blocks of 80 trials (1440 trials in total). There was a total of 1080 face trials (6 conditions x 60 phase coherence levels x 3 repetitions of each coherence level) and 360 texture trials. All trials and face identities were randomized across the entire experiment.

On each trial, participants were first presented with a small fixation cross (12 x 12 pixels, 0.35° x 0.35° of visual angle) displayed at the centre of the monitor screen for a random time interval of 500 to 1000 ms, followed by an image of a manipulated face (see Stimuli) or a texture presented for 10 frames (~83 ms). After the stimulus, a blank grey screen was displayed until the participant responded. During that time, participants categorized the image by pressing '1' for face, and '2' for texture on the numerical pad of a keyboard, using the index and middle fingers of their dominant hand. They were requested to respond as fast and accurately as possible.

After each block, participants could take a break, and they received feedback on their performance in the previous block and on their overall performance in the experiment (median reaction time and percentage of correct responses). The next block started after participants pressed a key indicating they were ready to move on.

Stimuli were displayed on a VIEWPixx monitor (1920 x 1200 pixels; 22.5 inch diagonal display size; 120 Hz refresh rate). The fixation cross, the stimulus and the blank response screen were all displayed on a uniform grey background. The viewing distance measured from the chinrest to the monitor screen was 45 cm. Each session lasted about 60 to 75 minutes, including breaks, but excluding EEG electrode application. The experiment was written in MATLAB using the Psychophysics Toolbox extensions (Brainard, 1997; Kleiner et al., 2007; Pelli, 1997).

EEG RECORDING AND PRE-PROCESSING

EEG data were recorded at 512 Hz using a 128-channel Biosemi Active Two EEG system (Biosemi, Amsterdam, the Netherlands). Four additional UltraFlat Active Biosemi

electrodes were placed below and at the outer canthi of both eyes. Electrode offsets were kept between $\pm 20 \mu\text{V}$.

EEG data were pre-processed using MATLAB 2013b and the open-source EEGLAB toolbox (Delorme et al., 2011; Delorme & Makeig, 2004). Data were first average-referenced and detrended. Two types of filtering were then performed. First, data were band-pass filtered between 1 Hz and 30 Hz using a non-causal fourth order Butterworth filter. Independently, another dataset was created in which data were pre-processed with fourth order Butterworth filters: high-pass causal filter at 2 Hz and low-pass non-causal filter at 30 Hz, to preserve accurate timing of onsets (D. J. Acunzo, Mackenzie, & van Rossum, 2012; Luck, 2005; Rousselet, 2012; Widmann & Schröger, 2012b).

Data from both datasets were then downsampled to 500 Hz, and epoched between -300 and 1000 ms around stimulus onset. Mean baseline was removed from the causal-filtered data, and channel mean was removed from each channel in the non-causal-filtered data in order to increase reliability of Independent Component Analysis (ICA) (Groppe, Makeig, & Kutas, 2009). Noisy electrodes and trials were then detected by visual inspection of the non-causal dataset, and rejected on a subject-by-subject basis. On average, more noisy channels were removed from older than from young participants' datasets (young participants: median 15, min 6, max 28; older participants: median 21, min 8, max 42; median difference = 7, 95% confidence interval = [2, 11]).

Subsequently, ICA was performed on the non-causal filtered dataset using the Infomax algorithm as implemented in the *runica* function in EEGLAB (Delorme & Makeig, 2004; Delorme et al., 2007). The ICA weights were then applied to the causal filtered dataset to ensure removal of the same components, and artifactual components were rejected from both datasets (young: median = 4.5, min = 1, max = 13; older: median = 3, min = 1, max = 20). Then, baseline correction was performed again, and data epochs were removed based on an absolute threshold value larger than $100 \mu\text{V}$ and the presence of a linear trend with an absolute slope larger than $75 \mu\text{V}$ per epoch and R^2 larger than 0.3. Due to battery failure, data from 1360 trials were recorded for one young participant and from 738 trials for one older participant. The median number of trials accepted for analysis was, for young participants: median 1402, min 1233, max 1434; for older participants: median 1403, min 713, max 1429 (median difference = -2 [-17, 10]). Finally, we computed single-trial spherical spline current source density waveforms using the CSD toolbox (Kayser, 2009; Tenke & Kayser, 2012). CSD waveforms were computed using parameters 50 iterations, $m=4$, $\lambda=10^{-5}$. The head radius was arbitrarily set to 10 cm, so that the ERP units are $\mu\text{V}/\text{cm}^2$. The CSD transformation is a spatial high-pass

filtering of the data, which sharpens ERP topographies and reduces the influence of volume-conducted activity. CSD waveforms also are reference-free.

STATISTICAL ANALYSES

Statistical analyses were conducted using Matlab 2013b. Throughout this chapter, square brackets indicate 95% confidence intervals computed using the percentile bootstrap technique, with 1000 bootstrap samples. Unless otherwise stated, median values are Harrell-Davis (Harrell & Davis, 1982) estimates of the 2nd quartile.

MEASURES OF EFFECT SIZE

We estimated the size of the between-group differences using two robust techniques: Cliff's *delta* and the median of all pairwise differences. Cliff's *delta* (Cliff, 1996; Wilcox, 2006) is related to the Wilcoxon-Mann-Whitney *U* statistic and estimates the probability that a randomly selected observation from one group is larger than a randomly selected observation from another group, minus the reverse probability. Cliff's *delta* ranges from 1 when all values from one group are higher than the values from the other group, to -1 when the reverse is true. Completely overlapping distributions have a Cliff's *delta* of 0. In line with Cliff's *delta* approach, we also calculated all pairwise differences between young and older participants on the measures of interest (reaction times, percent corrects, N170 latencies and amplitudes), and took the median of the distribution of these differences. This way of measuring effect sizes enabled us to provide information about the typical difference between any members of two groups (Wilcox, 2012).

MUTUAL INFORMATION

We used mutual information (MI) to quantify the dependence between the level of eye visibility (phase coherence) and behavioural and brain responses. MI is a non-parametric measure that quantifies (in bits) the reduction in uncertainty about one variable after observation of another and has been used to study the selectivity of neural and behavioural responses to external stimuli (Ince et al., 2009; Magri, Whittingstall, Singh, Logothetis, & Panzeri, 2009b; Panzeri et al., 2010; Schyns et al., 2011). The advantage of using the MI lies in its ability to detect associations of any order, whether linear or non-linear.

Here, we used a new estimator of MI that can be used with continuous variables (Ince, Giordano, et al., 2016) and utilizes the concept of copulas (Nelsen, 2007), statistical structures that express the relationship between two random variables, independently of

their marginal distributions. Previously (Jaworska et al., in prep), we used an approach where data were quantized into a number of bins, and MI was estimated over the resulting discrete spaces. However, the binning approach is sensitive to the problem of limited sampling bias. The copula method does not require the binning step and overcomes this problem while being computationally efficient (Ince, Giordano, et al., 2016).

We calculated several MI quantities in single participants: MI(eye, RT) to establish the relationship between visibility of the eye (i.e. phase coherence) and reaction times, as well as MI(eye, EEG) to establish the relationship between the visibility of the eye and EEG voltage over the time period of -300 ms before to 1000 ms after stimulus onset. These quantities were computed separately for each experimental condition (see Stimuli).

We also computed the temporal gradient of the EEG voltage (dEEG) on each trial in order to account for the temporal relationship between neighbouring time points, and then combined the EEG voltage and its temporal gradient into a bivariate response. We then calculated the time course of MI about the eye visibility in the bivariate response: MI(eye, [EEG dEEG]). Considering the gradient response together with the voltage smoothes out the artifactual dips in MI time courses, occurring at time points of zero-crossings when EEG voltages change the sign. It also introduces information about the shape of the ERP, otherwise missing from just considering instantaneous amplitudes. As such, the bivariate time course provides a clearer picture of the time window(s) over which the EEG signal is modulated by the changing stimulus (Ince, Giordano, et al., 2016).

50% INTEGRATION TIME

In order to estimate the time course of information processing that takes into account the entire waveform and not just the peaks, we determined how long it took participants to integrate 50% of their MI time courses (Rousselet et al., 2010). For each participant, we computed the cumulated sum of the maximum MI across electrodes in both hemispheres in the time window of 0-500 ms. We then normalized that cumulated sum between 0 and 1, such that it had a value of 0 at stimulus onset and a value of 1 at 500 ms after stimulus onset. Finally, we computed the time necessary to reach 50% of that function using a linear interpolation.

ELECTRODE SELECTION

We selected three subsets of electrodes in each participant independently (Figure 9): midline electrodes (CE), posterior-lateral electrodes on the left hemisphere (LE) and on the right hemisphere (RE). Analyses were restricted to LE and RE. In order to avoid defining a single electrode of interest, we calculated the time courses of the maximum MI across all electrodes of interest in each hemisphere independently. We also checked that we did not miss any local maxima by repeating our group analyses on the maximum MI taken across all scalp electrodes.

For ERP analyses, we selected two electrodes by measuring the difference between face mean ERPs and noise mean ERPs at posterior-lateral electrodes of interest, squaring it, and selecting the left and the right electrodes that showed the maximum difference in the period of 120-220 ms. The selected lateral electrodes were P7/8, or PO7/8, or their immediate neighbours, which are electrodes typically associated with large face ERPs in the literature.

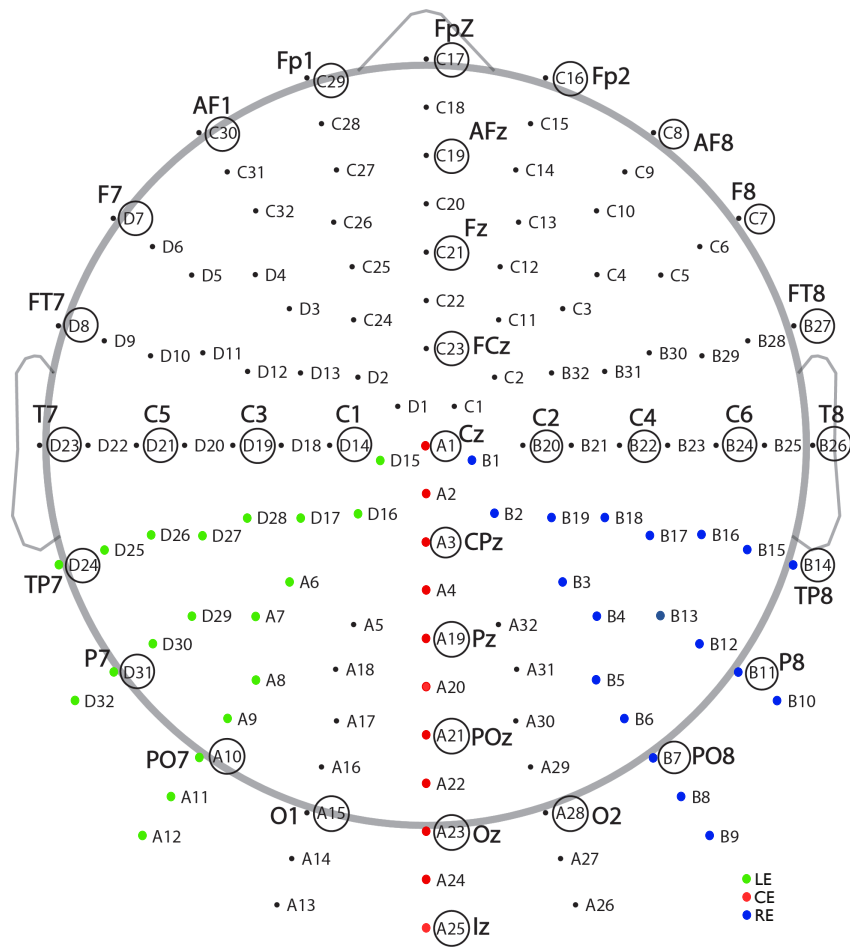


Figure 9 Electrode locations.

Location of electrodes included in three subsets: midline (CE, red), posterior-lateral in the left hemisphere (LE, green) and in the right hemisphere (RE, blue).

RESULTS

BEHAVIOURAL RESULTS

Regardless of the condition, young participants were generally faster than older participants by about 130 ms [107, 151] (median of the median RTs in young participants = 419 ms [401, 437]; older = 545 ms [521, 564]). However, participants from the two groups had similar levels of accuracy (mean accuracy in young participants = 86% [83, 89]; older = 87% [84, 90]; $\text{difference}_{\text{older-young}} = 1$ percentage point (PP) [0, 2]). The average performance was brought down by the conditions in which the face context was absent (Table 7). Conditions in which the face context was present could be regarded as trivial given the amount of information available in the stimulus to make a correct response, and elicited ceiling performance in both groups, thus limiting the scope of considerations that could be made. As such, we report analyses comparing accuracies between two conditions when the face context was absent within each group, before moving to discuss reaction time differences in more detail.

Average behavioural results for each condition are presented in Tables 7 and 8, and depicted graphically in Figure 10A. Both groups were more accurate in condition 5 (sampling of the left eye) compared with condition 6 (sampling of the right eye) by 5 PP [2, 7] (young), and by 4 PP [2, 6] (older), suggesting an advantage of the presence of the left eye, as seen by observers in the picture plane (hereafter, the left eye) for accuracy scores. However, this effect could also be due to assigning a 'texture' response to the '2' button on the numerical computer keyboard, which was also on the right side of the set of two response buttons. As such, when participants saw the right eye revealed through the noisy texture, they could have been more likely to erroneously respond it was a texture.

In terms of reaction times, both groups were fastest when the left eye was present and the right eye was sampled (condition 4), and slowest when the left eye was absent and the right eye was sampled (condition 3), confirming the face detection advantage afforded by the presence of the left eye (Rousselet et al., 2014; Jaworska et al., in prep).

We then looked at pairwise comparisons between each and every other condition (Figure 10B). In face context conditions, both groups were slower in condition 3 compared with condition 2 (sampling of the left eye while the right eye is present; young = 19 ms [10, 25], older = 28 ms [19, 38]), and with condition 4 (sampling of the right eye when the left eye is present; young = 20 ms [12, 30], older = 38 ms [24, 52]). There was

a significant age x RT difference interaction for condition 3 vs. 4 comparison: on average, RT differences among older participants were larger by about 16 ms [3, 34].

Participants were also slower on condition 3 compared with condition 1 (sampling of the left eye while the right eye is absent: young = 8 ms [-16, 1]; older = 18 ms [10, 30]). Here, the interaction was also significant: RT differences among older participants were larger by about 12 ms [1, 22], suggesting that the absence of the left eye, compared with the right eye has a greater effect on RTs in older participants.

Both groups also showed an RT advantage of sampling the left eye compared with sampling the right eye in no-face context conditions (young = 17 ms [7, 30], older = 54 ms [36, 70]; interaction: 35 ms [16, 54]).

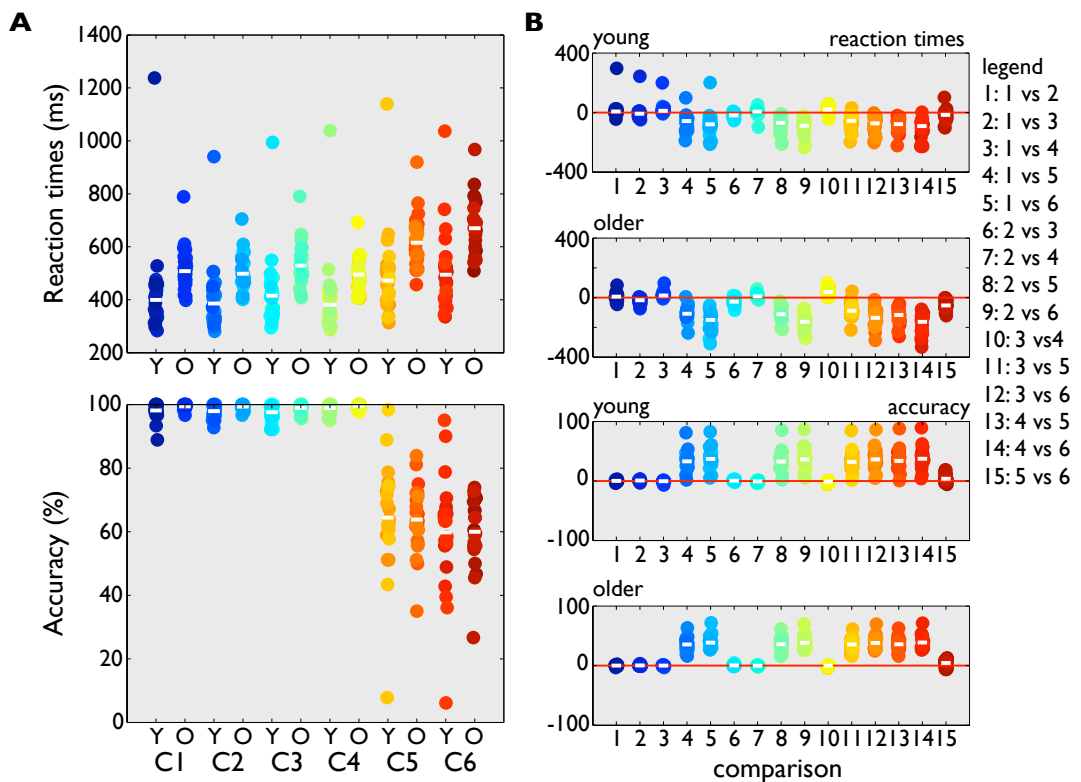


Figure 10 Behavioural results.

(A) Median RT (top panel) and mean accuracy (bottom panel). Each dot in the plot corresponds to one participant. Dots are grouped by age (young participants, Y; older participants, O) and condition (C1 – C6). White horizontal lines mark the median (for RTs) or mean (for accuracy scores) across participants for each age group and condition. White solid line in each scatterplot corresponds to the median (for RTs) or the mean (for accuracy scores) across participants. **(B)** Pairwise differences between conditions. Each dot corresponds to one participant's difference in median RTs (top two panels) or mean accuracy scores (bottom two panels) between the

corresponding conditions (e.g. comparison 1 corresponds to the difference between conditions 1 and 2; see legend). Differences for young and older participants are plotted in separate panels.

Table 7 Behavioural results: accuracy scores.

Values correspond to the median across young and older participants separately, as well as the group difference, for each of the six experimental conditions and for textures. The last column shows median RT differences between older and young participants for each condition. Square brackets indicate 95% confidence intervals. Within face context conditions, there was a small but consistent group effect: older participants were, on average, better by about 1 PP. There were no group differences on accuracies in trials without the face context.

Condition	Young	Older	Older-Young
Sample LE/ RE absent	98 [97, 99]	99 [99, 100]	1 [0, 2] <i>0.37 [0.04, 0.63]</i>
Sample LE/ RE present	98 [97, 99]	99 [99, 100]	1 [0, 2] <i>0.46 [0.14, 0.70]</i>
Sample LE/ RE absent	98 [97, 98]	99 [98, 99]	1 [0, 2] <i>0.39 [0.06, 0.65]</i>
Sample LE/ RE present	99 [98, 99]	100 [99, 100]	0 [0, 1] <i>0.35 [0.05, 0.59]</i>
Sample LE	64 [57, 70]	64 [59, 68]	-1 [-8, 4] <i>-0.07 [-0.39, 0.26]</i>
Sample RE	60 [52, 67]	60 [55, 64]	1 [-7, 7] <i>0.03 [-0.31, 0.35]</i>
Textures	85 [78, 90]	93 [89, 95]	4 [0, 9] <i>0.28 [-0.07, 0.56]</i>

Table 8 Behavioural results: reaction times.

Values correspond to the median across young and older participants separately, as well as the group difference, for each of the six experimental conditions and for textures. The last column shows median RT differences between older and young participants for each condition. Square brackets indicate 95% confidence intervals. Older participants were generally slower than young participants in each condition.

Condition	Young	Older	Older-Young
Sample LE/ RE absent	396 [353, 441]	508 [477, 540]	113 [68, 157] <i>0.71 [0.41, 0.87]</i>
Sample LE/ RE present	387 [345, 431]	504 [473, 548]	119 [71, 165] <i>0.71 [0.41, 0.87]</i>
Sample LE/ RE absent	409 [359, 446]	530 [497, 570]	126 [76, 169] <i>0.71 [0.41, 0.87]</i>
Sample LE/ RE present	380 [343, 421]	494 [466, 524]	113 [70, 149] <i>0.74 [0.45, 0.89]</i>
Sample LE	470 [415, 510]	613 [566, 662]	149 [93, 206] <i>0.72 [0.43, 0.88]</i>
Sample RE	487 [432, 530]	669 [619, 713]	181 [123, 240] <i>0.75 [0.45, 0.90]</i>
Textures	476 [437, 510]	628 [593, 698]	166 [110, 222] <i>0.77 [0.47, 0.91]</i>

MUTUAL INFORMATION

Looking at median RTs in each condition is not, however, the same as quantifying the relationship between the visibility of the eye and RTs. To investigate this, we computed Mutual Information (MI) between eye visibility and RTs ($MI(\text{eye}, \text{RT})$) in each condition and for each participant independently. We then computed the median MI across young and older participants (Table 9). Generally, MI values across conditions and groups were rather low, suggesting that manipulating the visibility of the eye either with face context present or absent did not have a large influence on reaction times. In both age groups, highest MI was observed in condition 5, in which the left eye was sampled without face context present. MI in this condition was also higher in older than in young participants ($\text{difference}_{\text{older-young}} = 0.039 \text{ bits [0.002, 0.116]}$), suggesting that increasing the visibility of the left eye modulated reaction times in older participants more, contrary to previous findings (Jaworska et al., in prep). Higher MI in older participants was also found in condition 6 (sampling of the right eye when no face context is present), as well as in condition 1 (sampling of the left eye when the right eye was absent in face context).

Table 9 MI(eye, RT).

Values correspond to the median MI (expressed in bits) across young and older participants separately, for each of the six experimental conditions. The last column shows median differences between older and young participants for each condition. Square brackets indicate 95% confidence intervals.

Condition	Young	Older	Older-Young
Sample LE/ RE absent	0.004 [-0.001, 0.012]	0.042 [0.026, 0.060]	0.031 [0.015, 0.047] <i>0.60 [0.27, 0.80]</i>
Sample LE/ RE present	0 [-0.002, 0.009]	0.009 [-0.004, 0.027]	0.003 [-0.001, 0.022] <i>0.22 [-0.13, 0.52]</i>
Sample LE/ RE absent	0.001 [-0.001, 0.008]	0 [-0.002, 0.004]	0 [-0.006, 0.002] <i>-0.09 [-0.40, 0.25]</i>
Sample LE/ RE present	-0.001 [-0.003, 0.001]	-0.001 [-0.004, 0.002]	0 [-0.002, 0.003] <i>0.05 [-0.28, 0.38]</i>
Sample LE	0.023 [0.009, 0.039]	0.077 [0.028, 0.154]	0.039 [0.002, 0.116] <i>0.38 [0.04, 0.65]</i>
Sample RE	0.004 [-0.002, 0.025]	0.037 [0.009, 0.092]	0.016 [0.004, 0.070] <i>0.39 [0.05, 0.65]</i>

To directly test if there was an advantage of manipulating the visibility of the left, as opposed to the right eye for RTs, we then compared MI between pairs of conditions: sampling of the left eye (LE) vs. sampling of the right eye (RE) when the other eye was absent; sampling of LE vs. sampling of RE when the other eye was present; and sampling of LE vs. sampling of RE when no face context was present (Table 10). We did not find any significant differences between modulation of RTs by the left vs. the right eye in young participants. In older participants, increasing the visibility of the left eye modulated RTs to a higher extent than the right eye in two instances: in face context trials, when the opposite eye was absent; as well as in no face context trials.

Table 10 Condition differences in MI(eye, RT): left eye advantage.

Values correspond to the difference in MI (expressed in bits) between sampling of the left and the right eye while the other eye is absent (first row), sampling of the left eye and the right eye while the other eye is present (second row); and sampling of the left and the right eye when there is no face context present (third row). Last column shows median group difference for each of the comparisons.

Comparison	Young	Older	Older-Young
Sample LE/RE abs. – Sample RE/LE abs.	0.003 [-0.002, 0.009]	0.024 [0.010, 0.040]	0.020 [0.002, 0.038] <i>0.39 [0.03, 0.66]</i>
Sample LE/RE pres. – Sample RE/LE pres.	0 [-0.001, 0.006]	0.002 [-0.002, 0.005]	0 [-0.008, 0.004] <i>-0.03 [-0.36, 0.30]</i>
Sample LE – Sample RE	0.008 [-0.002, 0.021]	0.029 [0.013, 0.060]	0.021 [0.002, 0.050] <i>0.35 [0.01, 0.62]</i>

Stronger modulation of RTs by the presence of the left eye when the opposite eye, or the face context was absent, suggested that degrading the visibility of some face regions had an impact on RTs in older participants. To test this, we ran pairwise comparisons between conditions 1, 3, and 5. In all these conditions, visibility of the left eye was manipulated. In addition, the three conditions could be thought of as different levels of stimulus information degradation: the face stimulus was most intact in condition 3, where the face context and the opposite eye were present ('high context information'). In condition 1, some face information was degraded because the right eye was absent while the face context remained intact ('medium context information'). Finally, trials in condition 5 presented the most degraded stimulus, where only the left eye was revealed but the rest of the face was absent ('low context information'). Results are presented in Table 11. Overall, older participants had stronger RT modulation in medium compared with high context information conditions, and weaker RT modulation in medium, as well as high context compared with low context information conditions.

Table 11 Condition differences in MI(eye, RT): effects of decreasing stimulus information available from the face.

Values correspond to the difference in MI (expressed in bits) between: sampling of the left eye while the right eye is absent, and sampling of the left eye while the right eye is present (first row); sampling of the left eye while the right eye is absent, and sampling of the left eye without face context (second row); as well as sampling of the left eye while the right eye is present, and sampling of the left eye without face context (third row). Last column shows median group difference for each of the comparisons.

Comparison	Young	Older	Older-Young
Sample LE/RE abs. – Sample LE/RE pres.	0.002 [-0.000, 0.009]	0.041 [0.026, 0.057]	0.034 [0.019, 0.053] <i>0.70 [0.39, 0.86]</i>
Sample LE/RE abs. – Sample LE	-0.007 [-0.028, 0.004]	-0.039 [-0.102, -0.003]	-0.025 [-0.082, 0.011] <i>-0.20 [-0.51, 0.16]</i>
Sample LE/RE pres. – Sample LE	-0.021 [-0.034, -0.009]	-0.074 [-0.149, -0.024]	-0.046 [-0.117, -0.002] <i>-0.37 [-0.64, -0.02]</i>

In sum, here we show that increasing the visibility of the left eye modulates RTs more than the right eye in older participants when the face context is present, as well as when it is absent. In contrast, young participants do not show preferential modulation of RTs by increasing the visibility of the left eye. In addition, modulation of RTs by the left eye visibility in older participants changes according to the amount of face information available: larger modulation of RTs was found on trials in which the opposite eye was absent compared with trials in which it was present. Similarly, larger modulation of RTs was found on trials where the face context was absent compared with those where face context was present, with a slightly larger difference found for trials where the right eye was also present. In young participants, this pattern was found only for the difference between the most intact condition (sampling of the left eye + the right eye present in face context) and the least intact condition (sampling of the left eye when face context is absent). As such, here we show that despite high accuracy in discriminating a face from noise, degrading the visibility of part of the face, especially the left eye, has a small effect on reaction times in older, but not young participants.

AGE-RELATED DIFFERENCES IN EYE SENSITIVITY WHEN FACE CONTEXT IS PRESENT

Previously, using Bubbles we have shown that processing of the contralateral eye in older adults is delayed by about 40 ms in both hemispheres, and weaker by about 43% in the left, and by about 58% in the right hemisphere. Here, we revisit this question and compare the time courses of MI about contralateral, as well as ipsilateral eye visibility when face context is present.

First, we consider whether there are any group differences in eye sensitivity regardless of the presence or absence of the opposite eye. To this end, we ran MI on concatenated conditions 1 and 2 (sampling of the left eye: contralateral to the right hemisphere, and ipsilateral to the left hemisphere), and concatenated conditions 3 and 4 (sampling of the right eye: contralateral to the left hemisphere, and ipsilateral to the right hemisphere) when face context is present. We present results regardless of the hemisphere in Figure 11.

Contrary to previous findings, the time course of EEG sensitivity about the contralateral eye was weak and did not show a clear peak either in young or in older participants (Figure 11). Only a small deflection from baseline could be seen between 100 and 200 ms in both groups of participants, followed by another deflection that occurred between 200 and 300 ms in young participants. Maximum MI values taken across all time points were generally low: median maximum MI in young participants was 0.03 bits [0.03, 0.04], and 0.03 bits [0.02, 0.04] in older participants. There were no group differences either in maximum MI or its latency (max MI difference = 0.003 bits [-0.004, 0.010]; latency difference = -9 ms [-61, 37]). MI peaked on average around 200 ms in young and 211 ms in older participants. However, the variability of peak latencies was large in both groups (inter-quartile range (IQR), young = 135 ms, 25th and 75th percentiles = [142, 277]; IQR, older = 156 ms [142, 298]).

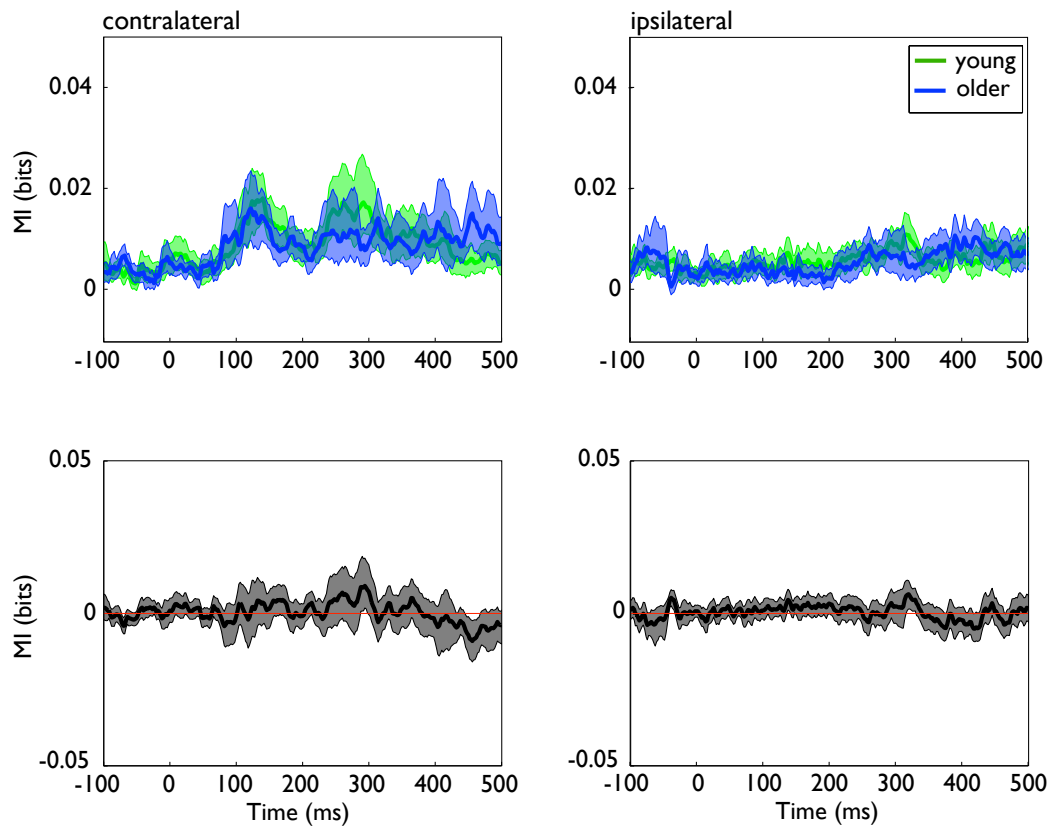


Figure 11 Age-related differences in eye sensitivity with face context present.

Top panel shows MI time courses for processing of the contralateral (left) and the ipsilateral (right) eye, separately for young (green) and older (blue) participants. Time courses show maximum MI across sensors on the left and the right hemisphere. Bottom panels show the difference between groups. Shaded areas correspond to 95% confidence intervals.

Next, we looked at processing of the eye when no face context was present (Figure 12). This condition was hypothesized to be similar to Bubbles stimuli used previously, in which only a small portion of the face was revealed on any given trial (Jaworska et al., in prep). We first report results on the contralateral eye sensitivity, separately for the left and the right hemisphere (Figure 12A) before moving on to report ipsilateral eye sensitivity (Figure 12B).

In conditions when face context was absent, we observed a pattern of MI that was different from previous findings (Rousselet et al., 2014; Jaworska et al., in prep). Average MI time courses about the contralateral eye tended to rise slowly and peak in the time window of 250-350 ms both in young (OTL: 285 ms [232, 319]; OTR: 262 ms [218, 286]) and older (OTL: 327 ms [299, 383]; OTR: 299 ms [263, 352]) observers. Maximum MI was delayed in older compared to young participants ($\text{difference}_{\text{young-older}}$, OTL: -48 ms [-120, -2]; OTR: -56 ms [-121, -6]), but not significantly weaker ($\text{difference}_{\text{young-older}}$, OTL: 0 bits [-0.02, 0.01], OTR: 0.02 bits [-0.03, 0.06]). Median 50% ITs were delayed by 23 ms [7, 40] in older participants compared with young participants.

Sensitivity to the ipsilateral eye was generally weak in both groups (Figure 12B). Maximum MI was similar across the two groups ($\text{difference}_{\text{young-older}}$, OTL: 0.01 bits [-0.02, 0.02], OTR: 0.01 bits [-0.01, 0.03]), but delayed in older observers by about 80 ms in both hemispheres (OTL: 78 ms [1, 148], OTR: 78 ms [2, 147]). 50% ITs were delayed by about 33 ms [14, 54] in older compared with young participants.

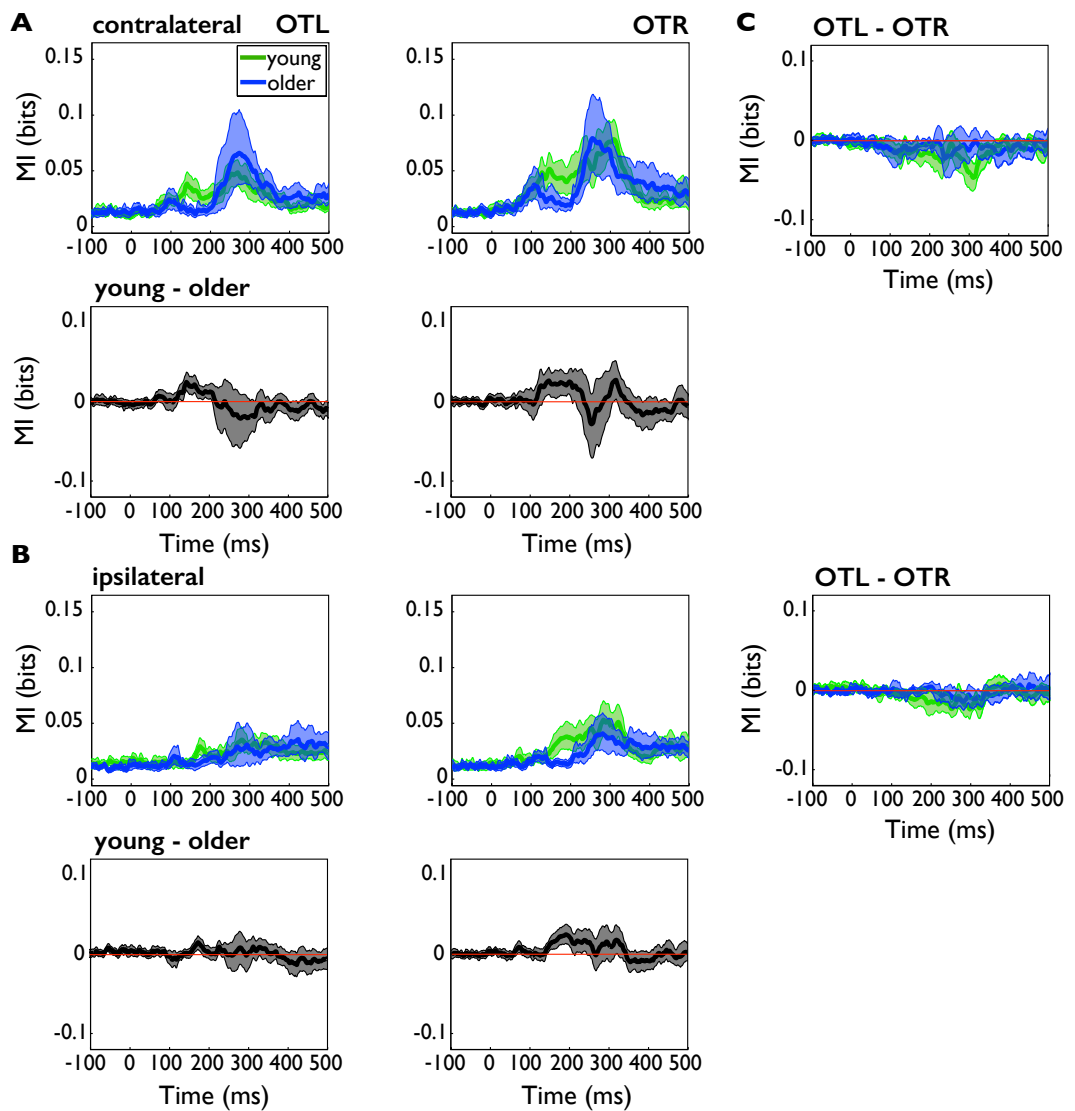


Figure 12 Age-related differences in eye sensitivity with face context absent.

(A) Contralateral eye sensitivity. Plotted are MI time courses for processing of the eye contralateral to the occipital-temporal sensor on the left hemisphere (OTL) and on the right hemisphere (OTR). Separate MI time courses are plotted for young (green) and older (blue) participants, with the difference between groups plotted in the bottom row. Shaded areas correspond to 95% confidence intervals. **(B)** Ipsilateral eye sensitivity. **(C)** Top panel: MI time courses for the difference in contralateral eye sensitivity between OTL and OTR, for young and older participants separately. MI was slightly stronger at OTR than OTL around 300 ms in young (0.04 bits [0.02, 0.06]), but not in older (0.03 bits [-0.01, 0.06]) participants. Bottom panel: MI time courses for the difference in ipsilateral eye sensitivity between OTL and OTR. MI was slightly stronger at OTR than OTL in young (difference: 0.01 bits [0.0003, 0.03]) but not older adults (difference: 0 bits [-0.01, 0.01]).

We then compared processing of the contralateral eye with the ipsilateral eye. Maximum MI about the contralateral eye was stronger than about the ipsilateral eye at OTR in young and older participants alike: by about 0.03 bits [0.02, 0.05] in young, and 0.03 bits [0.003, 0.06] in older participants. No differences were found at OTL: young participants = 0.004 bits [-0.002, 0.018], older participants = 0.02 bits [-0.001, 0.03]. Latencies of maximum MI did not differ between conditions in young (difference_{contra-ipsi}, OTL: -7 ms [-49, 30], OTR: 5 ms [-35, 40]) or older participants at OTL (-27 ms [-94, 37]). There was, however, a delay of 30 ms [6, 70] in processing the ipsilateral eye with respect to contralateral eye at OTR in older participants, a result confirmed with integration times difference of 27 ms [13, 39] (difference_{contra-ipsi}, young: -12 ms [-26, 8]). Looking at individual participants' time courses (Figure S7 in Appendix B), however, revealed that the time courses of ipsilateral eye sensitivity in when face context is absent were generally flat and the results should be treated with caution.

MUTUAL INFORMATION ABOUT CATEGORICAL DIFFERENCES BETWEEN FACE AND TEXTURE

In order to relate our experimental design to previous studies in the lab (Bieniek et al., 2013; Rousselet et al., 2009, 2010), next we ran MI analysis about categorical differences between ERP responses to face and texture trials in each condition. To this end, we compared trials with the highest phase coherence level (between 50% and 60%) with textures.

MI was higher at OTR than OTL in young and in older participants (Table S5 in Appendix B), in line with the reported dominance of the right hemisphere for face processing (Sergent et al., 1992). There were no group differences in the hemispheric differences in maximum MI or its latency (Tables S5 – S6 in Appendix B). As such, here we present results only for the right hemisphere (Figure 13; for detailed depiction of results at OTL, see Figure S8 and Tables S2 – S4 in Appendix B).

In line with previous findings (Rousselet et al., 2009, 2010; Bieniek et al., 2013), categorical MI about the face/texture contrast measured in young participants tended to peak in the 100-200 ms time window in face context conditions (Figure 13). Median MI latencies in each condition are presented in Table 13.

In contrast to that, we observed a qualitative change in the MI time courses in older adults (Figure 13). Specifically, older adults tended to show face sensitivity in two time windows: the first one, weaker, around 140 ms and the second, stronger, around 230 –

250 ms. As such, older participants' maximum MI latency was delayed by about 50 – 90 ms in face context conditions (for group differences in MI latencies, see Table 13). Looking at 50% integration times revealed group differences of about 30 – 45 ms depending on condition (Table 14). The time courses of the difference between young and older participants (Figure 13) revealed that MI was stronger in the group of young participants in the early time window, but weaker in the later time window. In fact, taking the maximum MI across all time points revealed no significant group differences in any condition (Table 12).

Using unplanned comparisons, we found some differences between face context conditions in a group of young participants. Specifically, it appeared that contrasting textures with trials where either the left or the right eye was present, while the opposite eye was sampled, was associated with higher MI than when the eye was absent (contra/ipsi abs. – contra/ipsi pres. = -0.05 bits [-0.09, -0.003]; contra/ipsi abs. – ipsi/contra pres. = -0.05 bits [-0.09, 0.01]; ipsi/contra abs. – contra/ipsi pres. = -0.07 bits [-0.12, -0.002]; ipsi/contra abs. – ipsi/contra pres. = -0.07 bits [-0.13, -0.01]). The absence of the left or the right eye was also associated with slightly later MI latency (contra/ipsi abs. – contra/ipsi pres. = 13 ms [2, 20]; ipsi/contra abs. – contra/ipsi pres. = 16 ms [5, 28]; ipsi/contra abs. – ipsi/contra pres. = 15 ms [-1, 30]). These results could point to a facilitatory effect of the visibility of both eyes in driving categorical responses to face stimuli. However, the effects from these unplanned comparisons were weak and would need to be replicated before drawing any strong conclusions.

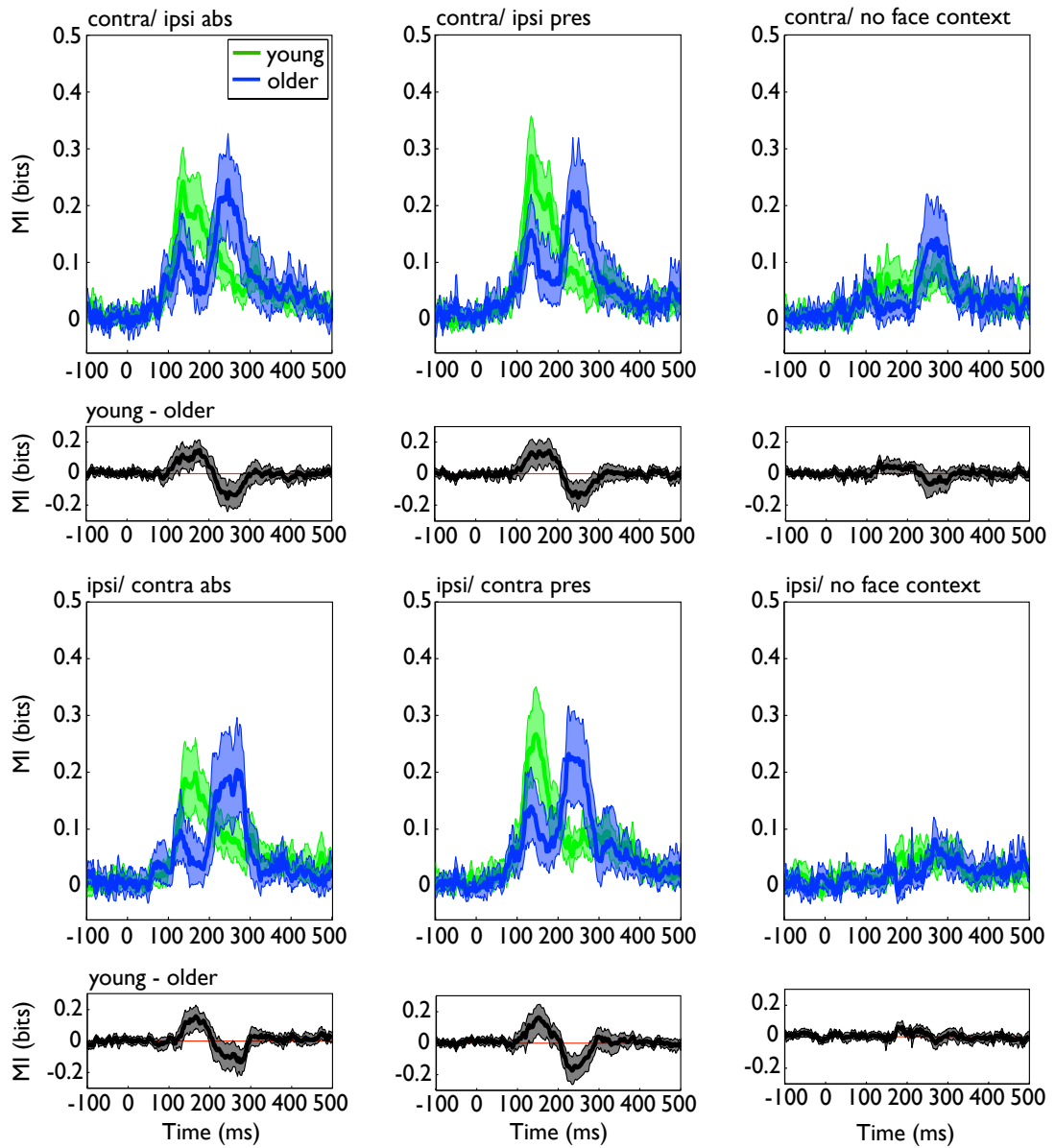


Figure 13 MI(face/noise, ERP) at OTR.

MI time courses are presented for each condition and separately for young (green) and older (blue) participants. The mean difference between young and older participants is plotted in black in separate panels. Shaded areas correspond to 95% confidence interval.

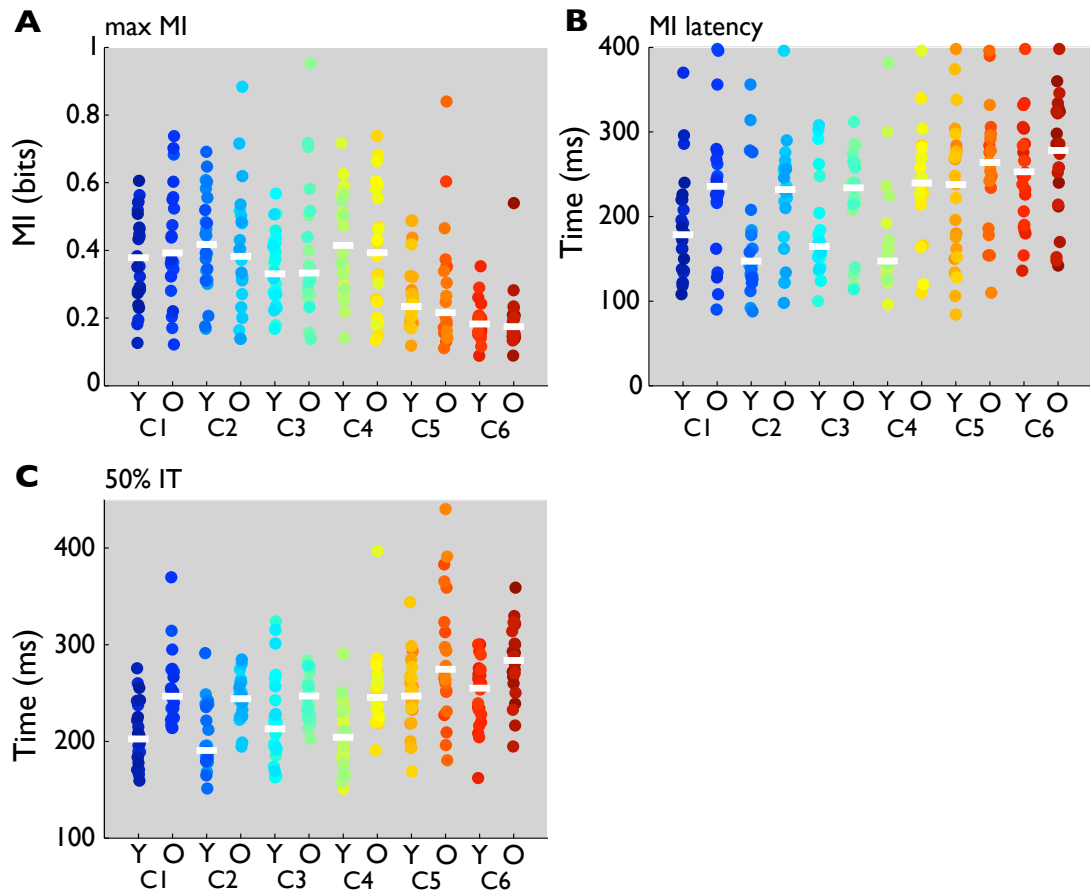


Figure 14 Scatterplots of individual maximum MI, latency and 50% integration times.

Each dot corresponds to individual participant's measure of interest: maximum MI (**A**), max MI latency (**B**), or 50% integration time (**C**). Dots are grouped by age (young participants: Y, older participants: O) and condition (C1: sampling of the contralateral eye when the ipsilateral eye is absent; C2: sampling of the contralateral eye when the ipsilateral eye is present; C3: sampling of the ipsilateral eye when the contralateral eye is absent; C4: sampling of the ipsilateral eye when the contralateral eye is present; C5: sampling of the contralateral eye without face context; C6: sampling of the ipsilateral eye without face context). Maximum MI and its latency were taken across the cluster of electrodes in the right hemisphere, whereas 50% integration times were computed across all sensors in the left and the right hemisphere. White lines correspond to the median across participants in each group and condition.

Table 12 Categorical differences: maximum MI.

Values correspond to the median of the maximum MI across time points (expressed in bits), separately for young and older participants, for the categorical differences between each of the experimental conditions and textures. The last column shows the median of pairwise differences between older and young participants. Square brackets indicate 95% confidence intervals. Cliff's *delta* estimates are presented in italics.

	Young	Older	Older-Young
Contra/ Ipsi abs.	0.38 [0.30, 0.46]	0.39 [0.33, 0.51]	0.03 [-0.07, 0.13] <i>0.13 [-0.22, 0.44]</i>
Contra/ Ipsi pres.	0.42 [0.35, 0.50]	0.38 [0.30, 0.47]	-0.04 [-0.14, 0.06] <i>-0.11 [-0.43, 0.23]</i>
Ipsi/ Contra abs.	0.33 [0.28, 0.40]	0.33 [0.28, 0.43]	0.01 [-0.06, 0.09] <i>0.06 [-0.28, 0.38]</i>
Ipsi/ Contra pres.	0.42 [0.34, 0.51]	0.39 [0.29, 0.51]	-0.02 [-0.14, 0.08] <i>-0.08 [-0.41, 0.26]</i>
Contra	0.23 [0.20, 0.28]	0.22 [0.17, 0.31]	-0.02 [-0.07, 0.05] <i>-0.13 [-0.46, 0.22]</i>
Ipsi	0.18 [0.16, 0.20]	0.17 [0.15, 0.20]	-0.01 [-0.03, 0.02] <i>-0.06 [-0.39, 0.28]</i>

Table 13 Categorical differences: MI latency.

Values correspond to the median of the maximum MI latency (expressed in milliseconds), separately for young and older participants, for the categorical differences between each of the experimental conditions and textures. The last column shows the median of pairwise differences between older and young participants. Square brackets indicate 95% confidence intervals. Cliff's *delta* estimates are presented in italics.

	Young	Older	Older-young
Contra/ Ipsi abs.	179 [155, 204]	236 [212, 257]	52 [7, 88] <i>0.39 [0.03, 0.67]</i>
Contra/ Ipsi pres.	147 [132, 174]	232 [203, 251]	72 [23, 101] <i>0.43 [0.06, 0.69]</i>
Ipsi/ Contra abs.	165 [155, 186]	234 [213, 256]	61 [18, 85] <i>0.40 [0.02, 0.67]</i>
Ipsi/ Contra pres.	147 [135, 163]	240 [224, 262]	89 [53, 110] <i>0.63 [0.27, 0.83]</i>
Contra	238 [184, 272]	264 [238, 289]	23 [-11, 82] <i>0.20 [-0.15, 0.49]</i>
Ipsi	253 [221, 279]	278 [241, 317]	20 [-22, 63] <i>0.17 [-0.18, 0.47]</i>

Table 14 Categorical differences: 50% integration times.

Values correspond to the median of time to integrate 50% of the MI time course (expressed in milliseconds), separately for young and older participants, for the categorical differences between each of the experimental conditions and textures. The last column shows the median of pairwise differences between older and young participants. Square brackets indicate 95% confidence intervals. Cliff's *delta* estimates are presented in italics.

	Young	Older	Older-young
Contra/ Ipsi abs.	203 [190, 219]	247 [232, 262]	45 [27, 62] <i>0.67 [0.36, 0.84]</i>
Contra/ Ipsi pres.	191 [183, 210]	244 [232, 255]	46 [33, 61] <i>0.72 [0.42, 0.88]</i>
Ipsi/ Contra abs.	213 [196, 235]	247 [235, 257]	32 [11, 49] <i>0.44 [0.08, 0.70]</i>
Ipsi/ Contra pres.	204 [183, 227]	246 [235, 261]	44 [20, 65] <i>0.61 [0.29, 0.81]</i>
Contra	247 [234, 261]	275 [255, 309]	31 [5, 67] <i>0.39 [0.04, 0.65]</i>
Ipsi	255 [236, 268]	284 [267, 303]	31 [8, 53] <i>0.47 [0.13, 0.71]</i>

REVERSE ANALYSIS

In previous studies, we have shown that a reverse analysis – whereby stimulus information is linked to modulations of the N170 amplitude and latency – can provide important information about the age-related differences in coding of the eye by the N170, which is otherwise missing from MI analysis (Rousselet et al., 2014; Jaworska et al., in prep). Visibility of the eye revealed through Bubble masks was associated with significantly earlier and larger N170 in young participants, particularly in the right hemisphere. In older participants, on the other hand, only modulation of amplitude but not latency was found for trials with higher eye visibility, and the effect was similar across hemispheres (Jaworska et al., in prep).

Here, we performed the reverse analysis in a similar vein, separately for each of the six experimental conditions in order to check whether a small MI deflection from baseline observed in Figure 11 was associated with a qualitatively similar modulation of the N170 as in the previous studies. To this end, we binned the visibility of the sampled eye in each condition into 6 discrete bins, such that bin 1 contained trials with the lowest eye visibility (1 – 10% phase coherence), and bin 6 contained trials with the highest eye visibility (51 – 60% phase coherence). We then averaged ERPs corresponding to trials in each of the bins, and plotted them separately for each condition and age group (Figure 15). Since the pattern of results was similar in both hemispheres, we only present results at OTR (for detailed depiction of results at OTL, see Figures S9 – S10 and Tables S8 – S9 in Appendix B).

From the graphical depiction of results in Figure 15 it can be seen that a small modulation of ERPs by binned eye visibility was present in young participants for sampling of the contralateral eye (Figure 15A). Considerable modulation of amplitude was also present in conditions where face context was absent (Figure 15A, rightmost panels). In older participants, on the other hand, ERPs seemed to be rather similar regardless of the bin or condition (Figure 15B). In order to quantify these differences, or lack thereof, we computed the N170 latency and amplitude modulation indices in a similar vein to previous studies (Rousselet et al., 2014; Jaworska et al., in prep). Specifically, in individual participants we subtracted average latencies in bin 1 from those in bin 6, and divided average amplitudes in bin 1 by those in bin 6 to obtain a ratio of amplitudes (Figure 16; for numerical values, see Table 15). We then computed the median of pairwise differences between young and older participants for each condition (Figure 16, Table 16).

We found a significant N170 latency modulation by contralateral eye visibility in young participants, in both conditions: when the ipsilateral eye was present, and when it was absent. Compared to trials with low eye visibility, high eye visibility was associated with the N170 latency shorter by 4 ms [2, 7] when the ipsilateral eye was absent, and by 3 ms [1, 6] when the ipsilateral eye was present. In older participants, latency modulation was also 4 ms in both conditions, although the confidence intervals were a bit wider ([-8,1] in both conditions). No other modulation of latency was found in young participants or older participants (Table 15). Likewise, the only significant amplitude modulation in young participants was found for contralateral eye sensitivity. On those trials, higher eye visibility was associated with amplitudes that were 1.17 times the size of those on trials with low eye visibility (95% CI: ipsilateral absent, [1.01, 1.35]; ipsilateral present, [0.95, 1.44]). No significant modulations of amplitude were found in older participants in any condition.

Although it appears from Figure 15 that in young participants there was a considerable modulation of amplitude in conditions without face context present, quantifying the modulation in individual participants revealed large inter-individual variability. This can be seen in large confidence intervals depicted by vertical lines in Figure 16, such that amplitudes on high visibility trials could be anything from 0.36 to 1.73 times the size of amplitudes on low visibility trials (contralateral eye sampling, Table 15).

Instead, ERPs recorded from both groups displayed a non-linear response to the visibility of the eye after 200 ms. Specifically, binning ERPs according to the level of eye visibility revealed that ERPs falling in the first two bins (i.e. lowest eye visibility) were qualitatively different from the rest (i.e. medium and high visibility). As such, we witness a possibly categorical response that might reflect participants' perception of whether the eye (the face) was there (high visibility) or not (low visibility), and that started after 200 ms following stimulus onset. Because the modulation of ERPs by eye visibility occurred late and was not tied to any ERP peak, we could observe a trend of accumulation of sensitivity to the eye over a longer period of time, particularly visible in the MI time course of contralateral eye sensitivity in young participants (Figure 12).

Comparing the N170 latency and amplitude modulation between young and older participants revealed no group differences either in latency or amplitude modulation in any condition (Figure 16, Table 16).

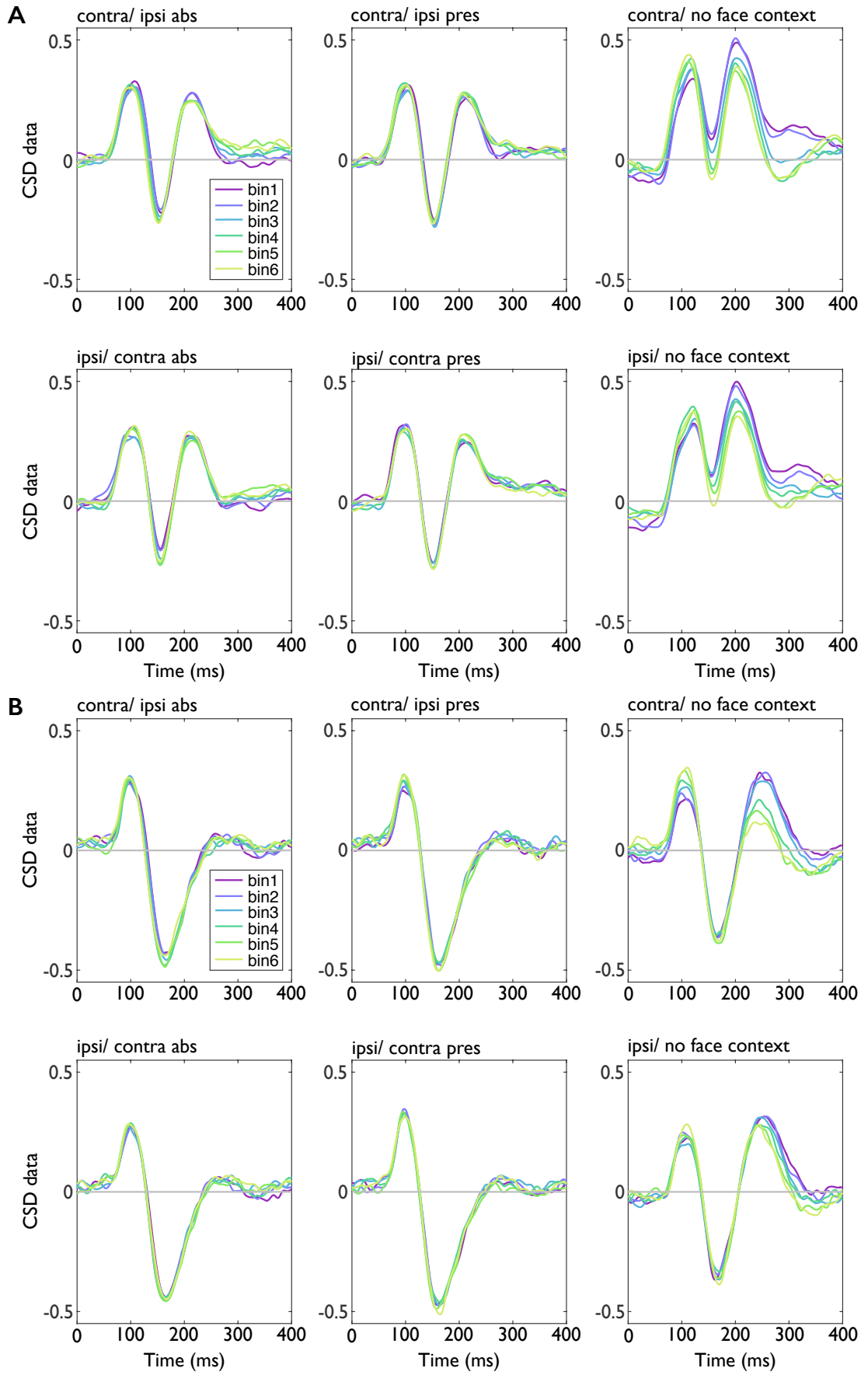


Figure 15 Modulation of ERPs by eye visibility at OTR.

ERPs from each condition are averaged across trials falling in one of six bins corresponding to different levels of eye visibility (bin 1: lowest visibility, bin 6: highest visibility). Average ERPs are presented separately for young **(A)** and older **(B)** participants.

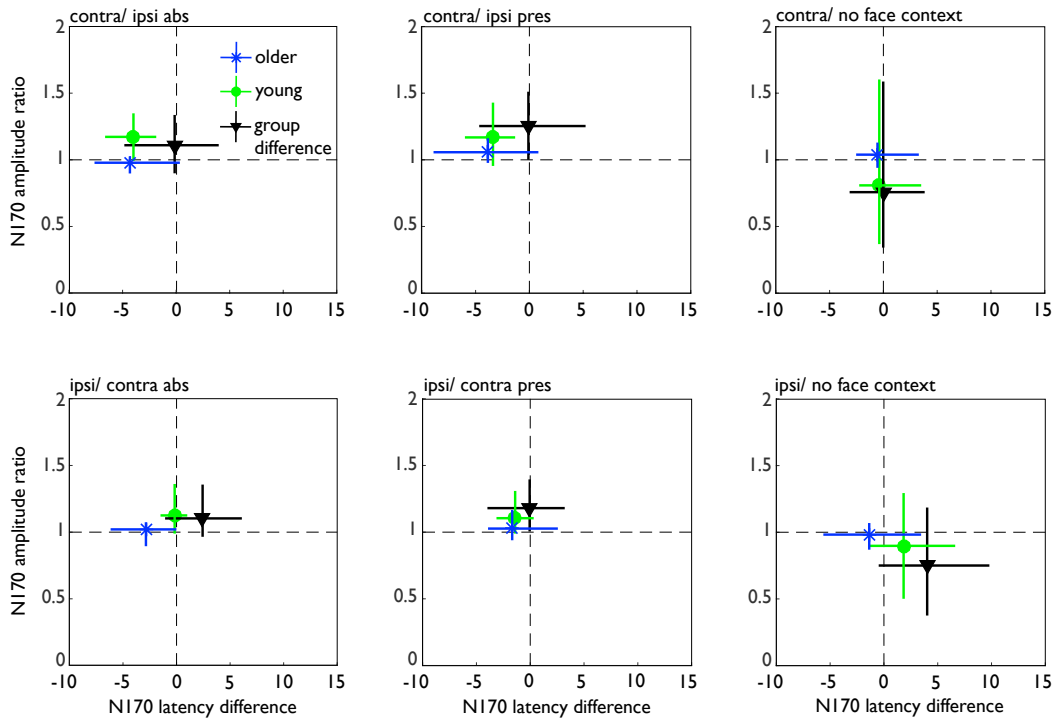


Figure 16 Group-average modulation of the N170 by eye visibility at OTR.

Effects of eye visibility on the N170 latency and amplitude were quantified as a difference between latencies in bin 6 (high visibility) and in bin 1 (low visibility), and as a ratio of amplitudes in bin 1 to amplitudes in bin 6, separately for each condition. For example, negative values on the x-axis (latency modulation, expressed in milliseconds) indicate shorter latencies in bin 6 than bin 1, and positive values on the y-axis (amplitude modulation, expressed as a ratio) indicate larger amplitudes in bin 6 than bin 1. Green circles correspond to the median across young participants, whereas blue stars – to median across older participants. Black squares show median group differences between young and older participants, expressed as a difference in median latency modulations, and a ratio of median amplitude modulations. Vertical and horizontal lines correspond to 95% confidence intervals.

Table 15 Group-average N170 latency and amplitude modulation by eye visibility at OTR.

Values correspond to median of individual participants' latency modulation expressed in milliseconds, and median ratio of amplitudes. In individual participants, latency modulation was calculated by subtracting average latency across trials in bin 1 (low eye visibility) from trials in bin 6 (high eye visibility). Amplitude modulation was calculated by dividing average bin 1 amplitude by average bin 6 amplitude. Square brackets correspond to 95% confidence intervals.

	N170 Latency		N170 Amplitude	
	Young	Older	Young	Older
Contra/Ipsi abs.	-4 [-7, -2]	-4 [-8, 1]	1.17 [1.01, 1.35]	0.98 [0.90, 1.03]
Contra/Ipsi pres.	-3 [-6, -1]	-4 [-8, 1]	1.17 [0.95, 1.44]	1.06 [0.98, 1.16]
Contra/ no face context	0 [-2, 3]	0 [-2, 3]	0.81 [0.36, 1.73]	1.04 [0.95, 1.13]
Ipsi/Contra abs.	0 [-2, 1]	-3 [-6, 0]	1.13 [0.99, 1.37]	1.01 [0.89, 1.07]
Ipsi/Contra pres.	-1 [-3, 0]	-2 [-4, 2]	1.11 [0.98, 1.32]	1.03 [0.94, 1.17]
Ipsi/ no face context	2 [-1, 6]	-1 [-5, 3]	0.90 [0.49, 1.28]	0.98 [0.87, 1.07]

Table 16 Group differences in the N170 latency and amplitude modulation at OTR.

For latency modulation, a median difference between individual latency modulations in the groups of young and older participants was computed. For amplitude modulation, a median ratio of individual amplitude modulations in both groups (young/older) was computed (first row of values), as well as the difference between individual values in young and older groups (second row of values). Corresponding Cliff's *delta* estimates are presented in italics. Square brackets indicate 95% confidence intervals.

	N170 Latency	N170 Amplitude
Contra/Ipsi abs.	0 [-5, 4]	1.11 [0.93, 1.33]
	<i>-0.03 [-0.35, 0.31]</i>	0.15 [-0.03, 0.36] <i>0.36 [0.01, 0.63]</i>
Contra/Ipsi pres.	0 [-4, 4]	1.25 [1.04, 1.54]
	<i>-0.01 [-0.34, 0.33]</i>	0.24 [0.01, 0.45] <i>0.14 [-0.22, 0.46]</i>
Contra/ no face context	0 [-3, 4]	0.76 [0.36, 1.59]
	<i>-0.01 [-0.33, 0.32]</i>	-0.00 [-0.59, 0.87] <i>-0.11 [-0.45, 0.25]</i>
Ipsi/Contra abs.	2 [0, 6]	1.10 [0.96, 1.42]
	<i>0.30 [-0.06, 0.58]</i>	0.10 [-0.05, 0.34] <i>0.30 [-0.05, 0.58]</i>
Ipsi/Contra pres.	0 [-4, 2]	1.18 [1, 1.40]
	<i>-0.03 [-0.35, 0.31]</i>	0.17 [-0.00, 0.36] <i>0.17 [-0.17, 0.48]</i>
Ipsi/ no face context	4 [-1, 10]	0.75 [0.38, 1.18]
	<i>0.25 [-0.08, 0.54]</i>	-0.03 [-0.45, 0.43] <i>0.02 [-0.33, 0.37]</i>

EVENT-RELATED POTENTIALS

The absence of effects in reverse analysis, particularly in older participants, could not be attributed to a lack of evoked responses to face stimuli. To the contrary, both young and older participants had a large N170 to both face and texture images in all conditions, with older participants showing enhanced responses with respect to the young.

Average ERPs are presented in Figure 17. Both young (top panels) and older participants (bottom panels) had a large N170 in each condition with face context present. In addition to that, older participants also had a strong N170-like component towards stimuli without the face context, as well as for textures. In young participants, the responses to textures, as well as to stimuli without face context were weaker than those to stimuli with face context present.

Average N170 latencies and amplitudes for each condition are presented in Table 17, and group differences are presented in Table 18. In general, the N170 was delayed in older compared with young participants, albeit not significantly in most conditions. The differences ranged from 4 ms [-18, 13] for sampling the contralateral eye when the ipsilateral eye was absent (at OTL) to 17 ms [2, 33] when the contralateral eye was sampled on trials without the face context and 20 ms [6, 44] when the ipsilateral eye was sampled and the contralateral eye was present (at OTR). Amplitudes were consistently larger in older than in young participants at both sensors and in all conditions (Table 18).

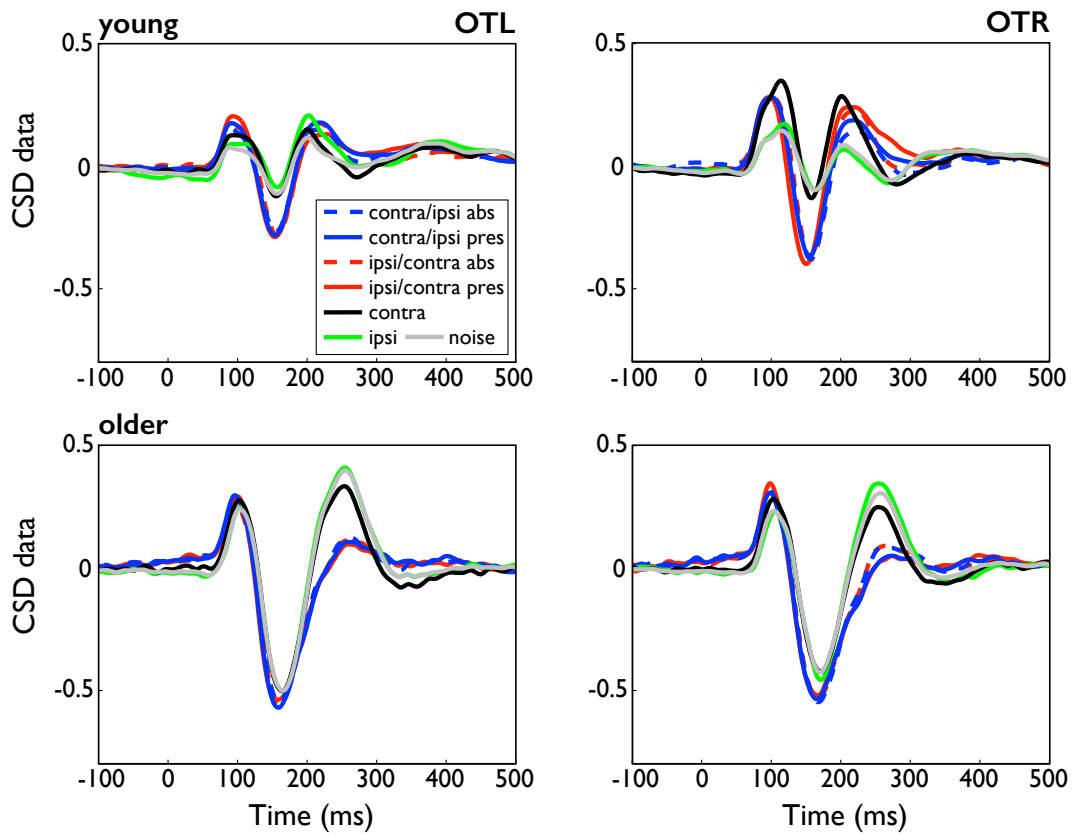


Figure 17 Event-related potentials.

Event-related responses are averaged across young (top) and older (bottom) participants in each of the six experimental conditions and textures, separately at OTL and OTR. CSD data are expressed in $\mu\text{V}/\text{cm}^2$.

Table 17 N170 latency and amplitude averaged across young and older participants.

Latencies are expressed in milliseconds and amplitudes in $\mu\text{V}/\text{cm}^2$. Square brackets indicate 95% confidence intervals.

Condition	OTL		OTR	
	young	older	young	older
N170 latency				
Contra/Ipsi abs.	159 [147, 181]	162 [153, 174]	157 [152, 167]	164 [155, 173]
Contra/Ipsi pres.	158 [144, 219]	160 [152, 173]	157 [152, 168]	162 [156, 177]
Ipsi/Contra abs.	158 [148, 171]	163 [154, 175]	157 [152, 163]	164 [157, 175]
Ipsi/Contra pres.	152 [142, 164]	159 [149, 173]	149 [143, 154]	165 [154, 183]
Contra	163 [147, 182]	169 [158, 181]	156 [141, 166]	172 [162, 182]
Ipsi	165 [148, 184]	169 [158, 182]	163 [156, 176]	171 [163, 182]
N170 amplitude				
Contra/Ipsi abs.	-0.33 [-0.43, -0.26]	-0.59 [-0.72, -0.44]	-0.37 [-0.49, -0.27]	-0.57 [-0.73, -0.44]
Contra/Ipsi pres.	-0.33 [-0.43, -0.28]	-0.62 [-0.75, -0.45]	-0.41 [-0.50, -0.30]	-0.57 [-0.76, -0.43]
Ipsi/Contra abs.	-0.32 [-0.43, -0.26]	-0.59 [-0.71, -0.42]	-0.39 [-0.48, -0.30]	-0.57 [-0.73, -0.43]
Ipsi/contra pres.	-0.34 [-0.44, -0.28]	-0.61 [-0.75, -0.45]	-0.41 [-0.50, -0.29]	-0.58 [-0.76, -0.47]
Contra	-0.25 [-0.32, -0.21]	-0.55 [-0.76, -0.38]	-0.25 [-0.36, -0.19]	-0.50 [-0.66, -0.37]
Ipsi	-0.23 [-0.29, -0.20]	-0.53 [-0.73, -0.37]	-0.25 [-0.31, -0.19]	-0.50 [-0.65, -0.35]

Table 18 Group differences in the N170.

Differences in N170 latency (expressed in ms) and amplitude (expressed in $\mu\text{V}/\text{cm}^2$) between young and older participants. Square brackets indicate 95% confidence intervals for the difference.

	OTL		OTR	
	amplitude	latency	amplitude	latency
Contra/Ipsi abs.	0.22 [0.09, 0.39]	-4 [-18, 13]	0.17 [0.02, 0.38]	-6 [-17, 5]
Contra/Ipsi pres.	0.24 [0.06, 0.44]	-5 [-19, 13]	0.15 [-0.02, 0.33]	-6 [-21, 5]
Ipsi/Contra abs.	0.20 [0.07, 0.38]	-7 [-21, 6]	0.16 [0.01, 0.31]	-8 [-20, 2]
Ipsi/contra pres.	0.22 [0.06, 0.38]	-8 [-21, 6]	0.18 [0.01, 0.33]	-20 [-44, -6]
Contra	0.26 [0.11, 0.45]	-8 [-24, 7]	0.20 [0.07, 0.36]	-17 [-33, -2]
Ipsi	0.27 [0.11, 0.47]	-6 [-23, 10]	0.22 [0.09, 0.39]	-6 [-20, 5]

DISCUSSION

Previously, using Bubbles we have shown that presence of the left eye in the image is associated with faster responses in young and older adults, with more accurate responses in older adults, and with modulation of ERPs recorded on the contralateral hemisphere in the time window of the N170, that was weaker and delayed in older adults. In the present study, we sought to replicate the eye sensitivity in both groups using stimuli in which face context was either present, or absent. To this end, in face context conditions, we manipulated the visibility of either the left or the right eye while the opposite eye was present or absent at the same time. In conditions without face context, visibility of either the left or the right eye was modulated while the rest of the face was phase-randomized.

Investigating the effects of eye visibility on reaction times (RTs) using Mutual Information (MI) revealed that the absence of, or modulating the visibility of the left eye had a greater effect on RTs across older participants, and this RT modulation in older adults increased with decreasing face context information. These results are in line with those reported previously (Jaworska et al., in prep), where modulating the visibility of the left eye, but not the right eye, had a greater effect on RTs in older participants. Notably, in our previous study (Jaworska et al., in prep), older participants also relied much more on the presence of the eyes in the image to make correct responses, in contrast to young adults who could use any feature to correctly discriminate a face from a texture. Here, both groups of participants were equally accurate regardless of whether the face context was present or absent. High accuracy on face context trials, coupled with an effect of the left eye visibility on RTs might suggest that processing of local facial information (such as the eye) is less efficient in older adults (Meinhardt-Injac, Persike, & Meinhardt, 2014), although the effect might be mitigated by increasing the face context available during the task.

In terms of brain sensitivity to the visibility of the eye, quantified with MI, a small deflection from baseline was visible between 100 and 200 ms post-stimulus for the contralateral eye visibility in face context conditions in both groups. However, MI time courses did not show the clear peak observed in previous studies in either group (Rousselet et al., 2014; Jaworska et al., in prep). Comparing maximum MI and its latency between young and older adults revealed no differences. As such, in face context conditions, we did not replicate contralateral eye sensitivity revealed in the Bubbles study either in young or in older participants (Rousselet et al., 2014; Jaworska et al., in prep). We also did not observe any group differences on MI latency or maximum amplitude.

The lack of eye sensitivity could be due to a saturation of face information from other parts of the face, which could be used in the detection task. Provided with this wealth of information in the form of the face context, participants could simply ignore the eyes in making responses as they get used to the stimuli. As such, it would be interesting to run a control experiment in which participants had to attend to the eye region to make a correct response, for example by reporting the number of eyes that could be perceived in the face context, ranging from 0 if both eye regions were phase-randomized to 2 if both eyes were clearly visible.

We then investigated eye sensitivity in the complementary conditions, in which the face context was absent and the eye visibility was modulated. These conditions were hypothesized to be more related to the Bubbles stimulus in a way that only a portion of the image was revealed through an eye aperture. However, modulating eye visibility in the absence of the face context also elicited a different pattern of results than that reported previously. Specifically, in both young and older participants MI peaked in the time window of 250 – 350 ms, which was much later than the peaks of MI reported in the Bubbles study (164 ms [158, 168] in young, and 204 ms [184, 221] in older participants; Jaworska et al., in prep). In the absence of face context, MI was delayed in older compared with young participants by about 50 ms – a delay similar to that reported in the Bubbles study where processing of the contralateral eye was delayed by about 40 ms [23, 57] in older participants (Jaworska et al., in prep). However, MI was not weaker in older participants in the present study, in contrast to the Bubbles study in which older participants' eye sensitivity was only about 57% [42, 82] the size of that of young participants (Jaworska et al., in prep). As such, two main findings emerge from conditions in which the face context was absent. First, similarly to face context conditions, we did not replicate the contralateral eye sensitivity in the first 200 ms of stimulus processing either in young or in older participants. On the other hand, we observed eye sensitivity that peaked much later (250 – 350 ms) in both groups and was delayed, but not weaker in older participants.

Altogether, our results show that strong eye sensitivity observed in a face detection task using Bubbles (Rousselet et al., 2014; Jaworska et al., in prep) is not generalizable to stimuli in which the face context is preserved, or stimuli in which the face context is absent.

The lack of eye sensitivity may suggest that the EEG activity in the first 200 ms of stimulus processing does not reflect encoding of a single feature – the contralateral eye. In order to test this possibility and to relate our findings to previous studies (Rousselet et

al., 2014; Jaworska et al., in prep) we conducted a reverse analysis in which we related eye visibility to the modulation of the latency and amplitude of the N170. Previously, we reported a large latency and amplitude modulation of the N170 in young participants when the contralateral eye visibility increased through Bubble masks (Rousselet et al., 2014; Jaworska et al., in prep): on average, in young adults the N170 recorded on the right hemisphere was 24 ms [17, 31] earlier and 153% [132, 175] larger when the left eye was visible compared to when it was not. On the other hand, in older adults it was 161% [141, 181] larger, and only 5 ms [2, 11] earlier. In the current study, in face context conditions we found a significant latency and amplitude modulation for the contralateral eye in young participants, but it was much smaller compared with previous results: with higher eye visibility, the N170 was earlier by about 3 – 4 ms [2, 7], whether the ipsilateral eye was present or absent. In both conditions, on trials with high eye visibility the N170 was also 1.17 times (or 117%) larger than that on trials with low eye visibility. There was no amplitude modulation in older adults, but their N170 was, on average, also earlier by 4 ms [-1, 8] on high visibility trials. There was no modulation of the N170 by the ipsilateral eye in either group, in line with flat M1time courses for the ipsilateral eye sensitivity. Importantly, the reverse analysis in the current study confirmed the results obtained with MI: that there were no age-related differences in coding of the contralateral eye by the N170 in face context conditions. Altogether, the reverse analysis revealed these findings:

- First, in both groups the N170 was earlier by about 4 ms when the eye visibility was high compared with low, and also slightly larger in amplitude in young, but not older participants.
- Second, the N170 amplitude and latency modulation by eye visibility in young, but not older participants was much smaller in the present study compared with that reported in the Bubbles study.
- Third, the N170 amplitude and latency modulation by eye visibility did not differ across the two age groups in the present study when face context was present, in contrast to the Bubbles study that revealed considerable age-related differences.

Contrary to previous findings (Rousselet et al., 2014), our results suggest that the N170 is not primarily concerned with coding the contralateral eye when face context is present. Instead, depending on the experimental paradigm and task demands, the N170 might reflect a number of processes, including but not limited to an automatic response to the eyes (Bentin et al., 1996; Itier et al., 2007; Schyns, Jentzsch, Johnson, Schweinberger, & Gosselin, 2003; Smith et al., 2004), structural encoding of the face components (Eimer, 1998), feature detection or the encoding of information diagnostic to the task at hand,

such as the mouth in emotion recognition task (Schyns et al., 2007; Van Rijsbergen & Schyns, 2009). Indeed, there is no reason to believe that an ERP peak, such as the N170 is equivalent to a single functional brain component (Luck, 2005). Instead, activity recorded at one EEG sensor on any given time point might reflect a mixture of sources and processes (Luck, 2005). For example, it has been suggested that at least three different brain areas are synchronously active in the time window of the N170: the occipital extrastriate area, the more anterior area around the fusiform gyrus (Itier, Herdman, George, Cheyne, & Taylor, 2006), as well as a region in the superior temporal sulcus (STS) (Itier & Taylor, 2004). Furthermore, Itier et al. (2007) suggested that both face-selective and eye-selective neurons coexist in STS and may contribute to the observed N170 depending on the stimulus characteristics. For example, single-cell recordings in monkeys revealed that majority of face-selective cells continue to respond even if parts of the face (e.g. the eyes) are obscured, whereas other, eye-selective cells respond to the eyes presented in isolation but fail to respond to the whole face when the eyes are obscured (Perrett, Rolls, & Caan, 1982). In a similar vein, eye-selective neurons may fail to respond when presented in a face context, but start responding when the face context/configuration is disrupted and the eye is no longer perceived in a normal face context in humans (Itier et al., 2007). For example, contrast reversal or inversion (or, perhaps, the use of Bubble masks) could lead to disruption of the normal face context and an additional activity of the eye-selective neurons, leading to an increase in the N170 amplitude (Itier et al., 2007). In our study, the modulation of eye visibility was associated with a small amplitude modulation in young participants, such that weaker eye visibility was associated with smaller amplitude. Weaker eye visibility was also associated with a longer N170 latency, in line with previous studies reporting a similar delay of 4 ms in responses to faces without the eyes compared with whole faces (Eimer, 1998; Itier et al., 2007). These results suggest a disruptive effect of manipulating eye visibility on the N170 that might affect structural face encoding (Eimer, 1998), or the additional involvement of eye-selective neurons that start responding when the normal face context is disrupted (Itier et al., 2007), or both. However, these two possibilities are difficult to disentangle in the current paradigm. Interestingly, we did not observe any eye sensitivity in the time window of the N170 in conditions where the face context was absent. Neither the latency nor the amplitude of the N170 was modulated by the visibility of the eye in either group. These results suggest that when face context was absent, the N170 did not code the presence of the eyes, in contrast to classic ERP studies showing that presenting the eyes in isolation leads to even larger responses than presenting a face (Bentin et al., 1996; Itier et al., 2007).

Our results are hard to compare with previous studies because of inherent differences in stimulus characteristics. Specifically, here we manipulated eye visibility in a parametric manner while keeping the face context present or not, whereas previous studies compared whole face images with images of faces without the eyes (Eimer, 1998; Itier et al., 2007), and images of isolated eyes (Itier et al., 2007). Also, whereas in previous studies the eyes were completely removed, thereby leaving the eye region blank, here we manipulated phase coherence of the eye region such that some local contrast in the eye region was preserved. Finally, in contrast to previous studies, we presented either the left or the right eye without the face context, but not *in isolation*. Instead, the face context was phase-randomized to preserve the overall contrast of the image, and the eye at different levels of visibility was presented in the periphery. As such, conclusions from past studies may not generalize to our current paradigm.

In terms of conditions in which the face context was absent, it could be argued that weak eye sensitivity was due to representation of noise at the fovea when participants fixated the centre of the screen. Information presented at the fovea is processed more efficiently than in the periphery, due to cortical magnification in V1 (Azzopardi & Cowey, 1993) that is then used to bias image representations in higher-level processing regions, such as in the inferotemporal cortex (Rolls, Aggelopoulos, & Zheng, 2003). The foveal bias (i.e. more efficient processing of stimuli presented at or near fixation) could explain faster responses to foveal than extra-foveal stimuli (Lueschow, Miller, & Desimone, 1994). In our study, since the task involved detecting a face, a stronger foveal representation of noise would be expected to hamper behavioural performance – which we indeed observed in both groups of participants who were slower and less accurate when face context was absent compared to when the face context was present. As such, the full account of face/eye detection mechanisms should consider the influence of cortical magnification and fixation locations that could either amplify or abolish sensitivity to eye features (de Lissa et al., 2014; Nemrodov, Anderson, Preston, & Itier, 2014; Rousselet et al., 2014; Zerouali et al., 2013).

Nevertheless, it remains clear that modulating the visibility of the eye in the face context has a small effect on the N170, and this effect is much larger when the face context is obscured with Bubble masks (in young participants). Future research should clarify whether same or different processes underlie the observed amplitude and latency modulations of the N170 in the two paradigms. Specifically, if the N170 reflects two independent processes: one responsible for feature detection, and another for face perception, it would be interesting to test how much face context is sufficient for the N170 to respond to the face, before switching to detecting an eye (or another feature). It

would also be interesting to see whether the same sources in the brain respond most strongly to the eye when the face context is preserved or disrupted, for example using magnetoencephalography (MEG).

Source localization could prove particularly useful in the context of ageing, in order to understand whether the same brain areas respond to the eyes with or without the face context. To date, only one study compared face processing in young and older adults using MEG, and did not report differences in source locations despite age-related delays on the M170, a magnetic counter-part of the N170 (Nakamura et al., 2001). However, the task in that study was not related to processing faces – instead, participants detected a cross within a stream of images. Furthermore, there was no stimulus variability within the face stimulus, therefore the observed neuro-magnetic response could have reflected general processing of any visual stimulus – unlike in our studies.

To recap our age-related effects, previously we found that single-trial EEG responses in both young and older participants alike were driven mostly by the presence of the contralateral eye revealed through Bubble masks (Jaworska et al., in prep). In older adults, this eye sensitivity was delayed and weaker, as well as associated with a modulation of the N170 amplitude and only a 4 ms modulation of the N170 latency. In young adults, presence of the eye was associated with much larger latency modulation and similar amplitude modulation as in older adults. In the current study, when face context was present the N170 latency and amplitude modulation by eye visibility was very small in both young and older participants. Crucially, we did not find any N170 group differences when the face context was present. These results suggest that neural processing of faces (and more specifically, the eye) might be differentially affected in older adults when revealed through Bubble masks, and remain unaffected when the face context is intact. This suggestion would be in line with a previous study showing that degradation of face stimuli had a greater effect on older adults, although the age difference was reduced when performance on non-degraded faces was taken into account (Grady et al., 2000). In that study, different brain regions displayed correlations with behaviour on degraded face matching – in young adults, it was an area in the fusiform gyrus; whereas in older adults, a posterior occipital region, in addition to the thalamus and hippocampus (Grady et al., 2000). As such, a degree of brain plasticity in terms of regions responsible for performance on the same perceptual task was observed in older adults. Given that we did not find age-related differences on the processing of the eye when presented in the face context, but we did find such differences on the processing of the eye revealed through Bubble masks, an outstanding question remains whether older adults use the same or different functional brain networks in an easy

(present study) and a difficult (Bubbles study) task, and whether these networks are different between young and older adults. Indeed, several fMRI studies reported that lower, or less differentiated (Park et al., 2004) activity in brain areas responsible for perceptual tasks in visual cortices are accompanied by a pattern of over-recruitment of frontal areas (Grady et al., 1994; Madden et al., 2004; Payer et al., 2006), often termed a posterior-anterior shift in ageing (Davis et al., 2008).

Although EEG lacks the spatial resolution of fMRI, and therefore would not be able to compare activity from separate brain regions and shed light on plasticity in functional brain networks, an MEG study could overcome such difficulties. Nevertheless, our previous studies seem to support the notion of de-differentiation of neural responses in the early visual processing to some extent (Rousselet et al., 2009). In particular, comparing responses elicited by full images of faces and textures revealed that whereas young adults had a clear peak of discriminatory activity in the 140 – 180 ms time window, in older adults it tended to be spread over a longer period of time and present over two peaks – one weaker, around 150 – 160 ms and one stronger that peaked around 230 ms (Rousselet et al., 2009, 2010; Bieniek et al., 2013). Importantly, the activity in the time window of the N170 seemed to become less face-sensitive with age (Rousselet et al., 2009). Here, using a categorical comparison between faces and textures in each experimental condition, we found a similar pattern of responses, where MI was weaker in older adults in the early time window and stronger in the later time window when face context was present. As such, in older adults the maximum discriminatory activity peaked in the second time window, and was delayed by 32 – 45 ms. The nature of the second peak of stimulus discriminability in older adults remains unclear and could be explained either as a delayed processing of visual stimulus, where a later time window becomes functionally equivalent to the N170 in older subjects, or be a consequence of additional attentional resources required by older subjects to perform the task. The first possibility is rather unlikely given our two sets of findings: first, in our Bubbles study, processing of the same information (the contralateral eye) occurred in the same time window of the N170, albeit the N170 was delayed in older participants with respect to the young. Second, in the present study we found no group differences in the modulation of the N170 by eye visibility. With regards to the second possibility, a peak of activity occurring after 200 ms has been related to task difficulty (Philiastides & Sajda, 2006) or increased processing demands due to adding noise to images (Bankó, Gál, Körtvélyes, Kovács, & Vidnyánszky, 2011), albeit only in young adults. A third and simple possibility is that the difference between face and noise ERPs is driven by a peculiar pattern of activity in response to noise trials only. Indeed, we already reported that largest age-

related differences were found for trials with the lowest coherence level, i.e. textures (Rousselet et al., 2009). Textures elicit very strong responses in the time window of the N170, as well as after 200 ms and might contribute to the observed age-related differences. As such, it would be interesting to determine if similar differences were obtained by contrasting faces with other stimulus categories (e.g. letters, houses) apart from textures, and whether processing speed of other categories was similarly affected.

CHAPTER 4: TOP-DOWN EFFECTS ON THE PERCEPTION OF TEXTURES IN THE CONTEXT OF OBJECT DETECTION TASKS

INTRODUCTION

Recent studies investigating age-related differences in the time course of face processing revealed strong early visual evoked responses to noise textures in older adults (Bieniek, Bennett, Sekuler, & Rousselet, 2015; Jaworska et al., in prep; Rousselet et al., 2009, 2010). In the original study (Rousselet et al., 2009), phase information of face images was manipulated parametrically by introducing phase noise. The largest age-related differences were found for trials with the lowest phase coherence, such that images contained relatively unstructured noise textures. Specifically, older participants had a pronounced negative-going peak in the time window of the N170, whereas young participants did not. Group differences diminished as phase coherence of the images increased. It remained unclear whether such responses arose because of de-differentiation of neural responses in the occipital-temporal brain regions in ageing (Park et al., 2004, 2012), due to processing of textures as meaningful stimuli by older adults, or some other influence, such as increased attention or expectation to perceive a particular image category.

Recently, we ran a study to investigate the information content of ERPs to face and texture images in young and older adults (Jaworska et al., in prep). On each trial, participants were presented with an image of either a face or a texture revealed through randomly placed Gaussian apertures (“bubbles”, Gosselin & Schyns, 2001) and asked to perform a face detection task. Similarly to previous studies, older adults had a strong response to textures in the time window of the N170. However, single-trial ERPs to textures were not consistently modulated by any region in the image in either young or older participants, suggesting that the strong response to textures in older adults is not likely to be driven by spatial attention. The lack of any information content on ERPs to textures also suggested that older adults did not process textures as faces, leaving open the question of the origin of the strong responses to noise.

Even if older participants did not process textures as faces, the nature of the detection task could have influenced the neural responses to textures in some way. In the detection task, the two responses do not have the same status because of the nature of the stimuli. Specifically, structure in the image is associated with a face, whereas no structure – with a texture. As such, a texture is an absence of a face and an easier

strategy adopted in the task could be to simply respond whether a face was there or not, instead of discriminating whether the image was a face, or a texture – processing of which is more difficult and takes longer because of its inherent lack of structure. An interesting question is thus whether older adults develop some kind of an expectation to detect a face, which would then enhance their N170 responses to noise in a top-down manner. Top-down modulation can be thought of as any mechanism by which cognitive influences and higher-order representations, such as attention or expectation, impinge upon earlier steps in information processing (Gilbert & Li, 2013). Such influences can either enhance neural responses to relevant stimuli, or suppress responses to irrelevant information (Gazzaley, Cooney, Rissman, & D’Esposito, 2005). To our knowledge, the modulation of the N170 by expectation or context effects in older adults has only been tested in a working memory task (Gazzaley, Cooney, McEvoy, Knight, & D’Esposito, 2005; Gazzaley et al., 2008). In a paradigm where participants had to remember, ignore, or passively view faces (or scenes), older adults did not modulate the N170 latency in response to ignored compared to passively viewed stimuli whereas young participants did (Gazzaley et al., 2008), suggesting a selective impairment in suppression of irrelevant information in a working memory task. Both groups also showed an earlier N170 to attended, compared with passively viewed stimuli, suggesting a preservation of the capacity to enhance relevant information in ageing. Interestingly, in later studies using the same paradigm larger N170 amplitudes to *ignored* faces were found compared with attended or passively viewed in both age groups (Deiber et al., 2010; Zanto, Hennigan, Oestberg, Clapp, & Gazzaley, 2010), whereas no such effect was observed for letter stimuli. This pattern of responses suggested that faces might attract attention to a greater extent than other stimuli, even if presented in a task-irrelevant manner. As such, if the observed strong responses to textures in our studies were driven by a top-down effect of the face detection task, this influence could potentially be abolished in detection tasks using different stimuli, which do not attract attention to such an extent.

Although top-down effects on the N170 in older adults have only been tested in a working memory paradigm, there are some studies involving young participants, which suggest that expectation to see a face can produce strong N170-like responses to meaningless stimuli or even to textures. In young adults, top-down influence on the N170 has been tested, for example, by manipulating the context in which visual objects were presented (Bentin & Golland, 2002; Bentin, Sagiv, Mecklinger, Friederici, & von Cramon, 2002; Kato et al., 2004). Specifically, pairs of dots separated horizontally evoked only a weak N170 when presented in isolation (Bentin et al., 2002). The same dots were then presented in a face context, such that they were interpretable as the eyes. After priming

with the face context, the N170 response to dots alone increased to resemble that of full-face images, suggesting that the N170 is susceptible to modulation of context or expectation. In another study, Wild and Busey (2004) tested how the N170 was modulated by expectation to see a face or a word. Interestingly, they used noise-only displays to test the effects of expectation, and reported a larger N170 in response to noise when participants expected to see a face.

In light of these findings, it remains unclear whether the strong N170 responses to textures observed in our previous studies (Rousselet et al., 2009, 2010; Jaworska et al., in prep) could reflect a similar expectation effect to that observed in young adults expecting to see a face in a meaningless stimulus, possibly explained by the age-related inability to suppress irrelevant information (Gazzaley et al., 2005, 2008). As such, in the current study we sought to investigate whether the large N170 in response to textures in older adults is an outcome of attending to, or expecting to see a particular image category. Specifically, we hypothesized that if the N170 to noise is driven by top-down enhancement, we should be able to manipulate it by changing task requirements. As such, in addition to faces we introduced two other stimulus categories: letters and houses, and asked participants to perform a detection task with each of the stimulus categories in separate blocks. Participants' expectation was modulated at the beginning of each block of trials, when they were instructed to discriminate one image category (faces, houses, or letters) from textures. If the N170 to noise was modulated by the expectation to see a particular stimulus category, we hypothesized that differences in the N170 to noise in older adults would resemble categorical differences between objects in terms of their time courses and topographies.

METHODS

PARTICIPANTS

Twenty-four young (15 females, 3 left-handed; median age = 22, min = 20, max = 39) and twenty-four older adults (13 females, 3 left-handed; median age = 67.5, min = 59, max = 85) participated in the study. All young participants were recruited from the student body at the University of Glasgow. Older participants were local residents who had already taken part in the Bubbles study before (Jaworska et al., in prep) or were recruited from a local Active Age fitness class, the Retired Staff Association at the University of Glasgow, or through advertisement at a local optometrist. Young participants were recruited from the student body at the University of Glasgow. Volunteers were excluded from participation if they reported any current eye condition (i.e., lazy eye, glaucoma, macular degeneration, cataract, diabetic retinopathy), had a history of mental illness, were currently taking psychotropic medications or used to take them, suffered from any neurological condition, or had suffered a stroke or a serious head injury. Volunteers were also excluded from participation if they had their eyes tested more than a year (for older volunteers) or two years (for younger volunteers) prior to the study taking place, in order to minimise the chances that volunteers did not have knowledge of an underlying eye condition. Participants' visual acuity was assessed during their first experimental session using a Colenbrander mixed contrast card set (Colenbrander & Fletcher, 2004) for the 40 cm and 63 cm viewing distances, and the 6 m Bailey-Lovie Chart (Bailey & Lovie, 1980). Participants' contrast sensitivity was assessed with the Mars Letter Contrast Sensitivity set (Arditi, 2005). All participants had normal or corrected to normal visual acuity (Table 19) and contrast sensitivity of 1.72 log units and above, which fell within the normal range of contrast sensitivity for each age group (Haymes et al., 2006). In addition, older participants completed the Montreal Cognitive Assessment (MOCA) to screen for age-related cognitive impairment. MOCA scores of three older participants were one point below the normal threshold (more than or equal to 26 out of 30, Table 19) and the median score was 28 (min = 25, max = 30). Older participants also completed the Trail Making Test – part of the Delis-Kaplan Executive Function System (D-KEFS) (Delis et al., 2001) battery of tests to assess higher-order cognitive and executive functioning. Results of the Trail Making Test are reported in Table 19. During the experimental session, participants wore their habitual correction if needed.

The study was approved by the local ethics committee at the College of Science and Engineering, University of Glasgow (approval no. 300150007), and conducted in line with the British Psychological Society ethics guidelines. Informed written consent was obtained from each participant before they took part in the study. Participants were compensated £6 per hour.

Table 19 Visual and cognitive test scores.

Visual acuity and contrast sensitivity (CS) scores for young and older participants, as well as MOCA and Trail Making Test Scores for older participants. Visual acuity scores are reported for high contrast (HC) and low contrast (LC) charts presented at the 40 cm, 63 cm and 6 m viewing distances, and expressed as raw visual acuity scores (VAS). Their corresponding logMAR scores are presented below in italics, where higher values indicate poorer vision and negative values represent normal vision (logMAR score of 0 corresponds to 20/20 vision). For Trail Making Test, scores are age-scaled composite scores for Number-Letter Switching (NLS) task versus: Visual Scanning (VS), Number Sequencing (NS), Letter Sequencing (LS), Composite Scaled Score (CSS), and Motor Speed (MS). Scores correspond to median across all participants in each age group. Square brackets indicate the minimum and maximum scores across participants in each age group.

	HC 40	LC 40	HC 63	LC 63	HC 600	LC 600	CS
young	103	95	105	94	103	95	1.84
	[93, 105]	[83, 103]	[97, 111]	[86, 105]	[89, 110]	[65, 103]	[1.72, 1.92]
	<i>-0.06 [0.14,</i>	<i>0.10 [0.34,</i>	<i>-0.10 [0.06,</i>	<i>0.12 [0.28,</i>	<i>-0.06 [0.22,</i>	<i>0.10 [0.70,</i>	
	<i>-0.10]</i>	<i>-0.06]</i>	<i>-0.22]</i>	<i>-0.10]</i>	<i>-0.20]</i>	<i>-0.06]</i>	
older	92	83	101	90	100	91	1.80
	[75, 105]	[65, 98]	[85, 110]	[75, 100]	[88, 105]	[75, 99]	[1.68, 1.88]
	<i>0.16 [0.50,</i>	<i>0.34 [0.70,</i>	<i>-0.02 [0.30,</i>	<i>0.20 [0.50,</i>	<i>0.00 [0.24,</i>	<i>0.18 [0.50,</i>	
	<i>-0.10]</i>	<i>0.04]</i>	<i>-0.20]</i>	<i>0.00]</i>	<i>-0.10]</i>	<i>0.02]</i>	
D-KEFS Trail Making test: NLS vs. XXX							
	MOCA	VS	NS	LS	CSS	MS	
older	28	12	11	12	11	10	
	[25, 30]	[10, 15]	[9, 15]	[9, 15]	[9, 15]	[9, 13]	

STIMULI

We used three sets of objects in this experiment (Figure 18): a set of 10 grey-scaled front view photographs of faces (5 males and 5 females), a set of 10 images of the uppercase letters A, F, G, J, L, P, E, R, T, Y in the Geneva font (Gold, Bennett, & Sekuler, 1999), and a set of front-view photographs of houses (Husk, Bennett, &

Sekuler, 2007). All stimuli had the same amplitude spectrum and contrast variance of 0.05. Images were presented at 90% phase coherence level. Textures in each of the detection blocks were created by randomizing the phase spectrum of an image selected at random from the same stimulus category. Generating textures from the same object category was performed in order to preserve any low-level differences (that might have been left after controlling for amplitude spectrum and contrast variance) between textures in different detection tasks, as well as to match the stimulus design from previous experiments (Rousselet et al., 2009, 2010; Bieniek et al., 2015).

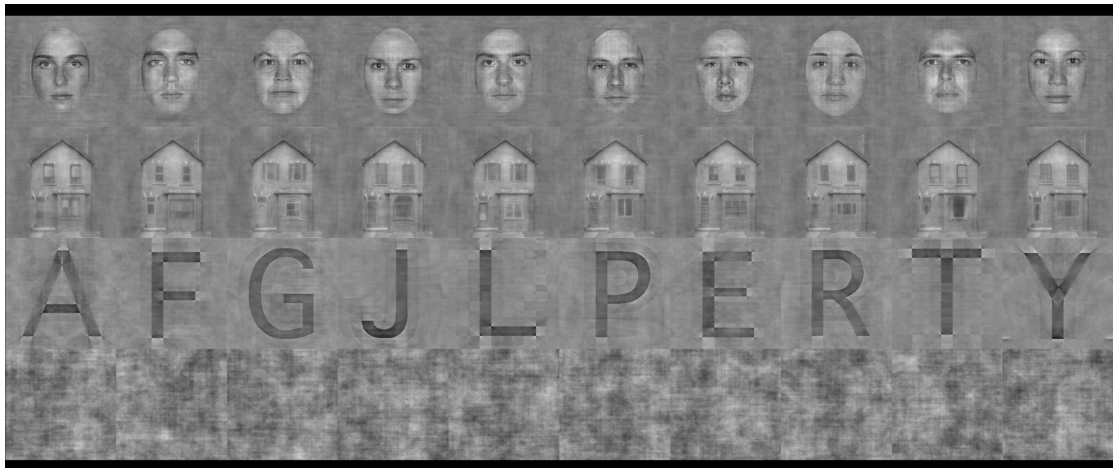


Figure 18 Stimuli.

Top row shows all ten identities of faces, the second row shows all ten images of houses, and the third row shows images of the ten letters used in this study. All images are presented at 100% phase coherence. The bottom row shows ten examples of textures created by randomizing the phase coherence of one of the 30 object images presented above.

PROCEDURE

All participants were tested in one experimental session consisting of a behavioural task with simultaneous EEG recordings. Participants sat in a dimly lit and sound-attenuated booth, and were given experimental instructions including a request to minimize movement and blinking, or to blink when hitting a response button.

The session consisted of 7 blocks of 100 trials (700 trials in total). In the first block, participants were presented with a set of 100 textures. Textures were created by randomizing the phase spectrum of one image randomly drawn among the thirty objects. The remaining six blocks presented textures intermixed with images of objects from only one category.

Throughout the experiment, participants completed four tasks. In the first block, the task was to always press one key on the keyboard ('2') to move on to the next trial after a texture had been presented. In the remaining six blocks, participants completed three detection tasks: the face, the house, or the letter detection. They responded by pressing '1' for the object (either a face, or a house, or a letter depending on the block), and '2' for texture, using the index and middle fingers of their dominant hand. In each of the detection blocks, participants were presented with 50 trials of textures and 50 trials of object images, randomly intermixed. Each object category was presented in two separate blocks over the course of the experiment, such that there was a total of 100 trials per object category.

The order of the detection blocks was predefined manually such that each participant within each age group followed a different block order. The first three of the six blocks presented the three object detection tasks, and the presentation of each category was then repeated in the remaining three blocks with the restriction that no category was repeated across the two adjacent blocks.

On each trial, participants were first presented with a small fixation cross (12 x 12 pixels, $0.35^\circ \times 0.35^\circ$ of visual angle) displayed at the centre of the monitor screen for a random time interval of 500 to 1000 ms. After the fixation cross disappeared, the stimulus was presented for 10 frames (~83 ms). After the stimulus, a blank grey screen was displayed until the participant responded, using the numerical pad of a keyboard. Participants were requested to respond as fast and accurately as possible.

After each block, participants could take a break, and they received feedback on their performance in the previous block and on their overall performance in the experiment (median reaction time and percentage of correct responses). The next block started after participants pressed a key indicating they were ready to move on.

Stimuli were displayed on a VIEWPixx monitor (1920 x 1200 pixels; 22.5 inch diagonal display size; 120 Hz refresh rate). The fixation cross, the stimulus and the blank response screen were all displayed on a uniform grey background. The viewing distance from the chinrest to the monitor screen was 45 cm. Each session lasted about 60 to 75 minutes, including breaks, but excluding EEG electrode application.

The experiment was written in MATLAB using the Psychophysics Toolbox extensions (Brainard, 1997; Kleiner et al., 2007; Pelli, 1997).

EEG RECORDING AND PRE-PROCESSING

EEG data were recorded at 512 Hz using a 128-channel Biosemi Active Two EEG system (Biosemi, Amsterdam, the Netherlands). Four additional UltraFlat Active Biosemi electrodes were placed below and at the outer canthi of both eyes. Electrode offsets were kept between ± 20 μV .

EEG data were pre-processed using MATLAB 2013b and the open-source EEGLAB toolbox (Delorme et al., 2011; Delorme & Makeig, 2004). Data were first average-referenced and detrended. Two types of filtering were then performed. First, data were band-pass filtered between 1 Hz and 30 Hz using a non-causal fourth order Butterworth filter. Independently, another dataset was created in which data were pre-processed with fourth order Butterworth filters: high-pass causal filter at 2 Hz and low-pass non-causal filter at 30 Hz, to preserve accurate timing of onsets (Acunzo, MacKenzie, & van Rossum, 2012; Luck, 2005; Rousselet, 2012; Widmann & Schröger, 2012).

Data from both datasets were then downsampled to 500 Hz, and epoched between -300 and 1000 ms around stimulus onset. Mean baseline was removed from the causal-filtered data, and channel mean was removed from each channel in the non-causal-filtered data in order to increase reliability of Independent Component Analysis (ICA; Groppe, Makeig, & Kutas, 2009). Noisy electrodes and trials were then detected by visual inspection of the non-causal dataset, and rejected on a subject-by-subject basis. On average, more noisy channels were removed from older than from young participants' datasets (older participants: median = 20, min = 6, max = 34; young participants: median = 10.5, min = 3, max = 30; median difference = 7, 95% confidence interval = [3, 11]).

Subsequently, ICA was performed on the non-causal filtered dataset using the Infomax algorithm as implemented in the *runica* function in EEGLAB (Delorme & Makeig, 2004; Delorme et al., 2007). The ICA weights were then applied to the causal filtered dataset to ensure removal of the same components, and artifactual components were rejected from both datasets (young: median = 4.5, min = 1, max = 11; older: median = 3, min = 1, max = 25; median difference = 1 [0, 3]). Then, baseline correction was performed again, and data epochs were removed based on an absolute threshold value larger than 100 μV and the presence of a linear trend with an absolute slope larger than 75 μV per epoch and R^2 larger than 0.3. The median number of trials accepted for analysis was, for young participants: median = 683, min = 648, max = 693; for older participants: median = 681.5, min = 604, max = 695 (median difference = -2 [-9, 5]). Finally, we computed single-trial

spherical spline current source density waveforms using the CSD toolbox (Kayser, 2009; Tenke & Kayser, 2012). CSD waveforms were computed using parameters 50 iterations, $m=4$, $\lambda=10^{-5}$. The head radius was arbitrarily set to 10 cm, so that the ERP units are $\mu\text{V}/\text{cm}^2$. The CSD transformation is a spatial high-pass filtering of the data, which sharpens ERP topographies and reduces the influence of volume-conducted activity. CSD waveforms also are reference-free.

STATISTICAL ANALYSES

Statistical analyses were conducted using Matlab 2013b. Throughout the paper, square brackets indicate 95% confidence intervals computed using the percentile bootstrap technique, with 1000 bootstrap samples. Unless otherwise stated, median values are Harrell-Davis (Harrell & Davis, 1982) estimates of the 2nd quartile.

MEASURES OF EFFECT SIZE

We estimated the size of the between-group differences using two robust techniques: Cliff's *delta* and the median of all pairwise differences. Cliff's *delta* (Cliff, 1996; Wilcox, 2006) is related to the Wilcoxon-Mann-Whitney *U* statistic and estimates the probability that a randomly selected observation from one group is larger than a randomly selected observation from another group, minus the reverse probability. Cliff's *delta* ranges from 1 when all values from one group are higher than the values from the other group, to -1 when the reverse is true. Completely overlapping distributions have a Cliff's *delta* of 0. In line with Cliff's *delta* approach, we also calculated all pairwise differences between young and older participants on the measures of interest (reaction times, percent corrects, N170 latencies and amplitudes), and took the median of the distribution of these differences. This way of measuring effect sizes enabled us to provide information about the typical difference between any members of two groups (Wilcox, 2012).

MUTUAL INFORMATION

Mutual Information (MI) is a non-parametric measure that quantifies (in bits) the reduction in uncertainty about one variable after observation of another and has been used to study the selectivity of neural and behavioural responses to external stimuli (Ince et al., 2009; Magri et al., 2009b; Panzeri et al., 2010; Schyns et al., 2011). The advantage of using the MI lies in its ability to detect associations of any order, whether linear or non-linear.

Here, we used a new estimator of MI that can be used with continuous variables (Ince,

Giordano, et al., 2016) and utilizes the concept of copulas (Nelsen, 2007), statistical structures that express the relationship between two random variables, independently of their marginal distributions. Previously (Jaworska et al., in prep), we used an approach where data were quantized into a number of bins, and MI was estimated over the resulting discrete spaces. The copula method does not require the quantization step and is computationally efficient (Ince, Giordano, et al., 2016).

We used MI to quantify the dependence between the category of the visual stimulus and brain responses. To do so, we computed the temporal gradient of the EEG voltage (dEEG) on each trial in order to account for the temporal relationship between neighbouring time points, and then combined the EEG voltage and its temporal gradient into a bivariate response. We then calculated the time course of MI about the eye visibility in the bivariate response: $MI(\text{eye}, [\text{EEG dEEG}])$. Considering the gradient response together with the voltage smoothes out the artifactual dips in MI time courses, occurring at time points of zero-crossings when EEG voltages change sign. It also introduces information about the shape of the ERP, otherwise missing from considering just the instantaneous amplitudes. As such, the bivariate time course provides a clearer picture of the time window(s) over which the EEG signal is modulated by the changing stimulus (Ince, Giordano, et al., 2016).

In single participants, we calculated several $MI(\text{image category}, \text{EEG})$ quantities to establish the relationship between the pair of categories in question and EEG voltage over the time period of -300 ms before to 1000 ms after stimulus onset. The pairs of categories were as follows: 1) *Objects versus texture*: Faces vs. textures, Houses vs. textures, and Letters vs. textures; 2) *Categorical differences of full images*: Faces vs. Houses, Faces vs. Letters, and Houses vs. Letters; 3) *Categorical differences of textures*: textures in the Face detection block vs. textures in the House detection block, textures in the Face vs. Letter detection blocks, and textures in House vs. Letter detection blocks; and finally 4) *Texture differences*: textures in block 1 (baseline) vs. each of the three object detection blocks (three comparisons).

50% INTEGRATION TIME

In order to estimate information processing speed, we determined how long it took participants to integrate 50% of their MI time-courses, a measure that takes into account the entire waveform and not just the peaks of MI (Rousselet et al., 2010). For each participant, we computed the cumulated sum of the maximum MI across electrodes in both hemispheres in the time window of 0-500 ms. We then normalized that cumulated

sum between 0 and 1, such that it had a value of 0 at stimulus onset and a value of 1 at 500 ms after stimulus onset. Finally, we computed the time necessary to reach 50% of that function using linear interpolation.

ELECTRODE SELECTION

We selected three subsets of electrodes in each participant independently (Figure 19): posterior-lateral electrodes on the left hemisphere (LE) and on the right hemisphere (RE). In order to avoid defining a single electrode of interest, we calculated the time-courses of the maximum MI across all electrodes of interest in each hemisphere independently. We also checked that we did not miss any local maxima by repeating our group analyses on the maximum MI taken across all electrodes.

For ERP analyses, we selected two electrodes by measuring the difference between mean ERPs elicited by face, house, or letter images and their corresponding textures. The differences were computed at all posterior-lateral electrodes in the left and the right hemisphere and then squared. We then selected the left and the right electrodes that showed the maximum difference in the period of 100-250 ms.

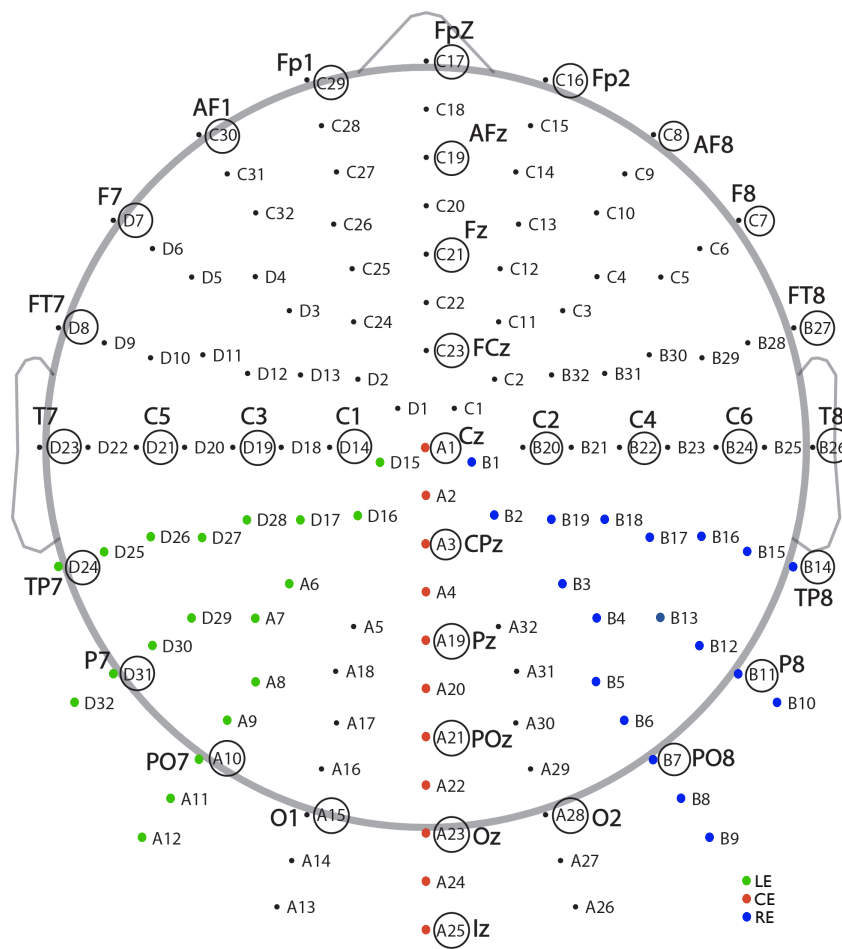


Figure 19 Electrode location.

Location of electrodes included in three subsets: midline (CE, red), posterior-lateral in the left hemisphere (LE, green) and in the right hemisphere (RE, blue).

TOPOGRAPHIC ANALYSES

Topographic maps for each participant were computed from the whole-scalp MI (image category, ERP) results at the individual MI peak latency. Individual topographic maps were normalised between 0 and 1, interpolated and rendered in a 67 x 67 pixel image using the EEGLAB function *topoplot*, and then averaged across participants in each age group. Using the interpolated head maps, we then computed a hemispheric lateralisation index for each participant. First, we saved the maximum pixel intensity in the left and the right hemisphere (lower left and right quadrants of the interpolated image), excluding the midline. Then, we computed the lateralisation index in each group as the ratio $(MI_{\text{left}} - MI_{\text{right}}) / (MI_{\text{left}} + MI_{\text{right}})$.

RESULTS

BEHAVIOURAL RESULTS

Across all conditions, older participants were generally slower than young participants ($\text{difference}_{\text{older-young}} = 92 \text{ ms}$ [37, 123]; median, young = 308 ms [290, 347], older = 413 ms [390, 437]). On the other hand, young participants were slightly less accurate than older ones ($\text{difference}_{\text{older-young}} = 1.7 \text{ percentage points (PP)}$ [0.3, 3.5]; median, young = 96.4% [94.8, 98.1], older = 98.4% [97.8, 99]), although no group differences were found within image categories (Table 21).

To investigate whether age affected reaction times (RTs) in simple versus more complex tasks differentially, we computed the difference between RTs to textures presented in the first block ('baseline') and those presented in object detection blocks for young and older participants. In the baseline block, only textures were presented so participants were only asked to press one key on the keyboard as soon as they saw a texture (simple-RT). In all other blocks, participants had to discriminate between an object (either a face, or a house, or a letter) and a texture by pressing one key for the object and another for the texture (choice-RT). Young adults were slower to respond on choice-RT trials than on simple-RT trials by 132 ms [114, 157], and older adults by 219 ms [190, 246]. The interaction between age and task complexity was significant: older adults were slower than young adults by 79 ms [47, 114] on choice-RT trials compared with simple-RT trials. In other words, there was no group difference on simple-RT trials ($\text{difference}_{\text{older-young}}: 11 \text{ ms}$ [-23, 49]), but older adults were consistently slower than young adults on choice-RT trials (for group differences in each stimulus category, see Table 20).

Regardless of the object category, younger adults were also faster to respond on object trials than on texture trials by 27 ms [18, 35], whereas older adults were faster by 14 ms [5, 26]. However, here the group difference was not significant (-9 ms [-24, 4]).

Table 20 Behavioural results: reaction times.

We report the median across participants of the median reaction times in milliseconds, for each stimulus category: faces, houses and letters; textures in face detection (Fnoise), house detection (Hnoise), and letter detection (Lnoise) tasks; as well as textures presented in the baseline block (base). Last column shows the median of pairwise differences between young and older participants. Cliff's *delta* estimates are shown in italics. Square brackets correspond to 95% confidence intervals.

	young	older	group difference
Faces	299 [275, 337]	405 [385, 435]	98 [54, 134] <i>0.59 [0.25, 0.80]</i>
Houses	319 [288, 367]	405 [385, 430]	83 [45, 119] <i>0.51 [0.16, 0.75]</i>
Letters	322 [285, 357]	419 [403, 444]	99 [58, 137] <i>0.60 [0.27, 0.81]</i>
Fnoise	324 [308, 380]	429 [398, 475]	87 [38, 130] <i>0.51 [0.16, 0.74]</i>
Hnoise	338 [324, 374]	441 [416, 470]	91 [43, 130] <i>0.51 [0.16, 0.75]</i>
Lnoise	333 [316, 373]	438 [402, 473]	87 [38, 129] <i>0.53 [0.19, 0.75]</i>
base	192 [169, 216]	206 [181, 247]	11 [-23, 49] <i>0.10 [-0.23, 0.41]</i>

Table 21 Behavioural results: percent correct.

We report the median across participants of median percent correct, for each stimulus category: faces, houses and letters; textures in face detection (Fnoise), house detection (Hnoise), and letter detection (Lnoise) tasks; as well as textures presented in the baseline block (base). Last column shows the median of pairwise differences between young and older participants. Cliff's *delta* estimates for the group difference are shown in italics. Square brackets correspond to 95% confidence intervals.

	young	older	group difference
Faces	97.5 [96, 98.5]	97.3 [94.7, 98.3]	-0.1 [-2, 1.1] <i>-0.05 [-0.36, 0.27]</i>
Houses	96.9 [94.7, 98.1]	95.4 [94.1, 97.4]	-0.8 [-3, 1.1] <i>-0.11 [-0.42, 0.22]</i>
Letters	96.5 [94.5, 97.8]	96.1 [93.9, 97.7]	-0.1 [-2.5, 2] <i>-0.03 [-0.35, 0.29]</i>
Fnoise	96.4 [94, 97.9]	96.6 [94.8, 98.1]	0.3 [-1.5, 2.1] <i>0.06 [-0.27, 0.37]</i>
Hnoise	95.3 [92.5, 97.3]	95.5 [93.3, 97.8]	0.3 [-1.7, 2.9] <i>0.06 [-0.27, 0.37]</i>
Lnoise	95.7 [93.1, 97.6]	95.4 [92.6, 97.2]	0 [-2.7, 2] <i>0 [-0.32, 0.32]</i>
base	100 [100, 100]	100 [100, 100]	

EVENT-RELATED POTENTIALS

Previously, in a face detection task where participants had to press one key if they saw a face and another if they saw a texture, we reported pronounced event-related potentials (ERPs) to textures in the time window of the N170 in older, but not young participants (Rousselet et al., 2009; Jaworska et al., in prep; Bieniek et al., 2015). Here, we show similarly large evoked responses, also in the time window of the N170, to textures in three detection tasks (Figure 20): face detection ('Fnoise'), house detection ('Hnoise'), and letter detection ('Lnoise'). We also observed a large N170 in response to textures presented in the baseline block ('base'), in which only textures were presented and, as such, participants did not engage in a detection task, but rather always pressed a unique key on the keyboard as soon as they saw a texture. These large responses to noise were only observed in older, but not in young participants.

Furthermore, older adults on average had larger N170 to *object* images: faces, houses, and letters, (Figure 3, insets; see Tables S10 – S11 in Appendix C for quantification of the N170 latency and amplitude for texture and object trials).

In order to investigate whether there were any categorical differences between ERP responses to textures, as well as among object images embedded within different detection tasks, we now turn to Mutual Information (MI) analyses.

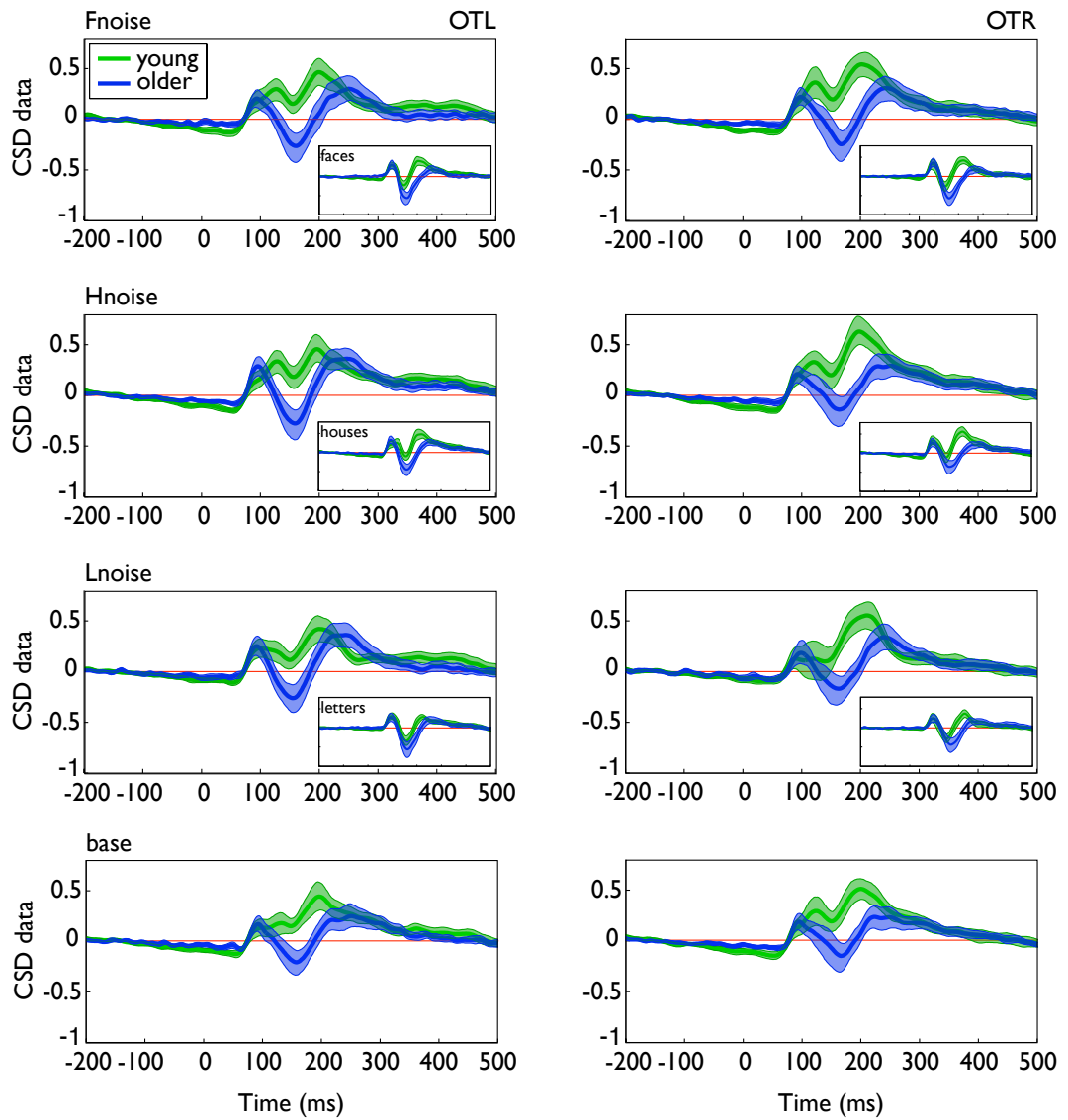


Figure 20 Event-related potentials.

In the main plots, responses are averaged across texture trials in each task: face detection (Fnoise), house detection (Hnoise), and letter detection (Lnoise), as well as in the baseline block (base). Young participants are in green, older participants in blue. ERPs are presented separately at OTL (left) and OTR (right). Insets present responses averaged across object trials in the corresponding detection tasks. CSD data are expressed in $\mu\text{V}/\text{cm}^2$. Shaded areas correspond to 95% confidence intervals.

BRAIN SENSITIVITY: MUTUAL INFORMATION

Analyses focusing on differences in ERP peak latencies and amplitudes can hide important information about the time course of information processing (Rousselet & Pernet, 2011; Rousselet et al., 2011; Schyns et al., 2007). In this study, peak analyses on ERPs to texture trials would be particularly problematic, because young adults do not have a clear peak in response to textures. To overcome the limitations associated with peak analyses, we calculated categorical Mutual Information (MI) to quantify the dependence between ERPs and image category.

In order to simplify the presentation of MI results for each of the comparisons, time courses displayed in Figures 21 – 24 depict the maximum MI taken across sensors of interest in the left and right hemispheres. We took the maximum MI from the time window of 80 ms to 400 ms post-stimulus, based on the recent finding that the earliest categorical differences start around 90 ms after stimulus onset regardless of age (Bieniek et al., 2015).

CATEGORICAL DIFFERENCES: OBJECTS

First of all, we sought to investigate how ERPs in response to objects, i.e. faces, houses and letters differed from each other. To this end, we computed MI for three comparisons: faces vs. letters, faces vs. houses, and letters vs. houses. Strong MI was found in both age groups for all three comparisons (Figure 21). For each comparison, MI peaked in the time window between 100 and 200 ms post-stimulus, but at slightly different times.

MI for the face vs. house contrast peaked at 131 ms [128, 137] in young, and at 140 ms [127, 147] in older participants, and did not differ significantly between groups ($\text{difference}_{\text{older-young}} = 5 \text{ ms} [-14, 15]$).

On the other hand, MI was stronger by 0.08 bits [0.01, 0.14] in young than in older participants (median MI, young = 0.25 bits [0.21, 0.31], older = 0.16 bits [0.12, 0.24]). MI was larger over right hemisphere electrodes in young (-0.17 [-0.23, -0.10]), but not in older participants (-0.03 [-0.21, 0.09]). However, the group difference was not significant (0.12 [-0.02, 0.23]).

MI for the face vs. letter contrast peaked at 158 ms [140, 176] in young, and at 151 ms [140, 173] in older participants, and there was no age-related delay in timings ($\text{difference} = 2 \text{ ms} [-19, 24]$). Again, MI about faces vs. letters contrast was stronger in young than in older participants by about 0.08 bits [0.01, 0.16] (young = 0.29 bits [0.23, 0.34], older =

0.20 bits [0.16, 0.25]). Information was symmetrical across hemispheres in both young and older participants (young = 0.06 [-0.10, 0.17], older = 0.00 [-0.07, 0.08], group difference = -0.03 [-0.15, 0.11]).

Finally, MI about the house vs. letter contrast peaked about 21 ms [6, 46] later in older than in young participants (young = 170 ms [156, 180], older = 189 ms [172, 221]) and was weaker by about 0.09 bits [0.04, 0.15] (young = 0.27 bits [0.21, 0.32], older = 0.15 bits [0.14, 0.20]). Here, MI was more left-lateralized in young (0.13 [0.04, 0.24]) but not older (0.07 [-0.06, 0.20]) participants (group difference = -0.06 [-0.19, 0.05]).

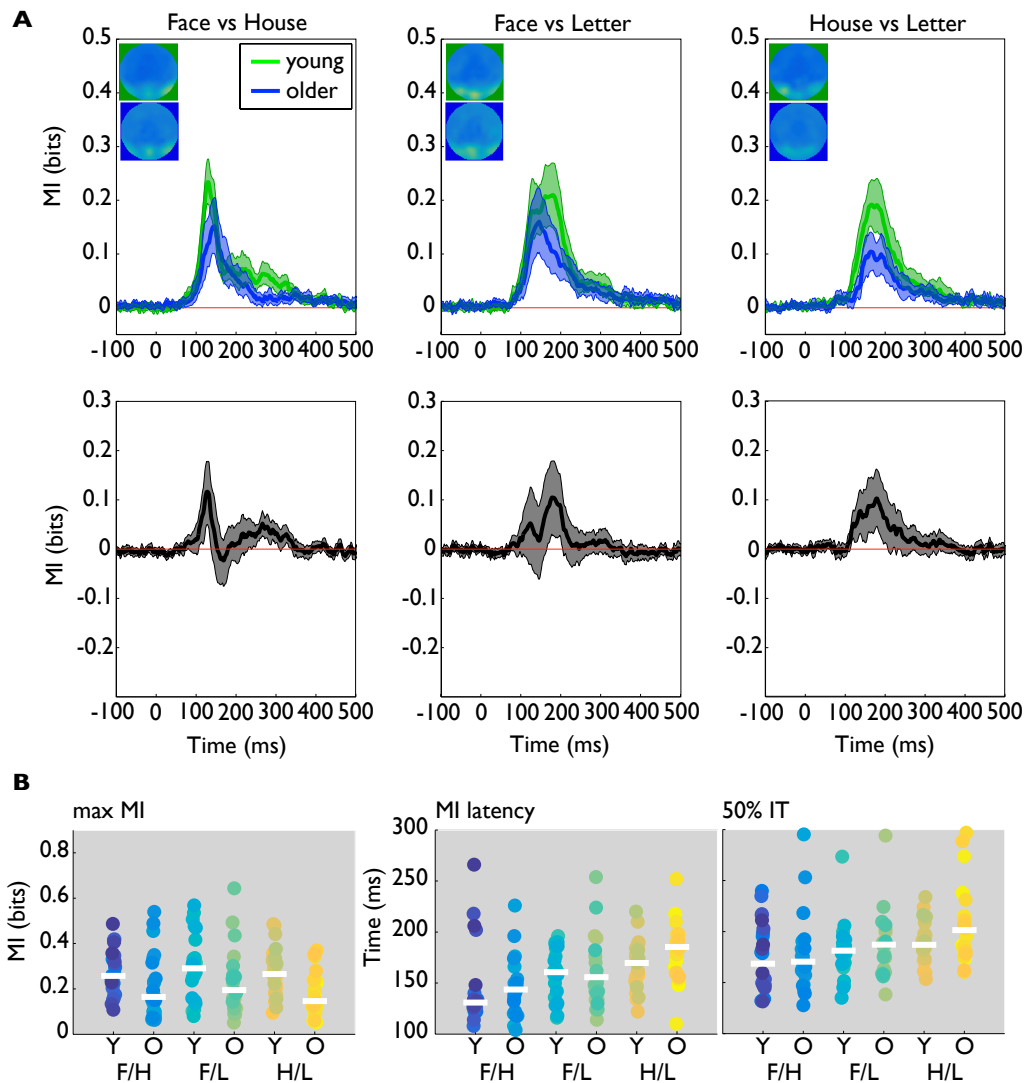


Figure 21 Categorical differences between full images.

(A) Top panel: MI time courses for the difference between faces and houses (left), faces and letters (middle), and houses and letters (right), averaged across young (green) and older participants (blue). Insets show MI topographies averaged across young and older participants (green and blue boxes, respectively). Bottom panel shows group differences between the average MI time courses. Shaded areas correspond to 95% confidence intervals. **(B)** Individual participants' maximum MI (left), max MI latency (middle), and 50% integration times (right). Each dot corresponds to one participant. Dots are grouped into young (Y) and older (O) participants, for each of the contrasts (faces vs houses - F/H, etc.). White horizontal bars correspond to median values.

CATEGORICAL DIFFERENCES: TEXTURES

Next, we quantified the categorical differences between textures presented in different detection tasks. We hypothesized that, if ERPs to textures in older participants were driven by the presence of the task at hand, then expecting to see a particular image category would influence responses to textures in a similar manner. As such, we expected categorical differences between textures embedded in the three detection tasks to resemble those between their corresponding objects, as presented in Figure 21.

However, contrary to our expectations, time courses of categorical MI between textures from different tasks were rather flat (Figure 22A) and did not resemble categorical MI to corresponding objects (Figure 21A). Plotting the average difference between young and older participants revealed only very weak age-related differences (Figure 22B).

Although the MI time courses were relatively flat, a very weak deflection of MI from baseline was observed between 200 and 300 ms post-stimulus for the difference between textures in the face and house tasks (“Fnoise vs. Hnoise”); as well as for the difference between textures in the face detection and letter detection tasks (“Fnoise vs. Lnoise”). Although the difference in average time courses for young and older participants (Figure 22B) seemed to reveal no group differences at all, comparing maximum MI did seem to differ between groups (Figure 22C). Specifically, max MI was stronger in older compared to young participants by about 0.01 bits [0.002, 0.03] (Cliff’s *delta* = 0.34 [0.01, 0.60]) in the Fnoise vs. Hnoise contrast (median MI, young = 0.06 bits [0.05, 0.07]; older = 0.07 bits [0.06, 0.09]). MI was also stronger by about 0.02 bits [0.002, 0.03] (Cliff’s *delta* = 0.35 [0.02, 0.62]) in older participants in the Fnoise vs. Lnoise contrast (median, young = 0.06 bits [0.05, 0.07]; older = 0.07 bits [0.06, 0.09]). No significant differences were found in the Hnoise vs. Lnoise contrast (difference_{young-older} = 0 bits [-0.01, 0.01]; median, young = 0.06 bits [0.05, 0.08]; older = 0.06 bits [0.05, 0.08]).

These moderate effects of detection category on brain responses to textures seem unrelated to the group-average MI time course (Figure 22B) because of considerable spread of maximum MI latencies across participants. The inter-quartile range (IQR) for max MI latencies in the Fnoise vs. Hnoise contrast was 99 ms in young, and 125 ms in older participants (25th and 75th percentiles, young = [203, 302]; older = [209, 334]). Even larger values were observed for the Fnoise vs. Lnoise contrast (IQR, young = 146 ms [169, 315]; older = 188 ms [158, 346]).

As such, despite the lack of clear categorical differences between textures perceived in various detection tasks, we found a moderate, task-related modulation of brain responses to textures in older participants. In particular, this effect is only present for textures perceived in the face detection task, and not the house, or the letter detection tasks.

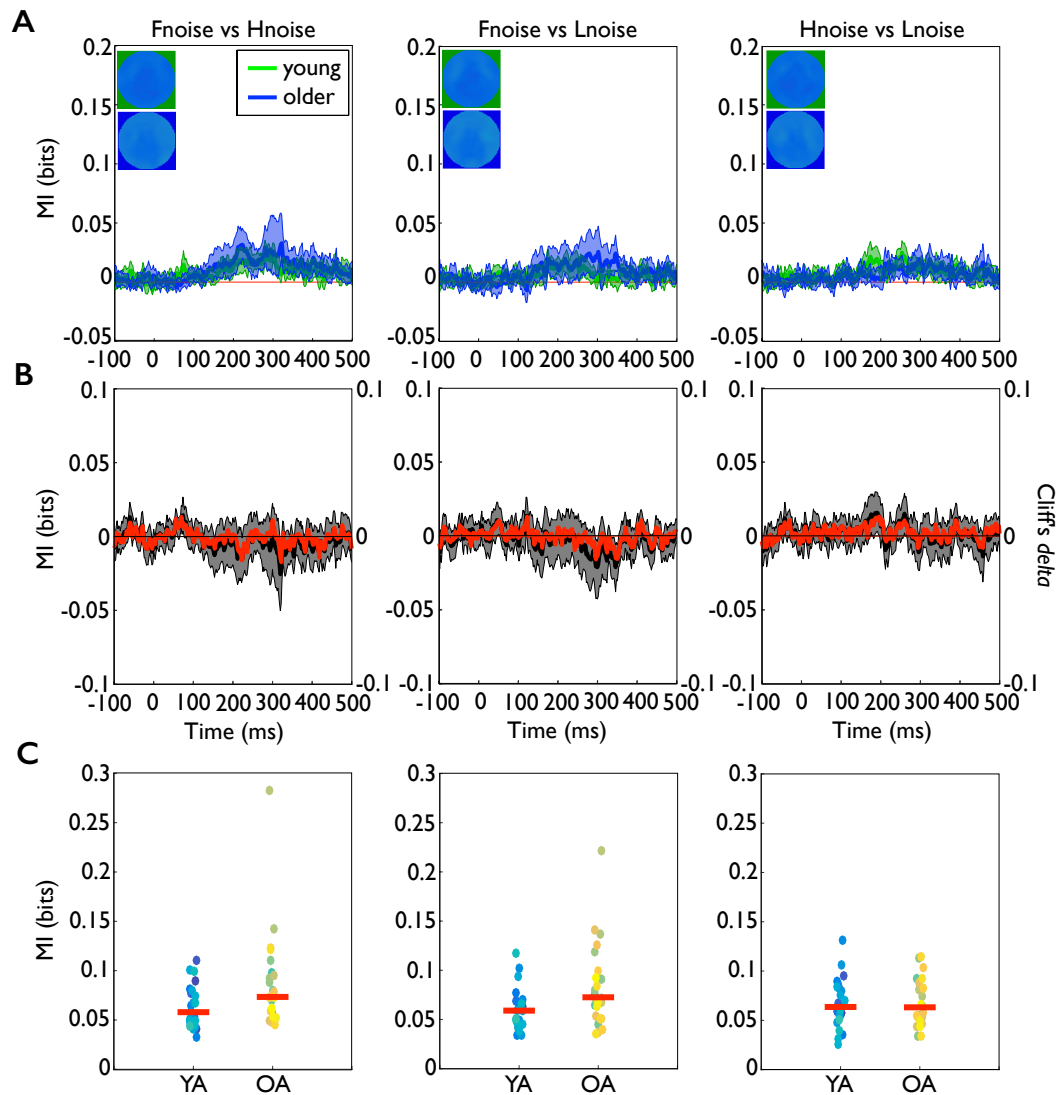


Figure 22 Age-related categorical differences between textures.

(A) MI time courses for the difference between textures in face detection block and in house detection block (left), in face detection and letter detection block (middle), and in house detection and letter detection (right), averaged across young (green) and older participants (blue). Insets show MI topographies averaged across young and older participants (green and blue boxes, respectively). **(B)** Group differences. Plotted are: the time course of MI group differences (black), and the time course of Cliff's *delta* (red). Shaded areas correspond to 95% confidence intervals. **(C)** Scatterplot of maximum MI across time points, separately for young adults (YA) and older adults (OA). Red horizontal bars correspond to median across participants in each age group.

AGE-RELATED DIFFERENCES IN BRAIN SENSITIVITY TO BASELINE VS. TASK-RELATED TEXTURES

We then wanted to investigate whether ERP responses to textures perceived in a detection task could be distinguished from those in the baseline block (where no detection task was present), and whether any age-related differences could be observed. We ran three comparisons: textures in baseline block were compared with textures perceived in the face detection task (“Fnoise vs. noise”), with textures perceived in the house detection task (“Hnoise vs. noise”) and with textures perceived in the letter detection task (“Lnoise vs. noise”). Figure 23 presents average MI time courses associated with these comparisons.

In each of the three comparisons, there was a clear difference that started around 100 ms post-stimulus and continued throughout the time window of interest, until 500 ms post-stimulus.

Comparing average time-courses between young and older adults revealed no significant group differences. Comparing maximum MI or its latency did not reveal any significant group differences either.

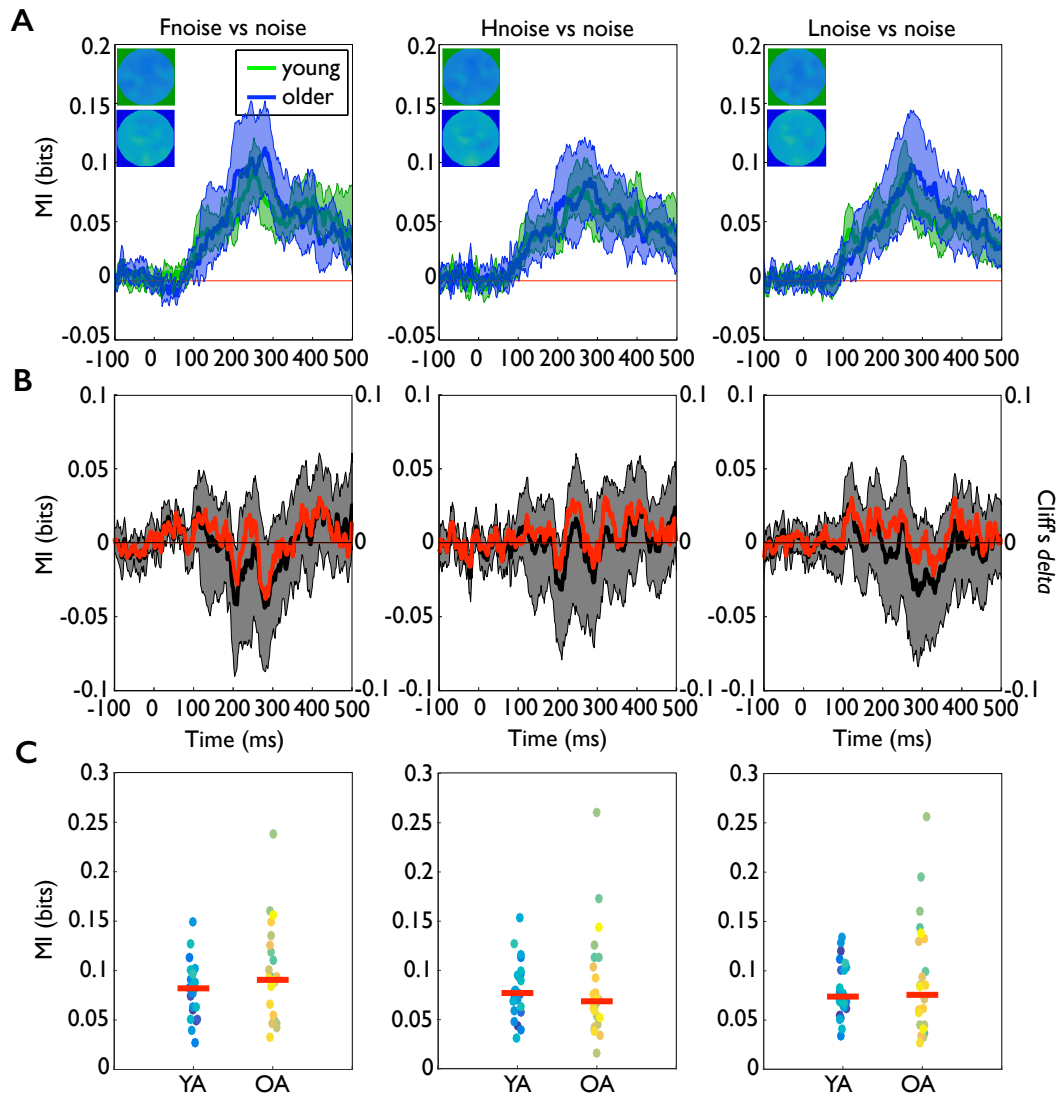


Figure 23 Age-related differences in brain sensitivity to baseline vs. task-related textures.

(A) MI time courses for the difference between textures in face detection block and baseline block (left), in house detection and baseline block (middle), and in letter detection and baseline block (right), averaged across young (green) and older participants (blue). Insets show MI topographies averaged across young and older participants (green and blue boxes, respectively). **(B)** Group differences. Plotted are: the time course of MI group differences (black), and the time course of Cliff's *delta* (red). Shaded areas correspond to 95% confidence intervals. **(C)** Scatterplot of maximum MI across time points, separately for young adults (YA) and older adults (OA). Red horizontal bars correspond to median across participants in each age group.

AGE-RELATED DIFFERENCES IN IMAGE STRUCTURE SENSITIVITY

In our last set of comparisons, we wanted to extend work previously conducted in the lab (Rousselet et al., 2009, 2010; Bieniek et al., 2013) and investigate age-related differences in the time courses of sensitivity to image structure, using images of houses and letters (in addition to previously used faces).

Results showing MI sensitivity to image structure are presented in Figure 24A. Both young and older participants showed a clear and strong MI peak in the 100 – 200 ms time window for each of the three contrasts between objects (faces, houses, letters) and textures. MI peaked at 134 ms [130, 139] for faces, at 170 ms [155, 200] for houses, and at 166 ms [160, 172] for letters in young participants. In older participants, MI peak latencies occurred at 164 ms [145, 190] for faces, 191 ms [181, 205] for houses, and 200 ms [182, 214] for letters.

Age-related differences depended on the image category. Overall, MI in older participants was delayed for faces and letters, but not for houses, and lower for letters, but not faces or houses.

Compared to young participants, MI was significantly delayed in older participants by 29 ms [13, 53] for faces, by 31 ms [16, 46] for letters, but not for houses, with a difference of 18 ms [-7, 37]. Similar results were obtained by looking at 50% integration times: it took older adults, on average, 33 ms longer [21, 48] to accumulate 50% of their MI time courses for the face contrast, 28 ms longer [18, 36] for the letter contrast, and 17 ms [-2, 32] for the house contrast.

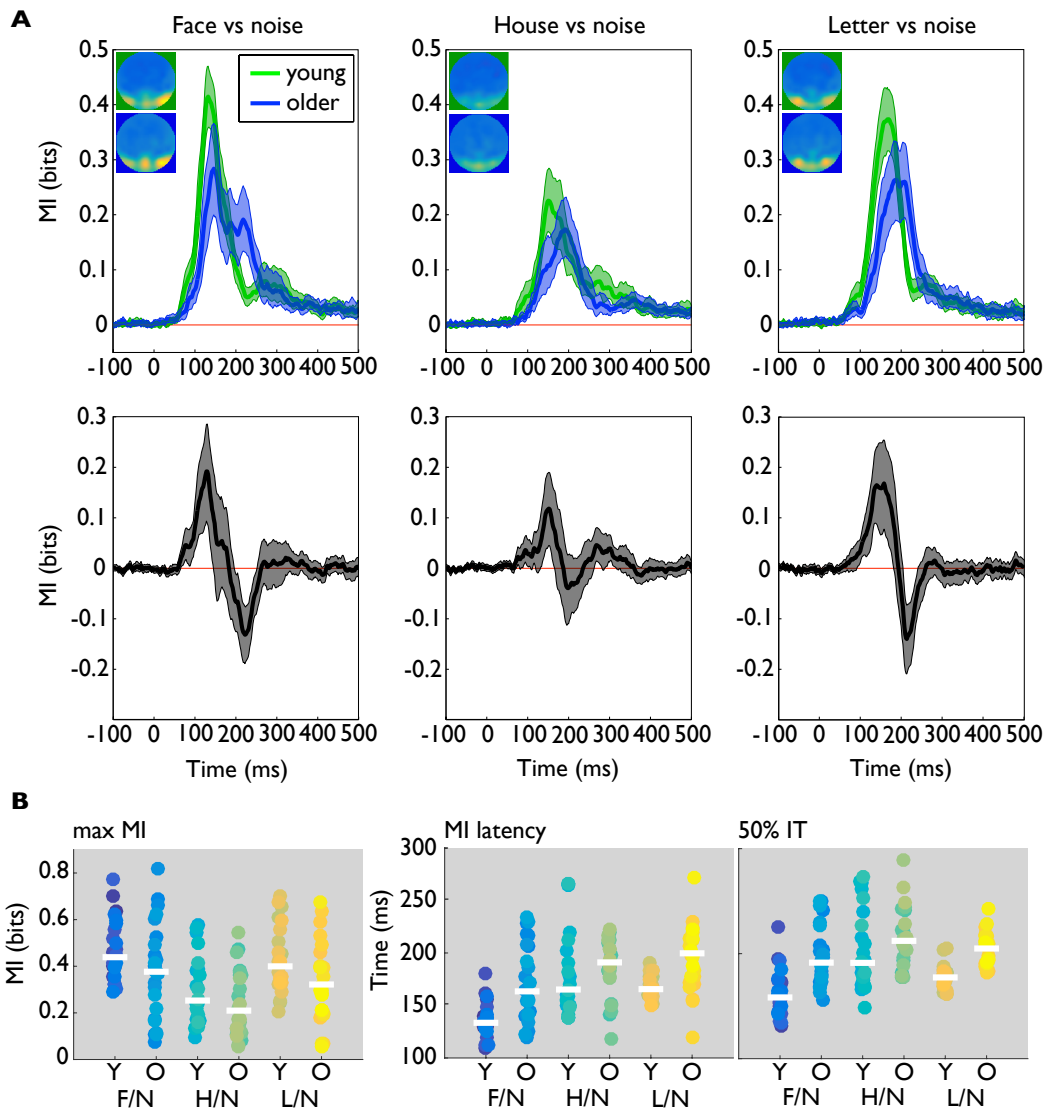


Figure 24 Age-related differences in sensitivity to image structure.

(A) Top panel, MI time courses for the difference between faces and textures (left), houses and textures (middle), and letters and textures (right), averaged across young (green) and older participants (blue). Insets show MI topographies averaged across young and older participants (green and blue boxes, respectively). Bottom panel shows differences between the average MI time course for young and older participants. Shaded areas correspond to 95% confidence intervals. **(B)** Individual participants' maximum MI (left), max MI latency (middle), and 50% integration times (right). Each dot corresponds to one participant. Dots are grouped into young (Y) and older (O) participants, for each of the contrasts (faces vs texture - F/N, etc.). White horizontal bars correspond to median values.

Maximum MI was similar across age groups for houses (difference: -0.05 bits [-0.12, 0.02]; young = 0.25 bits [0.20, 0.35], older = 0.21 bits [0.14, 0.31]). On the other hand, average max MI was stronger in young than in older participants for faces (difference = -0.09 bits [-0.18, 0.02]; median MI in young participants = 0.44 bits [0.39, 0.52], older participants = 0.38 bits [0.27, 0.46]) and letters (difference = -0.09 bits [-0.19, -0.01]; young = 0.4 bits [0.35, 0.48], older = 0.32 bits [0.24, 0.40]).

Average scalp topographies (Figure 24A, insets) revealed a clear right-lateralised pattern of MI for faces in both young (lateralization index = -0.16 [-0.23, -0.05]) and older (-0.12 [-0.21, -0.04]) participants. The average topographies for houses were mostly localised in the midline electrodes with a slight dominance of the right hemisphere (young = -0.09 [-0.19, 0.03], older = -0.08 [-0.18, 0.01]). The average topographies for letters were very slightly left-lateralised in young (0.05 [-0.01, 0.10]), but not in older participants (0.01 [-0.06, 0.06]). There were no group differences in lateralization indices for any comparison ($\text{difference}_{\text{faces}} = 0.01 [-0.10, 0.12]$; $\text{difference}_{\text{houses}} = 0.00 [-0.10, 0.12]$; $\text{difference}_{\text{letters}} = -0.05 [-0.13, 0.03]$).

DISCUSSION

The goal of the present study was to investigate the potential origin of the large visual evoked responses to textures in older adults. Our hypothesis was that early ERPs to noise were modulated by the expectations associated with the task at hand. Specifically, we hypothesized that textures perceived in the context of different tasks would elicit ERP differences similar qualitatively to those observed in response to full images of target objects in those tasks.

We found that, in comparison with young adults, older adults had elevated maximum Mutual Information (MI) values when comparing textures perceived in the face detection vs. house detection, and vs. letter detection tasks. There were no group differences when comparing textures perceived in the house detection vs. letter detection tasks. These results seem to suggest that ERPs recorded in response to textures might be susceptible to top-down effects to some extent, although this effect might be present in the context of the face detection task only. It should be noted, however, that MI was generally quite weak in most participants, with only a few participants showing elevated values. In some participants, MI peaked in the first 100 – 200 ms of stimulus processing, but in most of them it peaked between 200 ms and 300 ms post-stimulus, suggesting that the moderate effect observed in the face detection task relative to the house or letter detection tasks might not be related to the large N170.

Contrary to the small categorical differences between ERPs to textures, limited to trials in the face detection task, we found strong group differences between ERPs elicited by objects. Specifically, maximum MI was consistently stronger in young participants in each of the categorical comparisons. MI about categorical differences between objects also peaked between 130 ms and 190 ms post-stimulus in both groups, so roughly in the time window of the N170. As hypothesized, we found hemispheric differences: the face/house MI was stronger over the right hemisphere, whereas the house/letter MI was stronger over the left hemisphere. However, both the left-lateralization of letters and the right-lateralization of faces was only the case in young participants. Altogether, results from categorical comparisons of ERPs elicited by objects suggest that clear categorical differences can be found in both age groups, and that significant age-related differences can be observed for each pair of objects. These differences, however, were not paralleled in texture-only trials.

As a control condition in this study, at the beginning of the experimental session we presented participants with a set of textures without any object images. The reasoning

behind it was that if large ERP responses to textures in older adults were driven by the task at hand, we would see a strong difference between textures in the control ('baseline') block and textures in the detection blocks. MI revealed considerable differences between textures presented in those two types blocks in young and older participants: they began around 100 ms post-stimulus and were sustained for a long period of time (until 500 ms). However, there were no group differences, suggesting that large responses to textures in older adults are not driven by the presence of a detection task. A similar sustained difference in young participants was found in studies comparing the N1 elicited by foveally presented stimuli during two types of tasks, similar to ours. In simple RT tasks, participants pressed a single button upon detecting any stimulus, whereas in choice RT tasks participants pressed one of two buttons depending on the type of the stimulus (Ritter, Simson, & Vaughan, 1983; Vogel & Luck, 2000). Larger posterior N1 was elicited by stimuli during choice-RT tasks even in the absence of motor response, and was not due to greater arousal or task difficulty (Vogel & Luck, 2000). As such, the difference between textures in the two types of blocks in our study might reflect a general-purpose discrimination mechanism (Ritter et al., 1983; Vogel & Luck, 2000), which does not differ in ageing.

We also compared reaction times on these two types of the task, i.e. a simple task where participants had to press only one key as soon as they saw a texture, and a more complex task where they had to press one of the two keys to discriminate a texture from an object. Older participants had similar average reaction times to young participants on the simple task, but were significantly slower on the more complex task. These results can be thought of as an example of the complexity effect, where behavioural slowing increases with increasing task complexity (Salthouse, 2000). A similar finding was also reported in an ERP study investigating simple- and choice-reaction tasks to visually presented letters (J. Yordanova et al., 2004). Age-related behavioural slowing was attributed to motor response generation, and was specifically associated with a strongly enhanced and prolonged activity in the contralateral motor cortex (Falkenstein et al., 2006; Kolev et al., 2006; J. Yordanova et al., 2004), rather than a decline in perceptual speed marked with a prolonged N170.

Altogether, our results suggest that a small influence of the presence of the face detection task might have an effect on ERPs recorded from older adults. However, this effect might not be related to large amplitudes of the N170 specifically recorded in response to textures, and visible only in a few participants. The fact that the effect was not so clearly visible might also be related to the design of our experiment. In particular, since object images were not degraded or masked with addition of phase noise, they

were very clearly distinguishable from images of textures, therefore yielding the task trivial for both young and older observers. Introducing ambiguity or uncertainty into the visual object might probe the brain to execute more top-down control in order to perceive the image (Gilbert & Sigman, 2007). One such example of top-down specificity can be seen in priming (Bentin et al., 2002; Gilbert & Sigman, 2007; Kato et al., 2004). For example, it would be interesting to run Bentin et al.'s (2002) paradigm in a sample of older participants by comparing the magnitude of the N170 elicited in response to pairs of dots presented in isolation before and after seeing them embedded in a face context (thereby making them interpretable as the eyes). If older adults exerted greater top-down control over ambiguous stimuli, then we could expect a larger priming effect on the magnitude of the N170 than in young participants. Alternatively, participants could view images of textures intermixed with trials containing objects masked with different levels of noise (Mayer, Schwiedrzik, Wibrall, Singer, & Melloni, 2016; Philiastides & Sajda, 2006; Rousselet et al., 2009; Wild & Busey, 2004). Biasing older adults' expectations could produce larger effects on the N170 response to texture only trials. Finally, we used equal numbers of object and texture trials in this study, which might have been suboptimal at eliciting strong expectation effects. The original study included 84 trials per each of the 11 levels of phase coherence (Rousselet et al., 2009). Considering the fact that detecting a face was possible across several phase coherence levels (from ~30% to 100%), the expectation effect could have been stronger in the original study. On the other hand, we observed strong N170-like responses to textures in the current study, even though there was not enough evidence for categorical differences in textures presented in different detection blocks. As such, further research is needed in this area.

Recently, using magnetoencephalography (MEG) Mayer et al. (2016) reported that expectations about visually presented letters lead to increased prestimulus alpha oscillations in a network representing grapheme/morpheme associations. Furthermore, larger expectation-driven effects in prestimulus alpha power were associated with larger differences in early evoked (P1/N1) component (Fellinger, Gruber, Zauner, Freunberger, & Klimesch, 2012; Gruber, Klimesch, Sauseng, & Doppelmayr, 2005). As such, it would be interesting to test whether older adults modulate prestimulus alpha power when expecting to see a particular stimulus category and if so, whether this modulation is related to large N170 amplitudes on texture trials.

On the other hand, larger evoked responses in older adults not specific to any stimulus category might be a feature of healthy ageing and linked to age-related differences in inhibitory processing (De Sanctis et al., 2008). An age-related deficit in suppression of irrelevant information in older adults was previously found using EEG in a working

memory task (Gazzaley et al., 2008). However, the suppression deficit was described as an inability to modulate the N1 latency, not amplitude (Gazzaley et al., 2008). Larger amplitudes in older adults were previously reported for visually presented faces (Rousselet et al., 2009), letters (Falkenstein et al., 2006; Yordanova et al., 2004), and letter-number pairs (De Sanctis et al., 2008), although two studies reported an attenuation of the N1 amplitude to letters in very old participants (80+ years old) and no difference between young (18-32 years old) and young-old (65-79 years old) participants (Daffner, Haring, & Alperin, 2013; Zhuravleva et al., 2014).

Evidence for an age-related deterioration in inhibitory control that was related to increased visual response amplitudes comes from single-neuron recordings in animals. Monkey studies reported significant degradation of orientation and direction selectivity in single neurons from V1 (Schmolesky et al., 2000), V2 (Wang et al., 2005; Yu et al., 2006) and MT (Yang et al., 2008), possibly related to deterioration in GABA-mediated inhibition (Hua et al., 2008; Leventhal et al., 2003). These changes were accompanied by enhanced visual response amplitudes to preferred as well as non-preferred stimuli, higher signal-to-noise ratios, and higher levels of spontaneous activity. In humans, similar de-differentiation of responses was found using functional magnetic resonance imaging (fMRI) in brain areas that respond maximally to certain stimulus categories in young adults, such as faces or words (Burianová, Lee, Grady, & Moscovitch, 2013; Park et al., 2004; Park et al., 2012; Voss et al., 2008). For example, the area in fusiform gyrus responding most strongly to faces in young adults (fusiform face area, FFA; Kanwisher, McDermott, & Chun, 1997) showed increased responses to other stimulus categories in older adults (Park et al., 2004; Park et al., 2012; Payer et al., 2006). Voss et al. (2008) computed a differentiation index providing a measure of discriminability, or specificity of neural responses in certain brain areas and reported a significant age-related reduction in neural specificity in regions responding to faces and places. However, to our knowledge no study to date assessed de-differentiation of neural responses using EEG. In this study, results showing lower MI in categorical differences between objects in older adults might suggest that neural responses elicited by faces, houses and letters are less differentiated than in young adults. On the other hand, comparing responses elicited by objects and their corresponding textures revealed similar MI in young and older adults alike for faces and houses, but not letters, where MI was stronger in young participants. Similar MI for faces and houses is in line with previous findings from our lab in which we reported no age-related differences in effect sizes for the difference between face and texture trials (Rousselet et al., 2009, 2010; Jaworska et al., in prep), suggesting that these two types of evoked responses can be discriminated similarly in the two groups.

As such, further research is needed in order to assess whether large N170 in response to textures might be driven by deterioration of inhibitory control and a resulting de-differentiation of neural responses. For example, local variations in GABA levels found in visual cortices of young and older adults could be measured in the same individuals performing object detection task using EEG to investigate the relationship between levels of GABA and amplitudes of the N170 elicited in response to textures. It would also be interesting to compare responses elicited by our stimuli using MEG, which offers better spatial resolution and similar temporal resolution as EEG. A differentiation index similar to that used by Voss and colleagues (2008) could then be computed in regions responding most strongly to stimuli used in our study.

In our final set of comparisons, we looked at MI between objects and textures to investigate processing speed differences between young and older adults. Previous studies in our lab only contrasted face stimuli with textures (Rousselet et al., 2009, 2010; Bieniek et al., 2013, 2015; Jaworska et al., in prep) and reported a 1 ms/year slowing in processing speed (Rousselet et al, 2010; Bieniek et al., 2013). Here, in comparison to textures, processing of faces and letters (but not houses) was delayed by about 30 ms in older participants. This difference was somehow smaller than in previous studies, in which a delay of about 50 ms was reported, and could be attributed to a difference in the shape of the time courses. Previous studies reported that, in older adults, sensitivity to image structure was spread over two time windows, one weaker around 150 ms following stimulus onset, similarly to young adults, and one stronger after 200 ms (Rousselet et al, 2009, 2010). Here, MI peaked only once, and in the same time window both in young and older participants. The reason for this discrepancy might be in the stimuli used. Specifically, in previous studies phase noise was added to images of faces in a parametric manner (Rousselet et al., 2009, 2010) or such that faces had 70% phase coherence (Bieniek et al., 2013). Here, phase coherence of object images was kept at 90% and only randomized to create textures. As such, the second period of face processing, observed in previous studies and occurring after 200 ms in older adults could reflect differences introduced by the presence of a higher level of phase noise in the images. The second peak, occurring after 200 ms and corresponding to the P2 component, has been reported previously in young participants processing stimuli with added noise and suggested to reflect task difficulty (Philiastides and Sajda, 2006) or increased sensory processing demands of noisy stimuli (Bankó et al., 2011). Notably, in our previous studies, the second peak was not observed in young participants with the same stimuli with added noise, suggesting that older adults specifically are less able to

tolerate distortion in the stimulus that occurs with introduction of noise (Grady et al., 2000).

CHAPTER 5: GENERAL DISCUSSION

The ultimate goal of cognitive neuroscience is to understand the brain as an organ of information processing, for example when detecting faces in the surroundings. Although face detection might seem trivial from a behavioural point of view, our understanding of the exact computational stages that the brain goes through from the moment when the input arrives from the retina to the visual cortex, until this input is categorized in order to allow for decision making to take place is still far from comprehensive. Furthermore, given that the brain ages as dramatically as the body, we cannot be certain that these information-processing stages remain the same throughout the lifespan.

One of the most prominent accounts of cognitive ageing proposed that behavioural impairments on a variety of perceptual and cognitive tasks can be accounted for by a generalized slowing down of the neural information processing (Salthouse, 1996). Although there exist human and monkey studies (reviewed in Chapter 1) showing evidence for the structural and physiological differences and changes in the brain that could account for the observed behavioural slowing of responses and deterioration in accuracy, little research has in fact directly tested the slowing hypothesis on a neural level. Recent studies using EEG have tackled this problem and investigated processing of faces in comparison to textures (Rousselet et al., 2009, 2010; Bieniek et al., 2013, 2015) to show that ageing slows down visual processing speed by 1 [0.79, 1.25] ms per year and that this effect has a cortical, rather than optical origin. As such, two groups of participants whose mean or median ages are separated by 50 years will be expected to show a 50 [39.5, 62.5] ms delay in processing the same stimulus. However, although similar statistical properties of the image were shown to drive the electrophysiological visual responses, it remained unclear what actual *face information* was associated with these responses.

In this thesis, we aimed to shed light on this issue by investigating some of the information processing steps in the ageing brain using the most basic task for social cognition: face detection. In order to understand how the aged brain processes information in a face detection task, we must begin by asking questions: *what* information the brain processes when it detects a face, and *when* this information is processed with respect to the young brain. We tackled these two questions in Chapter 2. In order to find out what facial information is used by young and older adults alike, we employed the Bubbles paradigm which samples stimulus space in a randomized yet principled manner, and reverse-correlated the stimulus information revealed in single

trials with behavioural and brain responses. We have shown that the same information (the eye region) is associated with faster reaction times in both young and older adults alike, although older adults relied on the presence of the eyes more to make a correct discrimination. Furthermore, single-trial EEG responses were also modulated by the presence of the contralateral eye in the image, thereby extending similar results found previously in a sample of young adults (Rousselet et al., 2014) to a sample of older adults. Importantly, this association was weaker and delayed by 40 ms in older compared with young participants, although the delay amounted to only 20 ms when measured with the 50% integration times – the same technique employed previously by Rousselet et al. (2009). This modulation of EEG responses by eye visibility was demonstrated at the level of the N170 – an ERP component frequently associated with face categorization (Bentin et al., 1996). In young adults, higher eye visibility was associated with earlier and larger N170, whereas in older adults – only with larger responses. This pattern of responses was also more pronounced in the right hemisphere in young, but not older adults, suggesting a differential coding of the eye by the N170 in ageing. It should be kept in mind that the observed delay was smaller than the increase in reaction times, suggesting that both sensory and post-perceptual (decision-making, motor execution) slow with age. As such, it would be interesting to track information transmission across visual processing stages with newly developed techniques, such as Directed Information (DFI, Ince et al., 2016). Also, it would be interesting to extend analyses to later ERPs, such as the P300, which is considered an index of post-sensory evaluation processes.

Altogether, the results from this study fill the big gap in the literature concerned with age-related slowing of information processing: we have presented direct evidence that processing of the same facial information is slower (and weaker) in ageing, in line with Salthouse's (1996) theory.

In a follow-up study (Chapter 3), we sought to understand whether the age-related differences in eye sensitivity were preserved in a face context, on a notion that incomplete or occluded stimuli (such as Bubbled images) might differentially affect older adults' ability to perform a perceptual task. The results confirmed our suspicions in a way that contralateral eye sensitivity was still observed in young and older adults alike, but to a lesser degree than in the Bubbles study. Importantly, we did not observe any age-related differences on the N170 coding of the eye, and the observed weak eye sensitivity was not weaker or delayed in older adults. As such, in the second experiment we demonstrated that processing of the eye is *not* delayed or weaker in older, compared with young adults when the face context is preserved, in contrast to the theory of slower

processing speed in ageing. However, a categorical comparison of ERP activity elicited by faces and textures revealed similar differences as those observed in previous studies (Rousselet et al., 2009, 2010). In the present study, processing of faces with respect to textures was delayed by 32 – 46 ms depending on the condition. As such, we observed the age-related delay reported in previous studies but only when making a categorical comparison between faces and textures, suggesting that this difference might be due to larger responses to textures in older adults.

In order to explore the origins of these large responses to textures reported already in previous studies (Rousselet et al., 2009), in particular on the N170, we conducted the third experiment (Chapter 4) in which we employed a series of simple detection tasks involving faces, houses and letters. We analysed differences between *texture* trials, in order to test if perceiving textures in the context of different detection tasks would influence ERP responses to textures in a top-down manner. However, we did not find an effect of the presence of the detection task on early (<200 ms) responses to textures, although there was a weak effect of a face detection task on later responses (>200 ms). We concluded that this effect did not present enough evidence to suggest a top-down influence on the responses to textures, and that an alternative explanation could be related to an inhibition, or de-differentiation of cortical responses in ageing. In terms of visual processing speed, we found that running categorical comparisons between textures and faces, houses or letters revealed group differences of about 17 – 33 ms; however, comparing ERPs elicited by objects only revealed no age-related delays between faces and houses or faces and letters, and only a small difference between houses and letters. Given that the age difference between the two samples used in this study was 45.5 years, the observed processing-speed differences were smaller than the reported 1 [0.79, 1.25] ms/year delay observed for faces previously (Rousselet et al., 2009), even after taking into account confidence intervals associated with the original finding.

How do our findings tie in with the existing theories of ageing? In a recent study age has been shown to have dissociable effects on neural processing speed in visual and auditory evoked responses (Price et al., 2016), suggesting that neural delay should not be thought of as unitary concept that affects all brain regions equally. Furthermore, Price et al. (2016) provided evidence for dissociation in structural differences of functionally relevant brain regions responsible for transfer and processing of information: whereas visual delays were linked to white matter integrity, auditory delays were underlined by local differences in grey matter. Here, although our first study provided evidence for slower information processing in ageing, results from the other two experiments yielded

mixed results suggesting that slowing within a visual system might not be generalizable across visual stimuli, thereby extending results of Price et al. (2016) to within-domain.

On the other hand, consistently across studies we found large N170-like responses to textures. Elevated early sensory responses to visual stimuli in older adults seem to be a ubiquitous observation in the ERP literature (Falkenstein et al., 2006; De Sanctis et al., 2008; Rousselet et al., 2009; Bieniek et al., 2015). Large ERP amplitudes to redundant information in older adults could be explained in terms of a decrease in efficiency of inhibitory processing, or some general activation to a visual stimulus without functional significance (De Sanctis et al., 2008). Notably, we also found weaker brain sensitivity to visual information in older adults, which could be suggestive of de-differentiation of early ERPs (Park et al., 2004, 2012) although further confirmatory research is needed to support this idea. As pointed out in Introduction, de-differentiation of neural responses could arise as a result of decreased signal-to-noise ratio of neuronal responses (Schmolsky et al., 2000), which itself could be related to weaker inhibitory processing due to changes in neurotransmitter function (Leventhal et al., 2003). Increased neural noise might, in turn, result in higher sensory thresholds and slower rates of neural information processing (Salthouse & Meinz, 1995; Salthouse, 1996). As such, the results presented in this thesis could be due to a combination of neurophysiological causes and it is impossible to disentangle the underlying factors with the current methods.

Future studies should investigate these issues further by merging a variety of neuroimaging and stimulation methods with different behavioural tasks. For example, continuous theta burst stimulation (cTBS) with transcranial magnetic stimulation (TMS) (Huang, Rothwell, Chen, Lu, & Chuang, 2011; Pascual-Leone et al., 2011) could perhaps be used to increase neural inhibition over the lateral-occipital regions in older adults. It would be interesting to investigate not only whether increased inhibitory processing led to a reduction in the N170 amplitude to meaningless stimuli and whether representation of diagnostic information was stronger in older adults, but also if speed of information processing would be affected. On a behavioural level, paradigms merging careful stimulus control with inhibitory processing, such as garden path sentences, Stroop tasks, negative priming or go no-go tasks could in principle shed more light on the involvement of inhibitory processing in ageing. Likewise, according to Salthouse's (1996) theory, generalized slowing should be more pronounced as task complexity increases, suggesting a simple to test hypothesis that more difficult tasks should produce neural delays of larger magnitudes. For example, future studies should investigate and replicate age-related differences of information content on more complex and socially relevant tasks, such as gender or age discrimination, identity judgments or emotion

categorization, and assess task-dependent delay of information coding with respect to the N170 in both groups. Finally, future studies should attempt to employ multimodal imaging techniques, for example MRI and MEG (Price et al., 2016), as well as MR spectroscopy in order to better understand the relationship between structural, physiological and functional age-related differences in information processing. In summary, future research should aim to integrate across behavioural, information-processing and neurobiological levels in order to obtain an integrative understanding of cognitive ageing phenomena (Li, Lindenberger, & Sikström, 2001).

Overall, the experimental work described in this thesis has furthered the knowledge with regards to *what* information is processed by the aged brain in a face detection task, and *when*. As such, we have explicitly addressed the hypothesis arising from Salthouse's (1996) account of a generalized slowing down of information-processing speed by showing that in both age groups, the contralateral eye (the *what*) is processed in the time window of the N170 (the *when*), and is delayed by 40 ms (or 20 ms measured with 50% integration times) with respect to young participants. However, there were no age-related differences on the eye coding by the N170 when face context was present. Furthermore, we have replicated the previous account of a slower visual processing speed (Rousselet et al., 2009) only to some extent. Depending on the stimulus and the comparison, we have either observed age-related differences of about 17 – 46 ms in visual processing speed or no differences at all. Altogether, these results suggest that the age-related delay of 1 ms/year observed in earlier studies might be due to a peculiar form of the ERP wave in response to textures, and might not hold true for categorical differences obtained with other object categories. Alternatively, the distinctive shape of the face vs. texture waveform in older adults could be driven by the response to images of faces that have been phase-randomized. This pattern was observed in studies where phase coherence of entire face images was phase randomized in a parametric manner (Rousselet et al., 2009, 2010), or kept at 70% (Bieniek et al., 2015), or where phase coherence of the eye region was modulated between 0% and 60% (Chapter 3), but not when face images were presented at 90% phase coherence (Chapter 4). As such, it would be interesting to revisit the datasets analysed in Rousselet et al. (2009, 2010) to check whether a similar pattern of responses is present at different levels of face visibility.

It has been shown previously that stimulus degradation has an adverse effect on a face matching task in older adults (Grady et al., 2000). In our three studies, we have used three different stimulus manipulations to study visual processing speed: in the first study, the images of faces were degraded to the largest extent by revealing portions of the image through the Gaussian apertures. In the second study, we modulated the visibility

of the eye parametrically by introducing different levels of phase coherence, whereas the face context remained intact. In the third study, the stimuli were manipulated to the smallest extent: all objects in the three categories were presented at 90% phase coherence. Each of these approaches might have advantages and disadvantages depending on the research question being answered. The use of Bubbles seems to be ideally suited for investigating the information processing in the brain. This is because the stimulus itself acts as its own control condition (Schyns et al., 2003) – we are not interested in comparing categorical responses elicited by, for example faces and textures. Instead, we can study single-trial fluctuations of activity that crucially depend on the information available from the stimulus. However, this paradigm might not be ideal to study age-related differences in information processing because older adults seem to benefit from the available contextual information, as we have shown when the whole face context was preserved (thereby providing a more ecologically valid stimulus) in Chapter 3. In light of these findings, it would be interesting to investigate whether the eye sensitivity can be preserved in ageing when more informative stimuli are used, albeit not as revealing as in our second study (Chapter 3). For example, a number of apertures could be increased for older participants so that their performance is matched to that of young participants (in our first study, the same number of Bubbles was used in both groups). Alternatively, a more meaningful stimulus set could be used that, for example, contains coloured faces and reveals external features aiding detection (such as hair). Another possibility would be to use 3-D Bubbles sampling (Gosselin & Schyns, 2001; Schyns et al., 2007, 2011; Schyns, Petro, & Smith, 2009), rather than 2-D sampling used in Chapter 2 of this thesis. With 3-D Bubbles, sampling is performed independently in different spatial frequency bands in addition to sampling over a two-dimensional image plane. Adding Bubbles sampled over a wide range of spatial frequencies allows for presentation of face features visible at lower spatial frequencies than presented here (therefore preserving the face context). Presenting a stimulus sampled over different spatial scales might reveal more global features of the face (such as the oval of the face against the background), in addition to fine detail preserved in high spatial frequencies. All in all, our results point to the need for carefully and tightly controlled visual stimuli in ageing research, and careful selection of control stimuli for comparisons.

LIMITATIONS AND FUTURE DIRECTIONS

There are certain limitations present in the experimental work that constituted this thesis that we acknowledge and address in turn. First, we did not record eye movements in either experiment. Although participants were instructed to fixate the cross presented at

the centre of the screen, and the stimulus duration (about 83 ms) was too short to initiate saccadic eye movements, we cannot rule out the possibility that participants fixated slightly off the cross in a systematic way that could have affected our results. This could be problematic because information presented at the fovea is processed more efficiently than in the periphery, due to cortical magnification in V1 (Azzopardi & Cowey, 1993) as well as in higher-level processing regions, such as the inferotemporal cortex (Rolls et al., 2003). Furthermore, when allowed a variable number of fixations on the face stimulus, humans tend to land their first fixation just to the left of the centre of the nose (Hsiao & Cottrell, 2008), suggesting a left-side perceptual bias in face perception (Gilbert & Bakan, 1973), also found in older participants (Williams, Grealy, Kelly, Henderson, & Butler, 2016). In addition, eye movements associated with left perceptual bias did not differ between young and older participants (Williams et al., 2016), although age-related disruptions in sampling behaviour (more fixations and more transitions) were found in a different experimental setting (Firestone, Turk-Browne, & Ryan, 2007). Future studies should employ eye tracking at least in order to make sure that participants are fixating the correct position on the screen. Ideally, the full account of face/eye detection mechanisms should consider the influence of cortical magnification and fixation locations that could either amplify or abolish sensitivity to eye features (de Lissa et al., 2014; Nemrodov et al., 2014; Rousselet et al., 2014; Zerouali et al., 2013).

Furthermore, older participants wore habitual correction if needed. However, given presbyopia (i.e. age-related blurring of close-up vision due to loss of elasticity of the lens of the eye) this solution could be sub-optimal as a corrective measure. Specifically, use of either reading or distance glasses might be inefficient at computer distance, which is often considered intermediate. As a result, habitual correction might be inefficient at correcting blur in older participants, which could, in turn, lead to age-related differences at the behavioural level. For example, the observed reliance on the eye region to detect a face in older adults (Chapter 2) could be due to a behavioural strategy to focus on the face region with more contrast, to compensate for potentially increased blur. To overcome this issue in ideal world, visual acuity at the exact computer distance used in the study should be assessed and optimal correction at this distance should be given to each participant. However, limitations to this approach include the need for non-standard distance tests, and a range of correction spectacles available for use in the laboratory, associated with a significant increase in costs needed to run a study.

Furthermore, all studies reported in this thesis used relatively small sampled and unusual participants. In particular, studies were conducted at the University of Glasgow, and recruitment of participants (both young and older alike) was conducted in the vicinity of

the university. As such, it is likely that our sample of older adults over-represented those healthy, well-educated, highly motivated and generally high-functioning volunteers, some of whom were retired university staff. It should be kept in mind that sampling bias might be particularly problematic in ageing studies in general. Less healthy persons could be less able to participate in research studies, and health itself might deteriorate in ageing. As such, progressively older adults who do participate in studies may be progressively less representative of the group they are intended to reflect (Golomb et al., 2012). Although we cannot say whether better health or education would influence brain activity, especially that related to a simple face detection task, this issue should be explored further. One way to ensure the separation of age-related factors from other sources of individual variation is to provide a sufficient sample size in each age group. Recent study from our lab suggested that testing at least 20 participants per group appears to reduce the variability of data points considerably (Bieniek et al., 2015). In order to meet this requirement, we tested 23 participants in the second study, and 24 in the third study, but only 18 participants in the Bubbles study. Given that not all older participants had significant Mutual Information between stimulus space and ERPs (Chapter 2), the time courses and the resulting group differences could have been due to only a few individuals displaying strong effects. As such, information processing speed should ideally be quantified using large samples of individual participants. Additionally, collaborative efforts could address the issue of sample size by attempting to combine datasets collected in multiple locations and performing analyses on an enlarged dataset (Babiloni et al., 2006; Fennema-Notestine et al., 2007; Gaetz, Roberts, Singh, & Muthukumaraswamy, 2012).

Furthermore, to ensure that observed age-related patterns of neural change are relevant to population at large, to it advisable to use a population-based representative sample, for example using primary care population list of residents as the sampling frame (Shafto et al., 2014). However, recruitment of older adults for participation in research is a recognized difficulty due to several barriers, such as mistrust and transportation obstacles, caregiver burden, medical concerns and indifference (McHenry et al., 2015). Increasing efforts to recruit larger and representative samples should thus become an area of systematic planning and evaluation in labs undertaking ageing research. For example, McHenry et al. (2015) reported a successful recruitment plan for a medical study, detailing four strategies as important for representative participant recruitment and retention:

- 1) Accessing an appropriate population, e.g. by maintaining solid relationships with community-based organizations in multiple geographical locations;

- 2) Communication and trust-building, e.g. by maintaining face-to-face contact;
- 3) Providing for comfort and security, e.g. by limiting perceived burden such as discomfort, fatigue, time and travel;
- 4) Expression of gratitude.

Overall, ageing studies should start considering sampling and recruitment as critical components of the experimental design (Falk et al., 2013).

Apart from the sampling bias, we used cross-sectional designs, meaning that cohort effects (e.g. in educational attainment, nutritional differences) could also potentially confound results in a yet unknown manner. For example, Nyberg et al. (2010) reported qualitative differences in recruitment of frontal regions in older adults for cross-sectional versus longitudinal designs, suggesting that longitudinal designs might be needed to confirm or disprove the results obtained with cross-sectional designs.

Finally, due to low spatial resolution of EEG, we have no way of saying which brain areas contributed to the reported effects, and whether the same sources (or processes) were responsible for the effects reported in the two age groups. This question is particularly relevant in light of the two findings reported in Chapters 2 and 3, i.e. large group differences on the latency and amplitude coding of the eye in the Bubbles study versus similar coding of the eye in the face context. This issue could be addressed, for example, by using MEG, which offers similar temporal resolution and better spatial resolution than EEG. Investigating *where* the task-diagnostic information is processed is another step in trying to understand the information-processing networks in the brain. This is particularly important in ageing, which has been associated with de-differentiation of neural responses in face-selective areas in the ventral visual stream (Park et al., 2004) and increased functional connectivity with frontal and parietal regions (Burianova et al., 2013; Lee et al., 2011), suggesting that task-related brain networks lose some specificity and become less modular in nature (Meunier, Achard, Morcom, & Bullmore, 2009) in older adults. As a result, very different cortical networks could mediate equivalent performance in the brains of young and older adults.

APPENDICES

APPENDIX A

Supplementary material for Chapter 2.

SUPPLEMENTARY RESULTS

EFFECT SIZES FOR BRAIN SENSITIVITY TO IMAGE STRUCTURE

In order to establish similar brain response sensitivity across the two age groups, we computed Cliff's *delta* estimates for the difference between ERPs to face and noise trials (for practice and Bubble trials separately) for every time point and every electrode in each participant separately. Then, we saved the maximum *delta* value across time points and electrodes in each participant, and computed the median across participants in each age group.

The brain response sensitivity to full images was similar across the two groups in practice trials (difference (young-older): 0.01 [-0.07, 0.09]; median Cliff's *delta* in young participants = 0.64 [0.58, 0.68], median Cliff's *delta* in older participants = 0.60 [0.54, 0.69]).

This effect was smaller in Bubble trials in both groups: 0.35 [0.32, 0.40] in young, and 0.30 [0.25, 0.35] in older participants (difference: 0.06 [0.01, 0.11]). This small difference, however, is difficult to interpret given sparse sampling of face information on single-trial level. Therefore, similar values of the Cliff's *delta* estimates in both groups in *practice* trials are an indication of similar brain response sensitivity across age groups.

COMPARISON OF MI VALUES OBTAINED WITH DIFFERENT METHODS

In the main manuscript, we used an approach where data were quantized into a number of bins, and MI was estimated over the resulting discrete spaces. However, the binning approach can be sensitive to the problem of limited sampling bias. In order to test the results described in the main manuscript, here we computed a new estimator of MI that can be used with continuous variables (Ince, Giordano, et al., 2016) and utilizes the concept of copulas (Nelsen, 2007), statistical structures that express the relationship between two random variables, independently of their marginal distributions. The copula method does not require the binning step and overcomes this problem while being computationally efficient (Ince, Giordano, et al., 2016).

In single participants, we calculated MI between visibility of the left eye (a scalar value obtained as a sum of pixel visibility within the circular left eye mask on each trial, cf. main manuscript) and EEG voltage over the time period of -300 ms before to 1000 ms after stimulus onset (*regular* MI, Table S1). We also computed the temporal gradient of the EEG voltage (dEEG) on each trial in order to account for the temporal relationship between neighbouring time points, and then combined the EEG voltage and its temporal gradient into a bivariate response (*gradient* MI, Table S1). We then calculated the time course of MI about the eye visibility in the bivariate response: MI(eye, [EEG dEEG]). Considering the gradient response together with the voltage smoothes out the artifactual dips in MI time courses, occurring at time points of zero-crossings when EEG voltages change the sign. It also introduces information about the shape of the ERP, otherwise missing from just considering instantaneous amplitudes. As such, the bivariate time course provides a clearer picture of the time window(s) over which the EEG signal is modulated by the changing stimulus (Ince, Giordano, et al., 2016). Finally, in order to check whether information about the eye visibility was coded in a more distributed manner across the scalp in older compared with young participants, we ran Principal Component Analysis (PCA) on each time point in individual participants. Then, we computed MI between the top four components and eye visibility (*multivariate* MI, Table S1).

All analyses yielded group differences comparable to those obtained with the binning method and described in the main manuscript: MI about the left eye was delayed by about 37 - 47 ms in older compared with young participants, and peak MI in older participants was 49 - 59% the size of that in young participants. As such, the binning method was sensitive enough to provide a good description of age-related differences in eye coding.

Table S 1 Comparison of MI obtained with different methods.

We computed continuous MI between eye visibility and EEG (**regular**), bivariate MI between eye visibility and combined EEG and its temporal gradient (**gradient**) and MI between eye visibility and PCA components (**multivariate**) in single subjects. Values correspond to the Harrell-Davis estimates of the median latency (expressed in milliseconds) of maximum MI, and maximum MI (expressed in bits) computed across young and older participants and at the left occipito-temporal (LE) and the right occipito-temporal sensors separately. Group differences are expressed as the median of all pairwise differences between participants in each group. Additionally, the group difference in MI amplitudes is expressed as a ratio of the median amplitude in young to the median amplitude in older participants. Square brackets indicate 95% confidence intervals.

	Latency (ms)		Amplitude (bits)	
	LE	RE	LE	RE
regular				
young	165 [158, 177]	162 [158, 172]	0.07 [0.04, 0.11]	0.12 [0.09, 0.14]
older	212 [195, 249]	201 [191, 218]	0.04 [0.03, 0.06]	0.05 [0.04, 0.08]
difference	47 [29, 89]	39 [25, 58]	-0.03 [-0.07, 0]	-0.06 [-0.09, -0.03]
			<i>ratio:</i>	<i>ratio:</i>
			0.59 [0.39, 1.03]	0.51 [0.35, 0.77]
gradient				
young	166 [157, 188]	164 [156, 175]	0.07 [0.05, 0.11]	0.12 [0.09, 0.14]
older	213 [196, 256]	201 [189, 219]	0.04 [0.03, 0.05]	0.05 [0.04, 0.08]
difference	47 [19, 84]	37 [21, 56]	-0.03 [-0.07, 0]	-0.07 [-0.09, -0.03]
			<i>ratio:</i>	<i>ratio:</i>
			0.58 [0.36, 1.04]	0.49 [0.33, 0.72]
multivariate				
young	171 [166, 183]		0.09 [0.08, 0.12]	
older	210 [195, 237]		0.06 [0.04, 0.08]	
difference	38 [20, 70]		-0.03 [-0.07, -0.01]	
			<i>ratio: 0.57 [0.39, 0.85]</i>	

SUPPLEMENTARY FIGURES

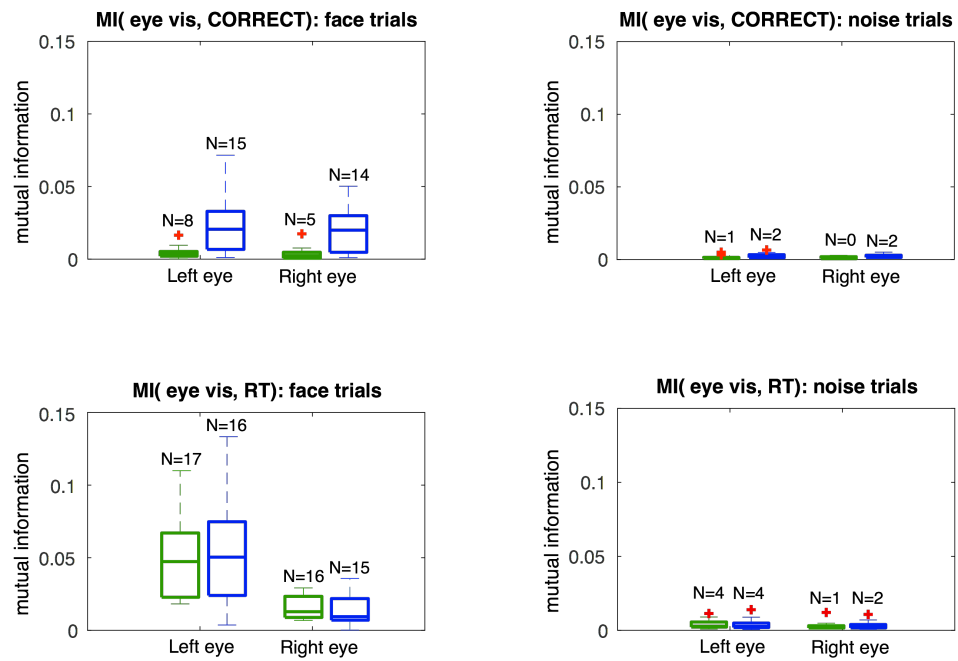


Figure S 1 Boxplots of MI results. Presented are boxplots for MI between eye visibility (summed within the left and the right eye aperture) and correct responses (top) and reaction times (bottom), separately for young (green) and older (blue) participants and for face (left) and noise (right) trials. Numbers above each boxplot present the number of participants showing significant MI for each condition.

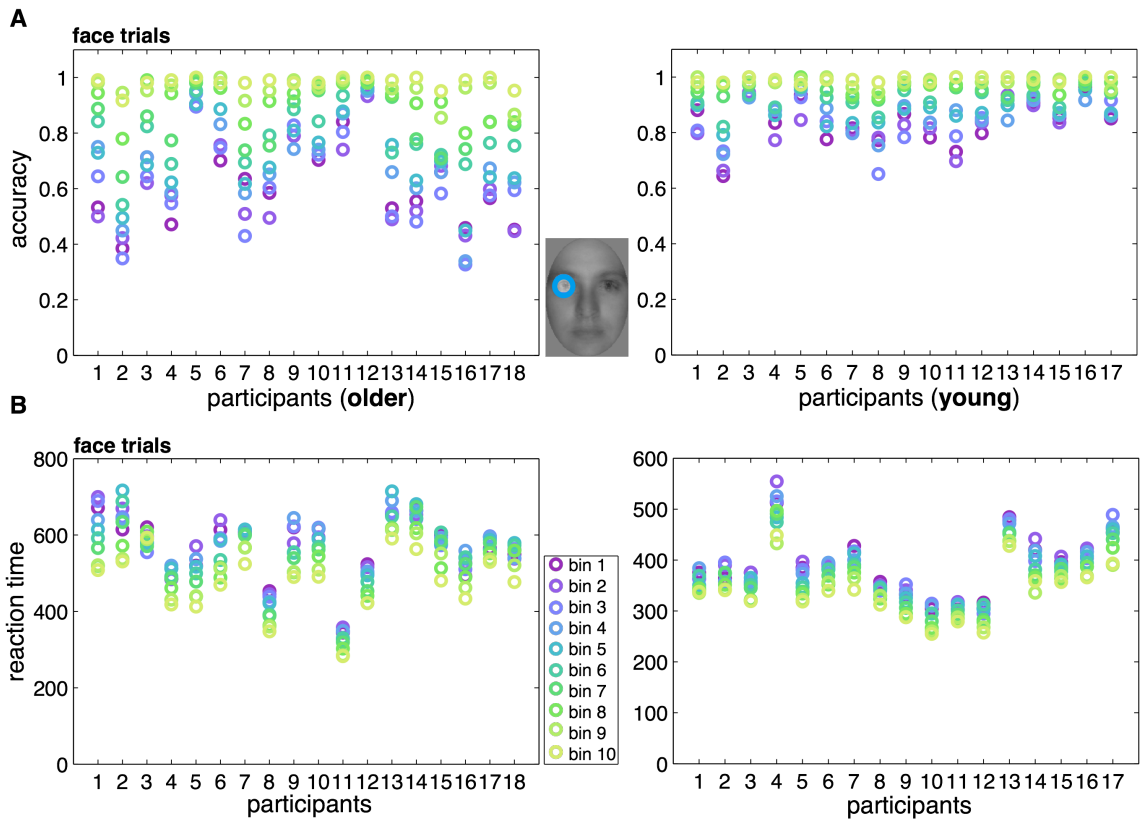


Figure S 2 Reverse analysis: Left eye (face trials). Each column of dots presents one participant's accuracy scores (top) and reaction times (bottom) averaged within each of the 10 bins of left eye visibility in face trials (bin 1: low visibility, bin 10: high visibility). Young (right) and older (left) participants' scores are presented separately. Low eye visibility (low bin numbers and purple to blue colours) were associated with lower accuracies and slower reaction times. This association was particularly visible in older participants' accuracies.

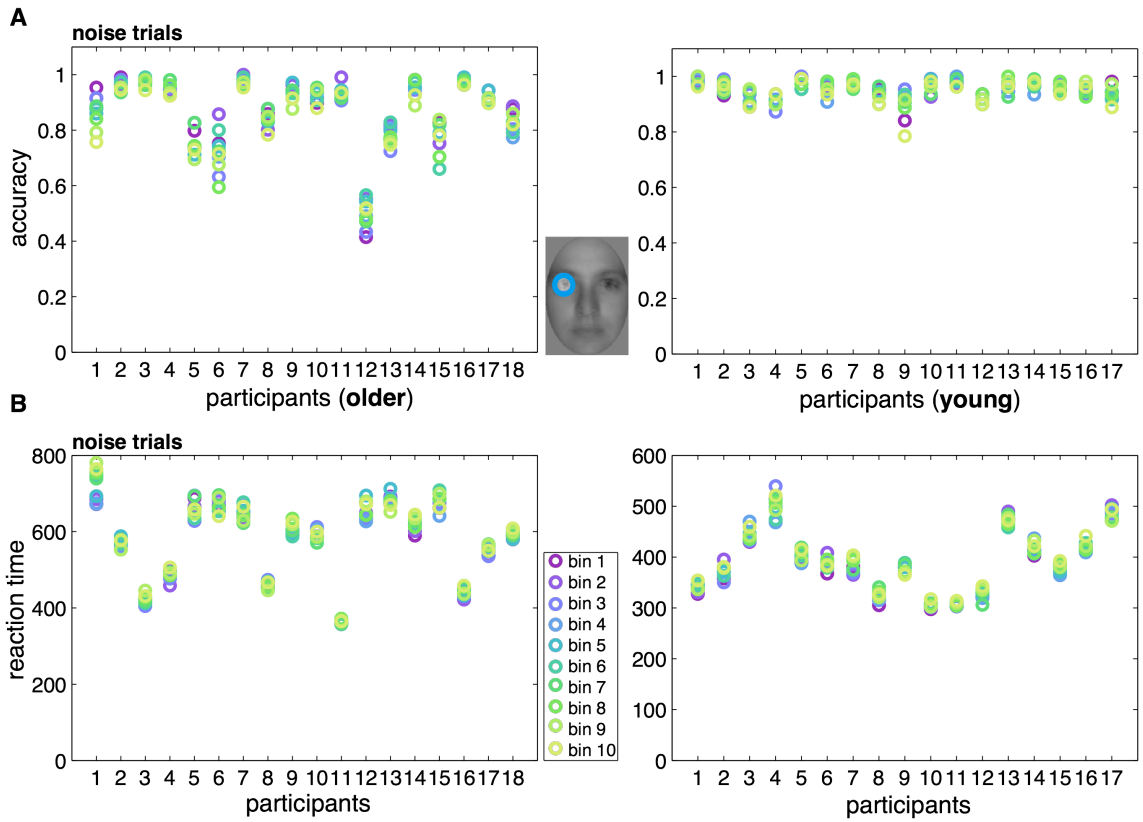


Figure S 3 Reverse analysis: Left eye (noise trials). For details, see Figure S 2 caption.

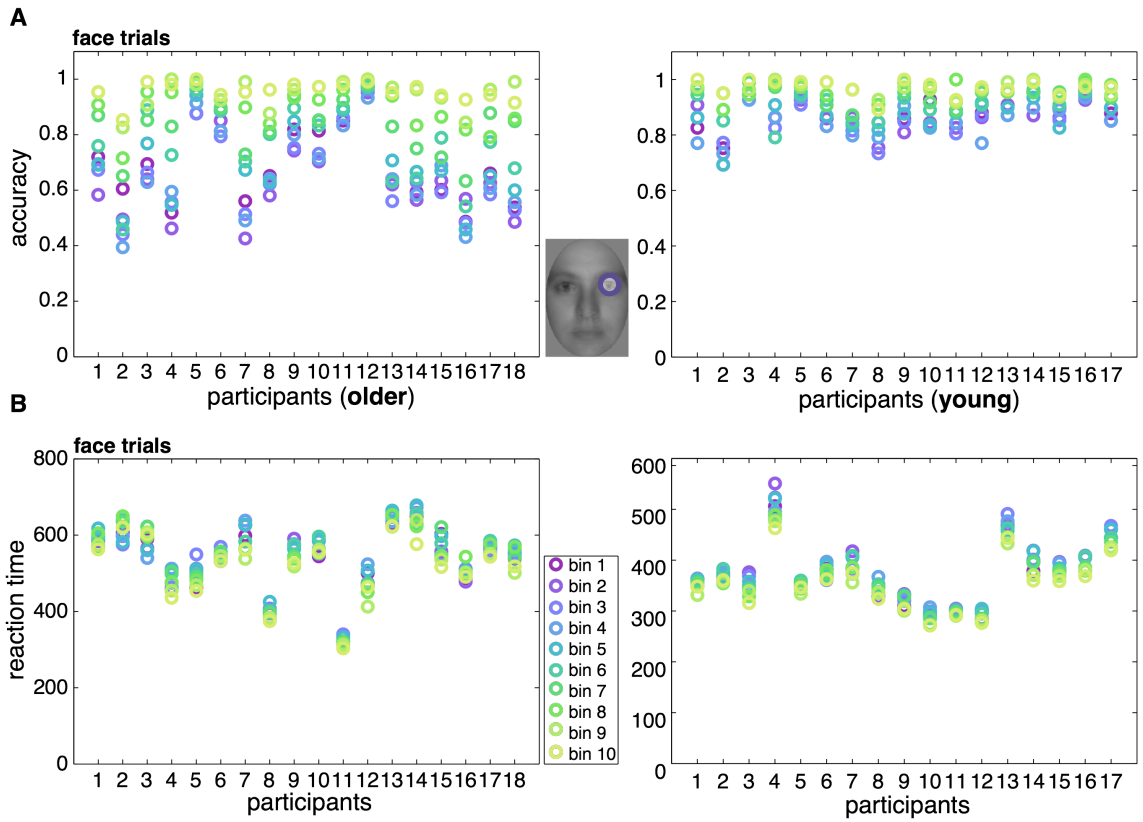


Figure S 4 Reverse analysis: Right eye (face trials). For details, see Figure S 2 caption.

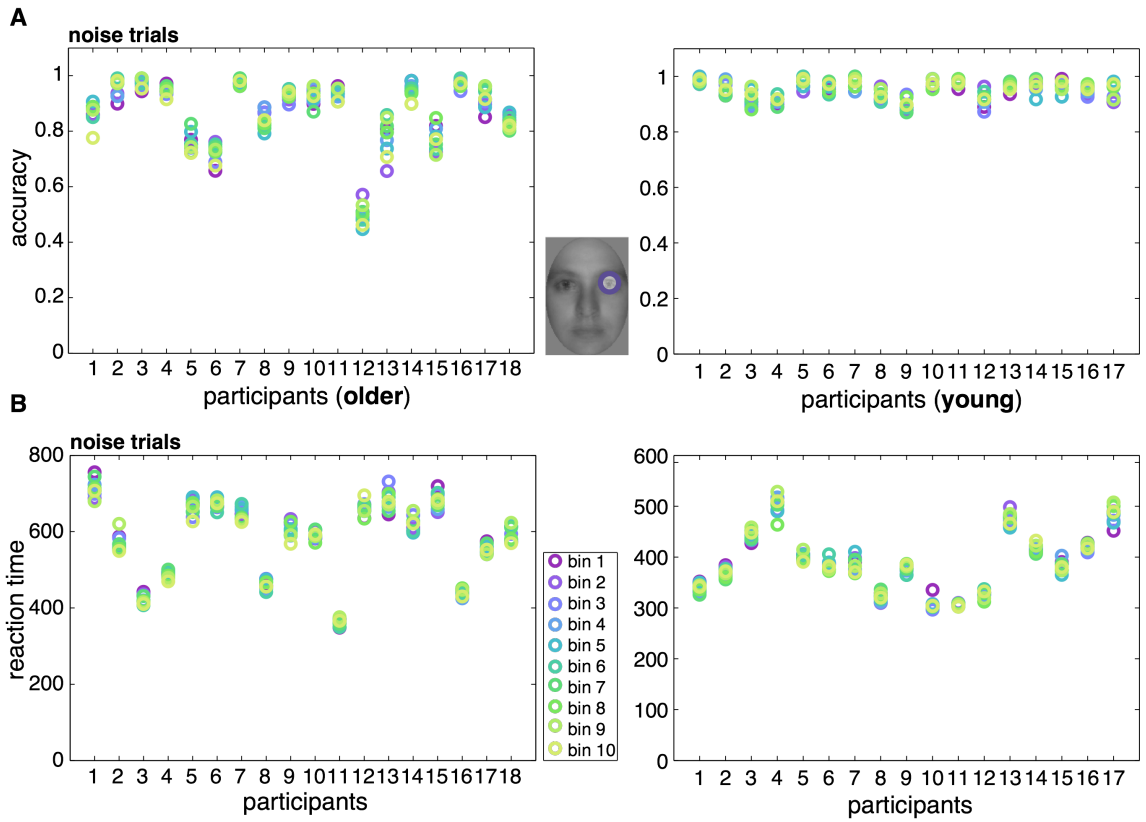


Figure S 5 Reverse analysis: Right eye (noise trials). For details, see Figure S 2 caption.

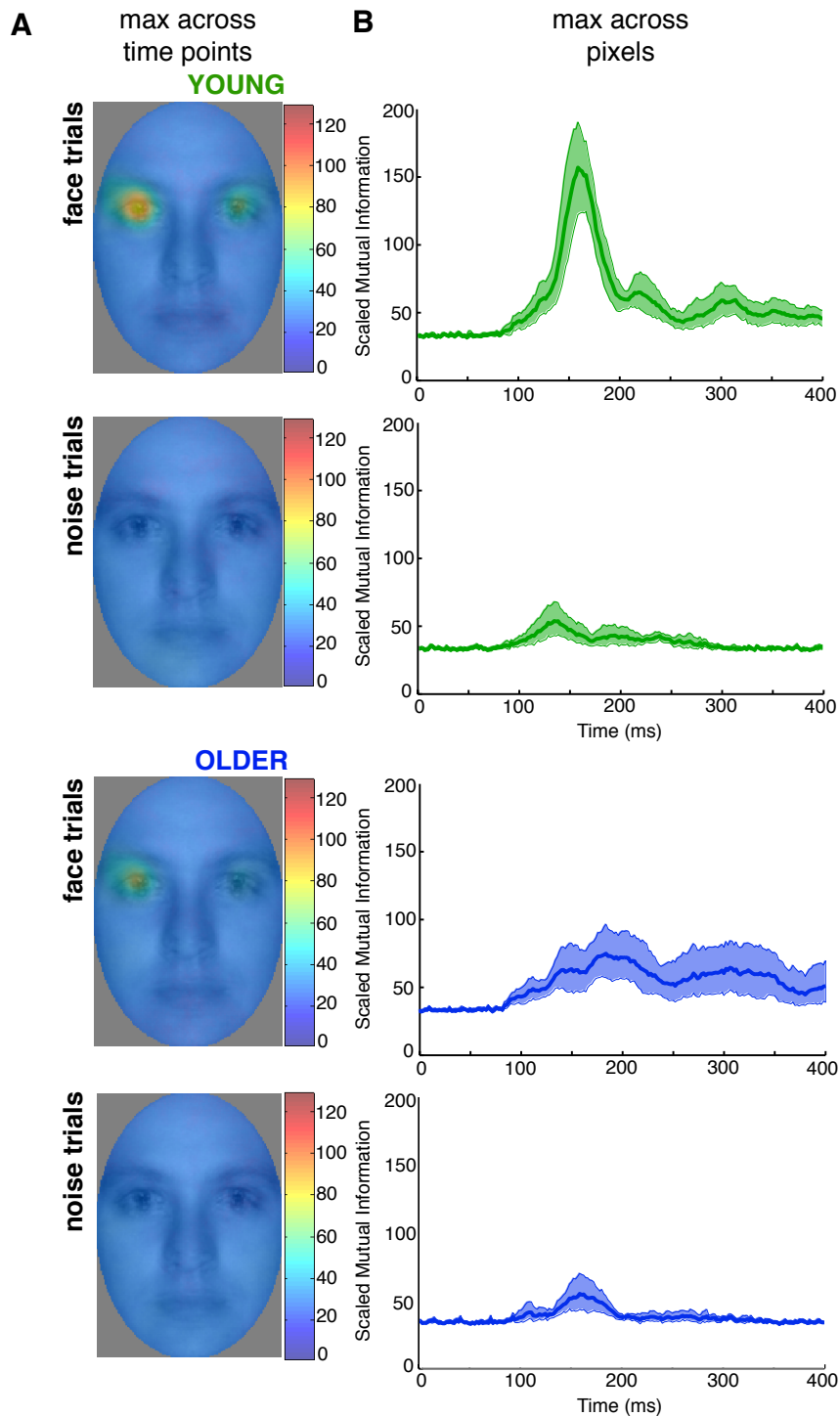


Figure S 6 MI(pix, ERP): all electrodes.

We ran the MI(PIX, ERP) analysis on all electrodes, and at all time points between 0 and 400 ms following stimulus onset, for each participant individually. **(A)** Classification images averaged from individual classification images showing the highest MI values across all time points and electrodes, for face and noise trials in young participants (top two images), and for face and noise trials in older participants (bottom two images). Across both young and older observers, the left eye area was strongly associated with ERPs on face trials. No MI was found on noise trials. **(B)**

Time courses of the maximum MI across all electrodes and pixels, averaged across young and older participants, for face and noise trials separately. Both time courses averaged for young and older participants were very similar to those obtained in the main analysis.

APPENDIX B

Supplementary material for Chapter 3.

SUPPLEMENTARY RESULTS

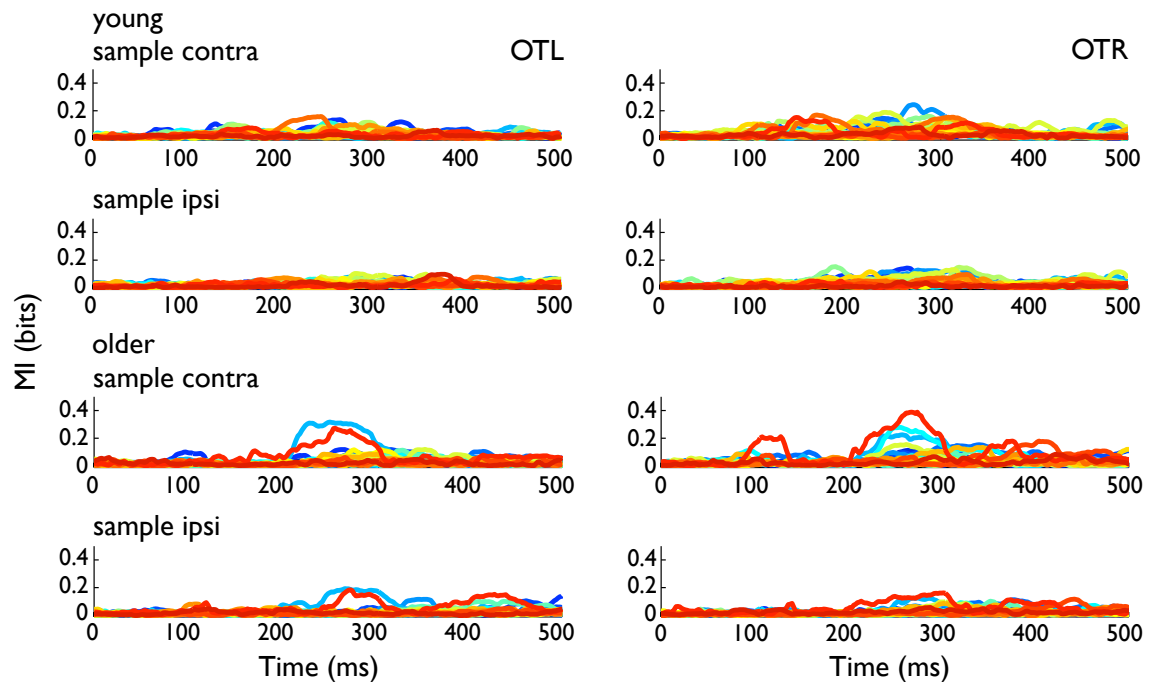


Figure S 7 Individual participants' MI time courses. Presented are time courses for conditions in which face context was absent: sampling of the contralateral and the ipsilateral eye, separately for the left hemisphere (OTL) and the right hemisphere (OTR). Individual participants' time courses are presented separately for young (top) and older (bottom) participants.

MUTUAL INFORMATION ABOUT CATEGORICAL DIFFERENCES BETWEEN FACE AND TEXTURE (OTL)

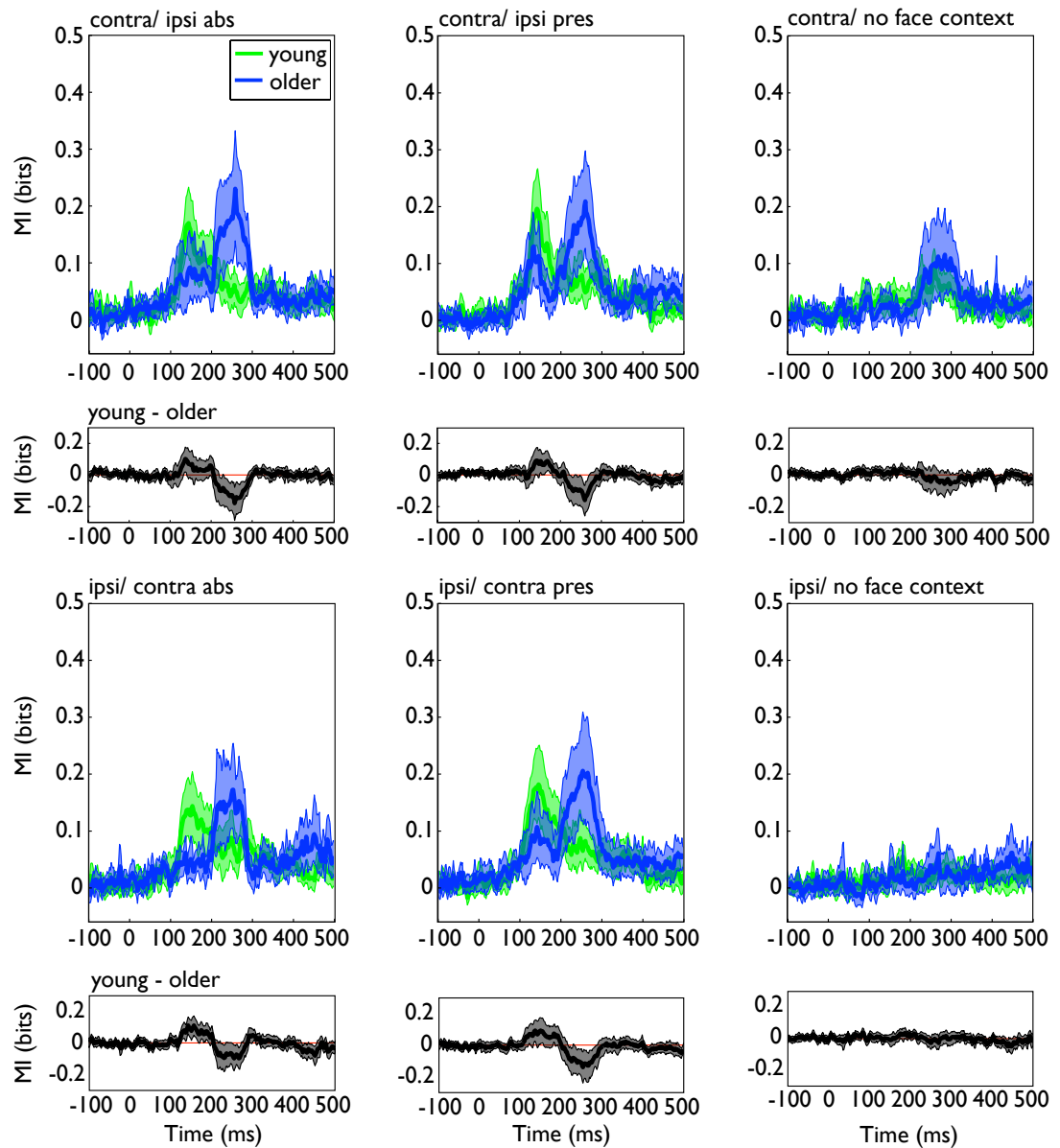


Figure S 8 MI(face/noise, ERP) at OTL.

MI time courses are presented for each condition and separately for young (green) and older (blue) participants. The mean difference between young and older participants is plotted in black in separate panels. Shaded areas correspond to 95% confidence interval.

Table S 2 Categorical differences: maximum MI (OTL).

Values correspond to the median of the maximum MI across time points (expressed in bits), separately for young and older participants, for the categorical differences between each of the experimental conditions and textures. The last column shows the median of pairwise differences between older and young participants. Square brackets indicate 95% confidence intervals. Cliff's *delta* estimates are presented in italics.

	Young	Older	Older-Young
Contra/ Ipsi abs.	0.26 [0.22, 0.30]	0.26 [0.21, 0.36]	0.01 [-0.05, 0.10] <i>0.05 [-0.29, 0.38]</i>
Contra/ Ipsi pres.	0.27 [0.23, 0.32]	0.29 [0.24, 0.35]	0.01 [-0.05, 0.08] <i>0.07 [-0.27, 0.39]</i>
Ipsi/ Contra abs.	0.25 [0.21, 0.31]	0.28 [0.23, 0.37]	0.03 [-0.04, 0.11] <i>0.14 [-0.20, 0.45]</i>
Ipsi/ Contra pres.	0.31 [0.27, 0.37]	0.32 [0.27, 0.38]	-0.004 [-0.08, 0.06] <i>-0.02 [-0.35, 0.31]</i>
Contra	0.21 [0.18, 0.23]	0.19 [0.16, 0.24]	-0.01 [-0.05, 0.03] <i>-0.05 [-0.37, 0.29]</i>
Ipsi	0.15 [0.14, 0.18]	0.16 [0.14, 0.19]	-0.001 [-0.03, 0.03] <i>-0.02 [-0.35, 0.31]</i>

Table S 3 Categorical differences: MI latency (OTL).

Values correspond to the median of the maximum MI latency (expressed in milliseconds), separately for young and older participants, for the categorical differences between each of the experimental conditions and textures. The last column shows the median of pairwise differences between older and young participants. Square brackets indicate 95% confidence intervals. Cliff's *delta* estimates are presented in italics.

	Young	Older	Older-young
Contra/ Ipsi abs.	200 [158, 274]	261 [247, 270]	57 [-15, 103] <i>0.26 [-0.11, 0.57]</i>
Contra/ Ipsi pres.	174 [154, 213]	257 [237, 268]	71 [32, 99] <i>0.54 [0.20, 0.76]</i>
Ipsi/ Contra abs.	179 [150, 224]	241 [220, 265]	60 [20, 90] <i>0.48 [0.14, 0.72]</i>
Ipsi/ Contra pres.	166 [144, 217]	253 [231, 272]	72 [22, 107] <i>0.50 [0.15, 0.74]</i>
Contra	221 [153, 277]	271 [202, 308]	22 [-28, 89] <i>0.15 [-0.19, 0.46]</i>
Ipsi	240 [189, 298]	276 [235, 342]	42 [-14, 86] <i>0.24 [-0.11, 0.53]</i>

Table S 4 Categorical differences: 50% integration time (OTL).

Values correspond to the median of time to integrate 50% of the MI time course (expressed in milliseconds), separately for young and older participants, for the categorical differences between each of the experimental conditions and textures. The last column shows the median of pairwise differences between older and young participants. Square brackets indicate 95% confidence intervals. Cliff's *delta* estimates are presented in italics.

	Young	Older	Older-young
Contra/ Ipsi abs.	217 [193, 250]	246 [235, 258]	28 [-4, 58] <i>0.30 [-0.06, 0.59]</i>
Contra/ Ipsi pres.	205 [184, 229]	259 [238, 282]	55 [25, 82] <i>0.56 [0.24, 0.78]</i>
Ipsi/ Contra abs.	220 [185, 256]	264 [245, 308]	59 [19, 86] <i>0.48 [0.14, 0.71]</i>
Ipsi/ Contra pres.	203 [185, 231]	249 [234, 268]	44 [18, 69] <i>0.50 [0.17, 0.73]</i>
Contra	246 [214, 266]	293 [265, 314]	43 [-1, 81] <i>0.33 [-0.03, 0.61]</i>
Ipsi	254 [227, 296]	285 [230, 353]	24 [-30, 93] <i>0.15 [-0.20, 0.47]</i>

Table S 5 Maximum MI: hemispheric difference (OTR-OTL).

Values correspond to the median of the difference (OTR-OTL) in maximum MI across time points (expressed in bits), separately for young and older participants, for the categorical differences between each of the experimental conditions and textures. The last column shows the median of pairwise differences between older and young participants. Square brackets indicate 95% confidence intervals. Cliff's *delta* estimates are presented in italics.

	Young	Older	Older-Young
Contra/ Ipsi abs.	0.10 [0.05, 0.15]	0.10 [0, 0.19]	0 [-0.10, 0.10] <i>0.01 [-0.33, 0.34]</i>
Contra/ Ipsi pres.	0.13 [0.06, 0.18]	0.09 [0.004, 0.15]	-0.04 [-0.12, 0.04] <i>-0.16 [-0.46, 0.18]</i>
Ipsi/ Contra abs.	0.06 [0.01, 0.12]	0.06 [-0.01, 0.15]	0 [-0.08, 0.08] <i>-0.02 [-0.34, 0.32]</i>
Ipsi/ Contra pres.	0.09 [0.01, 0.17]	0.05 [-0.03, 0.13]	-0.03 [-0.12, 0.05] <i>-0.11 [-0.42, 0.23]</i>
Contra	0.04 [0.01, 0.08]	0.01 [-0.03, 0.06]	-0.04 [-0.10, 0.03] <i>-0.19 [-0.49, 0.16]</i>
Ipsi	0.03 [-0.001, 0.05]	0.02 [-0.02, 0.05]	-0.01 [-0.05, 0.03] <i>-0.08 [-0.40, 0.26]</i>

Table S 6 MI latency: hemispheric differences (OTR-OTL).

Values correspond to the median of the differences (OTR-OTL) in maximum MI latency (expressed in milliseconds), separately for young and older participants, for the categorical differences between each of the experimental conditions and textures. The last column shows the median of pairwise differences between older and young participants. Square brackets indicate 95% confidence intervals. Cliff's *delta* estimates are presented in italics.

	Young	Older	Older-Young
Contra/ Ipsi abs.	-20 [-75, 17]	-14 [-36, 6]	0 [-47, 64] <i>0 [-0.33, 0.33]</i>
Contra/ Ipsi pres.	-28 [-73, 11]	-16 [-55, 2]	-1 [-40, 47] <i>0 [-0.33, 0.33]</i>
Ipsi/ Contra abs.	5 [-36, 23]	-7 [-44, 10]	-12 [-48, 17] <i>-0.14 [-0.45, 0.20]</i>
Ipsi/ Contra pres.	-11 [-66, 8]	0 [-23, 19]	14 [-19, 64] <i>0.16 [-0.19, 0.46]</i>
Contra	-4 [-33, 44]	13 [-17, 46]	10 [-44, 57] <i>0.05 [-0.28, 0.37]</i>
Ipsi	-12 [-55, 70]	0 [-49, 42]	-6 [-87, 55] <i>-0.01 [-0.34, 0.32]</i>

Table S 7 50% integration time: hemispheric differences (OTR-OTL).

Values correspond to the median of the differences (OTR-OTL) in time to integrate 50% of the MI time course (expressed in milliseconds), separately for young and older participants, for the categorical differences between each of the experimental conditions and textures. The last column shows the median of pairwise differences between older and young participants. Square brackets indicate 95% confidence intervals. Cliff's *delta* estimates are presented in italics.

	Young	Older	Older-Young
Contra/ Ipsi abs.	-23 [-70, 0]	-1 [-12, 30]	38 [0, 86] <i>0.30 [-0.05, 0.58]</i>
Contra/ Ipsi pres.	-20 [-36, 1]	-12 [-35, 1]	2 [-27, 27] <i>0.03 [-0.31, 0.35]</i>
Ipsi/ Contra abs.	-12 [-38, 1]	-13 [-67, 6]	-4 [-54, 29] <i>-0.05 [-0.37, 0.29]</i>
Ipsi/ Contra pres.	-7 [-36, 23]	-12 [-34, 1]	-13 [-55, 14] <i>-0.15 [-0.46, 0.19]</i>
Contra	-2 [-33, 41]	-23 [-51, 18]	-15 [-66, 34] <i>-0.11 [-0.42, 0.24]</i>
Ipsi	-8 [-33, 21]	-10 [-43, 41]	0 [-44, 59] <i>0.01 [-0.32, 0.34]</i>

REVERSE ANALYSIS (OTL)

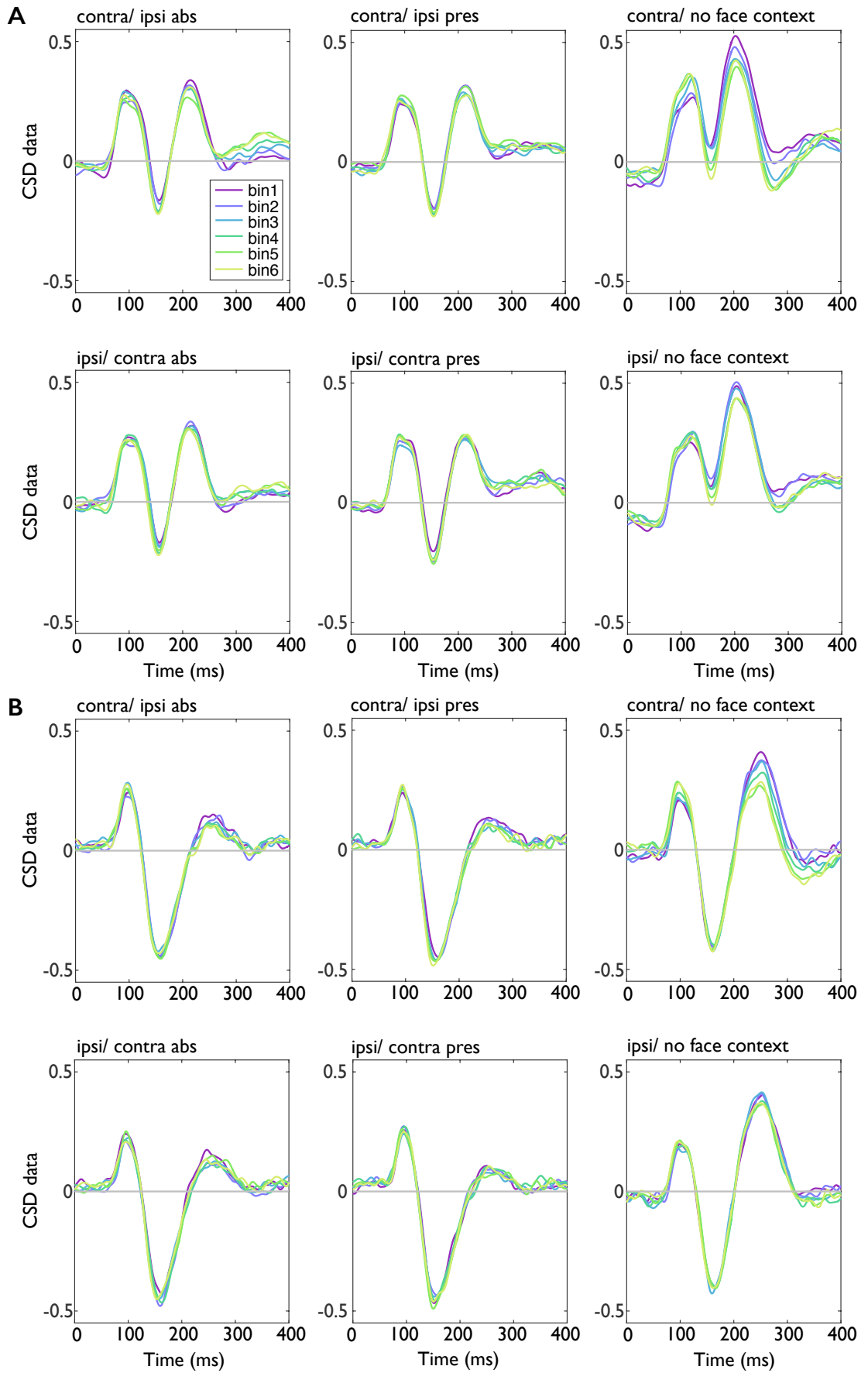


Figure S 9 Modulation of ERPs by eye visibility at OTL.

ERPs from each condition are averaged across trials falling in one of six bins corresponding to different levels of eye visibility (bin 1: lowest visibility, bin 6: highest visibility). Average ERPs are presented separately for young **(A)** and older **(B)** participants.

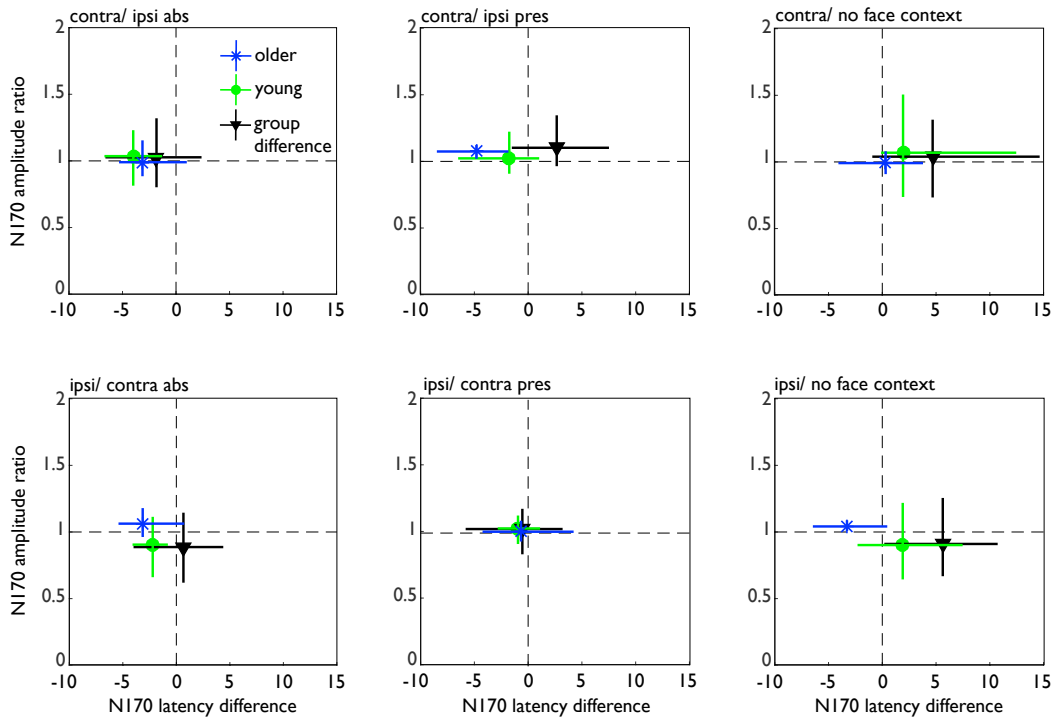


Figure S 10 Group-average modulation of the N170 by eye visibility at OTR.

Effects of eye visibility on the N170 latency and amplitude were quantified as a difference between latencies in bin 6 (high visibility) and in bin 1 (low visibility), and as a ratio of amplitudes in bin 1 to amplitudes in bin 6, separately for each condition. For example, negative values on the x-axis (latency modulation, expressed in milliseconds) indicate shorter latencies in bin 6 than bin 1, and positive values on the y-axis (amplitude modulation, expressed as a ratio) indicate larger amplitudes in bin 6 than bin 1. Green circles correspond to the median across young participants, whereas blue stars – to median across older participants. Black squares show median group differences between young and older participants, expressed as a difference in median latency modulations, and a ratio of median amplitude modulations. Vertical and horizontal lines correspond to 95% confidence intervals.

Table S 8 Group-average N170 latency and amplitude modulation by eye visibility at OTL.

Values correspond to median of individual participants' latency modulation expressed in milliseconds, and median ratio of amplitudes. In individual participants, latency modulation was calculated by subtracting average latency across trials in bin 1 (low eye visibility) from trials in bin 6 (high eye visibility). Amplitude modulation was calculated by dividing average bin 1 amplitude by average bin 6 amplitude. Square brackets correspond to 95% confidence intervals.

	N170 Latency		N170 Amplitude	
	Young	Older	Young	Older
Contra/Ipsi abs.	-4 [-7, -1]	-3 [-5, 1]	0.82 [0.51, 0.98]	1.02 [0.88, 1.13]
Contra/Ipsi pres.	-2 [-6, 1]	-5 [-9, -2]	0.91 [0.75, 1.05]	0.93 [0.89, 0.99]
Contra	2 [0, 12]	0 [-4, 4]	0.78 [0.42, 1.05]	1.01 [0.93, 1.12]
Ipsi/Contra abs.	-2 [-4, -1]	-3 [-6, 1]	1.00 [0.86, 1.36]	0.94 [0.85, 1.04]
Ipsi/Contra pres.	-1 [-3, 1]	-1 [-4, 4]	0.93 [0.80, 1.01]	0.99 [0.91, 1.08]
Ipsi	2 [-2, 7]	-3 [-7, 0]	0.98 [0.71, 1.40]	0.96 [0.92, 0.99]

Table S 9 Group differences in the N170 latency and amplitude modulation at OTL.

For latency modulation, a median difference between individual latency modulations in the groups of young and older participants was computed. For amplitude modulation, a median ratio of individual amplitude modulations in both groups (young/older) was computed (first row of values), as well as the difference between individual values in young and older groups (second row of values). Corresponding Cliff's *delta* estimates are presented in italics. Square brackets indicate 95% confidence intervals.

	N170 Latency	N170 Amplitude
Contra/Ipsi abs.	-2 [-6, 2]	0.79 [0.48, 0.97]
		-0.23 [-0.50, -0.02]
	<i>-0.12 [-0.44, 0.22]</i>	<i>-0.34 [-0.61, 0.00]</i>
Contra/Ipsi pres.	3 [-2, 7]	0.96 [0.78, 1.12]
		-0.04 [-0.21, -0.12]
	<i>0.20 [-0.14, 0.50]</i>	<i>-0.08 [-0.41, 0.26]</i>
Contra	5 [-1, 13]	0.76 [0.53, 1.04]
		-0.24 [-0.62, -0.02]
	<i>0.26 [-0.09, 0.55]</i>	<i>-0.35 [-0.64, 0.03]</i>
Ipsi/Contra abs.	1 [-4, 4]	1.07 [0.86, 1.42]
		0.06 [-0.14, 0.30]
	<i>0.06 [-0.28, 0.38]</i>	<i>0.09 [-0.25, 0.41]</i>
Ipsi/Contra pres.	-1 [-6, 4]	0.92 [0.76, 1.05]
		-0.08 [-0.25, 0.06]
	<i>-0.05 [-0.38, 0.29]</i>	<i>-0.22 [-0.51, 0.13]</i>
Ipsi	6 [-1, 10]	0.97 [0.71, 1.46]
		-0.03 [-0.24, 0.45]
	<i>0.31 [-0.03, 0.58]</i>	<i>-0.04 [-0.39, 0.32]</i>

APPENDIX C

Supplementary material for Chapter 4.

Table S 10 ERP amplitudes and latencies: object trials.

Values correspond to the median N170 latency and amplitude across young and older participants, averaged for face, house and letter trials and presented separately for OTL and OTR. The column labelled 'difference' shows median differences between older and young participants, and the corresponding Cliff's *delta* estimate of the group difference is shown in italics. Amplitude is expressed in $\mu\text{V}/\text{cm}^2$ and latency is expressed in milliseconds. Square brackets correspond to 95% confidence intervals.

N170 latency	OTL			OTR		
	young	older	difference	young	older	difference
Faces	147 [138, 153]	154 [146, 162]	8 [-2, 18] <i>0.27 [-0.06, 0.55]</i>	147 [144, 151]	158 [149, 167]	12 [1, 22] <i>0.35 [0.01, 0.62]</i>
Houses	155 [144, 166]	162 [151, 173]	8 [-6, 23] <i>0.17 [-0.16, 0.47]</i>	155 [144, 162]	166 [161, 176]	14 [3, 30] <i>0.39 [0.04, 0.65]</i>
Letters	157 [153, 163]	161 [152, 169]	3 [-7, 14] <i>0.09 [-0.23, 0.41]</i>	154 [148, 159]	166 [159, 176]	13 [3, 25] <i>0.41 [0.07, 0.66]</i>
N170 amplitude						
Faces	-0.32 [-0.46, -0.15]	-0.61 [-0.73, -0.55]	-0.31 [-0.51, -0.16] <i>-0.57 [-0.77, -0.25]</i>	-0.36 [-0.46, -0.23]	-0.61 [-0.81, -0.46]	-0.26 [-0.46, -0.13] <i>-0.47 [-0.70, -0.14]</i>
Houses	-0.18 [-0.28, -0.09]	-0.49 [-0.67, -0.35]	-0.32 [-0.50, -0.16] <i>-0.62 [-0.80, -0.32]</i>	-0.16 [-0.27, -0.08]	-0.45 [-0.60, -0.32]	-0.27 [-0.42, -0.13] <i>-0.55 [-0.76, -0.23]</i>
Letters	-0.41 [-0.55, -0.28]	-0.62 [-0.87, -0.41]	-0.22 [-0.50, -0.04] <i>-0.34 [-0.60, -0.00]</i>	-0.42 [-0.54, -0.33]	-0.48 [-0.72, -0.36]	-0.08 [-0.28, 0.09] <i>-0.17 [-0.47, 0.17]</i>

Table S 11 ERP amplitudes and latencies: texture trials.

Values correspond to the median N170 latency and amplitude across young and older participants, averaged for texture trials in the face detection (Fnoise), house detection (Hnoise) and letter detection (Lnoise) tasks and presented separately for OTL and OTR. The column labelled 'difference' shows median differences between older and young participants, and the corresponding Cliff's *delta* estimate of the group difference is shown in italics. Amplitude is expressed in $\mu\text{V}/\text{cm}^2$ and latency is expressed in milliseconds. Square brackets correspond to 95% confidence intervals.

N170 latency	OTL			OTR		
	young	older	difference	young	older	difference
Fnoise	160 [130, 192]	171 [158, 186]	33 [-10, 60] <i>0.30 [-0.07, 0.60]</i>	140 [113, 171]	173 [156, 188]	55 [19, 78] <i>0.50 [0.14, 0.75]</i>
Hnoise	128 [105, 152]	156 [148, 165]	48 [21, 64] <i>0.53 [0.17, 0.76]</i>	151 [122, 182]	161 [148, 174]	27 [-2, 56] <i>0.32 [-0.04, 0.61]</i>
Lnoise	163 [136, 191]	159 [147, 172]	6 [-27, 34] <i>0.07 [-0.27, 0.39]</i>	141 [116, 166]	159 [145, 174]	30 [2, 55] <i>0.35 [0.01, 0.63]</i>
N170 amplitude						
Fnoise	-0.07 [-0.12, -0.03]	-0.39 [-0.53, -0.22]	-0.30 [-0.46, -0.13] <i>-0.64 [-0.82, -0.33]</i>	-0.06 [-0.17, 0.02]	-0.35 [-0.45, -0.23]	-0.24 [-0.38, -0.09] <i>-0.53 [-0.75, -0.21]</i>
Hnoise	-0.07 [-0.12, -0.00]	-0.30 [-0.45, -0.17]	-0.22 [-0.37, -0.11] <i>-0.62 [-0.81, -0.33]</i>	-0.00 [-0.10, 0.05]	-0.26 [-0.37, -0.15]	-0.22 [-0.34, -0.11] <i>-0.55 [-0.76, -0.22]</i>
Lnoise	-0.10 [-0.16, -0.05]	-0.33 [-0.48, -0.24]	-0.23 [-0.37, -0.11] <i>-0.64 [-0.82, -0.34]</i>	-0.12 [-0.25, -0.03]	-0.29 [-0.36, -0.20]	-0.15 [-0.27, -0.03] <i>-0.37 [-0.63, -0.04]</i>

REFERENCES

- Acunzo, D. J., Mackenzie, G., & van Rossum, M. C. (2012). Systematic biases in early ERP and ERF components as a result of high-pass filtering. *Journal of Neuroscience Methods*, *209*(1), 212–218.
- Acunzo, D. J., MacKenzie, G., & van Rossum, M. C. W. (2012). Systematic biases in early ERP and ERF components as a result of high-pass filtering. *Journal of Neuroscience Methods*, *209*(1), 212–218. <https://doi.org/10.1016/j.jneumeth.2012.06.011>
- Arditi, A. (2005). Improving the design of the letter contrast sensitivity test. *Investigative Ophthalmology & Visual Science*, *46*(6), 2225–9. <https://doi.org/10.1167/iovs.04-1198>
- Azzopardi, P., & Cowey, A. (1993). Preferential representation of the fovea in the primary visual cortex. *Nature*, *361*(6414), 719–21. <https://doi.org/10.1038/361719a0>
- Babiloni, C., Binetti, G., Cassarino, A., Dal Forno, G., Del Percio, C., Ferreri, F., ... Rossini, P. M. (2006). Sources of cortical rhythms in adults during physiological aging: A multicentric EEG study. *Human Brain Mapping*, *27*(2), 162–172. <https://doi.org/10.1002/hbm.20175>
- Bailey, I. L., & Lovie, J. E. (1980). The design and use of a new near-vision chart. *American Journal of Optometry and Physiological Optics*, *57*(6), 378–87. Retrieved from <http://www.ncbi.nlm.nih.gov/pubmed/7406006>
- Baltes, P. B., & Lindenberger, U. (1997). Emergence of a powerful connection between sensory and cognitive functions across the adult life span: A new window to the study of cognitive aging? *Psychology and Aging*, *12*(1), 12–21. <https://doi.org/10.1037/0882-7974.12.1.12>
- Bankó, E. M., Gál, V., Körtvélyes, J., Kovács, G., & Vidnyánszky, Z. (2011). Dissociating the effect of noise on sensory processing and overall decision difficulty. *The Journal of Neuroscience: The Official Journal of the Society for Neuroscience*, *31*(7), 2663–2674. <https://doi.org/10.1523/JNEUROSCI.2725-10.2011>
- Bar, M. (2003). A cortical mechanism for triggering top-down facilitation in visual object recognition. *Journal of Cognitive Neuroscience*, *15*(4), 600–9. <https://doi.org/10.1162/089892903321662976>

- Bartzokis, G. (2001). Age-related changes in frontal and temporal lobe volumes in men: a magnetic resonance imaging study. *Arch. Gen. Psychiatry*, *58*(9), 461–465. <https://doi.org/10.1001/archpsyc.58.5.461>.Text
- Bashore, T. R., Van Der Molen, M. W., Ridderinkhof, K. R., & Wylie, S. A. (1997). Is the age-complexity effect mediated by reductions in a general processing resource? *Biological Psychology*, *45*(1), 263–282. [https://doi.org/10.1016/S0301-0511\(96\)05231-3](https://doi.org/10.1016/S0301-0511(96)05231-3)
- Bender, A. R., Völkle, M. C., & Raz, N. (2016). Differential aging of cerebral white matter in middle-aged and older adults: A seven-year follow-up. *NeuroImage*, *125*(October), 74–83. <https://doi.org/10.1016/j.neuroimage.2015.10.030>
- Bennett, P. J., Sekuler, R., & Sekuler, A. B. (2007). The effects of aging on motion detection and direction identification. *Vision Research*, *47*(6), 799–809. <https://doi.org/10.1016/j.visres.2007.01.001>
- Bentin, S., Allison, T., Puce, A., Perez, E., & McCarthy, G. (1996). Electrophysiological studies of face perception in humans. *Journal of Cognitive Neuroscience*, *8*(6), 551–565.
- Bentin, S., & Golland, Y. (2002). Meaningful processing of meaningless stimuli: The influence of perceptual experience on early visual processing of faces. *Cognition*, *86*(1). [https://doi.org/10.1016/S0010-0277\(02\)00124-5](https://doi.org/10.1016/S0010-0277(02)00124-5)
- Bentin, S., Sagiv, N., Mecklinger, A., Friederici, A., & von Cramon, Y. D. (2002). Priming Visual Face-Processing Mechanisms: Electrophysiological Evidence. *Psychological Science*, *13*(2), 190–193. <https://doi.org/10.1111/1467-9280.00435>
- Betts, L. R., Sekuler, A. B., & Bennett, P. J. (2007). The effects of aging on orientation discrimination. *Vision Research*, *47*(13), 1769–1780. <https://doi.org/10.1016/j.visres.2007.02.016>
- Bieniek, M. M., Bennett, P. J., Sekuler, A. B., & Rousselet, G. A. (2015). A robust and representative lower bound on object processing speed in humans. *European Journal of Neuroscience*, 1–11. <https://doi.org/10.1111/ejn.13100>
- Bieniek, M. M., Frei, L. S., & Rousselet, G. A. (2013). Early ERPs to faces: Aging, luminance, and individual differences. *Frontiers in Psychology*, *4*(MAY). <https://doi.org/10.3389/fpsyg.2013.00268>

- Boutet, I., & Faubert, J. (2006). Recognition of faces and complex objects in younger and older adults. *Memory & Cognition*, 34(4), 854–864. <https://doi.org/10.3758/BF03193432>
- Boutet, I., Taler, V., & Collin, C. A. (2015). On the particular vulnerability of face recognition to aging: a review of three hypotheses. *Frontiers in Psychology*, 6, 1139. <https://doi.org/10.3389/FPSYG.2015.01139>
- Brainard, D. H. (1997). The Psychophysics Toolbox. *Spatial Vision*, 10(4), 433–436.
- Brickman, A. M., Meier, I. B., Korgaonkar, M. S., Provenzano, F. A., Grieve, S. M., Siedlecki, K. L., ... Zimmerman, M. E. (2012). Testing the white matter retrogenesis hypothesis of cognitive aging. *Neurobiology of Aging*, 33(8), 1699–1715. <https://doi.org/10.1016/j.neurobiolaging.2011.06.001>
- Burianová, H., Lee, Y., Grady, C. L., & Moscovitch, M. (2013). Age-related dedifferentiation and compensatory changes in the functional network underlying face processing. *Neurobiology of Aging*, 34(12), 2759–2767. <https://doi.org/10.1016/j.neurobiolaging.2013.06.016>
- Cabeza, R. (2002). Hemispheric asymmetry reduction in older adults: the HAROLD model. *Psychology and Aging*, 17(1), 85–100. <https://doi.org/10.1037/0882-7974.17.1.85>
- Chaby, L., George, N., Renault, B., & Fiori, N. (2003). Age-related changes in brain responses to personally known faces: An event-related potential (ERP) study in humans. *Neuroscience Letters*, 349(2), 125–129. [https://doi.org/10.1016/S0304-3940\(03\)00800-0](https://doi.org/10.1016/S0304-3940(03)00800-0)
- Chaby, L., Jemel, B., George, N., Renault, B., & Fiori, N. (2001). An ERP Study of Famous Face Incongruity Detection in Middle Age. *Brain and Cognition*, 45(3), 357–377. <https://doi.org/10.1006/brcg.2000.1272>
- Chaby, L., Narme, P., & George, N. (2011). Older adults' configural processing of faces: role of second-order information. *Psychology and Aging*, 26(1), 71–79. <https://doi.org/10.1037/a0020873>
- Charlton, R. A., Barrick, T. R., McIntyre, D. J., Shen, Y., O'Sullivan, M., Howe, F. A., ... Markus, H. S. (2006). White matter damage on diffusion tensor imaging correlates with age-related cognitive decline. *Neurology*, 66(2), 217–22. <https://doi.org/10.1212/01.wnl.0000194256.15247.83>

- Charlton, R. a, Schiavone, F., Barrick, T. R., Morris, R. G., & Markus, H. S. (2010). Diffusion tensor imaging detects age related white matter change over a 2 year follow-up which is associated with working memory decline. *Journal of Neurology, Neurosurgery, and Psychiatry*, *81*(1), 13–19. <https://doi.org/10.1136/jnnp.2008.167288>
- Cliff, N. (1996). *Ordinal methods for behavioural data analysis*. Mahwah, NJ: Lawrence Erlbaum Associates.
- Colenbrander, A., & Fletcher, D. C. (2004). Evaluation of a new Mixed Contrast Reading Card. *Investigative Ophthalmology & Visual Science*, *45*(13), 4352–4352.
- Cremer, R., & Zeef, E. J. (1987). What Kind of Noise Increases With Age? *Journal of Gerontology*, *42*(5), 515–518.
- Csete, G., Bognár, A., Csibri, P., Kaposvári, P., & Sáry, G. (2015). Aging alters visual processing of objects and shapes in inferotemporal cortex in monkeys. *Brain Research Bulletin*, *110*, 76–83. <https://doi.org/10.1016/j.brainresbull.2014.11.005>
- Daffner, K., Haring, A., & Alperin, B. (2013). The impact of visual acuity on age-related differences in neural markers of early visual processing. *Neuroimage*, *67*(617), 127–136. <https://doi.org/10.1016/j.neuroimage.2012.10.089>.The
- Dakin, S. C., & Watt, R. J. (2009). Biological "bar codes" in human faces. *Journal of Vision*, *9*(4), 2.1-10. <https://doi.org/10.1167/9.4.2>
- Daniel, S., & Bentin, S. (2012). Age-related changes in processing faces from detection to identification: ERP evidence. *Neurobiology of Aging*, *33*(1), 206.e1-206.e28. <https://doi.org/10.1016/j.neurobiolaging.2010.09.001>
- Danziger, W. L., & Salthouse, T. A. (1978). Age and the perception of incomplete figures. *Exp Aging Res*, *4*(1), 67–80. <https://doi.org/10.1080/03610737808257127>
- Davis, S. W., Dennis, N. A., Daselaar, S. M., Fleck, M. S., & Cabeza, R. (2008). Que PASA? The posterior-anterior shift in aging. *Cerebral Cortex* , *18*(5), 1201–9. <https://doi.org/10.1093/cercor/bhm155>
- de Lissa, P., McArthur, G., Hawelka, S., Palermo, R., Mahajan, Y., & Hutzler, F. (2014). Fixation location on upright and inverted faces modulates the N170. *Neuropsychologia*, *57*, 1–11. <https://doi.org/10.1016/j.neuropsychologia.2014.02.006>

- De Sanctis, P., Katz, R., Wylie, G. R., Sehatpour, P., Alexopoulos, G. S., & Foxe, J. J. (2008). Enhanced and lateralized visual sensory processing in the ventral stream may be a feature of normal aging. *Neurobiology of Aging*, *29*(10), 1576–1586. <https://doi.org/10.1016/j.neurobiolaging.2007.03.021>
- Deiber, M. P., Rodriguez, C., Jaques, D., Missonnier, P., Emch, J., Millet, P., ... Ibanez, V. (2010). Aging effects on selective attention-related electroencephalographic patterns during face encoding. *Neuroscience*, *171*(1), 173–186. <https://doi.org/10.1016/j.neuroscience.2010.08.051>
- Delis, D. C., Kaplan, E., & Kramer, J. H. (2001). *Delis-Kaplan Executive Function System (D-KEFS)*. San Antonio, TX: The Psychological Corporation.
- Delorme, A., & Makeig, S. (2004). EEGLAB: an open source toolbox for analysis of single-trial EEG dynamics including independent component analysis. *Journal of Neuroscience Methods*, *134*, 9–21. <https://doi.org/10.1016/j.jneumeth.2003.10.009>
- Delorme, A., Mullen, T., Kothe, C., Akalin Acar, Z., Bigdely-Shamlo, N., Vankov, A., ... Makeig, S. (2011). EEGLAB, SIFT, NFT, BCILAB, and ERICA: new tools for advanced EEG processing. *Computational Intelligence and Neuroscience*, *2011*, 130714. <https://doi.org/10.1155/2011/130714>
- Delorme, A., Sejnowski, T., & Makeig, S. (2007). Enhanced detection of artifacts in EEG data using higher-order statistics and independent component analysis. *NeuroImage*, *34*(4), 1443–9. <https://doi.org/10.1016/j.neuroimage.2006.11.004>
- Druzgal, T. J., & D'Esposito, M. (2003). Dissecting Contributions of Prefrontal Cortex and Fusiform Face Area to Face Working Memory. *Journal of Cognitive Neuroscience*, *15*(6), 771–784. <https://doi.org/10.1162/089892903322370708>
- Eckert, M. A. (2011). Slowing down: Age-related neurobiological predictors of processing speed. *Frontiers in Neuroscience*, *5*(MAR), 1–13. <https://doi.org/10.3389/fnins.2011.00025>
- Eimer, M. (1998). Does the face-specific N170 component reflect the activity of a specialized eye processor? *Neuroreport*, *9*(13), 2945–2948. Retrieved from http://journals.lww.com/neuroreport/Abstract/1998/09140/Does_the_face_specific_N170_component_reflect_the.5.aspx
- Éthier-Majcher, C., Joubert, S., & Gosselin, F. (2013). Reverse correlating trustworthy faces in young and older adults. *Frontiers in Psychology*, *4*, 592.

<https://doi.org/10.3389/fpsyg.2013.00592>

- Falk, E. B., Hyde, L. W., Mitchell, C., Faul, J., Gonzalez, R., Heitzeg, M. M., ... Schulenberg, J. (2013). What is a representative brain? Neuroscience meets population science. *Proceedings of the National Academy of Sciences of the United States of America*, *110*(44), 17615–22. <https://doi.org/10.1073/pnas.1310134110>
- Falkenstein, M., Yordanova, J., & Kolev, V. (2006). Effects of aging on slowing of motor-response generation. *International Journal of Psychophysiology*, *59*(1), 22–29. <https://doi.org/10.1016/j.ijpsycho.2005.08.004>
- Fellinger, R., Gruber, W., Zauner, A., Freunberger, R., & Klimesch, W. (2012). Evoked traveling alpha waves predict visual-semantic categorization-speed. *NeuroImage*, *59*(4), 3379–3388. <https://doi.org/10.1016/j.neuroimage.2011.11.010>
- Fennema-Notestine, C., Gamst, A. C., Quinn, B. T., Pacheco, J., Jernigan, T. L., Thal, L., ... Gollub, R. L. (2007). Feasibility of Multi-site Clinical Structural Neuroimaging Studies of Aging Using Legacy Data. *Neuroinformatics*, *5*(4), 235–245. <https://doi.org/10.1007/s12021-007-9003-9>
- Firestone, A., Turk-Browne, N. B., & Ryan, J. D. (2007). Age-related deficits in face recognition are related to underlying changes in scanning behavior. *Aging, Neuropsychology, and Cognition*, *14*(6), 594–607. <https://doi.org/10.1080/13825580600899717>
- Foxe, J. J., & Simpson, G. V. (2002). Flow of activation from V1 to frontal cortex in humans: A framework for defining “early” visual processing. *Experimental Brain Research*, *142*(1), 139–150. <https://doi.org/10.1007/s00221-001-0906-7>
- Friedman, D. (2011). The Components of Aging. In S. J. Luck & E. S. Kappenman (Eds.), *The Oxford Handbook of Event-Related Potential Components*. Oxford: Oxford University Press.
- Friedman, J. H. (1991). Multivariate Adaptive Regression Splines. *The Annals of Statistics*, *19*(1), 1–67. <https://doi.org/10.1214/aos/1176347963>
- Gaetz, W., Roberts, T. P. L., Singh, K. D., & Muthukumaraswamy, S. D. (2012). Functional and structural correlates of the aging brain: relating visual cortex (V1) gamma band responses to age-related structural change. *Human Brain Mapping*, *33*(9), 2035–46. <https://doi.org/10.1002/hbm.21339>

- Gao, L., Xu, J., Zhang, B., Zhao, L., Harel, A., & Bentin, S. (2009). Aging effects on early-stage face perception: An ERP study. *Psychophysiology*, *46*(5), 970–983. <https://doi.org/10.1111/j.1469-8986.2009.00853.x>
- Gazzaley, A., Clapp, W., Kelley, J., McEvoy, K., Knight, R. T., & D'Esposito, M. (2008). Age-related top-down suppression deficit in the early stages of cortical visual memory processing. *Proceedings of the National Academy of Sciences*, *105*(35), 13122–13126. <https://doi.org/10.1073/pnas.0806074105>
- Gazzaley, A., Cooney, J. W., McEvoy, K., Knight, R. T., & D'Esposito, M. (2005). Top-down enhancement and suppression of the magnitude and speed of neural activity. *Journal of Cognitive Neuroscience*, *17*(3), 507–517. <https://doi.org/10.1162/0898929053279522>
- Gazzaley, A., Cooney, J. W., Rissman, J., & D'Esposito, M. (2005). Top-down suppression deficit underlies working memory impairment in normal aging. *Nature Neuroscience*, *8*(10), 1298–1300. <https://doi.org/10.1038/nn1543>
- Gazzaley, A., & D'Esposito, M. (2007). Top-down modulation and normal aging. *Annals of the New York Academy of Sciences*, *1097*, 67–83. <https://doi.org/10.1196/annals.1379.010>
- Gilbert, C., & Bakan, P. (1973). Visual asymmetry in perception of faces. *Neuropsychologia*, *11*(3), 355–362. [https://doi.org/10.1016/0028-3932\(73\)90049-3](https://doi.org/10.1016/0028-3932(73)90049-3)
- Gilbert, C. D., & Li, W. (2013). Top-down influences on visual processing. *Nature Reviews. Neuroscience*, *14*(5), 350–63. <https://doi.org/10.1038/nrn3476>
- Gilbert, C. D., & Sigman, M. (2007). Brain States: Top-Down Influences in Sensory Processing. *Neuron*, *54*(5), 677–696. <https://doi.org/10.1016/j.neuron.2007.05.019>
- Gittings, N. S., & Fozard, J. L. (1986). Age related changes in visual acuity. *Experimental Gerontology*, *21*(4–5), 423–33. Retrieved from <http://www.ncbi.nlm.nih.gov/pubmed/3493168>
- Goffaux, V., & Dakin, S. C. (2010). Horizontal information drives the behavioral signatures of face processing. *Frontiers in Psychology*, *1*(SEP), 1–14. <https://doi.org/10.3389/fpsyg.2010.00143>
- Gold, J., Bennett, P. J., & Sekuler, A. B. (1999). Identification of band-pass filtered letters and faces by human and ideal observers. *Vision Research*, *39*(21), 3537–3560.

[https://doi.org/10.1016/S0042-6989\(99\)00080-2](https://doi.org/10.1016/S0042-6989(99)00080-2)

- Golomb, B. A., Chan, V. T., Evans, M. A., Koperski, S., White, H. L., & Criqui, M. H. (2012). The older the better: are elderly study participants more non-representative? A cross-sectional analysis of clinical trial and observational study samples. *BMJ Open*, 2(6), e000833. <https://doi.org/10.1136/bmjopen-2012-000833>
- Gosselin, F., & Schyns, P. G. (2001). Bubbles: A technique to reveal the use of information in recognition tasks. *Vision Research*, 41(17), 2261–2271. [https://doi.org/10.1016/S0042-6989\(01\)00097-9](https://doi.org/10.1016/S0042-6989(01)00097-9)
- Gosselin, F., & Schyns, P. G. (2004). No troubles with bubbles: A reply to Murray and Gold. *Vision Research*, 44(5), 471–477. <https://doi.org/10.1016/j.visres.2003.10.007>
- Grady, C. (2012). The cognitive neuroscience of ageing. *Nature Reviews. Neuroscience*, 13(7), 491–505. <https://doi.org/10.1038/nrn3256>
- Grady, C. L. (2008). Cognitive neuroscience of aging. *Annals of the New York Academy of Sciences*, 1124, 127–144. <https://doi.org/10.1196/annals.1440.009>
- Grady, C. L., Maisog, J. M., Horwitz, B., Ungerleider, L. G., Mentis, M. J., Salerno, J. A., ... Haxby, J. V. (1994). Age-related changes in cortical blood flow activation during visual processing of faces and location. *The Journal of Neuroscience*, 14(3 Pt 2), 1450–62. Retrieved from <http://www.ncbi.nlm.nih.gov/pubmed/8126548>
- Grady, C. L., Randy McIntosh, A., Horwitz, B., & Rapoport, S. I. (2000). Age-Related Changes in the Neural Correlates of Degraded and Nondegraded Face Processing. *Cognitive Neuropsychology*, 17(1–3), 165–186. <https://doi.org/10.1080/026432900380553>
- Grill-Spector, K., Knouf, N., & Kanwisher, N. (2004). The fusiform face area subserves face perception, not generic within-category identification. *Nature Neuroscience*, 7(5), 555–562. <https://doi.org/10.1038/nn1224>
- Groppe, D. M., Makeig, S., & Kutas, M. (2009). Identifying reliable independent components via split-half comparisons. *NeuroImage*, 45(4), 1199–211. <https://doi.org/10.1016/j.neuroimage.2008.12.038>
- Gruber, W. R., Klimesch, W., Sauseng, P., & Doppelmayr, M. (2005). Alpha Phase Synchronization Predicts P1 and N1 Latency and Amplitude Size. *Cerebral Cortex*, 15(4), 371–377. <https://doi.org/10.1093/cercor/bhh139>

- Gunning-Dixon, F. M., Brickman, A. M., Cheng, J. C., & Alexopoulos, G. S. (2009). Aging of cerebral white matter: a review of MRI findings. *International Journal of Geriatric Psychiatry, 24*(2), 109–117. <https://doi.org/10.1002/gps.2087>
- Habak, C., Wilkinson, F., & Wilson, H. R. (2008). Aging disrupts the neural transformations that link facial identity across views. *Vision Research, 48*(1), 9–15. <https://doi.org/10.1016/j.visres.2007.10.007>
- Harrell, F. E., & Davis, C. E. (1982). A new distribution-free quantile estimator. *Biometrika, 69*(3), 635–640. <https://doi.org/10.1093/biomet/69.3.635>
- Hasher, L., & Zacks, R. T. (1988). Working memory, comprehension, and aging: A review and a new view. In G. H. Bower (Ed.), *The Psychology of Learning and Motivation, Vol. 22* (pp. 193–225). New York, NY: Academic Press.
- Haxby, Hoffman, & Gobbini. (2000). The distributed human neural system for face perception. *Trends in Cognitive Sciences, 4*(6), 223–233. Retrieved from <http://www.ncbi.nlm.nih.gov/pubmed/10827445>
- Haymes, S. A., Roberts, K. F., Cruess, A. F., Nicolela, M. T., LeBlanc, R. P., Ramsey, M. S., ... Artes, P. H. (2006). The letter contrast sensitivity test: clinical evaluation of a new design. *Investigative Ophthalmology & Visual Science, 47*(6), 2739–45. <https://doi.org/10.1167/iovs.05-1419>
- Hildebrandt, A., Wilhelm, O., Schmiedek, F., Herzmann, G., & Sommer, W. (2011). On the specificity of face cognition compared with general cognitive functioning across adult age. *Psychology and Aging, 26*(3), 701–715. <https://doi.org/10.1037/a0023056>
- Hsiao, J. H., & Cottrell, G. (2008). Two fixations suffice in face recognition. *Psychological Science, 19*(10), 998–1006. <https://doi.org/10.1111/j.1467-9280.2008.02191.x>
- Hua, T., Kao, C., Sun, Q., Li, X., & Zhou, Y. (2008). Decreased proportion of GABA neurons accompanies age-related degradation of neuronal function in cat striate cortex. *Brain Research Bulletin, 75*(1), 119–125. <https://doi.org/10.1016/j.brainresbull.2007.08.001>
- Huang, Y.-Z., Rothwell, J. C., Chen, R.-S., Lu, C.-S., & Chuang, W.-L. (2011). The theoretical model of theta burst form of repetitive transcranial magnetic stimulation. *Clinical Neurophysiology, 122*(5), 1011–8. <https://doi.org/10.1016/j.clinph.2010.08.016>

- Husk, J. S., Bennett, P. J., & Sekuler, A. B. (2007). Inverting houses and textures: Investigating the characteristics of learned inversion effects. *Vision Research*, 47(27), 3350–3359. <https://doi.org/10.1016/j.visres.2007.09.017>
- Ince, R. A. A., Giordano, B. L., Kayser, C., Rousselet, G. A., Gross, J., & Schyns, P. G. (2016). A statistical framework for neuroimaging data analysis based on mutual information estimated via a Gaussian copula, 1–53. <https://doi.org/10.1101/043745>
- Ince, R. A. A., Jaworska, K., Gross, J., Panzeri, S., Rijsbergen, J. Van, Rousselet, G. A., & Schyns, P. G. (2016). The Deceptively Simple N170 Reflects Network Information Processing Mechanisms Involving Visual Feature Coding and Transfer Across Hemispheres.
- Ince, R. A. A., Mazzoni, A., Bartels, A., Logothetis, N. K., & Panzeri, S. (2012). A novel test to determine the significance of neural selectivity to single and multiple potentially correlated stimulus features.
- Ince, R. A. A., Petersen, R. S., Swan, D. C., & Panzeri, S. (2009). Python for information theoretic analysis of neural data. *Frontiers in Neuroinformatics*, 3, 4. <https://doi.org/10.3389/neuro.11.004.2009>
- Ishai, A. (2008). Let's face it: It's a cortical network. *NeuroImage*. <https://doi.org/10.1016/j.neuroimage.2007.10.040>
- Ishai, A., Schmidt, C. F., & Boesiger, P. (2005). Face perception is mediated by a distributed cortical network. *Brain Research Bulletin*, 67(1), 87–93. <https://doi.org/10.1016/j.brainresbull.2005.05.027>
- Issa, E. B., & DiCarlo, J. J. (2012). Precedence of the Eye Region in Neural Processing of Faces. *Journal of Neuroscience*, 32(47). Retrieved from <http://www.jneurosci.org/content/32/47/16666.full>
- Itier, R. J., Alain, C., Sedore, K., & McIntosh, A. R. (2007). Early face processing specificity: It's in the eyes! *Journal of Cognitive Neuroscience*, 19(11), 1815–1826. <https://doi.org/10.1162/jocn.2007.19.11.1815>
- Itier, R. J., Herdman, A. T., George, N., Cheyne, D., & Taylor, M. J. (2006). Inversion and contrast-reversal effects on face processing assessed by MEG. *Brain Research*, 1115(1), 108–20. <https://doi.org/10.1016/j.brainres.2006.07.072>
- Itier, R. J., & Taylor, M. J. (2004). Source analysis of the N170 to faces and objects.

Neuroreport, 15(8), 1261–5. Retrieved from <http://www.ncbi.nlm.nih.gov/pubmed/15167545>

Jaworska, K., Yi, F., Ince, R. A. A., Schyns, P. G., & Rousselet, G. A. (n.d.). Processing of the same face features is delayed by 40 ms and weaker in healthy ageing.

Jekabsons, G. (2015). ARESLab: Adaptive Regression Splines toolbox for Matlab/Octave.

Kanwisher, N., McDermott, J., & Chun, M. M. (1997). The Fusiform Face Area: A Module in Human Extrastriate Cortex Specialized for Face Perception. *Journal of Neuroscience*, 17(11). Retrieved from <http://www.jneurosci.org/content/17/11/4302.short>

Kanwisher, N., McDermott, J., & Chun, M. M. (1997). The fusiform face area: a module in human extrastriate cortex specialized for face perception. *The Journal of Neuroscience*, 17(11), 4302–11. Retrieved from <http://www.ncbi.nlm.nih.gov/pubmed/9151747>

Kato, Y., Muramatsu, T., Kato, M., Shintani, M., Yoshino, F., Shimono, M., & Ishikawa, T. (2004). An earlier component of face perception detected by seeing-as-face task. *Neuroreport*, 15(2), 225–229. <https://doi.org/None>

Kayser, J. (2009). Current source density (CSD) interpolation using spherical splines - CSD Toolbox (Version 1.1). New York State Psychiatric Institute: Division of Cognitive Neuroscience.

Kennedy, K. M., & Raz, N. (2005). Age, sex and regional brain volumes predict perceptual-motor skill acquisition. *Cortex*, 41(4), 560–9. Retrieved from <http://www.ncbi.nlm.nih.gov/pubmed/16042032>

Kleiner, M., Brainard, D. H., & Pelli, D. (2007). What's new in Psychtoolbox-3? *Perception*, 36(ECVP Abstract Supplement).

Kolev, V., Falkenstein, M., & Yordanova, J. (2006). Motor-response generation as a source of aging-related behavioural slowing in choice-reaction tasks. *Neurobiology of Aging*, 27(11), 1719–1730. <https://doi.org/10.1016/j.neurobiolaging.2005.09.027>

Kurylo, D. D. (2006). Effects of aging on perceptual organization: efficacy of stimulus features. *Experimental Aging Research*, 32(2), 137–52. <https://doi.org/10.1080/03610730600553901>

- Learmonth, G., Benwell, C. S. Y., Thut, G., & Harvey, M. (2017). Age-related reduction of hemispheric lateralisation for spatial attention: An EEG study. *NeuroImage*, *153*, 139–151. <https://doi.org/10.1016/j.neuroimage.2017.03.050>
- Lee, Y., Grady, C. L., Habak, C., Wilson, H. R., & Moscovitch, M. (2011). Face Processing Changes in Normal Aging Revealed by fMRI Adaptation. *Journal of Cognitive Neuroscience*, *23*(11), 3433–3447. https://doi.org/10.1162/jocn_a_00026
- Leventhal, A. G., Wang, Y., Pu, M., Zhou, Y., & Ma, Y. (2003). GABA and its agonists improved visual cortical function in senescent monkeys. *Science*, *300*(5620), 812–5. <https://doi.org/10.1126/science.1082874>
- Li, S.-C. (2005). Neurocomputational perspectives linking neuromodulation, processing noise, representational distinctiveness, and cognitive aging. In R. Cabeza, L. Nyberg, & D. C. Park (Eds.), *Cognitive Neuroscience of Aging* (pp. 354–379). New York, NY: Oxford University Press.
- Li, S. C., Lindenberger, U., & Sikström, S. (2001). Aging cognition: from neuromodulation to representation. *Trends in Cognitive Sciences*, *5*(11), 479–486. Retrieved from <http://www.ncbi.nlm.nih.gov/pubmed/11684480>
- Liang, Z., Li, H., Yang, Y., Li, G., Tang, Y., Bao, P., & Zhou, Y. (2012). Selective effects of aging on simple and complex cells in primary visual cortex of rhesus monkeys. *Brain Research*, *1470*, 17–23. <https://doi.org/10.1016/j.brainres.2012.06.017>
- Liang, Z., Yang, Y., Li, G., Zhang, J., Wang, Y., Zhou, Y., & Leventhal, A. G. (2010). Aging affects the direction selectivity of MT cells in rhesus monkeys. *Neurobiology of Aging*, *31*(5), 863–873. <https://doi.org/10.1016/j.neurobiolaging.2008.06.013>
- Lindfield, K. C., & Wingfield, A. (1999). An experimental and computational analysis of age differences in the recognition of fragmented pictures: inhibitory connections versus speed of processing. *Experimental Aging Research*, *25*(3), 223–42. <https://doi.org/10.1080/036107399244002>
- Lindfield, K. C., Wingfield, A., & Bowles, N. L. (1994). Identification of fragmented pictures under ascending versus fixed presentation in young and elderly adults: Evidence for the inhibition-deficit hypothesis. *Aging, Neuropsychology, and Cognition*, *1*(4), 282–291. <https://doi.org/10.1080/13825589408256582>
- Lott, L. A., Haegerstrom-Portnoy, G., Schneck, M. E., & Brabyn, J. A. (2005). Face recognition in the elderly. *Optometry and Vision Science*, *82*(10), 874–881.

- Lu, P. H., Lee, G. J., Raven, E. P., Tingus, K., Khoo, T., Thompson, P. M., & Bartzokis, G. (2011). Age-related slowing in cognitive processing speed is associated with myelin integrity in a very healthy elderly sample. *Journal of Clinical and Experimental Neuropsychology*, 33(10), 1059–1068. <https://doi.org/10.1080/13803395.2011.595397>
- Luck, S. J. (2005). *An introduction to the event-related potential technique*. MIT Press.
- Lueschow, A., Miller, E. K., & Desimone, R. (1994). Inferior temporal mechanisms for invariant object recognition. *Cerebral Cortex*, 4(5), 523–31. Retrieved from <http://www.ncbi.nlm.nih.gov/pubmed/7833653>
- Lustig, C., Hasher, L., & Zacks, R. T. (2007). Inhibitory deficit theory: Recent developments in a “new view.” *Inhibition in Cognition*, (571), 145–162. <https://doi.org/http://dx.doi.org/10.1037/11587-008>
- Macke, J. H., & Wichmann, F. a. (2010). Estimating predictive stimulus features from psychophysical data: The decision image technique applied to human faces. *Journal of Vision*, 10, 22. <https://doi.org/10.1167/10.5.22>
- Madden, D. J., Whiting, W. L., Huettel, S. A., White, L. E., MacFall, J. R., & Provenzale, J. M. (2004). Diffusion tensor imaging of adult age differences in cerebral white matter: Relation to response time. *NeuroImage*, 21(3), 1174–1181. <https://doi.org/10.1016/j.neuroimage.2003.11.004>
- Magri, C., Whittingstall, K., Singh, V., Logothetis, N. K., & Panzeri, S. (2009a). A toolbox for the fast information analysis of multiple-site LFP, EEG and spike train recordings. *BMC Neuroscience*, 10(1), 81. <https://doi.org/10.1186/1471-2202-10-81>
- Magri, C., Whittingstall, K., Singh, V., Logothetis, N. K., & Panzeri, S. (2009b). A toolbox for the fast information analysis of multiple-site LFP, EEG and spike train recordings. *BMC Neuroscience*, 10, 81. <https://doi.org/10.1186/1471-2202-10-81>
- Marner, L., Nyengaard, J. R., Tang, Y., & Pakkenberg, B. (2003). Marked loss of myelinated nerve fibers in the human brain with age. *Journal of Comparative Neurology*, 462(2), 144–152. <https://doi.org/10.1002/cne.10714>
- Maurer, D., Grand, R. Le, & Mondloch, C. J. (2002). The many faces of configural processing. *Trends in Cognitive Sciences*, 6(6), 255–260. Retrieved from <http://www.ncbi.nlm.nih.gov/pubmed/12039607>

- Maurer, D., O'Craven, K. M., Le Grand, R., Mondloch, C. J., Springer, M. V., Lewis, T. L., & Grady, C. L. (2007). Neural correlates of processing facial identity based on features versus their spacing. *Neuropsychologia*, *45*(7), 1438–1451. <https://doi.org/10.1016/j.neuropsychologia.2006.11.016>
- Mayer, A., Schwiedrzik, C. M., Wibral, M., Singer, W., & Melloni, L. (2016). Expecting to See a Letter: Alpha Oscillations as Carriers of Top-Down Sensory Predictions. *Cerebral Cortex*, *26*(7), 3146–60. <https://doi.org/10.1093/cercor/bhv146>
- McHenry, J. C., Insel, K. C., Einstein, G. O., Vidrine, A. N., Koerner, K. M., & Morrow, D. G. (2015). Recruitment of Older Adults: Success May Be in the Details. *The Gerontologist*, *55*(5), 845–853. <https://doi.org/10.1093/geront/gns079>
- McKone, E., & Robbins, R. (2011). Are faces special? In G. Rhodes, A. J. Calder, J. Johnson, & J. V Haxby (Eds.), *Oxford Handbook of Face Perception* (p. 149). Oxford: Oxford University Press.
- Meinhardt-Injac, B., Persike, M., & Meinhardt, G. (2014). Holistic processing and reliance on global viewing strategies in older adults' face perception. *Acta Psychologica*, *151*, 155–163. <https://doi.org/10.1016/j.actpsy.2014.06.001>
- Meunier, D., Achard, S., Morcom, A., & Bullmore, E. (2009). Age-related changes in modular organization of human brain functional networks. *NeuroImage*, *44*(3), 715–23. <https://doi.org/10.1016/j.neuroimage.2008.09.062>
- Murray, R. F., & Gold, J. M. (2004). Troubles with bubbles. *Vision Research*, *44*(5), 461–470. <https://doi.org/10.1016/j.visres.2003.10.006>
- Nakamura, A., Yamada, T., Abe, Y., Nakamura, K., Sato, N., Horibe, K., ... Ito, K. (2001). Age-related changes in brain neuromagnetic responses to face perception in humans. *Neuroscience Letters* (Vol. 312). [https://doi.org/10.1016/S0304-3940\(01\)02168-1](https://doi.org/10.1016/S0304-3940(01)02168-1)
- Neath, K. N., & Itier, R. J. (2014). Facial expression discrimination varies with presentation time but not with fixation on features: a backward masking study using eye-tracking. *Cognition & Emotion*, *28*(1), 115–31. <https://doi.org/10.1080/02699931.2013.812557>
- Nelsen, R. B. (2007). *An introduction to copulas. An Introduction to Copulas*. New York, NY: Springer. https://doi.org/10.1007/0-387-28678-0_1

- Nemrodov, D., Anderson, T., Preston, F. F., & Itier, R. J. (2014). Early sensitivity for eyes within faces: a new neuronal account of holistic and featural processing. *NeuroImage*, *97*, 81–94. <https://doi.org/10.1016/j.neuroimage.2014.04.042>
- Nyberg, L., Salami, A., Andersson, M., Eriksson, J., Kalpouzos, G., & Kauppi, K. (2010). Longitudinal evidence for diminished frontal cortex function in aging. *Pnas*, *107*(52), 22682–22686. <https://doi.org/10.1073/pnas.1012651108/-/DCSupplemental.www.pnas.org/cgi/doi/10.1073/pnas.1012651108>
- Obermeyer, S., Kolling, T., Schaich, A., & Knopf, M. (2012). Differences between old and young adults' ability to recognize human faces underlie processing of horizontal information. *Frontiers in Aging Neuroscience*, *4*(APR), 1–9. <https://doi.org/10.3389/fnagi.2012.00003>
- Owsley, C. (2011). Aging and vision. *Vision Research*, *51*(13), 1610–1622. <https://doi.org/10.1016/j.visres.2010.10.020>
- Owsley, C., Sekuler, R., & Boldt, C. (1981). Aging and low-contrast vision: face perception. *Investigative Ophthalmology and Visual Science*, *21*(2), 362–365.
- Owsley, C., Sekuler, R., & Siemsen, D. (1983). Contrast sensitivity throughout adulthood. *Vision Research*, *23*(7), 689–699. [https://doi.org/10.1016/0042-6989\(83\)90210-9](https://doi.org/10.1016/0042-6989(83)90210-9)
- Pakkenberg, B., & Gundersen, H. J. G. (1997). Neocortical neuron number in humans: Effect of sex and age. *The Journal of Comparative Neurology*, *384*(2), 312–320. [https://doi.org/10.1002/\(SICI\)1096-9861\(19970728\)384:2<312::AID-CNE10>3.0.CO;2-K](https://doi.org/10.1002/(SICI)1096-9861(19970728)384:2<312::AID-CNE10>3.0.CO;2-K)
- Panzeri, S., Brunel, N., Logothetis, N. K., & Kayser, C. (2010). Sensory neural codes using multiplexed temporal scales. *Trends in Neurosciences*, *33*(3), 111–120. <https://doi.org/10.1016/j.tins.2009.12.001>
- Park, D. C., Polk, T. A., Park, R., Minear, M., Savage, A., & Smith, M. R. (2004). Aging reduces neural specialization in ventral visual cortex. *Proceedings of the National Academy of Sciences of the United States of America*, *101*(35), 13091–5. <https://doi.org/10.1073/pnas.0405148101>
- Park, J., Carp, J., Kennedy, K. M., Rodrigue, K. M., Bischof, G. N., Huang, C.-M., ... Park, D. C. (2012). Neural broadening or neural attenuation? Investigating age-related dedifferentiation in the face network in a large lifespan sample. *Journal of*

Neuroscience, 32(6), 2154–2158. <https://doi.org/10.1523/JNEUROSCI.4494-11.2012>

Pascual-Leone, A., Freitas, C., Oberman, L., Horvath, J. C., Halko, M., Eldaief, M., ... Rotenberg, A. (2011). Characterizing Brain Cortical Plasticity and Network Dynamics Across the Age-Span in Health and Disease with TMS-EEG and TMS-fMRI. *Brain Topography*, 24(3–4), 302–315. <https://doi.org/10.1007/s10548-011-0196-8>

Payer, D., Marshuetz, C., Sutton, B., Hebrank, A., Welsh, R. C., & Park, D. C. (2006). Decreased neural specialization in old adults on a working memory task. *NeuroReport*, 17(5), 487–491. <https://doi.org/10.1097/01.wnr.0000209005.40481.31>

Pelli, D. G. (1997). The VideoToolbox software for visual psychophysics: transforming numbers into movies. *Spatial Vision*, 10(4), 437–42. Retrieved from <http://www.ncbi.nlm.nih.gov/pubmed/9176953>

Pernet, C. R., Chauveau, N., Gaspar, C., Rousselet, G. A., Pernet, C. R., Chauveau, N., ... Rousselet, G. A. (2011). LIMO EEG: a toolbox for hierarchical Linear MOdeling of ElectroEncephaloGraphic data. *Computational Intelligence and Neuroscience*, 2011, 831409. <https://doi.org/10.1155/2011/831409>

Pernet, C. R., Latinus, M., Nichols, T. E., & Rousselet, G. A. (2015). Cluster-based computational methods for mass univariate analyses of event-related brain potentials/fields: A simulation study. *Journal of Neuroscience Methods*, 250, 85–93. <https://doi.org/10.1016/j.jneumeth.2014.08.003>

Perrett, D. I., Rolls, E. T., & Caan, W. (1982). Visual neurones responsive to faces in the monkey temporal cortex. *Experimental Brain Research*, 47(3), 329–42. Retrieved from <http://www.ncbi.nlm.nih.gov/pubmed/7128705>

Peters, A. (2002). The effects of normal aging on myelin and nerve fibers: A review. *Journal of Neurocytology*, 31(8/9), 581–593. <https://doi.org/10.1023/A:1025731309829>

Peters, A. (2009a). The effects of normal aging on myelinated nerve fibers in monkey central nervous system. *Frontiers in Neuroanatomy*, 3(July), 11. <https://doi.org/10.3389/neuro.05.011.2009>

Peters, A. (2009b). The Effects of Normal Aging on Nerve Fibers and Neuroglia in the Central Nervous System. *Aging*, 593(2002), 1–26.

- Peters, A., Moss, M. B., & Sethares, C. (2000). Effects of aging on myelinated nerve fibers in monkey primary visual cortex. *The Journal of Comparative Neurology*, 419(3), 364–376. [https://doi.org/10.1002/\(SICI\)1096-9861\(20000410\)419:3<364::AID-CNE8>3.0.CO;2-R](https://doi.org/10.1002/(SICI)1096-9861(20000410)419:3<364::AID-CNE8>3.0.CO;2-R)
- Peters, A., Moss, M. B., & Sethares, C. (2001). The effects of aging on layer 1 of primary visual cortex in the rhesus monkey. *Cerebral Cortex*, 11(2), 93–103. <https://doi.org/10.1093/cercor/11.2.93>
- Peters, A., & Sethares, C. (2002). Aging and the myelinated fibers in prefrontal cortex and corpus callosum of the monkey. *Journal of Comparative Neurology*, 442(3), 277–291. <https://doi.org/10.1002/cne.10099>
- Pfütze, E.-M., Sommer, W., & Schweinberger, S. R. (2002). Age-related slowing in face and name recognition: evidence from event-related brain potentials. *Psychology and Aging*, 17(1), 140–160. <https://doi.org/10.1037/0882-7974.17.1.140>
- Philiastides, M. G., & Sajda, P. (2006). Temporal characterization of the neural correlates of perceptual decision making in the human brain. *Cerebral Cortex*, 16(4), 509–518. <https://doi.org/10.1093/cercor/bhi130>
- Piepers, D. W., & Robbins, R. A. (2012). A review and clarification of the terms “holistic,” “configural,” and “relational” in the face perception literature. *Frontiers in Psychology*, 3, 559. <https://doi.org/10.3389/fpsyg.2012.00559>
- Platek, S. M., Loughhead, J. W., Gur, R. C., Busch, S., Ruparel, K., Phend, N., ... Langleben, D. D. (2006). Neural substrates for functionally discriminating self-face from personally familiar faces. *Human Brain Mapping*, 27(2), 91–98. <https://doi.org/10.1002/hbm.20168>
- Polich, J. (1996). Meta-analysis of P300 normative aging studies. *Psychophysiology*, 33(4), 334–353. <https://doi.org/10.1111/j.1469-8986.1996.tb01058.x>
- Polich, J. (1997). EEG and ERP assessment of normal aging. *Electroencephalography and Clinical Neurophysiology/Evoked Potentials Section*, 104(3), 244–256. [https://doi.org/10.1016/S0168-5597\(97\)96139-6](https://doi.org/10.1016/S0168-5597(97)96139-6)
- Price, D., Tyler, L., Henriques, R. N., Campbell, K., Williams, N., Treder, J. T., ... Henson. (2016). Age-related delay in visual and auditory evoked responses is mediated by white- and gray-matter differences. *bioRxiv*, <http://dx>.

- Raz, N. (2005). The ageing obrain observed in vivo: differential changes and their modifiers. In R. Cabeza, L. Nyberg, & D. C. Park (Eds.), *Cognitive Neuroscience of Aging* (pp. 19–57). New York, NY: Oxford University Press.
- Raz, N., Lindenberger, U., Rodrigue, K. M., Kennedy, K. M., Head, D., Williamson, A., ... Acker, J. D. (2005). Regional brain changes in aging healthy adults: General trends, individual differences and modifiers. *Cerebral Cortex*, *15*(11), 1676–1689. <https://doi.org/10.1093/cercor/bhi044>
- Raz, N., & Rodrigue, K. M. (2006). Differential aging of the brain: Patterns, cognitive correlates and modifiers. *Neuroscience and Biobehavioral Reviews*, *30*(6), 730–748. <https://doi.org/10.1016/j.neubiorev.2006.07.001>
- Ritter, W., Simson, R., & Vaughan, H. G. (1983). Event-Related Potential Correlates of Two Stages of Information Processing in Physical and Semantic Discrimination Tasks. *Psychophysiology*, *20*(2), 168–179. <https://doi.org/10.1111/j.1469-8986.1983.tb03283.x>
- Rolls, E. T., Aggelopoulos, N. C., & Zheng, F. (2003). The receptive fields of inferior temporal cortex neurons in natural scenes. *The Journal of Neuroscience*, *23*(1), 339–48. Retrieved from <http://www.ncbi.nlm.nih.gov/pubmed/12514233>
- Roudaia, E., Bennett, P. J., & Sekuler, A. B. (2008). The effect of aging on contour integration. *Vision Research*, *48*(28), 2767–2774. <https://doi.org/10.1016/j.visres.2008.07.026>
- Rousselet, G. A. (2012). Does Filtering Preclude Us from Studying ERP Time-Courses? *Frontiers in Psychology*, *3*, 131. <https://doi.org/10.3389/fpsyg.2012.00131>
- Rousselet, G. A., Gaspar, C. M., Pernet, C. R., Husk, J. S., Bennett, P. J., & Sekuler, A. B. (2010). Healthy aging delays scalp EEG sensitivity to noise in a face discrimination task. *Frontiers in Psychology*, *1*(JUL), 1–14. <https://doi.org/10.3389/fpsyg.2010.00019>
- Rousselet, G. A., Husk, J. S., Bennett, P. J., & Sekuler, A. B. (2008). Time course and robustness of ERP object and face differences. *Journal of Vision*, *8*(2008), 3.1-18. <https://doi.org/10.1167/8.12.3>
- Rousselet, G. A., Husk, J. S., Pernet, C. R., Gaspar, C. M., Bennett, P. J., & Sekuler, A. B. (2009). Age-related delay in information accrual for faces: evidence from a parametric, single-trial EEG approach. *BMC Neuroscience*, *10*, 114.

<https://doi.org/10.1186/1471-2202-10-114>

- Rousselet, G. A., Ince, R. A. A., van Rijsbergen, N. J., & Schyns, P. G. (2014). Eye coding mechanisms in early human face event-related potentials. *Journal of Vision*, *14*(13), 1–24. <https://doi.org/10.1167/14.13.7>
- Rousselet, G. A., & Pernet, C. R. (2011). Quantifying the Time Course of Visual Object Processing Using ERPs: It's Time to Up the Game. *Frontiers in Psychology*, *2*, 107. <https://doi.org/10.3389/fpsyg.2011.00107>
- Rousselet, G. A., Pernet, C. R., Bennett, P. J., & Sekuler, A. B. (2008). Parametric study of EEG sensitivity to phase noise during face processing. *BMC Neuroscience*, *9*, 98. <https://doi.org/10.1186/1471-2202-9-98>
- Rousselet, G. A., Pernet, C. R., Caldara, R., & Schyns, P. G. (2011). Visual Object Categorization in the Brain: What Can We Really Learn from ERP Peaks? *Frontiers in Human Neuroscience*, *5*, 156. <https://doi.org/10.3389/fnhum.2011.00156>
- Royer, J., Blais, C., Gosselin, F., Duncan, J., & Fiset, D. (2015). When Less Is More: Impact of Face Processing Ability on Recognition of Visually Degraded Faces. *Journal of Experimental Psychology. Human Perception and Performance*, *41*(5), 1179–1183. <https://doi.org/10.1037/xhp0000095>
- Sala-Llonch, R., Bartres-Faz, D., & Junque, C. (2015). Reorganization of brain networks in aging: a review of functional connectivity studies. *Frontiers in Psychology*, *6*, 663. <https://doi.org/10.3389/fpsyg.2015.00663>
- Salthouse, T. a. (1996). The processing-speed theory of adult age differences in cognition. *Psychological Review*, *103*(3), 403–428. <https://doi.org/10.1037/0033-295X.103.3.403>
- Salthouse, T. A. (2000). Aging and measures of processing speed. *Biological Psychology*, *54*(1–3), 35–54. [https://doi.org/10.1016/S0301-0511\(00\)00052-1](https://doi.org/10.1016/S0301-0511(00)00052-1)
- Salthouse, T. A., & Ferrer-Caja, E. (2003). What needs to be explained to account for age-related effects on multiple cognitive variables? *Psychology and Aging*, *18*(1), 91–110. <https://doi.org/10.1037/0882-7974.18.1.91>
- Salthouse, T. A., & Lichty, W. (1985). Tests of the neural noise hypothesis of age-related cognitive change. *Journal of Gerontology*, *40*(4), 443–450. <https://doi.org/10.1093/geronj/40.4.443>

- Salthouse, T. A., & Meinz, E. J. (1995). Aging , Inhibition , Working Memory , and Speed, *50*(6), 297–306.
- Salthouse, T. A., & Prill, K. A. (1988). Effects of aging on perceptual closure. *The American Journal of Psychology*, *101*(2), 217–238.
- Sandell, J. H., & Peters, A. (2002). Effects of age on the glial cells in the rhesus monkey optic nerve. *The Journal of Comparative Neurology*, *445*(1), 13–28. <https://doi.org/10.1002/cne.10162>
- Sandell, J. H., & Peters, A. (2003). Disrupted myelin and axon loss in the anterior commissure of the aged rhesus monkey. *The Journal of Comparative Neurology*, *466*(1), 14–30. <https://doi.org/10.1002/cne.10859>
- Schiavone, F., Charlton, R. A., Barrick, T. R., Morris, R. G., & Markus, H. S. (2006). White Matter Damage on Diffusion Tensor Imaging Correlates with Age-Related Cognitive Decline. *Neurology*, *66*(2), 217–222. <https://doi.org/10.1002/jmri.21572>
- Schmiedt-Fehr, C., Mathes, B., & Basar-Eroglu, C. (2009). Alpha Brain Oscillations and Inhibitory Control. *Journal of Psychophysiology*, *23*(4), 208–215. <https://doi.org/10.1027/0269-8803.23.4.208>
- Schmolesky, M. T., Wang, Y., Pu, M., & Leventhal, A. G. (2000). Degradation of stimulus selectivity of visual cortical cells in senescent rhesus monkeys. *Nature Neuroscience*, *3*(4), 384–390. <https://doi.org/10.1038/73957>
- Schyns, P. G., Gosselin, F., & Smith, M. L. (2009). Information processing algorithms in the brain. *Trends in Cognitive Sciences*, *13*(1), 20–26. <https://doi.org/10.1016/j.tics.2008.09.008>
- Schyns, P. G., Jentzsch, I., Johnson, M., Schweinberger, S. R., & Gosselin, F. (2003). A principled method for determining the functionality of brain responses. *Neuroreport*, *14*(13), 1665–9. <https://doi.org/10.1097/01.wnr.0000088408.04452.e9>
- Schyns, P. G., Petro, L. S., & Smith, M. L. (2007). Dynamics of Visual Information Integration in the Brain for Categorizing Facial Expressions. *Current Biology*, *17*(18), 1580–1585. <https://doi.org/10.1016/j.cub.2007.08.048>
- Schyns, P. G., Petro, L. S., & Smith, M. L. (2009). Transmission of facial expressions of emotion co-evolved with their efficient decoding in the brain: Behavioral and brain evidence. *PLoS ONE*, *4*(5). <https://doi.org/10.1371/journal.pone.0005625>

- Schyns, P. G., Thut, G., & Gross, J. (2011). Cracking the code of oscillatory activity. *PLoS Biology*, 9(5). <https://doi.org/10.1371/journal.pbio.1001064>
- Sekuler, A. B., Gold, J. M., Murray, R. F., & Bennett, P. . (2000). Visual completion of partly occluded objects: insights from behavioral studies. *Neuro-Ophthalmology*, 23, 165–168.
- Sekuler, R., & Hutman, L. P. (1980). Spatial vision and aging. I: Contrast sensitivity. *Journal of Gerontology*, 35(5), 692–9. Retrieved from <http://www.ncbi.nlm.nih.gov/pubmed/7430565>
- Sergent, J., Ohta, S., & MacDonald, B. (1992). Functional neuroanatomy of face and object processing. A positron emission tomography study. *Brain: A Journal of Neurology*, 115 Pt 1(1), 15–36. <https://doi.org/10.1093/brain/115.1.15>
- Shafto, M. A., Tyler, L. K., Dixon, M., Taylor, J. R., Rowe, J. B., Cusack, R., ... Cam-CAN, F. E. (2014). The Cambridge Centre for Ageing and Neuroscience (Cam-CAN) study protocol: a cross-sectional, lifespan, multidisciplinary examination of healthy cognitive ageing. *BMC Neurology*, 14, 204. <https://doi.org/10.1186/s12883-014-0204-1>
- Slessor, G., Riby, D. M., & Finnerty, A. N. (2013). Age-related differences in processing face configuration: the importance of the eye region. *The Journals of Gerontology. Series B, Psychological Sciences and Social Sciences*, 68(2), 228–31. <https://doi.org/10.1093/geronb/gbs059>
- Smith, M. L., Gosselin, F., & Schyns, P. G. (2004). Receptive fields for flexible face categorizations. *Psychological Science*, 15(11), 753–761. <https://doi.org/10.1111/j.0956-7976.2004.00752.x>
- Smith, M. L., Gosselin, F., & Schyns, P. G. (2007). From a face to its category via a few information processing states in the brain. *NeuroImage*, 37(3), 974–984. <https://doi.org/10.1016/j.neuroimage.2007.05.030>
- Smith, S. M., & Nichols, T. E. (2009). Threshold-free cluster enhancement: Addressing problems of smoothing, threshold dependence and localisation in cluster inference. *NeuroImage*, 44(1), 83–98. <https://doi.org/10.1016/j.neuroimage.2008.03.061>
- Spear, P. D. (1993). Neural bases of visual deficits during aging. *Vision Research*, 33(18), 2589–2609. [https://doi.org/10.1016/0042-6989\(93\)90218-L](https://doi.org/10.1016/0042-6989(93)90218-L)

- Summerfield, C., Egner, T., Greene, M., Koechlin, E., Mangels, J., & Hirsch, J. (2006). Predictive Codes for Forthcoming Perception in the Frontal Cortex. *Science*, *314*(5803), 1311–1314. <https://doi.org/10.1126/science.1132028>
- Tang, H., Buia, C., Madhavan, R., Crone, N. E., Madsen, J. R., Anderson, W. S., & Kreiman, G. (2014). Spatiotemporal Dynamics Underlying Object Completion in Human Ventral Visual Cortex. *Neuron*, *83*(3), 736–748. <https://doi.org/10.1016/j.neuron.2014.06.017>
- Tang, Y., Nyengaard, J. R., Pakkenberg, B., & Gundersen, H. J. (1997). Age-induced white matter changes in the human brain: a stereological investigation. *Neurobiology of Aging*, *18*(6), 609–15. Retrieved from <http://www.ncbi.nlm.nih.gov/pubmed/9461058>
- Tenke, C. E., & Kayser, J. (2012). Generator localization by current source density (CSD): implications of volume conduction and field closure at intracranial and scalp resolutions. *Clinical Neurophysiology*, *123*(12), 2328–45. <https://doi.org/10.1016/j.clinph.2012.06.005>
- Thomas, C., Moya, L., Avidan, G., Humphreys, K., Jung, K. J., Peterson, M. A., & Behrmann, M. (2007). Reduction in White Matter Connectivity, Revealed by Diffusion Tensor Imaging, May Account for Age-related Changes in Face Perception. *Journal of Cognitive Neuroscience*, *20*(2), 268–284. <https://doi.org/10.1162/jocn.2008.20025>
- Uylings, H. B. M., & de Brabander, J. M. (2002). Neuronal Changes in Normal Human Aging and Alzheimer's Disease. *Brain and Cognition*, *49*(3), 268–276. <https://doi.org/10.1006/brcg.2001.1500>
- Van Rijsbergen, N. J., & Schyns, P. G. (2009). Dynamics of trimming the content of face representations for categorization in the brain. *PLoS Computational Biology*, *5*(11). <https://doi.org/10.1371/journal.pcbi.1000561>
- van Rijsbergen, N., Jaworska, K., Rousselet, G. A., & Schyns, P. G. (2014). With age comes representational wisdom in social signals. *Current Biology: CB*, *24*(23), 2792–2796. <https://doi.org/10.1016/j.cub.2014.09.075>
- VanRullen, R., & Thorpe, S. J. (2001). The time course of visual processing: from early perception to decision-making. *Journal of Cognitive Neuroscience*, *13*(4), 454–461. <https://doi.org/10.1162/08989290152001880>

- Verhaeghen, P., & Salthouse, T. a. (1997). Meta-analyses of age-cognition relations in adulthood: estimates of linear and nonlinear age effects and structural models. *Psychological Bulletin*, 122(3), 231–249. <https://doi.org/10.1037/0033-2909.122.3.231>
- Vernooij, M. W., de Groot, M., van der Lugt, A., Ikram, M. A., Krestin, G. P., Hofman, A., ... Breteler, M. M. B. (2008). White matter atrophy and lesion formation explain the loss of structural integrity of white matter in aging. *NeuroImage*, 43(3), 470–7. <https://doi.org/10.1016/j.neuroimage.2008.07.052>
- Vogel, E. K., & Luck, S. J. (2000). The visual N1 component as an index of a discrimination process. *Psychophysiology*, 37(2), 190–203. <https://doi.org/10.1111/1469-8986.3720190>
- Voss, M. W., Erickson, K. I., Chaddock, L., Prakash, R. S., Colcombe, S. J., Morris, K. S., ... Kramer, A. F. (2008a). Dedifferentiation in the visual cortex: An fMRI investigation of individual differences in older adults. *Brain Research*, 1244(0), 121–131. <https://doi.org/10.1016/j.brainres.2008.09.051>
- Voss, M. W., Erickson, K. I., Chaddock, L., Prakash, R. S., Colcombe, S. J., Morris, K. S., ... Kramer, A. F. (2008b). Dedifferentiation in the visual cortex: An fMRI investigation of individual differences in older adults. *Brain Research*, 1244(0), 121–131. <https://doi.org/10.1016/j.brainres.2008.09.051>
- Wang, Y., Zhou, Y., Ma, Y., & Leventhal, A. G. (2005). Degradation of signal timing in cortical areas V1 and V2 of senescent monkeys. *Cerebral Cortex*, 15(4), 403–408. <https://doi.org/10.1093/cercor/bhh143>
- Whitfield, K. E., & Elias, J. W. (1992). Age cohort differences in the ability to perform closure on degraded figures. *Experimental Aging Research*, 18(2), 67–73. <https://doi.org/10.1080/03610739208253913>
- Widmann, A., & Schröger, E. (2012a). Filter effects and filter artifacts in the analysis of electrophysiological data. *Frontiers in Psychology*, 3, 233. <https://doi.org/10.3389/fpsyg.2012.00233>
- Widmann, A., & Schröger, E. (2012b). Filter effects and filter artifacts in the analysis of electrophysiological data. *Frontiers in Psychology*, 3, 233. <https://doi.org/10.3389/fpsyg.2012.00233>
- Wiese, H., Schweinberger, S. R., & Hansen, K. (2008). The age of the beholder: ERP

evidence of an own-age bias in face memory. *Neuropsychologia*, 46(12), 2973–2985. <https://doi.org/10.1016/j.neuropsychologia.2008.06.007>

Wilcox, R. R. (2006). Graphical Methods for Assessing Effect Size: Some Alternatives to Cohen's *d*. *Journal of Experimental Education*, 74(4), 353–367. Retrieved from <http://ezproxy.library.capella.edu/login?url=http://search.ebscohost.com/login.aspx?direct=true&db=aph&AN=21333704&site=ehost-live&scope=site>

Wilcox, R. R. (2012). *Introduction to robust estimation and hypothesis testing*. Academic Press.

Wild, H., & Busey, T. (2004). Seeing faces in the noise: stochastic activity in perceptual regions of the brain may influence the perception of ambiguous stimuli. *Psychonomic Bulletin & Review*, 11(3), 475–481. <https://doi.org/10.3758/BF03196598>

Williams, L. R., Grealy, M. A., Kelly, S. W., Henderson, I., & Butler, S. H. (2016). Perceptual bias, more than age, impacts on eye movements during face processing. *Acta Psychologica*, 164, 127–135. <https://doi.org/10.1016/j.actpsy.2015.12.012>

Wilson, H. R., Mei, M., Habak, C., & Wilkinson, F. (2011). Visual bandwidths for face orientation increase during healthy aging. *Vision Research*, 51(1), 160–164. <https://doi.org/10.1016/j.visres.2010.10.026>

Xi, M.-C., Liu, R.-H., Engelhardt, J. K., Morales, F. R., & Chase, M. H. (1999). Changes in the axonal conduction velocity of pyramidal tract neurons in the aged cat. *Neuroscience*, 92(1), 219–225. [https://doi.org/10.1016/S0306-4522\(98\)00754-4](https://doi.org/10.1016/S0306-4522(98)00754-4)

Yang, Y., Liang, Z., Li, G., Wang, Y., Zhou, Y., & Leventhal, A. G. (2008). Aging affects contrast response functions and adaptation of middle temporal visual area neurons in rhesus monkeys. *Neuroscience*, 156(3), 748–757. <https://doi.org/10.1016/j.neuroscience.2008.08.007>

Yordanova, J., Kolev, V., Hohnsbein, J., & Falkenstein, M. (2004). Sensorimotor slowing with ageing is mediated by a functional dysregulation of motor-generation processes: Evidence from high-resolution event-related potentials. *Brain*, 127(2), 351–362. <https://doi.org/10.1093/brain/awh042>

Yordanova, J. Y., Kolev, V. N., & Başar, E. (1998). EEG theta and frontal alpha oscillations during auditory processing change with aging. *Electroencephalography*

and Clinical Neurophysiology/Evoked Potentials Section, 108(5), 497–505.
[https://doi.org/10.1016/S0168-5597\(98\)00028-8](https://doi.org/10.1016/S0168-5597(98)00028-8)

- Yu, S., Wang, Y., Li, X., Zhou, Y., & Leventhal, A. G. (2006). Functional degradation of extrastriate visual cortex in senescent rhesus monkeys. *Neuroscience*, 140(3), 1023–1029. <https://doi.org/10.1016/j.neuroscience.2006.01.015>
- Zanto, T. P., Hennigan, K., Oestberg, M., Clapp, W. C., & Gazzaley, A. (2010). Predictive knowledge of stimulus relevance does not influence top-down suppression of irrelevant information in older adults. *Cortex*, 46(4), 564–574. <https://doi.org/10.1016/j.cortex.2009.08.003>
- Zanto, T. P., Toy, B., & Gazzaley, A. (2010). Delays in neural processing during working memory encoding in normal aging. *Neuropsychologia*, 48(1), 13–25. <https://doi.org/10.1016/j.neuropsychologia.2009.08.003>
- Zerouali, Y., Lina, J.-M., Jemel, B., Rossion, B., Jacques, C., Jacques, C., ... Anderson, S. (2013). Optimal Eye-Gaze Fixation Position for Face-Related Neural Responses. *PLoS ONE*, 8(6), e60128. <https://doi.org/10.1371/journal.pone.0060128>
- Zhuravleva, T. Y., Alperin, B. R., Haring, A. E., Rentz, D. M., Holcomb, P. J., & Daffner, K. R. (2014). Age-related decline in bottom-up processing and selective attention in the very old. *Journal of Clinical Neurophysiology*, 31(3), 261–71. <https://doi.org/10.1097/WNP.0000000000000056>